

**NONEQUILIBRIUM SORPTION OF
VOLATILE PETROLEUM HYDROCARBONS BY
SURFACTANT-MODIFIED ZEOLITE**

by

Joshua Andrew Simpson

Submitted in Partial Fulfillment of
the Requirements for the Degree of
Master of Science in Hydrology

New Mexico Institute of Mining and Technology
Socorro, New Mexico

May 2008

ABSTRACT

The sorption process significantly affects the transport of reactive solutes through geologic media. Nonequilibrium sorption complicates breakthrough curve (BTC) predictions because early-time breakthrough and extended tailing occur. These conditions have adversely affected the accuracy of BTC predictions of volatile petroleum hydrocarbons—specifically benzene, toluene, ethylbenzene, and xylenes (BTEX)—through surfactant-modified zeolite (SMZ) columns.

According to our conceptual model, BTEX molecules are kinetically sorbed on bilayer surfactant sites where the solutes must penetrate external surfactant hydrophilic head groups before partitioning into the hydrophobic tail region of the SMZ. Monolayer SMZ sites allow instantaneous sorption because BTEX molecules immediately partition into the hydrophobic surfactant tail groups. Concentration effects on the kinetics of nonequilibrium sorption of BTEX by SMZ were studied by applying a first-order bicontinuum sorption model to batch experiment data. The modeling results indicate that a constituent's distribution coefficient (K_d) is not affected by concentration variations. However, the first-order sorption rate coefficient (k_2) and the fraction of instantaneous sorption sites (F) are both inversely related to the initial BTEX concentration. A 30 to 45% reduction in k_2 and a 35 to 45% reduction in F occurred as the total BTEX concentration increased from 0.25 to 1.5 mmol L⁻¹. According on the batch results, these nonequilibrium parameters are controlled by the total initial BTEX concentration rather than the concentrations of individual compounds. The variation in F was unexpected based upon a conceptual model of BTEX partitioning into surfactant monolayers and

bilayers. The batch-determined kinetic measurements were used to parameterize a nonequilibrium transport model to predict BTEX breakthrough curves for varying input concentrations.

Monolayer SMZ batch tests were run to test our conceptual model, and the results were in agreement with the conceptual model. As hypothesized, only minor variations between the monolayer and bilayer k_2 results were observed. The significant increase (3 to 10 times) in the monolayer F results was anticipated because of the increase in the fraction of surface covered by a surfactant monolayer. The monolayer K_d results, adjusted for partial coverage, agreed with the bilayer K_d results.

The nonequilibrium transport model fully parameterized with values from the batch experiments was not successful in predicting BTEX transport through SMZ laboratory columns. Predicted breakthrough was earlier than the observed breakthrough for each solute, with the degree of overestimation increasing with increasing hydrophobicity. Sensitivity analysis revealed that the retardation factor, R , (calculated from the distribution coefficient) limited the prediction capabilities. When R was inversely fit to the BTC data while retaining values of k_2 and F from the batch studies, the nonequilibrium model provided reasonable agreement for each constituent's transport behavior. On average, R values fitted to the transport results were three times those calculated from the batch-derived K_d s. Aqueous phase surfactant monomers are present in SMZ batch systems due to surfactant wash-off, but are constantly flushed from transport systems. Consequently, the BTEX solubility might increase in the batch systems, producing lower K_d values in SMZ/BTEX batch systems than transport systems.

ACKNOWLEDGEMENTS

First and foremost, I would like to thank God for allowing me to complete this research and for the knowledge that I have gained in the process.

I would like to thank the Department of Energy for funding this research under grant DE-PS26-04NT15546 to the University of Texas at Austin. I would also like to thank Conoco-Phillips for providing field facilities and field support during this research.

I would like to thank my advisor, Dr. Robert Bowman, for the countless ideas and knowledge provided during my time at New Mexico Tech. I would also like to thank my committee members, Dr. Fred Phillips and Dr. Frank Huang, for their input and advice over the course of my research. I am also thankful for the discussions and time spent with fellow students during my stay at New Mexico Tech. Special thanks go to Craig Altare for introducing me to the project and analytical techniques, Jaron Andrews for helping in the laboratory, and Tyler Munson for teaching me the procedure and analysis of hydrometer tests.

Finally, I am grateful to my family, Mindy, Levi, and Nathan, for their dedication, encouragement, and support for the past three years. This work could not have been completed without the sacrifice you have made. Thank you for all the special moments that took my mind off of work and allowed me to enjoy the little things in life. I love you all and am looking forward to seeing you more in the future.

TABLE OF CONTENTS

	Page
ACKNOWLEDGEMENTS.....	ii
TABLE OF CONTENTS.....	iii
LIST OF FIGURES	v
LIST OF TABLES	vii
LIST OF APPENDIX FIGURES.....	viii
LIST OF APPENDIX TABLES	xi
THESIS INTRODUCTION.....	1
MANUSCRIPT ENTITLED “NONEQUILIBRIUM SORPTION OF VOLATILE PETROLEUM HYDROCARBONS BY SURFACTANT MODIFIED ZEOLITE”	3
ABSTRACT.....	3
1. INTRODUCTION	6
2. MATERIALS AND METHODS.....	11
2.1. <i>Surfactant-Modified Zeolite</i>	11
2.2. <i>Kinetic Batch Experiments</i>	12
2.3. <i>Column Experiments</i>	13
2.4. <i>Analytical Methods</i>	15
2.5. <i>Data Analysis</i>	16
3. RESULTS AND DISCUSSION.....	19
3.1. <i>Bilayer Batch Tests</i>	19
3.2. <i>Monolayer Batch Tests</i>	23
3.3. <i>Column Experiments</i>	25

	Page
4. CONCLUSIONS.....	30
5. RECOMMENDATIONS FOR FUTURE WORK	32
ACKNOWLEDGEMENTS	34
REFERENCES	35
FIGURE CAPTIONS.....	41
APPENDIX A. SINGLE-SOLUTE BATCH EXPERIMENT DATA	67
APPENDIX B. MULTIPLE-SOLUTE BATCH EXPERIMENT DATA.....	75
APPENDIX C. MONOLAYER SMZ BATCH EXPERIMENT DATA	93
APPENDIX D. BTEX ISOTHERMS FROM BATCH EXPERIMENT'S EQUILIBRIUM DATA.....	98
APPENDIX E. TRITIUM BTC DATA.....	125
APPENDIX F. LABORATORY COLUMN BTEX BTC DATA.....	135
APPENDIX G. BICONTINUUM MODEL MODIFICATIONS AND CODE	186
APPENDIX H. PARTICLE SIZE ANALYSIS OF SURFACTANT MODIFIED ZEOLITE FROM THE 2005 FARMINGTON, NM PILOT TEST.	193
APPENDIX I. APPENDICES REFERENCES	226

LIST OF FIGURES

		Page
Figure 1.	Conceptual model of benzene partitioning into surfactant-modified zeolite's hydrophobic tail group	43
Figure 2.	Kinetics of ethylbenzene sorption to bilayer SMZ. A) ethylbenzene alone (single solute), B) ethylbenzene with equal concentrations of benzene, toluene, <i>o</i> -xylene, and <i>p</i> -xylene (multiple solute)	44
Figure 3.	Relationship between $\log K_d$ and $\log K_{ow}$ for BTEX compounds in single-solute and 1.0 mmol L^{-1} total BTEX multiple-solute batch experiments ..	45
Figure 4.	Relationships between $\log k_2$ and $\log K_d$ for BTEX compounds in single-solute and 1.0 mmol L^{-1} total BTEX multiple-solute batch experiments ..	46
Figure 5.	Relationship between F and K_{ow} for BTEX compounds in single-solute and 1.0 mmol L^{-1} total BTEX multiple-solute batch experiments	47
Figure 6.	Initial concentration effects on BTEX constituent distribution coefficients when all constituents have similar initial aqueous concentrations	48
Figure 7.	Initial concentration effects on BTEX constituent rate coefficients when all constituents have similar initial aqueous concentrations	49
Figure 8.	Initial concentration effects on the F of BTEX constituents when all constituents have similar initial aqueous concentrations	50
Figure 9.	Concentration effects of individual BTEX constituents on the benzene K_d . The initial concentration of benzene was 0.2 mmol L^{-1} for all experiments	51
Figure 10.	Concentration effects of individual BTEX constituents on the benzene k_2 . The initial concentration of benzene was 0.2 mmol L^{-1} for all experiments	52
Figure 11.	Concentration effects of individual constituents on the benzene F . The initial concentration of benzene was 0.2 mmol L^{-1} for all experiments	53
Figure 12.	<i>m</i> -Xylene kinetic batch-experiment k_2 data fit with a linear regression	54
Figure 13.	<i>m</i> -Xylene kinetic batch experiment F data fit with a polynomial trend line	55

	Page
Figure 14.	K_d results from three replicate monolayer and corresponding bilayer SMZ batch experiments56
Figure 15.	Results for k_2 from three replicate monolayer and corresponding bilayer SMZ batch experiments57
Figure 16.	F results from three replicate monolayer and corresponding bilayer SMZ batch experiments58
Figure 17.	Tritium breakthrough curve for column 2B fitted with the physical equilibrium, 1-D advection-dispersion model59
Figure 18.	BTEX breakthrough curves for Column 2B60
Figure 19.	Benzene Column 2B data with nonequilibrium model prediction and equilibrium and nonequilibrium model fits61
Figure 20.	<i>m</i> -Xylene Column 2B data with nonequilibrium model prediction and equilibrium and nonequilibrium model fits62
Figure 21.	The k_2 calculated from the nonequilibrium model having R , β , and ω inversely fit, termed transport-determined values63
Figure 22.	F calculated from the nonequilibrium model having R , β , and ω inversely fit, termed transport determined values64
Figure 23.	Nonequilibrium prediction model's individual parameter fits to Column 2B benzene data65
Figure 24.	Nonequilibrium prediction model's individual parameter fits to Column 2B <i>m</i> -xylene data66

LIST OF TABLES

	Page
Table I. Batch-determined nonequilibrium sorption parameter relationships used to parameterize the nonequilibrium transport model. Standard deviation for K_d is in parentheses	39
Table II. Input parameters used to predict nonequilibrium BTEX transport	39
Table III. Monolayer versus bilayer SMZ batch experiment results. For monolayer results, average values are reported with 95% confidence intervals. The multiple-solute, bilayer SMZ experiment with total BTEX C_o equaling 0.5 mmol L^{-1} represents the bilayer results.	40
Table IV. Column characteristics and tritium results from the column experiments	40
Table V. Nonequilibrium parameters from predicted model (predicted) and fit model (fit). Table presents average values over the six column runs with standard deviations in parentheses	40

LIST OF APPENDIX FIGURES

	Page
Figure D-1. Isotherm results for benzene equilibrium batch experiment data	115
Figure D-2. Isotherm results for toluene equilibrium batch experiment data.....	116
Figure D-3. Isotherm results for ethylbenzene equilibrium batch experiment data ...	117
Figure D-4. Isotherm results for <i>m</i> -xylene equilibrium batch experiment data.....	118
Figure D-5. Isotherm results for <i>o</i> -xylene equilibrium batch experiment data.....	119
Figure D-6. Twenty and ninety-minute data from the benzene batch experiments fitted with linear isotherms.....	120
Figure D-7. Twenty and ninety-minute data from the toluene batch experiments fitted with linear isotherms.....	121
Figure D-8. Twenty and ninety-minute data from the ethylbenzene batch experiments fitted with linear isotherms	122
Figure D-9. Twenty and ninety-minute data from the <i>m</i> -xylene batch experiments fitted linear isotherms	123
Figure D-10. Twenty and ninety-minute data from the <i>o</i> -xylene's batch experiments fitted with linear isotherms	124
Figure E-1. Tritium BTC data from column 1A. The solid line represents the physical equilibrium model inversely fit to the data.....	132
Figure E-2. Tritium BTC data from column 1B. The solid line represents the physical equilibrium model inversely fit to the data.....	132
Figure E-3. Tritium BTC data from column 2A. The solid line represents the physical equilibrium model inversely fit to the data.....	133
Figure E-4. Tritium BTC data from column 2B. The solid line represents the physical equilibrium model inversely fit to the data.....	133
Figure E-5. Tritium BTC data from column 3B. The solid line represents the physical equilibrium model inversely fit to the data.....	134

	Page
Figure E-6. Tritium BTC data from column 3B. The solid line represents the physical equilibrium model inversely fit to the data.....	134
Figure G-1. Figure G-1. A) Unmodified model fit to benzene batch data. B) Modified model fit to same benzene dataset.....	187
Figure H-1. Bar graph representation of particle size distribution of sample TA-1. Virgin SMZ represents unspent particle size distribution.....	214
Figure H-2. Bar graph representation of particle size distribution of sample TA-2. Virgin SMZ represents unspent particle size distribution.....	214
Figure H-3. Bar graph representation of particle size distribution of sample BA-1. Virgin SMZ represents unspent particle size distribution.....	215
Figure H-4. Bar graph representation of particle size distribution of sample BA-2. Virgin SMZ represents unspent particle size distribution.....	215
Figure H-5. Bar graph representation of particle size distribution of sample TB-1. Virgin SMZ represents unspent particle size distribution.....	216
Figure H-6. Bar graph representation of particle size distribution of sample TB-2. Virgin SMZ represents unspent particle size distribution.....	216
Figure H-7. Bar graph representation of particle size distribution of sample BB-1. Virgin SMZ represents unspent particle size distribution.....	217
Figure H-8. Bar graph representation of particle size distribution of sample BB-2. Virgin SMZ represents unspent particle size distribution.....	217
Figure H-9. Particle size distribution results for sample TA-1	218
Figure H-10. Particle size distribution results for sample TA-2.....	219
Figure H-11. Particle size distribution results for sample BA-1.....	220
Figure H-12. Particle size distribution results for sample BA-2.....	221

	Page
Figure H-13. Particle size distribution results for sample TB-1	222
Figure H-14. Particle size distribution results for sample TB-2	223
Figure H-15. Particle size distribution results for sample BB-1	224
Figure H-16. Particle size distribution results for sample BB-2	225

LIST OF APPENDIX TABLES

	Page
Table A-1. Data from benzene single-solute batch experiment	68
Table A-2. Data from toluene single-solute batch experiment	69
Table A-3. Data from ethylbenzene single-solute batch experiment	70
Table A-4. Data from <i>m</i> -xylene single-solute batch experiment	71
Table A-5. Data from <i>o</i> -xylene single-solute batch experiment	72
Table A-6. Data from <i>p</i> -xylene single-solute batch experiment	73
Table A-7. Results from the single-solute batch experiments	74
Table B-1. Multiple-solute kinetic batch experiment definitions. In description field: B = benzene, T = toluene, E = ethylbenzene, M = <i>m</i> -xylene, O = <i>o</i> -xylene	76
Table B-2. BTEX sorption data from MSB-0.05 batch experiment	77
Table B-3. BTEX sorption data from MSB-0.1 batch experiment	78
Table B-4. BTEX sorption data from MSB-0.2 batch experiment	79
Table B-5. BTEX sorption data from MSB-0.3 batch experiment	80
Table B-6. BTEX sorption data from MSB-0.5T batch experiment.....	81
Table B-7. BTEX sorption data from MSB-0.5E batch experiment.....	82
Table B-8. BTEX sorption data from MSB-0.5M batch experiment.....	83
Table B-9. BTEX sorption data from MSB-0.5O batch experiment	84
Table B-10. BTEX sorption data from MSB-0.35T batch experiment.....	85
Table B-11. BTEX sorption data from MSB-0.35E batch experiment.....	86
Table B-12. BTEX sorption data from MSB-0.35M batch experiment.....	87

	Page
Table B-13. BTEX sorption data from MSB-0.35O batch experiment	88
Table B-14. Overall results from MSB-0.05 batch experiment.....	89
Table B-15. Overall results from MSB-0.1 batch experiment.....	89
Table B-16. Overall results from MSB-0.2 batch experiment.....	89
Table B-17. Overall results from MSB-0.3 batch experiment.....	90
Table B-18. Overall results from MSB-0.35T batch experiment	90
Table B-19. Overall results from MSB-0.35E batch experiment	90
Table B-20. Overall results from MSB-0.35M batch experiment	91
Table B-21. Overall results from MSB-0.35O batch experiment.....	91
Table B-22. Overall results from MSB-0.5T batch experiment	91
Table B-23. Overall results from MSB-0.5E batch experiment	92
Table B-24. Overall results from MSB-0.5M batch experiment	92
Table B-25. Overall results from MSB-0.5O batch experiment.....	92
Table C-1. BTEX sorption data from M1 monolayer batch experiment	94
Table C-2. BTEX sorption data from M2 monolayer batch experiment	95
Table C-3. BTEX sorption data from M3 monolayer batch experiment	96
Table C-4. Overall results from M1 monolayer batch experiment.....	97
Table C-5. Overall results from M2 monolayer batch experiment.....	97
Table C-6. Overall results from M3 monolayer batch experiment.....	97
Table D-1. Benzene equilibrium data from kinetic batch experiments.....	99

	Page
Table D-2. Toluene equilibrium data from kinetic batch experiments	101
Table D-3. Ethylbenzene equilibrium data from kinetic batch experiments.....	103
Table D-4. <i>m</i> -Xylene equilibrium data from kinetic batch experiments.....	105
Table D-5. <i>o</i> -Xylene equilibrium data from kinetic batch experiments	107
Table D-6. Overall isotherm results from equilibrium data of batch experiments	109
Table D-7. Overall “quasi” equilibrium results from batch experiment data	109
Table D-8. Twenty and ninety-minute data from benzene batch experiments	110
Table D-9. Twenty and ninety-minute data from toluene batch experiments.....	111
Table D-10. Twenty and ninety-minute data from ethylbenzene batch experiments ..	112
Table D-11. Twenty and ninety-minute data from <i>m</i> -xylene batch experiments.....	113
Table D-12. Twenty and ninety-minute data from <i>o</i> -xylene batch experiments	114
Table E-1. Tritium BTC data from column 1A	126
Table E-2. Tritium BTC data from column 1B	127
Table E-3. Tritium BTC data from column 2A	128
Table E-4. Tritium BTC data from column 2B	129
Table E-5. Tritium BTC data from column 3A	130
Table E-6. Tritium BTC data from column 3B	131
Table F-1. BTEX BTC data from column 1A transport experiment.....	136
Table F-2. BTEX BTC data from column 1B transport experiment	138
Table F-3. BTEX BTC data from column 2A transport experiment	140

	Page
Table F-4.	BTEX BTC data from column 2B transport experiment142
Table F-5.	BTEX BTC data from column 3A transport experiment.....144
Table F-6.	BTEX BTC data from column 3B transport experiment146
Table F-7.	Nonequilibrium prediction model results for column 1A experiment.....148
Table F-8.	Nonequilibrium prediction model results for column 1B experiment150
Table F-9.	Nonequilibrium prediction model results for column 2A experiment.....152
Table F-10.	Nonequilibrium prediction model results for column 2B experiment154
Table F-11.	Nonequilibrium prediction model results for column 3A experiment.....156
Table F-12.	Nonequilibrium prediction model results for column 3B experiment158
Table F-13.	Equilibrium model inversely fit to column 1A data results160
Table F-14.	Equilibrium model inversely fit to column 1B data results162
Table F-15.	Equilibrium model inversely fit to column 2A data results164
Table F-16.	Equilibrium model inversely fit to column 2B data results166
Table F-17.	Equilibrium model inversely fit to column 3A data results168
Table F-18.	Equilibrium model inversely fit to column 3B data results170
Table F-19.	Nonequilibrium model inversely fit to column 1A data results.....172
Table F-20.	Nonequilibrium model inversely fit to column 1B data results174
Table F-21.	Nonequilibrium model inversely fit to column 2A data results.....176
Table F-22.	Nonequilibrium model inversely fit to column 2B data results178
Table F-23.	Nonequilibrium model inversely fit to column 3A data results.....180
Table F-24.	Nonequilibrium model inversely fit to column 3B data results182
Table F-25.	Parameters obtained from equilibrium fit model184

	Page
Table F-26. Parameters obtained from nonequilibrium fit model	186
Table H-1. Combined sieve and hydrometer data for sample TA-1	204
Table H-2. Combined sieve and hydrometer data for sample TA-2	205
Table H-3. Combined sieve and hydrometer data for sample BA-1	206
Table H-4. Combined sieve and hydrometer data for sample BA-2	207
Table H-5. Combined sieve and hydrometer data for sample TB-1	208
Table H-6. Combined sieve and hydrometer data for sample TB-2	209
Table H-7. Combined sieve and hydrometer data for sample BB-1	210
Table H-8. Combined sieve and hydrometer data for sample BB-2	211
Table H-9. Combined sieve and hydrometer data for sample Virgin SMZ	212
Table H-10. Overall parameter results from the particle size distribution data	213
Table H-11. Particle size breakdown results from particle size distribution data.....	213

THESIS INTRODUCTION

This document contains a manuscript written for submission to a professional journal and supporting appendices. It represents the results of a thesis project that partially fulfills the requirements for the Degree of Master of Science in Hydrology at the New Mexico Institute of Mining and Technology. This study furthered research on surfactant-modified zeolite (SMZ) removal of benzene, toluene, ethylbenzene, and xylenes (BTEX) from produced water. Previous research showed BTEX transport through SMZ columns is characterized by nonequilibrium sorption. These nonequilibrium processes were investigated through laboratory batch and column experiments. A first-order bicontinuum model was fit to kinetic batch sorption data in order to obtain three nonequilibrium sorption parameters: the distribution coefficient (K_d), a first-order sorption rate coefficient (k_2), and the fraction of instantaneous sorption (F). Since produced water contains highly variable organic hydrocarbon concentrations, the effect of initial BTEX concentrations on these nonequilibrium sorption parameters was investigated in batch experiments.

The nonequilibrium sorption conceptual model was investigated through batch experiments with monolayer SMZ. These studies also tested the experimental procedure's accuracy because three tests with identical experimental conditions were conducted. Finally, the monolayer batch experiments tested the sorption capacity of monolayer zeolite versus bilayer zeolite.

The nonequilibrium sorption parameters determined from the batch experiments were used to parameterize a chemical nonequilibrium transport model. The transport

model predictions were compared to column experiment results. Multiple influent concentrations were studied in order to test the nonequilibrium transport model's sensitivity to this variable.

The following manuscript entitled "Nonequilibrium Sorption of Volatile Petroleum Hydrocarbons by a Surfactant-Modified Zeolite" was prepared for submission to a professional journal. The article presents the introduction, methods, results, and conclusions of the research described above.

The appendices contain data from the batch, tritium, and column experiments, as well as discussion and results for unreported topics.

MANUSCRIPT:
**NONEQUILIBRIUM SORPTION OF VOLATILE PETROLEUM
HYDROCARBONS BY SURFACTANT-MODIFIED ZEOLITE**

Joshua A. Simpson and Robert S. Bowman

*Department of Earth and Environmental Science, New Mexico Institute of Mining and
Technology, Socorro, NM 87801*

ABSTRACT

The sorption process significantly affects the transport of reactive solutes through geologic media. Nonequilibrium sorption complicates breakthrough curve (BTC) predictions because early-time breakthrough and extended tailing occur. These conditions have adversely affected the accuracy of BTC predictions of volatile petroleum hydrocarbons—specifically benzene, toluene, ethylbenzene, and xylenes (BTEX)—through surfactant-modified zeolite (SMZ) columns.

According to our conceptual model, BTEX molecules are kinetically sorbed on bilayer surfactant sites where the solutes must penetrate external surfactant hydrophilic head groups before partitioning into the hydrophobic tail region of the SMZ. Monolayer SMZ sites allow instantaneous sorption because BTEX molecules immediately partition into the hydrophobic surfactant tail groups. Concentration effects on the kinetics of nonequilibrium sorption of BTEX by SMZ were studied by applying a first-order bicontinuum sorption model to batch experiment data. The modeling results indicate that a constituent's distribution coefficient (K_d) is not affected by concentration variations.

However, the first-order sorption rate coefficient (k_2) and the fraction of instantaneous sorption sites (F) are both inversely related to the initial BTEX concentration. A 30 to 45% reduction in k_2 and a 35 to 45% reduction in F occurred as the total BTEX concentration increased from 0.25 to 1.5 mmol L⁻¹. According on the batch results, these nonequilibrium parameters are controlled by the total initial BTEX concentration rather than the concentrations of individual compounds. The variation in F was unexpected based upon a conceptual model of BTEX partitioning into surfactant monolayers and bilayers. The batch-determined kinetic measurements were used to parameterize a nonequilibrium transport model to predict BTEX breakthrough curves for varying input concentrations.

Monolayer SMZ batch tests were run to test our conceptual model, and the results were in agreement with the conceptual model. As hypothesized, only minor variations between the monolayer and bilayer k_2 results were observed. The significant increase (3 to 10 times) in the monolayer F results was anticipated because of the increase in the fraction of surface covered by a surfactant monolayer. The monolayer K_d results, adjusted for partial coverage, agreed with the bilayer K_d results.

The nonequilibrium transport model fully parameterized with values from the batch experiments was not successful in predicting BTEX transport through SMZ laboratory columns. Predicted breakthrough was earlier than the observed breakthrough for each solute, with the degree of overestimation increasing with increasing hydrophobicity. Sensitivity analysis revealed that the retardation factor, R, (calculated from the distribution coefficient) limited the prediction capabilities. When R was inversely fit to the BTC data while retaining values of k_2 and F from the batch studies, the

nonequilibrium model provided reasonable agreement for each constituent's transport behavior. On average, R values fitted to the transport results were three times those calculated from the batch-derived K_d s. Aqueous phase surfactant monomers are present in SMZ batch systems due to surfactant wash-off, but are constantly flushed from transport systems. Consequently, the BTEX solubility might increase in the batch systems, producing lower K_d values in SMZ/BTEX batch systems than transport systems.

1. INTRODUCTION

Water brought to the earth's surface during the production of oil and gas (produced water) represents a significant waste stream within the United States and the single largest waste stream for the oil and gas industries. Within the United States, approximately 18-21 billion barrels (2.8-3.3 billion m³) of produced water are annually brought to the ground surface during oil and gas recovery (API, 2000; Sirivedhin and Dallbauman, 2004). Over the lifetime of an individual production well, approximately 10 barrels of water will be produced for every barrel of oil or gas. Since produced water contains high total dissolved solids, heavy metals, organic constituents, radionuclides, and chemicals added during the production process (Stephenson, 1992), approximately 92% of onshore produced water goes through a preliminary oil separation treatment process and is reinjected into the subsurface (API, 2000). Portions of this water maintain backpressures within the producing formations; however, large amounts of wastewater are pumped into surrounding formations.

Because large portions of the western United States are experiencing water shortages, beneficial use of produced water has been widely considered, and numerous produced water treatment technologies have been proposed (see Altare et al., 2007 and Ranck et al., 2005 for reviews). Since organic constituents foul filtration and membrane treatment systems, organic removal is necessary before reversed osmosis/ultrafiltration methods can be successfully applied to produced waters. According to the American Petroleum Institute (API, 2002), volatile one-ring aromatic hydrocarbons—benzene, toluene, ethylbenzene, and xylenes (BTEX)—and low molecular-weight saturated

hydrocarbons are the most abundant petroleum hydrocarbons within produced waters. Total BTEX concentrations in produced waters have been measured up to 578 mg L^{-1} (API, 2002). Benzene, a Class A carcinogen, is usually the most abundant BTEX constituent within produced waters. Benzene concentrations in produced waters have been measured up to 7,000 times the benzene maximum contaminant level (MCL) of $5 \text{ } \mu\text{g L}^{-1}$ for drinking water under the U.S. Environmental Protection Agency's National Primary Drinking Water Regulations (EPA, 2003).

Natural zeolites are hydrated aluminosilicate minerals and have rigid, cage-like crystal structures. They are characterized by high negative surface charges and high surface areas and, consequently, have high total and external cation exchange capacities (CEC). Many natural zeolites are mined as aggregates that can be crushed to any desired particle size. This characteristic, combined with their high porosity and rigid structure, make natural zeolites suitable for use as packed-bed sorbents.

The positive head groups of cationic surfactant molecules, for example hexadecyltrimethylammonium (HDTMA), are strongly attracted to the zeolite's negative surface and readily exchange for the original inorganic counterions. A stable surfactant monolayer forms on the zeolite surface, with hydrophobic tail groups exposed to the environment. When the aqueous surfactant concentration approaches the critical micelle concentration, admicelles are formed on the zeolite surface. Monolayer, bilayer, or patchy bilayer surfactant coverage is produced depending upon surfactant concentrations and the surfactant counterion (Li and Bowman, 1997; Sullivan et al., 1998). In this paper, we will use the term "monolayer" to refer to zeolite loaded to or below its external CEC. At this surfactant loading, the zeolite primarily has monolayer coverage but also

may exhibit patchy bilayer coverage. We will use the term “bilayer” to indicate a surfactant loading beyond that required to satisfy the external CEC of the zeolite. At this surfactant loading, the zeolite exhibits monolayer, patchy bilayer, and full bilayer coverage (Figure 1). Nonpolar organic solutes, such as BTEX, have an affinity for the hydrophobic surfactant tail group region formed on the SMZ.

Neel and Bowman (1992) examined the sorption of benzene, toluene, and *para*-xylene (BTX) by SMZ. They reported high sorption affinities, with SMZ distribution coefficients approximately 30 – 45 times those of natural zeolite. Based on linear isotherms, no competition between multiple constituents, and a strong correlation between BTEX sorption and octanol-water partitioning coefficients (K_{ow}), Neel and Bowman concluded that the sorption of BTX onto SMZ occurred primarily via a partitioning mechanism. Neel (1992) and Huddleston (1990) both showed that zeolites modified with long-chain alkyl quaternary amines (cationic surfactants with long tail groups) have the highest organic sorption affinities. Sorption equilibrium in batch systems also occur in less than twenty-four hours (Huddleston, 1990).

Ranck *et al.* (2005) studied the transport of BTEX through SMZ in laboratory and field experiments. Ranck *et al.* (2005) reported no statistically significant loss of sorption capacity over ten sorption/regeneration cycles (approximately 4500 PV). Altare *et al.* (2007) also investigated the long-term stability of SMZ in laboratory columns during extended treatment times. A weakly decreasing trend in sorption capacity over fifty sorption and regeneration cycles indicated that minimal surfactant washed off the SMZ during the transport experiments. Because SMZ was fully regenerated by simply blowing air through the columns, both studies concluded that SMZ presented an effective and

regenerable medium to remove BTEX from produced waters (Altare et al., 2007; Ranck et al., 2005). A pilot field test was also conducted in order to determine the suitability of the SMZ treatment system at larger scales (Katz et al., 2006). Continuous treatment successfully removed BTEX from produced water, and a vapor phase bioreactor (VPB) effectively removed BTEX from the off gas during the regeneration cycle, with carbon dioxide and water as the main byproducts.

Even though BTEX sorption onto SMZ is a rapid partitioning process (Neel, 1992), transport models assuming instantaneous sorption inadequately describe BTEX transport through packed beds of SMZ (Ranck et al., 2005). However, equilibrium models adequately describe the transport of tritium—a nonreactive solute—through SMZ (Altare et al., 2007; Ranck et al., 2005). As a result, the nonequilibrium transport of BTEX is apparently explained by chemical, or sorption-related, nonequilibrium.

The purpose of this research was to investigate the nonequilibrium sorption of BTEX by SMZ and to improve predictions of BTEX transport through SMZ. We began with the conceptual model shown in Figure 1. Monolayer SMZ sites allow instantaneous sorption because BTEX molecules immediately partition into the hydrophobic surfactant tail groups. However, BTEX molecules are kinetically sorbed on bilayer sites because the solutes must penetrate the external surfactant's hydrophilic head groups before partitioning into the hydrophobic region (Pignatello and Xing, 1996). Consequently, BTEX molecules are sorbed in the two domains (equilibrium and kinetic) in parallel and represent monolayer and patchy bilayer surfactant coverage on the bilayer SMZ, respectively. We conducted batch experiments with monolayer and bilayer SMZ in order

to obtain kinetic sorption parameters. Since produced water contains highly variable BTEX concentrations, we investigated competition and concentration effects on kinetic sorption parameters. The nonequilibrium sorption parameters obtained from bilayer SMZ batch experiments were used to parameterize a nonequilibrium transport model. We also conducted column experiments to determine the prediction capabilities of the nonequilibrium model. The sensitivity of model predictions to the batch-derived transport parameters was also determined.

2. MATERIALS AND METHODS

2.1. Surfactant-Modified Zeolite

The zeolite used in these studies was obtained from the St. Cloud mine located near Truth or Consequences, New Mexico. It is a natural clinoptilolite-rich tuff, with a mineral composition of 74% clinoptilolite, 10% quartz/cristobalite, 5% smectite, 10% feldspar, and 1% illite. The clinoptilolite's internal cation exchange capacity is 800 meq kg⁻¹, and the external CEC is 90-100 meq kg⁻¹. The St. Cloud zeolite's external surface area is approximately 15.7 m² g⁻¹ (Bowman et al., 2000). The clinoptilolite was crushed to 14-40 mesh size (1.4 to 0.4 mm diameter) for this research.

The bilayer SMZ used in batch and column tests was mass-produced at the St. Cloud mine and had a HDTMA-Cl loading of 180 mmol kg⁻¹ of zeolite (Bowman et al., 2001). Monolayer SMZ with a surfactant loading of 77 mmol kg⁻¹ of zeolite was prepared by the following procedure. Approximately 525 g of raw zeolite was packed into a 30-cm long, 5-cm diameter cast acrylic column (Soil Measurement Systems, LLC, Tucson, AZ). After running carbon dioxide through the column for four hours to remove air, approximately 2000 ml of 20-mmol L⁻¹ HDTMA-Cl (Aldrich, Milwaukee, WI) water (Milli-Q, Millipore, Billerica, MA) was circulated through the column at 5 ml min⁻¹ with a peristaltic pump for 10 days to allow equilibration to a monolayer configuration. Effluent samples were taken at two-day intervals to monitor the zeolite sorption of HDTMA. A constant effluent concentration of 0.03 mmol L⁻¹ was observed after four days. Following equilibration, the monolayer SMZ was removed from the column and allowed to air dry. Electrophoretic mobility analyses showed a net negative charge for

the monolayer zeolite, indicating that the final surfactant loading was less than the external CEC and that coverage was less than a complete monolayer.

2.2. Kinetic Batch Experiments

All BTEX solutions used in batch and column experiments were prepared in a 0.22-mol L⁻¹ NaCl solution, simulating the inorganic salt composition of San Juan Basin produced waters (Altare et al., 2007). Batch experiments, prepared in triplicate with appropriate blanks, were conducted as follows. Three grams of SMZ was added to an 11-mL glass headspace vial. Approximately 6 ml of 0.22-mol L⁻¹ NaCl solution was also added to the headspace vial. After placing (not crimping) a polytetrafluoroethylene (PTFE)-lined butyl septum on the vial, the vial was gently shaken and allowed to sit overnight to promote saturation of the SMZ by the NaCl solution. The vial was then completely filled with 0.22-mol L⁻¹ NaCl solution. Ten microliters of concentrated BTEX solution in methanol was injected into the vial below the air-water interface, and the vial was immediately capped and crimped (procedure adapted from Kolb and Ettre, 1997). The vial was placed on an end-over-end shaker and rotated for a period of 0.5 to 90 min at 9 rpm. The vial was then centrifuged for 2 minutes, and 3 mL of the supernatant solution was transferred into a separate 11-mL glass headspace vial using a rapid open-vial transfer technique (Fuierer, 2001). All procedures were carried out at room temperature (23 ± 2 °C). The solution was analyzed for aqueous BTEX concentration by gas chromatography.

Numerous batch tests were performed in order to examine the effects of single versus multiple solutes, initial solute concentrations, and surfactant loading (monolayer

versus bilayer) on BTEX sorption kinetics. Six single-solute (e.g. benzene alone, *m*-xylene alone) kinetic batch experiments were performed using bilayer SMZ. An initial aqueous solute concentration of approximately 0.2 mmol L^{-1} was used for each single-solute experiment.

Twelve multiple-solute tests were conducted with initial concentrations of each constituent ranging from 0.05 mmol L^{-1} to 0.5 mmol L^{-1} . For each multiple-solute test, all BTEX constituents were included except for *p*-xylene. *p*-Xylene was not included because it co-elutes with *m*-xylene during the GC analysis. The twelve tests were broken into two subgroups: 1) Four multiple-solute tests with the same initial aqueous concentration for all BTEX constituents (e.g. all constituents at 0.05 mmol L^{-1}); 2) Eight tests with the same initial concentration for four BTEX constituents while the initial concentration of one constituent varied (e.g., benzene, toluene, *m*-xylene, and *o*-xylene at 0.2 mmol L^{-1} , ethylbenzene at 0.35 mmol L^{-1}). These tests investigated the sensitivity of concentration variations of individual constituents on benzene nonequilibrium sorption parameters. For these eight multiple-solute tests, the initial aqueous concentration of benzene was always 0.2 mmol L^{-1} .

A monolayer SMZ, multiple-solute batch test with an initial aqueous concentration of each solute equaling 0.1 mmol L^{-1} (total BTEX equaled 0.5 mmol L^{-1}) was replicated three times.

2.3. Column Experiments

Bilayer SMZ was packed into duplicate 11-cm long, 2.5-cm diameter glass columns (Omnifit, Boonton, NJ) to a bulk density of 0.94 g cm^{-3} for BTEX transport

experiments. The columns contained one fixed end piece and one adjustable end piece (both Teflon) in order to eliminate voids. Both end pieces contained removable 100- μm frits (Aldrich, Milwaukee, WI).

Carbon dioxide was passed through each column for 4 hours to displace air and speed saturation. A 0.22-mol L^{-1} NaCl solution was passed through each column using a Model 510 HPLC pump (Waters Corp., Milford, MA) at 8 mL min^{-1} (specific discharge of 1.6 cm min^{-1}), conditions shown to exhibit nonequilibrium BTEX sorption (Altare et al., 2007; Ranck et al., 2005). Tritium tracer tests were conducted with each column in order to determine the hydraulic properties. After column saturation and steady flow conditions were achieved, a 2-pore volume (PV) slug of tritiated water was injected into the column at the same 8 mL min^{-1} flow rate, followed by tritium-free solution for an additional 5 PV. Effluent samples were collected every 0.5 min in 10-mL glass vials using a Retriever II fraction collector (ISCO Inc., Lincoln, NE). One milliliter of each sample was added to 5 mL of scintillation cocktail (ICN Biomedicals, Irvine, CA) in a 7-mL plastic scintillation vial. Samples were gently shaken and tritium was analyzed using a Model LS6500 liquid scintillation counter (Beckman Coulter Inc., Fullerton, CA).

Following the tritium test, a step input of BTEX at a total concentration of 0.60 mmol L^{-1} (approximately 0.12 mmol L^{-1} each of benzene, toluene, ethylbenzene, *m*-xylene, and *o*-xylene) was introduced into the duplicate columns. The influent was held in a 16-L PTFE gas sampling bag (Alltech, Deerfield, IL) to minimize BTEX volatilization losses. Influent samples were taken at 2-h intervals, while effluent samples were taken every 10 min for the first 80 min and at 20-min intervals for the remainder of each experiment. Approximately 250 PV of BTEX solution passed through each column.

The entire process was repeated with freshly packed bilayer SMZ columns and total BTEX concentrations of 0.75 and 0.9 mmol L⁻¹.

2.4. Analytical Methods

All BTEX samples were analyzed by gas chromatography. Samples were loaded into a Model 7694 headspace sampler attached to a Model 5890 GC (Hewlett Packard, Palo Alto, CA). The operating conditions for the headspace sampler were: 70 °C oven temperature, 90 °C transfer line temperature, 80 °C loop temperature, 8.3-min GC cycle time, 3.0-min vial equilibration time, 0.2-min pressurization time, 1.0-min loop fill time, 0.7-min loop equilibration time, and 0.07-min injection time. The operating conditions for the GC were: 35-mL min⁻¹ carrier gas (He) flow rate, 40-ml min⁻¹ split gas (He) flow rate, 55 °C oven temperature, 210 °C injector temperature, and 240 °C detector temperature. The BTEX compounds were separated using a 10-m long x 0.53-mm diameter x 2.65- μ m film thickness HP-5 column and detected with a flame ionization detector. Complete calibration curves—five standards encompassing typical experimental concentrations (0.05, 0.1, 0.2, 0.3, and 0.4 mmol L⁻¹)—were prepared prior to and after each experiment's set of 56 samples. In addition, calibration curves with three standards (0.1, 0.2, and 0.3 mmol L⁻¹) were run after every 10-12 samples.

High-performance liquid chromatography (HPLC) was used to analyze HDTMA, following the method of Li and Bowman (1997).

2.5. Data Analysis

Two bicontinuum models, physical (two-region) and chemical (two-site) nonequilibrium, have been widely used to explain nonequilibrium processes. Two-region nonequilibrium occurs between mobile and immobile water zones. Consequently, both sorbing and non-sorbing constituents experience physical nonequilibrium (Gamerding et al., 1991). Two-site nonequilibrium results from kinetic limitations during the sorption process (Brusseau and Rao, 1989). Only sorbing solutes experience chemical nonequilibrium. The sorption process is considered to occur in two domains; one domain that allows instantaneous sorption and one domain where sorption is rate-limited.

Since tritium (a non-sorbing solute) transport through SMZ is accurately explained by equilibrium models (Altare et al., 2007), the two-site linear bicontinuum model developed by Selim et al. (1976) was used to explain BTEX transport. This model assumes linear isotherms and first-order mass transfer into the rate-limited domain. Sorption is described by the following expressions (Larsen et al., 1992):

$$S_1 = FK_d C_{aq} \quad (1)$$

$$\frac{dS_2}{dt} = k_2 [(1 - F)K_d C_{aq} - S_2] \quad (2)$$

where S_1 represents solute sorbed on sites exhibiting instantaneous sorption ($M M^{-1}$), S_2 represents solute sorbed on sites exhibiting kinetic/ rate-limited sorption ($M M^{-1}$), F equals the fraction of instantaneous sorption sites, K_d is the distribution coefficient ($L^3 M^{-1}$), C_{aq} is the solute's aqueous concentration ($M L^{-3}$), and k_2 is the first-order kinetic rate coefficient for rate-limited sorption (T^{-1}).

Values of K_d were estimated from the equilibrium data of the batch experiments, while k_2 and F were fit to kinetic batch-experiment data using a least sums-of-squares

method. Similar to previous research (Connaughton et al., 1993; Farrell and Reinhard, 1994; Harmon and Roberts, 1994), early investigation of the bicontinuum model fits to batch data revealed that the single rate coefficient did not fully describe the entire kinetic portion of the sorption curve. Consequently, the fitting algorithm placed a lower weighting on early time data in order to obtain a k_2 estimation based on the kinetic sorption curve as it approached equilibrium. These data provide a more accurate representation of k_2 in our system. The values of K_d , k_2 , and F were used to parameterize a nonequilibrium transport model. The following equations describe one-dimensional transport of constituents subject to nonequilibrium chemical sorption in a homogeneous porous medium (Brusseau and Rao, 1991):

$$\beta R \frac{\partial C^*}{\partial p} + (1 - \beta) R \frac{\partial S^*}{\partial p} = \frac{1}{P} \frac{\partial^2 C^*}{\partial X^2} - \frac{\partial C^*}{\partial X} \quad (3)$$

$$(1 - \beta) R \frac{\partial S^*}{\partial p} = \omega (C^* - S^*) \quad (4)$$

where:

$$C^* = \frac{C_{aq}}{C_o} \quad (5)$$

$$S^* = \frac{S_2}{(1 - F) K_d C_o} \quad (6)$$

$$R = 1 + \frac{\rho}{\theta} K_d \quad (7)$$

$$P = \frac{vl}{D} \quad (8)$$

$$p = \frac{vt}{l} \quad (9)$$

$$X = \frac{x}{l} \quad (10)$$

$$\beta = \frac{\left(1 + F \left(\frac{\rho}{\theta}\right) K_d\right)}{R} \quad (11)$$

$$\omega = k_2 (1 - \beta) \frac{lR}{v} \quad (12)$$

and C_0 is the influent aqueous concentration, p is dimensionless time (pore volumes), R is the retardation factor (-), P is the Peclet number (-), l is the length of the column (L), D is the dispersion coefficient ($L^2 T^{-1}$), v is the linear pore water velocity ($L T^{-1}$), x is distance (L), ρ is the medium's bulk density ($M L^{-3}$), θ is the volumetric water content (-), β is the fraction of instantaneous sorption (-), and ω is the Damkohler number (-), which represents the ratio of hydrodynamic residence time to characteristic sorption time. The optimization program CXTFIT version 2.1 (Toride et al., 1999) was used with Eqs. (3) and (4) in the forward mode to predict solute transport from K_d , k_2 , and F values determined in batch studies, and in an inverse mode to estimate these parameters from observed column results.

3. RESULTS AND DISCUSSION

3.1. Bilayer Batch Tests

Six single-solute batch experiments (approximately 0.2 mmol L^{-1} initial concentration) were run, and the bicontinuum model was fit to the data. In order to determine the effect of multiple-solutes, these single-solute results were compared to the multiple-solute results with similar individual initial BTEX concentrations. Figure 2 presents the bicontinuum fit to ethylbenzene single-solute and the corresponding multiple-solute data. The presence of multiple solutes had minimal effect on the ethylbenzene K_d (5 % difference), but noticeably reduced the values of k_2 (30 % decrease) and F (65 % decrease). For all six constituents, sorption equilibrium was reached within 0.5 hr. The bicontinuum model fit all batch experimental data well, with all r^2 values greater than 0.90. Figure 3 presents the relationship between the batch K_d and the octanol-water partition coefficient (K_{ow}) for each BTEX compound from the single-solute and multiple-solute tests. Similar to previous findings (Neel, 1992; Bowman et al., 1995), there is a linear relationship between $\log K_d$ and $\log K_{ow}$, and the BTEX distribution coefficients are not significantly affected by the presence of multiple constituents. Figure 4 shows the k_2 results from these batch tests. An inverse relationship between the K_{ow} and k_2 of each constituent is seen. Competition or concentration effects are also seen, with a 5 – 35% decrease in rate coefficients in the multiple-solute results. The inverse relationship between k_2 and K_{ow} is consistent with k_2 versus K_d results involving natural sediments and organic solutes (Ball and Roberts, 1991; Brusseau and Rao, 1991; Karickhoff, 1984). Since BTEX diffusion coefficients

decrease and molecular size increases with increasing K_{ow} , k_2 of the more hydrophobic molecules may be limited by their larger molecular sizes and smaller diffusion coefficients.

F results from the multiple-solute and single-solute batch tests are presented in Figure 5. An inverse relationship is also observed between F and K_{ow} , and F decreased by 10 – 80% during the multiple-solute test.

Twelve additional multiple-solute experiments were run in order to determine concentration effects on the three nonequilibrium sorption parameters. The first set of four experiments contained a concentration of 0.05, 0.10, 0.20, or 0.30 mmol L⁻¹ for each of the five constituents (total BTEX concentrations of 0.25, 0.50, 1.00, or 1.50 mmol L⁻¹). Figure 6 shows the concentration effects on K_d . In agreement to the single-solute versus multiple-solute data, initial BTEX concentrations have minimal effects on the K_d of each constituent. Concentration effects on k_2 are presented in Figure 7. As initial aqueous BTEX concentrations increase in the batch systems, the kinetic rate coefficient decreases. Hu and Brusseau (1998) reported that k_2 increased with concentration in batch systems containing natural sediment and 2,4-dichlorophenoxyacetic acid. Since diffusive processes control rate-limited sorption, Hu and Brusseau suggested that increased concentration gradients would increase the rate of sorption. However, similar to our results, Gamerdinger et al. (1991) reported an inverse relationship between concentration and k_2 in batch experiments containing natural sediments and herbicides. Physical and/or chemical interactions between the constituents and the sorbent could cause the decrease in k_2 as concentration increases. Figure 8 shows concentration effects on F. According to the conceptual and numerical models, F should be independent of variations in initial

concentration. However, based on the multiple-solute results, F decreases as concentration increases. Because the determination of F is extremely sensitive to early-time data and a rapid partitioning process is present in the BTEX/SMZ system, these variations in F might be attributed to experimental limitations. Furthermore, a dependence of F on initial concentration is also seen in desorption processes and is not fully explained (Farrell and Reinhard, 1994; Grathwohl and Reinhard, 1993; Pignatello, 1990).

Eight additional multiple-solute batch experiments were run. Because benzene represents the first constituent to break through in transport experiments, the primary purpose of these eight tests was determining the sensitivity of benzene sorption kinetics to variations in individual BTEX constituent initial concentration. Benzene K_d results are seen in Figure 9. Similar to previous results, concentration variations of individual constituents do not significantly affect the K_d of benzene. Consequently, no individual constituent (i.e. toluene, *m*-xylene) is more influential on the benzene K_d than the other BTEX constituents. Figure 10 displays benzene k_2 results from these eight experiments. Increasing each constituent's concentration slightly lowered (<10%) the k_2 of benzene. Even though the benzene k_2 is affected by other constituent's initial concentration, it does not exhibit consistent sensitivity variations between individual constituents. Figure 11 presents the benzene F results from these experiments. An overall decrease in the F of benzene is observed as each constituent's concentration increases. The parabolic nature of the benzene F data is similar to the ethylbenzene, *m*-xylene, and *o*-xylene results seen in Figure 8. Similar to the k_2 results, no individual constituent consistently influences the F of benzene greater or less than any other constituent. Consequently, the k_2 and F

parameters of benzene, and the other BTEX constituents, are apparently affected by the total BTEX initial aqueous concentration.

Based upon the results from the multiple-solute, bilayer SMZ batch experiments, relationships between batch-determined nonequilibrium sorption parameters and total initial BTEX concentrations were developed (Table I). Since K_d does not vary significantly over the tested concentration ranges, Table I presents the average distribution coefficient for each constituent. Linear regressions accurately describe k_2 as a function of total concentration (r^2 greater than 0.89 for all constituents except toluene). Figure 12 shows the linear regression and the *m*-xylene multiple-solute batch test data. Since the slope of the linear regressions decreases with increasing hydrophobicity (Table I), concentration variations within batch systems have the greatest effect on the least hydrophobic constituent, benzene.

F shows a decreasing trend with increasing total BTEX concentrations from 0.2 to 1 mmol L⁻¹. However, when initial BTEX concentrations were greater than 1 mmol L⁻¹, an increasing F is observed with increasing concentration. As previously discussed, these variations in F might result from experimental (early-time sampling) limitations. The data was fit with a 2nd-order polynomial, with reasonable fits for all of the constituents (Table I). The polynomial fit of *m*-xylene to the multiple-solute batch test data is seen in Figure 13.

The relationships in Table I were used with Eqs. (7), (11), and (12) to calculate input parameters for the nonequilibrium transport model for various column conditions (Table II).

3.2. Monolayer Kinetic Batch Tests

A multiple-solute, monolayer batch test was replicated three times. The initial concentration of each BTEX compound was 0.1 mmol L^{-1} (total BTEX concentration of 0.5 mmol L^{-1}). The kinetic sorption results were compared to the identical bilayer, multiple-solute test in order to test our conceptual model, and amongst themselves to test each parameters sensitivity to the experimental procedure. According to the conceptual model, loading the zeolite to a complete surfactant monolayer should have minimal effects on K_d and k_2 , but should produce a significant increase in F .

Figure 14 shows that $\log K_d$ varies linearly with $\log K_{ow}$ for BTEX sorption on monolayer SMZ, with K_d values approximately 20% lower than the bilayer SMZ K_d values. The zeolite was loaded with 77 mmol kg^{-1} of surfactant for the monolayer experiments. Since the external CEC of the St. Cloud zeolite is $90 - 100 \text{ mmol kg}^{-1}$, approximately 80% monolayer coverage of the zeolite was achieved. Li and Bowman (1998) reported a linear decrease in K_d for perchloroethylene sorption by SMZ when surfactant loading was below full monolayer coverage; and a constant K_d above monolayer coverage. The average K_d values from the monolayer batch tests were divided by 0.8 and compared to the bilayer K_d results (Table III). In agreement to Li and Bowman's (1998) results, the adjusted monolayer K_d and bilayer K_d results are nearly identical.

Figure 15 shows the k_2 results from the monolayer and corresponding bilayer batch tests. An inverse relationship between k_2 and K_{ow} is also seen in the monolayer results, similar to the results for bilayer SMZ (see also Figure 4). Since the monolayer SMZ likely contains areas of patchy bilayer (Sullivan et al., 1998; Sullivan et al., 1997),

similar kinetic rate coefficients are expected between monolayer and bilayer results. The k_2 values for monolayer and bilayer systems are similar (Figure 15 and Table III).

The results for F from the monolayer and corresponding bilayer batch tests are presented in Figure 16. F decreases with $\log K_{ow}$ for both monolayer and bilayer SMZ. However, F increases from 0.03 – 0.16 for the bilayer system to 0.34 – 0.44 in the monolayer system (Table III). This ~3 to 11 fold increase in F is due to the significantly greater fraction of monolayer surfactant coverage, and the resultant higher proportion of the surface subject to instantaneous sorption.

Parameter sensitivity to the monolayer experimental procedure was also examined from the three replicate monolayer results. Table III presents the average nonequilibrium sorption parameter results and 95% confidence intervals (2σ) from the three replicate monolayer tests. A normal distribution was assumed for the 95% confidence intervals. The bilayer results in Table III present the 0.5 mmol L⁻¹ total BTEX multiple-solute batch test parameters. K_d shows strongly reproducible results based on the three replicate results; therefore, K_d is fairly insensitive to slight variations (e.g. time, temperature, human) in the experimental procedure. The 95% confidence intervals of F also indicate that reproducible F results are obtainable. According to Table III, k_2 represents the parameter with the most variability during the replicate monolayer tests. Furthermore, k_2 is also not applicable for the entire kinetic portion of the batch sorption data. For the single-solute results, a 25 – 35% decrease in k_2 was produced after applying the previously discussed modification to the k_2 fitting algorithm. Additionally, k_2 was sensitive to input parameter precision (e.g. initial concentration) for the bicontinuum model. Therefore, not only does k_2 show sensitivity to the experimental procedure, but it

is also sensitive to the data fitting algorithm and input parameters of the numerical model. Consequently, the variations in k_2 between the monolayer and bilayer tests (Figure 15) might result from k_2 imprecision (experimental shortcomings).

3.3. Column Experiments

Tritium transport experiments were run in order to obtain the dispersion coefficient for each column. Representative tritium results from column 2B are seen in Figure 17. CXTFIT version 2.1 (Toride et al., 1999) was used to inversely fit the 1-dimensional advection dispersion, physical equilibrium equation to the tritium breakthrough curve data:

$$R \frac{\partial C^*}{\partial p} = \frac{1}{P} \frac{\partial^2 C^*}{\partial X^2} - \frac{\partial C^*}{\partial X} \quad (13)$$

Flux-averaged effluent concentrations were assumed along with a 3rd-type upper boundary condition and a semi-infinite lower boundary condition. Three parameters were required for the inverse solution: v , R , and D . R and D were calculated from the model fit, while v was specified to the effluent discharge rate. The tritium modeling results and the column characteristics are seen in Table IV. The physical equilibrium model provides a very good fit to the tritium breakthrough data, with all six r^2 values greater than 0.988. Therefore, as seen in previous research (Altare et al., 2007), zones of immobile water (physical nonequilibrium) are not significant in the SMZ columns under these flow conditions.

Figure 18 shows the column 2B breakthrough curves of the BTEX compounds. The compounds break through the column in order of increasing hydrophobicity. The breakthrough curve (BTC) of each constituent was fit with chemical nonequilibrium and

equilibrium models, and the nonequilibrium model, with batch-determined input parameters (Table II), was used to predict BTEX transport. Figure 19 presents benzene effluent data from column 2B, along with the predicted nonequilibrium model and the inversely fit equilibrium and nonequilibrium models. Similar to previous research (Altare et al., 2007), the equilibrium fit model (v and D fixed; R fit) does not adequately describe benzene's early breakthrough and slow approach to complete breakthrough. The nonequilibrium prediction (v , D , R , β , and ω all fixed) also underestimates the time required for complete benzene breakthrough and over-predicts the amount of early-time breakthrough. The nonequilibrium model fit (v and D fixed; R , β , and ω fit) adequately describes the entire benzene BTC of column 2B. Consistent trends between the predicted versus fit models and equilibrium versus nonequilibrium models were observed for all six sets of benzene transport data.

An accurate prediction of the benzene BTC, especially early-time data, is vital because it elutes first from SMZ columns. Therefore, proper regeneration schemes (i.e. timing, length) depend on the early-time breakthrough of benzene. Even though the nonequilibrium model inadequately predicted benzene transport, it provides a conservative estimation of the benzene early-time breakthrough.

Figure 20 shows *m*-xylene transport data from column 2B and the nonequilibrium model prediction, and equilibrium and chemical nonequilibrium model fits. Similar to the benzene results (Figure 19), the equilibrium model does not fit the early-time breakthrough or extended tailing of *m*-xylene. The nonequilibrium prediction model vastly underestimates the time required for the entire *m*-xylene BTC. The

nonequilibrium model provides a good fit to *m*-xylene BTC data. Similar results were obtained for all of the BTEX compounds in the replicated column experiments.

A comparison of the averaged unknown parameters for the nonequilibrium fit and predicted models is seen in Table V. The Peclet number is identical for all scenarios (values provided in Table II). The fit parameters represent transport-determined values, while the predicted parameters represent batch-determined values. According to Table V, the constituents experienced greater retardation during the transport experiments than predicted from batch experiments. Equation (7) was used to calculate K_d values from the transport experiments. Similar to the batch results, the transport-determined K_d values were not concentration dependent and $\log K_d$ was linearly related to $\log K_{ow}$.

The transport-determined K_d values are 1.5 – 3.75 times greater than the batch-determined values. Ranck (2003) reported a similar relationship between batch and column K_d for BTEX sorption on SMZ. Since batch-determined distribution coefficients are typically greater than transport-determined distribution coefficients (Maraqa, 2001 and references therein), a BTEX/SMZ-specific process is producing anomalous results. HDTMA is released from the SMZ when exposed to aqueous solutions (Li et al., 2003). Micellar surfactant solutions are known to increase BTEX solubility (surfactant-enhanced remediation); consequently, HDTMA monomers could also produce an increase in BTEX solubility. In column systems, the surfactant wash-off is constantly flushed from the column; however, a static aqueous phase is present in batch systems. Therefore, higher concentrations of surfactant monomers present in batch systems might increase BTEX solubility and produce lower K_d values for the batch system than the column system.

The Damkohler number (ω) is 2 – 4 times greater for the batch-determined values than the transport-determined values. Since ω represents the residence time divided by the characteristic sorption time, it is inversely proportional to the magnitude of nonequilibrium processes present in contaminant transport systems. According to the transport-determined ω , the magnitude of chemical nonequilibrium is greater in the SMZ columns that predicted by the batch-determined values. The transport-determined k_2 of each constituent was calculated by Eqs. (7), (11), and (12). Transport-determined k_2 values range from 0.2 to 1.56 hr^{-1} , while batch-determined values range from 1.87 to 9.27 hr^{-1} . Similar to the batch results, the transport-determined rate coefficients are constituent dependent (Figure 21). The batch-experiment k_2 results appear to have greater initial concentration sensitivity than transport-experiment results.

Table V also reveals that the batch-determined values for the fraction of instantaneous retardation (β) are 0.2 – 0.7 times the transport-determined values. Equations (7) and (11) were utilized to calculate F; and F ranged from 0.2 to 0.4 for all constituents based on transport experiments, but ranged from 0.02 to 0.2 based on batch experiments. Figure 22 also shows that, contrary to batch results, F determined in transport experiments is relatively insensitive to total BTEX concentrations.

The limitations of individual input parameters on the nonequilibrium model prediction were also investigated. One input parameter (R , β , or ω) was inversely fit to benzene and *m*-xylene transport data while the other two input parameters were fixed with the values determined from the batch experiments. The various model fits to column 2B BTC data of benzene are seen in Figure 23. When β was inversely fit to the transport data (R and ω fixed with batch-determined values), the nonequilibrium model

still underestimated the time for early-time and full breakthrough of benzene. Similar results are seen when ω was inversely fit to the transport data. However, when R was inversely fit to the data (β and ω fixed with batch-determined values), the model adequately described the benzene BTC ($r^2 = 0.990$). Therefore, R is constraining the prediction capabilities of the nonequilibrium transport model, which is relatively insensitive to the values of β and ω in our system. Allowing both β and ω to vary while R was fixed with the batch-determined value did not improve the model's fit (Figure 23).

Figure 24 presents the various models fit inversely to *m*-xylene column 2B transport data. When β or ω (or both together) are fit inversely to the data (R fixed to batch-determined value), the nonequilibrium model immensely underestimates the time for early-time and full breakthrough of *m*-xylene. However, the model describes the *m*-xylene BTC reasonably well when β and ω are fixed but R is inversely fit ($r^2 = 0.929$). These results suggest that the β and ω values obtained from the batch experiments could provide acceptable predictions to BTEX transport data (with varying initial concentrations) if a better understanding of the transport K_d of each solute was obtained.

4. CONCLUSIONS

The first-order bicontinuum model accurately described the sorption process in kinetic batch experiments containing SMZ and volatile hydrocarbons (specifically BTEX). The K_d of each solute did not show competition effects between single-solute and multiple-solute batch experiments. However, a 5 – 35% decrease in k_2 occurred during the multiple-solute test. F also decreased during the multiple-solute test. Chemical or physical interaction or competition could possibly explain the decrease in k_2 ; however, F should not decrease based on the conceptual and numerical models. Because BTEX partitioning into SMZ is a rapid process, experimental limitations on early-time sampling might cause the variations in F . Additional batch results show an inverse relationship between k_2 or F and the initial total BTEX concentration over the studied concentration ranges. The K_d of each constituent was not affected by solute competition or concentration variations.

According to the conceptual model, BTEX molecules instantaneously sorb within portions of the SMZ covered by a surfactant monolayer, while bilayer surfactant patches kinetically limit BTEX sorption. The monolayer SMZ kinetic batch-test results were in agreement with the conceptual model. The monolayer K_d results, adjusted for partial coverage, agreed very well with the bilayer K_d results. The kinetic rate coefficient was expected to remain constant in both systems, and only minor variations between the monolayer and bilayer k_2 results were observed. Finally, the significant increase (3 to 10 times) in F seen in the monolayer tests was expected because of the increase in the fraction of surface covered by a monolayer of surfactant.

Because the equilibrium model does not accurately fit the BTEX breakthrough data, nonequilibrium processes are present during BTEX transport through the SMZ columns. The nonequilibrium transport model accurately fit transport data for all BTEX constituents when R , β , and ω were allowed to vary. The nonequilibrium transport model, using batch-determined parameters to calculate R , β , and ω , was unable to accurately predict BTEX breakthrough curves through SMZ columns. Complete effluent breakthrough time of each constituent was significantly underestimated with the model prediction. In addition, prediction accuracy decreased with increasing constituent hydrophobicity.

Investigation of each input parameter for the nonequilibrium prediction revealed the value used for R controlled the prediction capability of the nonequilibrium transport model. Adequate BTC predictions for benzene and *m*-xylene were obtained when using β and ω derived from the batch tests and simply adjusting R . A more accurate estimation of the BTEX distribution coefficients in transport systems would significantly improve the prediction of BTEX transport through SMZ columns.

5. RECOMMENDATIONS FOR FUTURE WORK

Since surfactant wash-off likely causes the variation between distribution coefficients in batch and transport systems, future research needs to determine the effect of aqueous-phase surfactant concentrations on BTEX sorption/solubility. BTEX solubility experiments, with varying surfactant concentrations, should be run in order to qualitatively test this hypothesis. Octanol-water partition tests, with surfactant-containing and surfactant-free water, should also be conducted in order to quantitatively determine surfactant wash-off effects on BTEX sorption. For the surfactant-containing water, bilayer and monolayer SMZ batch experiments (without BTEX included) should be initially completed. Aqueous samples should be taken after 90 minutes of shaking and used for the surfactant-containing water in the octanol-water partition tests. Surfactant wash-off might also affect the BTEX chromatographic analysis. Consequently, chromatographic analysis should be conducted with a constant BTEX aqueous concentration but varying surfactant concentrations.

BTEX distribution coefficients in dynamic systems should also be determined. Recirculation column experiments (similar to “circulation-through” experiments in Maraqa, 2001) should be conducted to complete BTEX breakthrough. Since the BTEX-laden water recirculates through the SMZ column in these experiments, aqueous-phase surfactant conditions in these transport experiments should be similar to batch experiment conditions. Distribution coefficients should be calculated when full BTEX breakthrough conditions are reached to determine if batch-determined K_d values can be replicated in the recirculation dynamic experiments. Flow-through column experiments should also be

conducted in order to improve the prediction capabilities of the nonequilibrium transport model. Step-input column experiments should be run to complete BTEX breakthrough. The column effluent should be collected, and an effluent sample should be taken after full BTEX breakthrough is achieved. The flow-through, transport-determined K_d values should be coupled with the batch-determined F and k_2 values in order to parameterize the nonequilibrium transport prediction model. These experiments would likely determine the role of surfactant wash-off in our systems and improve the prediction capabilities of our nonequilibrium transport model.

ACKNOWLEDGEMENTS

This work was funded by the Department of Energy under contract number DE-PS26-04NT15546 to the University of Texas at Austin. We would like to thank Kerry A. Kinney and Lynn E. Katz from the University of Texas at Austin and Enid J. Sullivan from Los Alamos National Lab for ongoing SMZ/produced water collaboration. Special thanks go to Thomas Kieft of New Mexico Tech for use of the liquid scintillation counter and Tianguang Fan of the Petroleum Recovery Research Center for completing the electrophoretic mobility analyses. Craig Altare and Jaron Andrews provided insight and assistance in the laboratory.

REFERENCES

- Altare, C.R., Bowman, R.S., Katz, L.E., Kinney, K.A. and Sullivan, E.J., 2007. Regeneration and long-term stability of surfactant-modified zeolite for removal of volatile organic compounds from produced water. *Microporous and Mesoporous Materials*, 105(No. 3): 305-316.
- API, 2000. Overview of exploration and production waste volumes and waste management practices in the United States. American Petroleum Institute, Washington, D.C.
- API, 2002. Predictors of water-soluble organics (WSOs) in produced water - a literature review. American Petroleum Institute. Washington, D.C.
- Ball, W.P. and Roberts, P.V., 1991. Long-Term Sorption of Halogenated Organic Chemicals by Aquifer Material. 2. Intraparticle Diffusion. *Environmental Science and Technology*, 25(No. 7): 1237-1249.
- Bowman, R.S., Haggerty, G.M., Huddleston, R.G., Neel, D., and Flynn, M.M., 1995. "Sorption of nonpolar organic compounds, inorganic cations, and inorganic oxyanions by surfactant-modified zeolites." *Surfactant-enhanced subsurface remediation*. D.A. Sabatini, R.C. Knox, and J.H. Harwell, eds., American Chemical Society, Washington DC, pp. 54-64
- Bowman, R.S., Li Z., Roy S.J., Burt T., Johnson T.L., Johnson R.L., 2001. "Pilot test of a surfactant-modified zeolite permeable barrier for groundwater remediation." *Physicochemical groundwater remediation*. Kluwer Academic/Plenum Publishers, New York, New York, pp. 161-185
- Bowman, R.S., Sullivan, E.J. and Li, Z., 2000. "Uptake of cations, anions, and nonpolar organic molecules by surfactant-modified clinoptilolite-rich tuff." *Natural zeolites for the third millennium*. De Frede Editore, Napoli, Italy, pp. 287-297
- Brusseau, M.L. and Rao, P.S.C., 1989. Sorption nonideality during organic contaminant transport in porous media. *Critical Reviews in Environmental Control*, 19(1): 33-99.
- Brusseau, M.L. and Rao, P.S.C., 1991. Influence of sorbate structure on nonequilibrium sorption of organic compounds. *Environmental Science & Technology*, 25(No. 8): 1501-1506.
- Connaughton, D.F., Stedinger, J.R., Lion, L.W. and Shuler, M.L., 1993. Description of time-varying desorption kinetics: releases of naphthalene from contaminated soils. *Environmental Science & Technology*, 27(No. 12): 2397-2403.

- EPA, U., 2003. National primary drinking water standards. In: Office of Water. US Environmental Protection Agency. Washington, D.C.
- Farrell, J. and Reinhard, M., 1994. Desorption of halogenated organics from model soils, sediments, and soil under unsaturated conditions. 2. Kinetics. *Environmental Science & Technology*, 28(No. 1): 63-72.
- Fuierer, A.M., 2001. Microbial degradation of toluene sorbed to surfactant-modified zeolite, unpublished M.S. Thesis, New Mexico Institute of Mining and Technology, Socorro, 113 pp.
- Gamerding, A.P., Lemley, A.T. and Wagenet, R.J., 1991. Nonequilibrium sorption and degradation of three 2-chloro-s-triazine herbicides in soil-water systems. *Journal of Environmental Quality*, 20: 815-822.
- Grathwohl, P. and Reinhard, M., 1993. Desorption of trichloroethylene in aquifer material: rate limitation at the grain scale. *Environmental Science & Technology*, 27(No. 12): 2360-2366.
- Harmon, T.C. and Roberts, P.V., 1994. Comparison of intraparticle sorption and desorption rates for a halogenated alkene in a sandy aquifer material. *Environmental Science & Technology*, 28(No. 9): 1650-1660.
- Hu, M.X. and Brusseau, M.L., 1998. Coupled effects of nonlinear, rate-limited sorption and biodegradation on transport of 2,4-dichlorophenoxyacetic acid in soil. *Environmental Toxicology and Chemistry*, 17(Number 9): 1673-1680.
- Huddleston, R.G., 1990. Surface-altered hydrophobic zeolites as sorbents for hazardous organic compounds, unpublished M.S. Independent Study, New Mexico Institute of Mining and Technology, Socorro, New Mexico.
- Karickhoff, S.W., 1984. Organic Pollutant Sorption in Aquatic Systems. *Journal of Hydraulic Engineering*, Volume 110(Number 6): 707-735.
- Katz, L.E., Kinney, K.A., Bowman, R.S., Sullivan, E.J., Kwon, S., Darby, E.B., Chen, L.J., Altare, C.R., 2006. Treatment of produced waters using a surfactant modified zeolite/vapor phase bioreactor system. Final DOE Technical Report: DE-FC26-02NT15461
- Kolb, B. and Ettre, L., 1997. Static headspace-gas chromatography: theory and practice. Wiley-VCH. New York, New York. 376 pp.
- Larsen, T., Christensen, T.H. and Brusseau, M., 1992. Predicting Nonequilibrium Transport of Naphthalene Through Aquifer Materials Using Batch Determined Sorption Parameters. *Chemosphere*, 24(No. 2): 141-153.

- Li, Z. and Bowman, R.S., 1997. Counterion effects on the sorption of cationic surfactant and chromate on natural clinoptilolite. *Environmental Science & Technology*, 31(Number 8): 2407-2412.
- Li, Z. and Bowman, R.S., 1998. Sorption of perchloroethylene by surfactant-modified zeolite as controlled by surface loading. *Environmental Science & Technology*, 32(15): 2278-2282.
- Li, Z., Willms, C., Roy, S., and Bowman R.S, 2003. Desorption of hexadecyltrimethylammonium from charged mineral surfaces. *Environmental Geosciences*, 10(No. 1): 37-45
- Maraqqa, M.A., 2001. Effects of fundamental differences between batch and miscible displacement techniques on sorption distribution coefficient. *Environmental Geology*, 41: 219-228.
- Neel, D., 1992. Quantification of BTX sorption to surface-altered zeolites, unpublished M.S. Thesis, New Mexico Institute of Mining and Technology, Socorro, NM, 88 pp.
- Pignatello, J.J., 1990. Slowly reversible sorption of aliphatic halocarbons in soils. II. Mechanistic aspects. *Environmental Toxicology and Chemistry*, 9: 1117-1126.
- Pignatello, J.J. and Xing, B., 1996. Mechanisms of slow sorption of organic chemicals to natural particles. *Environmental Science & Technology*, 30(1): 1-11.
- Ranck, J.M., 2003. BTEX removal from produced water using surfactant-modified zeolite, unpublished M.S. Thesis, New Mexico Institute of Mining and Technology, Socorro, NM, 181 pp.
- Ranck, J.M., Bowman, R.S., Weeber, J.L., Katz, L.E. and Sullivan, E.J., 2005. BTEX removal from produced water using surfactant-modified zeolite. *Journal of Environmental Engineering*, 131(No. 3): 434-442.
- Selim, H.M., Davidson, J.M. and Mansell, R.S., 1976. Evaluation of a two-site adsorption-desorption model for describing solute transport in soils, Proc. Summer Computer Simulation Conference, Washington D.C., pp. 444-448.
- Sirivedhin, T. and Dallbauman, L., 2004. Organic matrix in produced water from the Osage-Skiatook Petroleum Environmental Research site, Osage county, Oklahoma. *Chemosphere*, 57: 463-469.
- Stephenson, M.T., 1992. Components of produced water - a compilation of industry studies. *Journal of Petroleum Technology*, 44(No. 5): 548-603.

Sullivan, E., Carey, J. and Bowman, R., 1998. Thermodynamics of cationic surfactant sorption onto natural clinoptilolite. *Journal of Colloid and Interface Science*, 206(No. 2): 369-380.

Sullivan, E.J., Hunter, D.B. and Bowman, R.S., 1997. Topological and thermal properties of surfactant-modified clinoptilolite studied by tapping-mode atomic force microscopy and high-resolution thermogravimetric analysis. *Clays and Clay Minerals*, 45(No. 1): 42-53.

Toride, N., Leij, F.J. and van Genuchten, M.T., 1999. The CXTFIT code for estimating transport parameters from laboratory or field tracer experiments, Version 2.1. Research Report No. 137, US Salinity Laboratory, Agricultural Research Service, U.S. Department of Agriculture; Riverside, California.

Table I. Batch-determined nonequilibrium sorption parameter relationships used to parameterize the nonequilibrium transport model. Standard deviation for K_d is in parentheses.

Constituent	K_d (L/kg)	k_2 (hr ⁻¹)		F	
		Linear Regression	r^2	Polynomial Regression	r^2
Benzene	7.5 (0.23)	-2.14(C _o)+9.71	0.88	0.058(C _o) ² -0.158(C _o)+0.234	0.29
Toluene	17.7 (0.39)	-1.59(C _o)+5.77	0.59	0.068(C _o) ² -0.154(C _o)+0.147	0.64
Ethylbenzene	35.2 (0.53)	-1.36(C _o)+3.96	0.89	0.085(C _o) ² -0.160(C _o)+0.103	0.76
M-Xylene	37.4 (0.54)	-1.37(C _o)+3.74	0.92	0.108(C _o) ² -0.196(C _o)+0.102	0.96
O-Xylene	34.4 (0.58)	-1.25(C _o)+3.76	0.89	0.083(C _o) ² -0.159(C _o)+0.103	0.86

Table II. Input parameters used to predict nonequilibrium BTEX transport.

Column	Total BTEX C _o (mmol L ⁻¹)	P	Constituent	R	β	ω
1A	0.62	11.3	Benzene	11.7	0.23	5.2
			Toluene	26.3	0.11	7.8
			Ethylbenzene	51.4	0.06	10.5
			M-xylene	54.6	0.04	10.5
			O-xylene	50.3	0.06	9.8
1B	0.59	10.7	Benzene	12.3	0.23	5.7
			Toluene	27.7	0.11	8.4
			Ethylbenzene	54.1	0.06	11.5
			M-xylene	57.5	0.04	11.5
			O-xylene	52.9	0.06	10.7
2A	0.93	13.3	Benzene	12.5	0.21	5.3
			Toluene	28.2	0.10	7.6
			Ethylbenzene	55.0	0.05	9.9
			M-xylene	58.5	0.03	9.8
			O-xylene	53.9	0.05	9.3
2B	0.89	11.9	Benzene	13.0	0.21	5.3
			Toluene	29.5	0.10	7.7
			Ethylbenzene	57.7	0.05	10.0
			M-xylene	61.3	0.03	9.9
			O-xylene	56.5	0.04	9.5
3A	0.78	6.7	Benzene	12.2	0.22	5.4
			Toluene	27.6	0.10	7.9
			Ethylbenzene	54.0	0.05	10.4
			M-xylene	57.3	0.03	10.4
			O-xylene	52.8	0.05	9.8
3B	0.71	8.1	Benzene	12.0	0.22	5.2
			Toluene	27.2	0.11	7.6
			Ethylbenzene	53.0	0.05	10.2
			M-xylene	56.3	0.04	10.2
			O-xylene	51.9	0.05	9.6

Table III. Monolayer versus bilayer SMZ batch experiment results. For monolayer results, average values are reported with 95% confidence intervals. The multiple-solute, bilayer SMZ experiment with total BTEX C_0 equaling 0.5 mmol L^{-1} represents the bilayer results.

Constituent	$K_d \text{ (L kg}^{-1}\text{)}$		$k_2 \text{ (hr}^{-1}\text{)}$		F	
	Monolayer ¹	Bilayer	Monolayer	Bilayer	Monolayer	Bilayer
Benzene	7.3 ± 1.0	7.3	5.74 ± 1.2	8.52	0.42 ± 0.05	0.16
Toluene	16.8 ± 1.0	17.5	4.50 ± 1.0	4.96	0.37 ± 0.03	0.09
Ethylbenzene	34.1 ± 1.9	34.7	4.35 ± 1.2	3.4	0.35 ± 0.03	0.04
M-Xylene	36.2 ± 2.0	37.3	4.26 ± 0.8	2.95	0.34 ± 0.03	0.03
O-Xylene	32.5 ± 1.9	34.4	4.30 ± 1.2	3.19	0.35 ± 0.03	0.04

¹ Experimental monolayer K_d values divided by 0.8 to account for ~80% monolayer coverage (see text).

Table IV. Column characteristics and tritium results from the column experiments.

Column	Column Characteristics				Tritium Results			
	Velocity (cm/min)	Mass Zeolite (g)	Porosity (Vv/Vt)	Bulk Density (g/cm ³)	R	D (cm ² /min)	P (vL/D)	Equil. Fit (r ²)
1A	2.65	47.13	61.0%	0.873	1.17	2.57	11.32	0.996
1B	2.62	50.52	60.9%	0.936	1.15	2.75	10.69	0.989
2A	2.62	50.59	61.0%	0.937	1.1	2.17	13.29	0.988
2B	2.77	49.56	57.0%	0.918	1.15	2.56	11.9	0.999
3A	2.63	48.9	60.2%	0.906	1.17	4.32	6.69	0.988
3B	2.67	47.15	60.2%	0.873	1.2	3.55	8.11	0.991

Table V. Nonequilibrium parameters from predicted model (predicted) and fit model (fit). Table presents average values over the six column runs with standard deviations in parentheses.

Constituent	R		β		ω	
	Predicted	Fit	Predicted	Fit	Predicted	Fit
Benzene	12.29 (0.45)	18.22 (1.64)	0.22 (0.01)	0.31 (0.05)	5.36 (0.17)	2.58 (0.69)
Toluene	27.76 (1.06)	58.27 (10.35)	0.10 (0.01)	0.40 (0.11)	7.83 (0.31)	1.60 (0.81)
Ethylbenzene	54.21 (2.11)	199.00 (23.48)	0.05 (0.01)	0.22 (0.09)	10.41 (0.56)	3.36 (1.10)
M-Xylene	57.58 (2.24)	212.83 (24.30)	0.03 (0.01)	0.23 (0.09)	10.37 (0.61)	3.70 (2.08)
O-Xylene	53.05 (2.06)	187.20 (28.39)	0.05 (0.01)	0.22 (0.05)	9.78 (0.50)	3.28 (0.65)

FIGURE CAPTIONS

- Figure 1. Conceptual model of benzene partitioning into surfactant-modified zeolite's hydrophobic tail group.
- Figure 2. Kinetics of ethylbenzene sorption to bilayer SMZ. A) ethylbenzene alone (single solute), B) ethylbenzene with equal concentrations of benzene, toluene, *o*-xylene, and *p*-xylene (multiple solute).
- Figure 3. Relationship between $\log K_d$ and $\log K_{ow}$ for BTEX compounds in single-solute and 1.0 mmol L^{-1} total BTEX multiple-solute batch experiments.
- Figure 4. Relationships between $\log k_2$ and $\log K_d$ for BTEX compounds in single-solute and 1.0 mmol L^{-1} total BTEX multiple-solute batch experiments.
- Figure 5. Relationship between F and K_{ow} for BTEX compounds in single-solute and 1.0 mmol L^{-1} total BTEX multiple-solute batch experiments.
- Figure 6. Initial concentration effects on BTEX constituent distribution coefficients when all constituents have similar initial aqueous concentrations.
- Figure 7. Initial concentration effects on BTEX constituent rate coefficients when all constituents have similar initial aqueous concentrations.
- Figure 8. Initial concentration effects on the F of BTEX constituents when all constituents have similar initial aqueous concentrations.
- Figure 9. Concentration effects of individual BTEX constituents on the benzene K_d . The initial concentration of benzene was 0.2 mmol L^{-1} for all experiments.
- Figure 10. Concentration effects of individual BTEX constituents on the benzene k_2 . The initial concentration of benzene was 0.2 mmol L^{-1} for all experiments.
- Figure 11. Concentration effects of individual constituents on the benzene F . The initial concentration of benzene was 0.2 mmol L^{-1} for all experiments.
- Figure 12. *m*-Xylene kinetic batch-experiment k_2 data fit with a linear regression.
- Figure 13. *m*-Xylene kinetic batch-experiment F data fit with a polynomial trend line.
- Figure 14. K_d results from three replicate monolayer and corresponding bilayer SMZ batch experiments.
- Figure 15. Results for k_2 from three replicate monolayer and corresponding bilayer SMZ batch experiments.

- Figure 16. F results from three replicate monolayer and corresponding bilayer SMZ batch experiments.
- Figure 17. Tritium breakthrough curve for column 2B fitted with the physical equilibrium, 1-D advection-dispersion model.
- Figure 18. BTEX breakthrough curves for Column 2B.
- Figure 19. Benzene Column 2B data with nonequilibrium model prediction and equilibrium and nonequilibrium model fits.
- Figure 20. *m*-Xylene Column 2B data with nonequilibrium model prediction and equilibrium and nonequilibrium model fits.
- Figure 21. The k_2 calculated from the nonequilibrium model having R , β , and ω inversely fit, termed transport-determined values.
- Figure 22. F calculated from the nonequilibrium model having R , β , and ω inversely fit, termed transport-determined values.
- Figure 23. Nonequilibrium prediction model's individual parameter fits to Column 2B benzene data.
- Figure 24. Nonequilibrium prediction model's individual parameter fits to Column 2B *m*-xylene data.

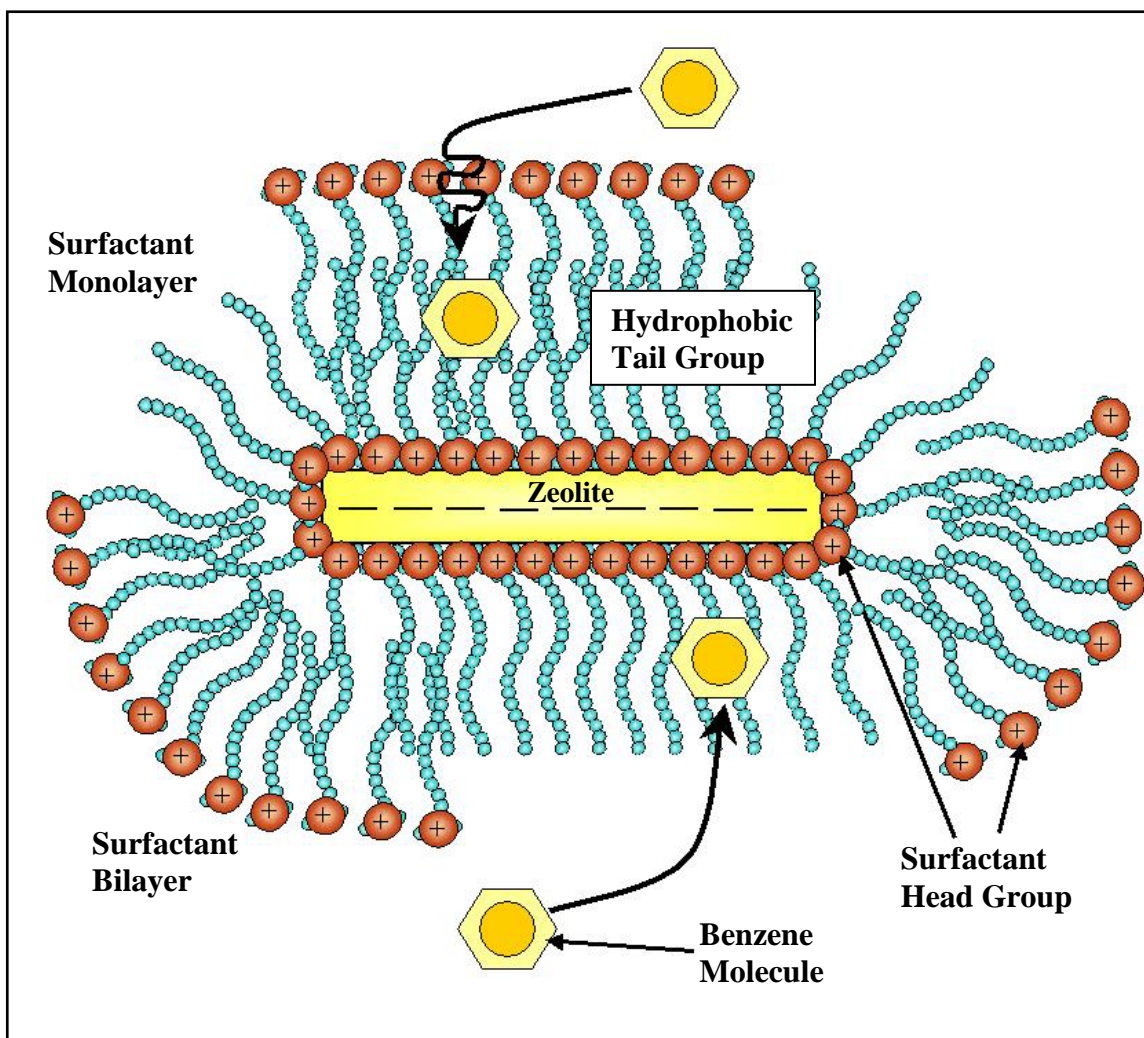


Figure 1. Conceptual model of benzene partitioning into surfactant-modified zeolite's hydrophobic tail group.

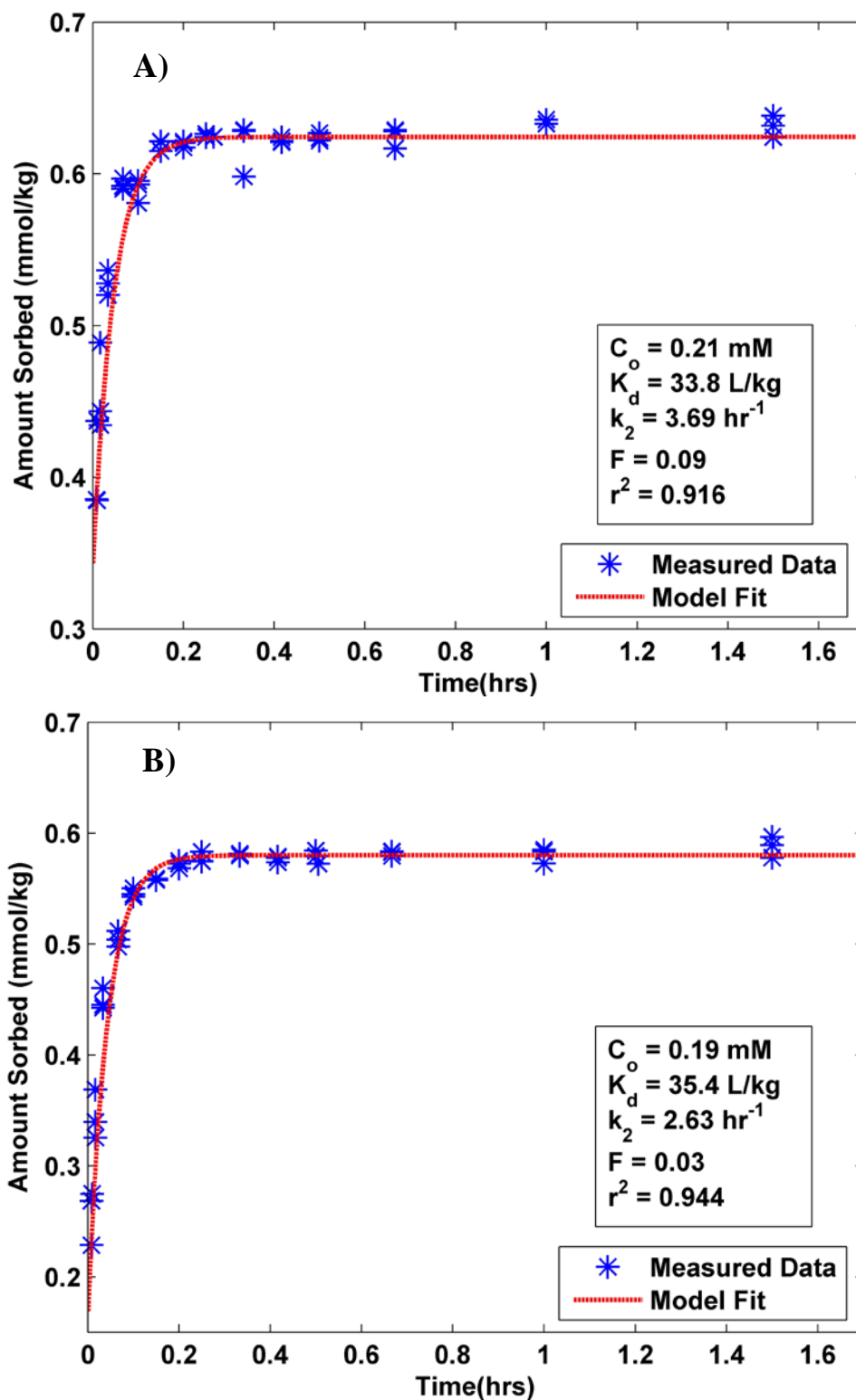


Figure 2. Kinetics of ethylbenzene sorption to bilayer SMZ. A) ethylbenzene alone (single solute), B) ethylbenzene with equal concentrations of benzene, toluene, *o*-xylene, and *p*-xylene (multiple solute).

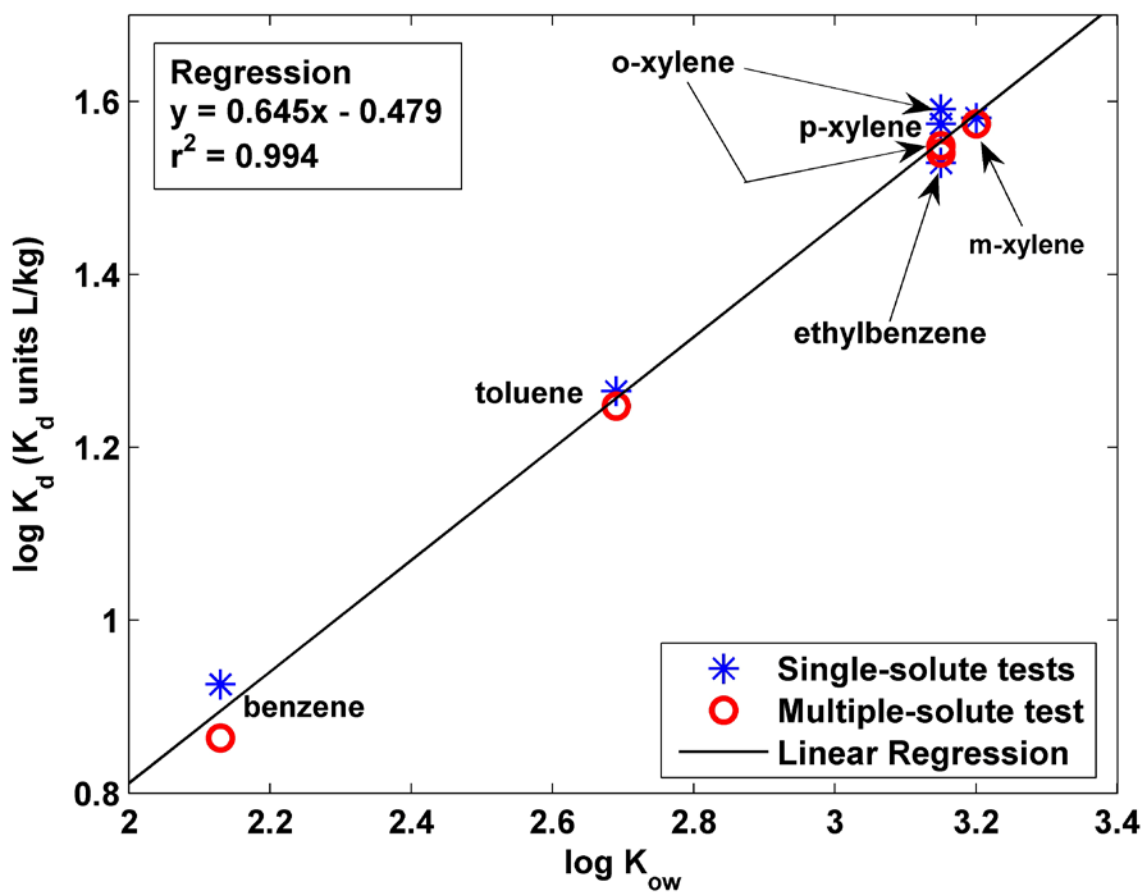


Figure 3. Relationship between $\log K_d$ and $\log K_{ow}$ for BTEX compounds in single-solute and 1.0 mmol L^{-1} total BTEX multiple-solute batch experiments.

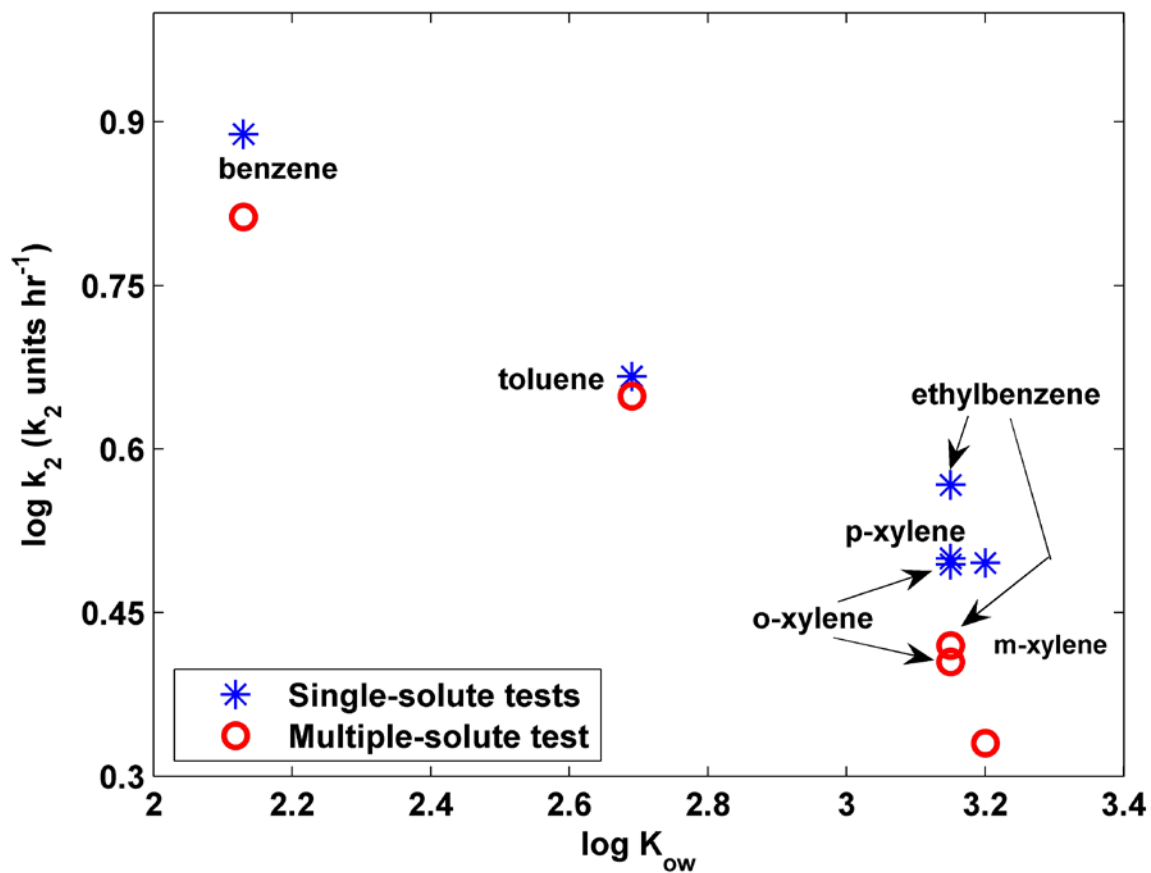


Figure 4. Relationships between $\log k_2$ and $\log K_d$ for BTEX compounds in single-solute and 1.0 mmol L^{-1} total BTEX multiple-solute batch experiments.

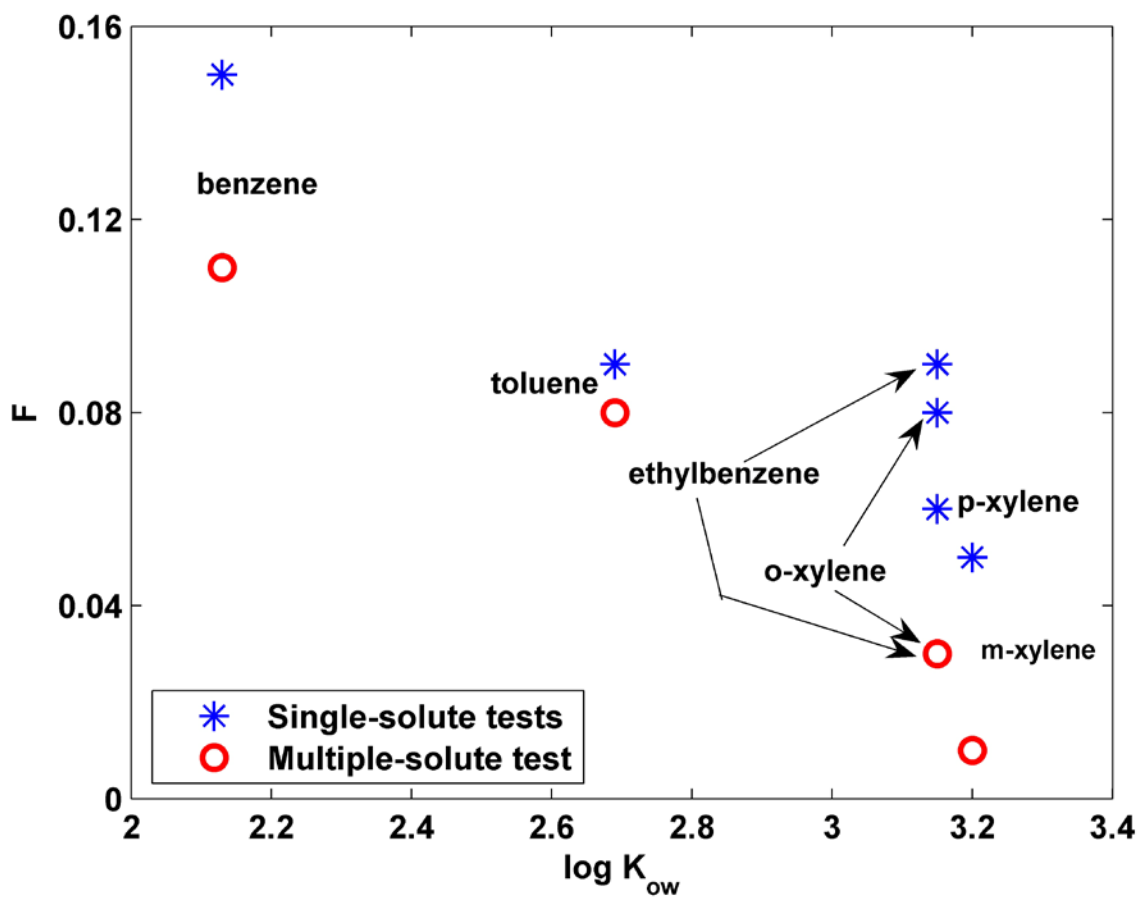


Figure 5. Relationship between F and K_{ow} for BTEX compounds in single-solute and 1.0 mmol L^{-1} total BTEX multiple-solute batch experiments.

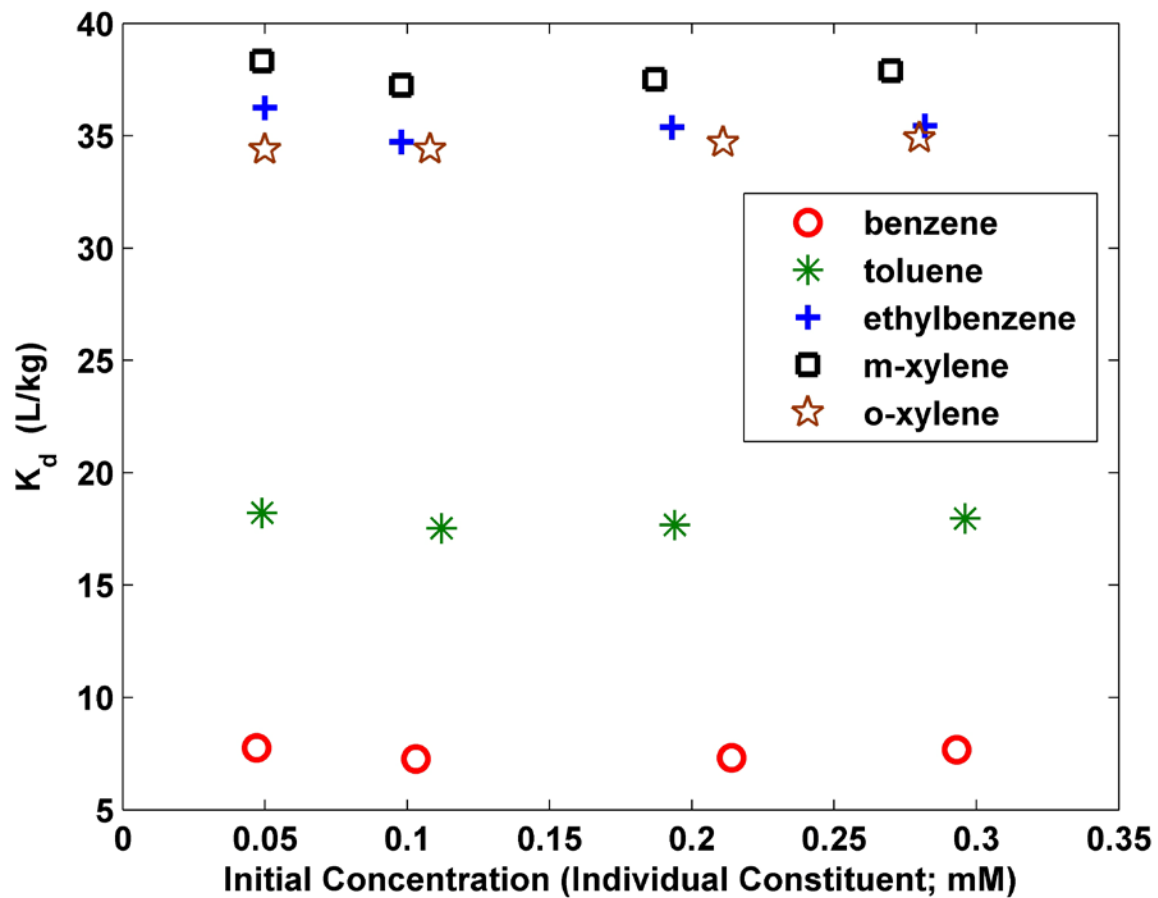


Figure 6. Initial concentration effects on BTEX constituent distribution coefficients when all constituents have similar initial aqueous concentrations.

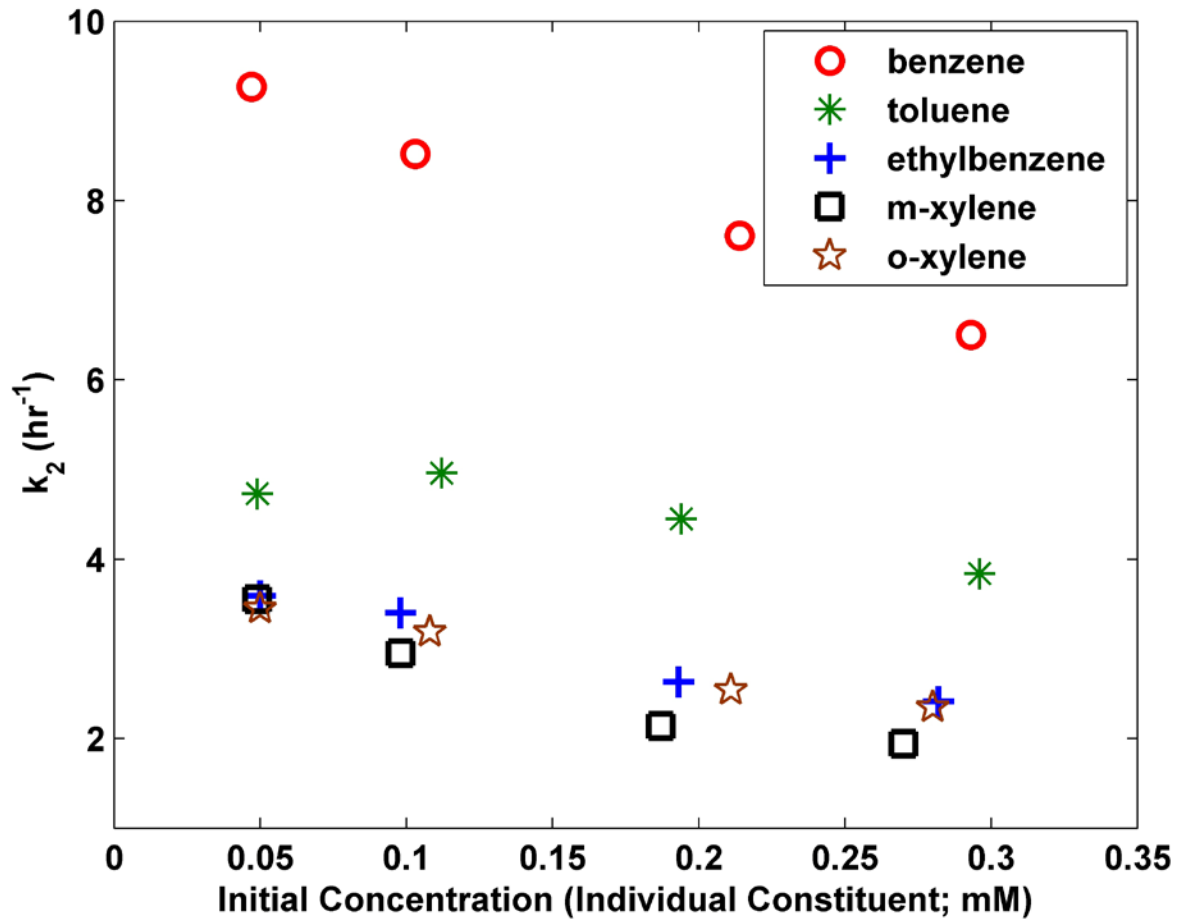


Figure 7. Initial concentration effects on BTEX constituent rate coefficients when all constituents have similar initial aqueous concentrations.

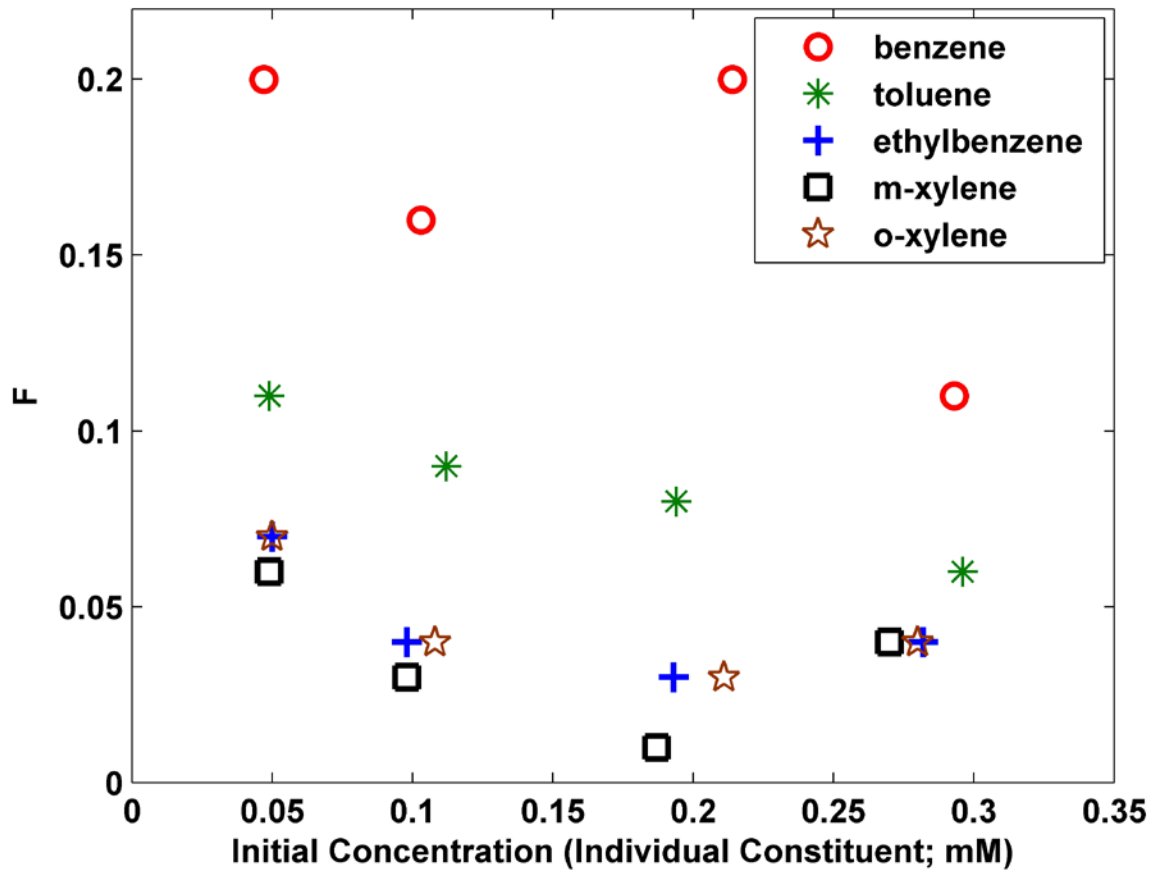


Figure 8. Initial concentration effects on the F of BTEX constituents when all constituents have similar initial aqueous concentrations.

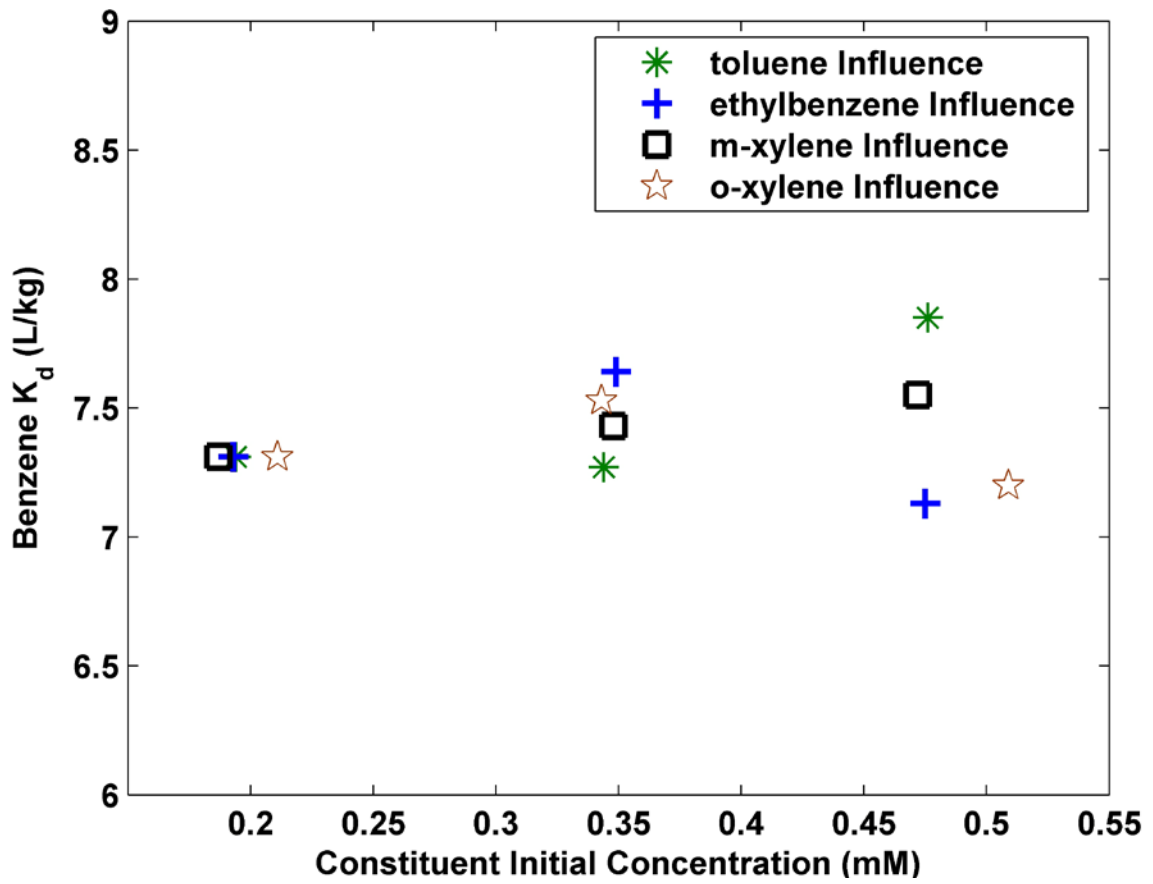


Figure 9. Concentration effects of individual BTEX constituents on the benzene K_d . The initial concentration of benzene was 0.2 mmol L^{-1} for all experiments.

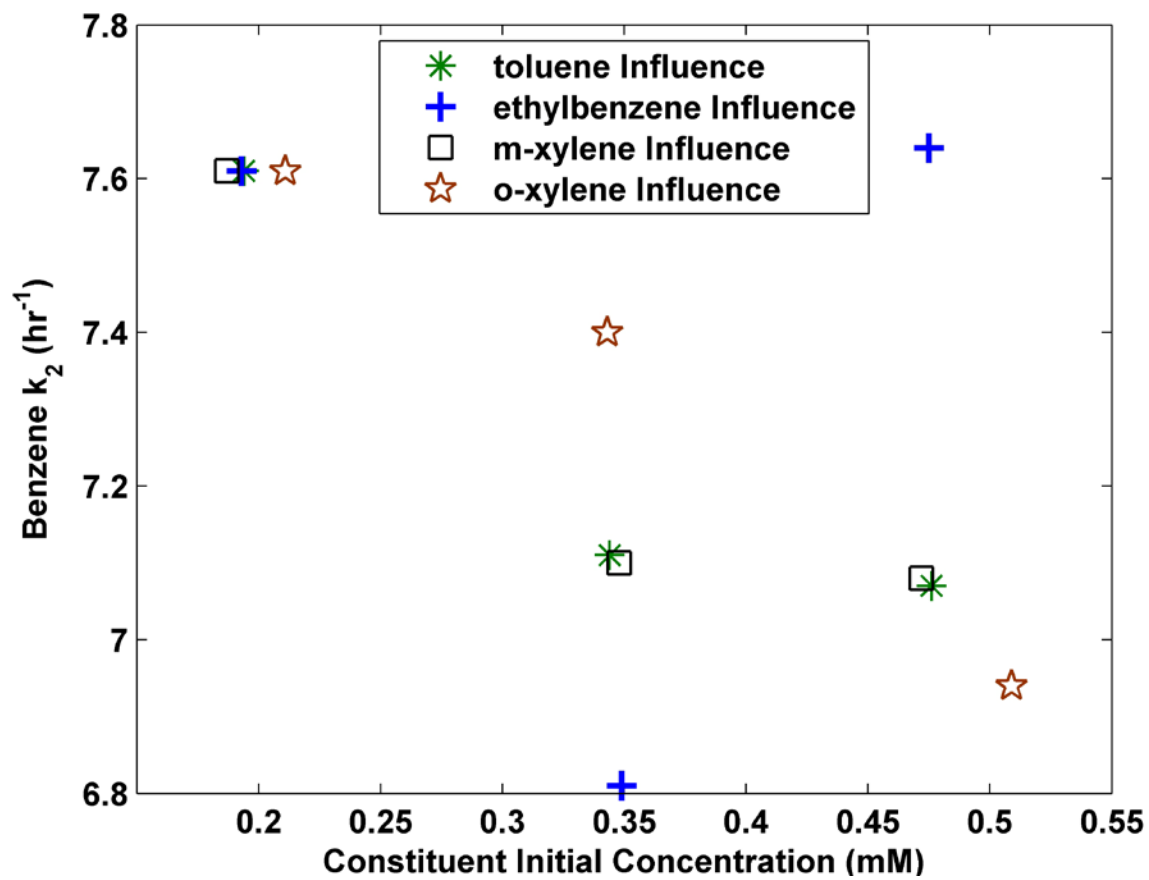


Figure 10. Concentration effects of individual BTEX constituents on the benzene k_2 . The initial concentration of benzene was 0.2 mmol L^{-1} for all experiments.

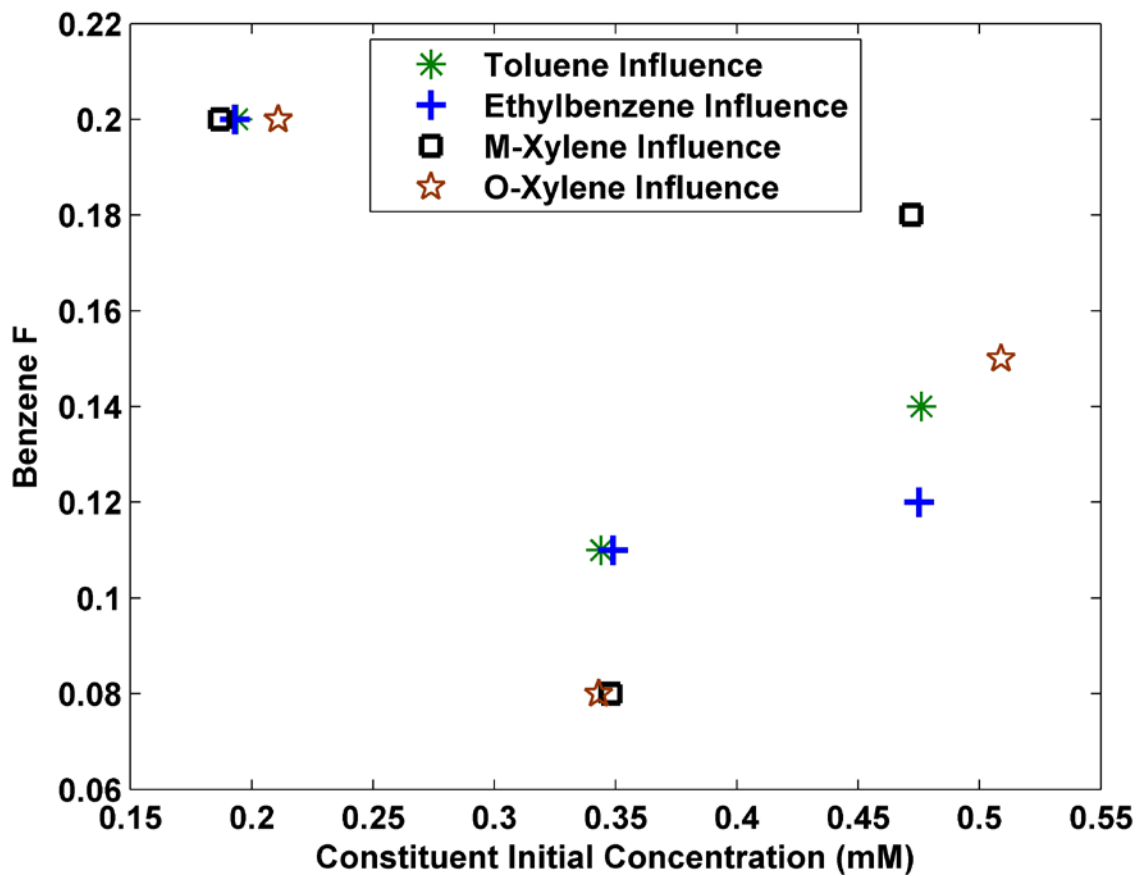


Figure 11. Concentration effects of individual constituents on the benzene F. The initial concentration of benzene was 0.2 mmol L^{-1} for all experiments.

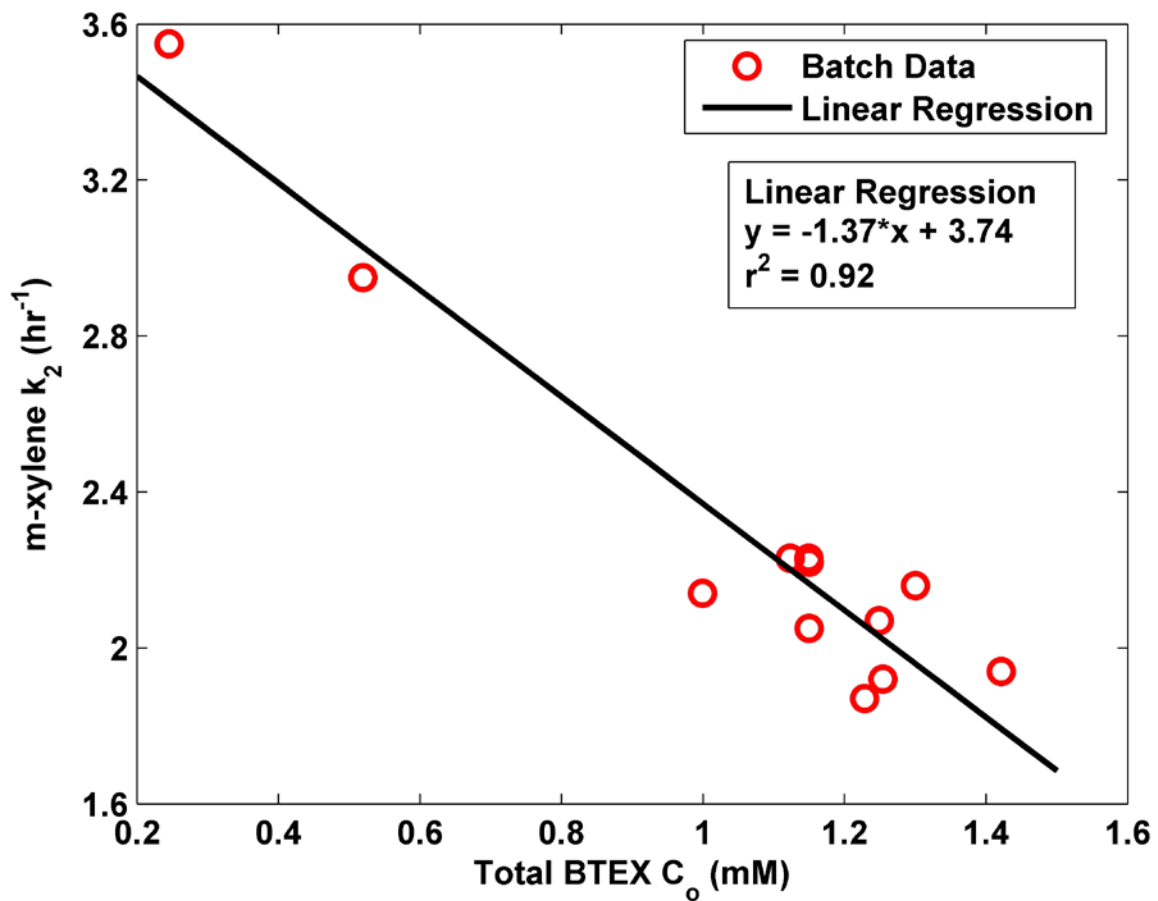


Figure 12. *m*-Xylene kinetic batch-experiment k_2 data fit with a linear regression.

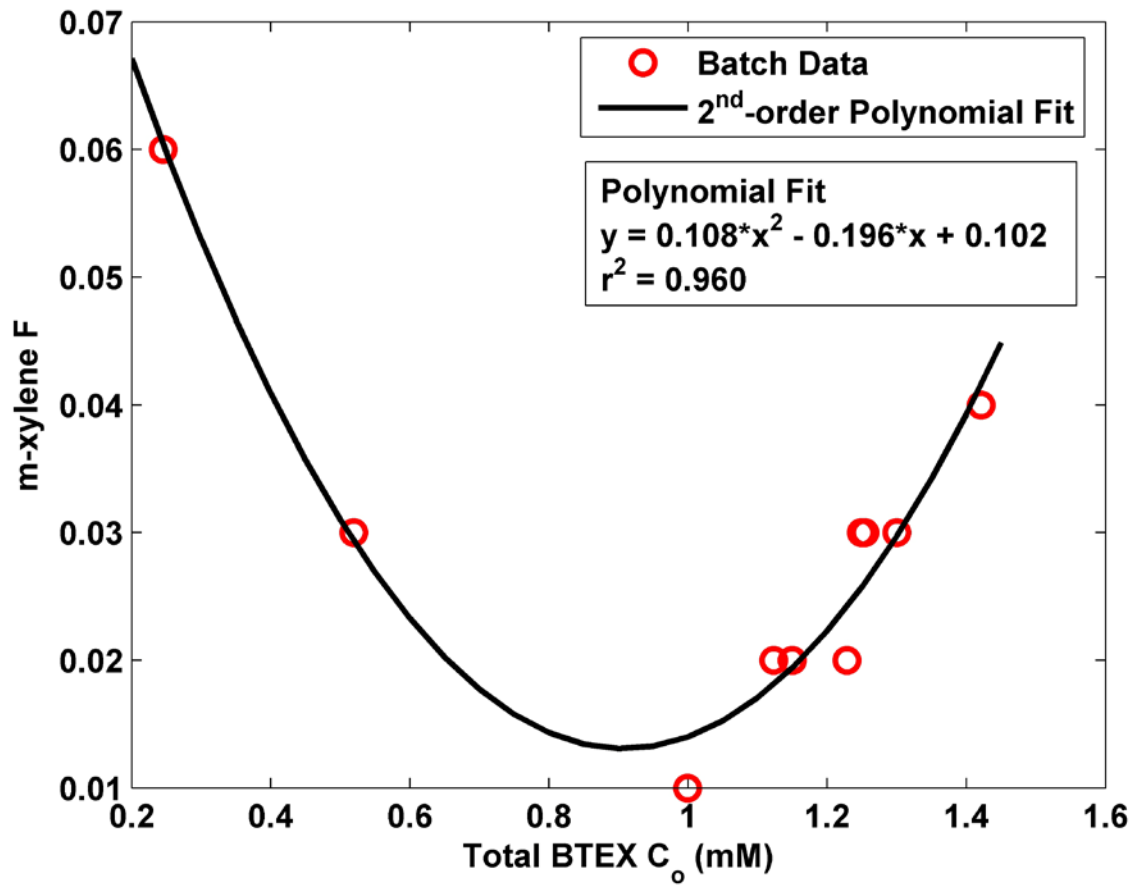


Figure 13. *m*-Xylene kinetic batch-experiment F data fit with a polynomial trend line.

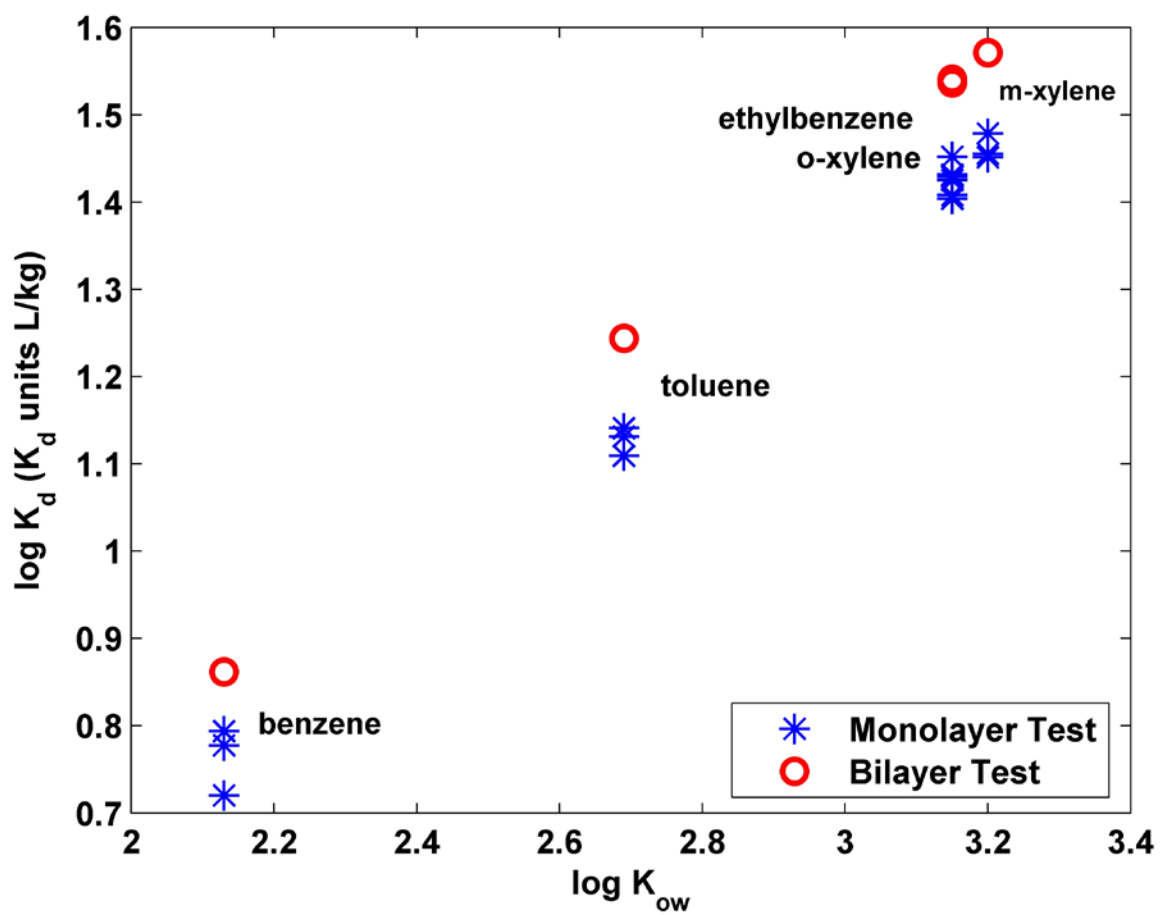


Figure 14. K_d results from three replicate monolayer and corresponding bilayer SMZ batch experiments.

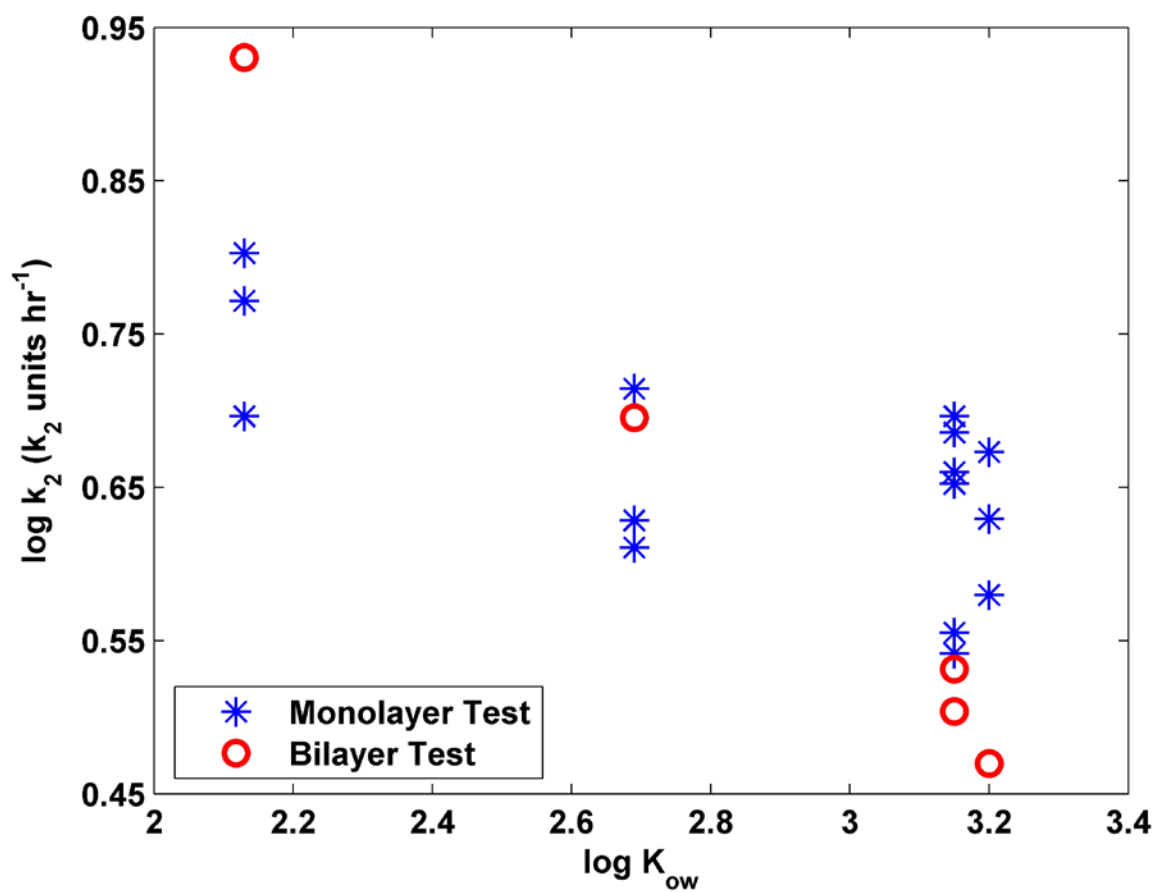


Figure 15. Results for k_2 from three replicate monolayer and corresponding bilayer SMZ batch experiments.

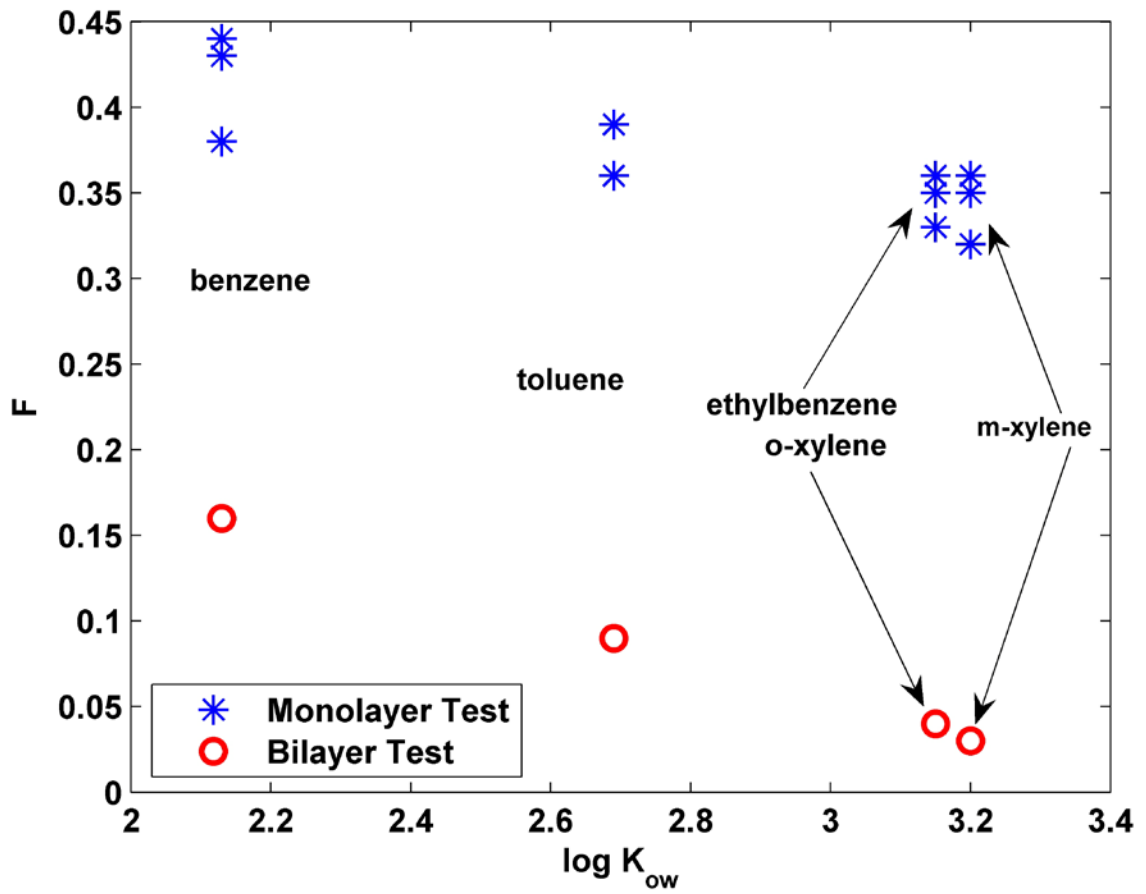


Figure 16. F results from three replicate monolayer and corresponding bilayer SMZ batch experiments.

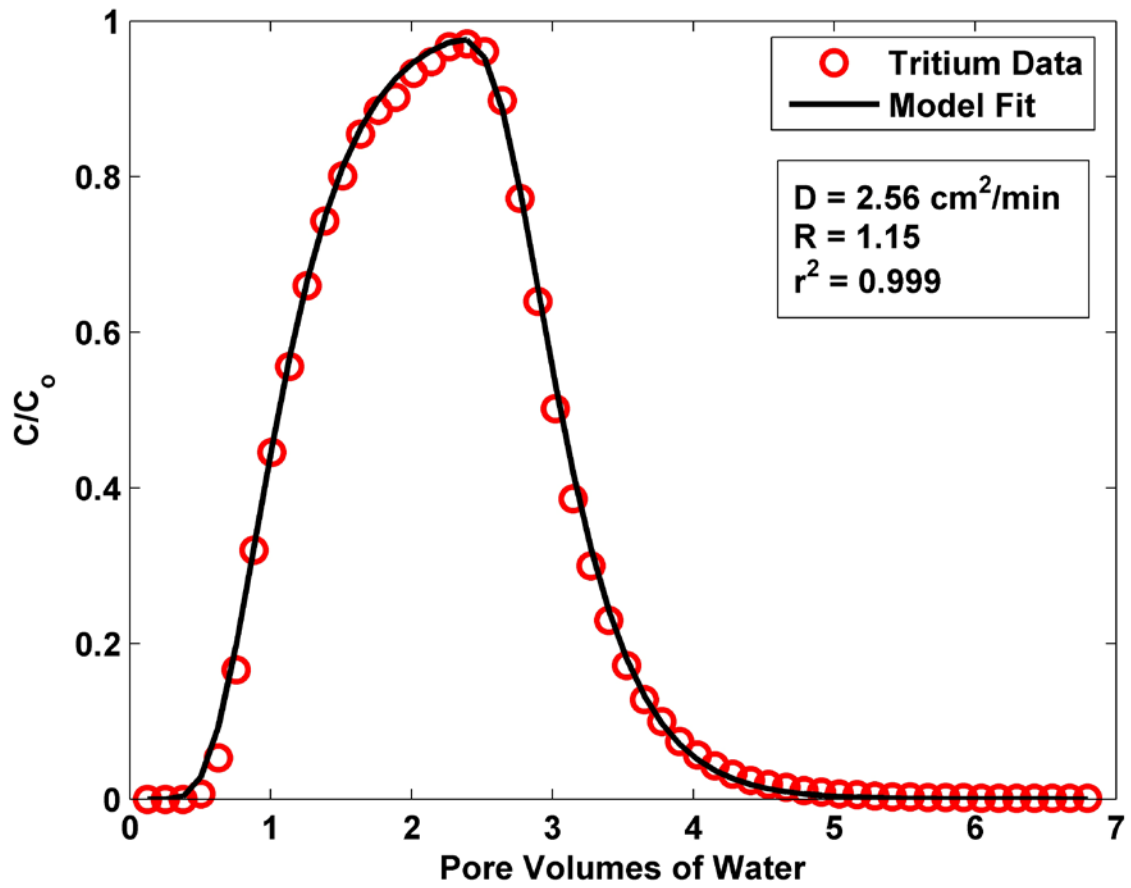


Figure 17. Tritium breakthrough curve for column 2B fitted with the physical equilibrium, 1-D advection-dispersion model.

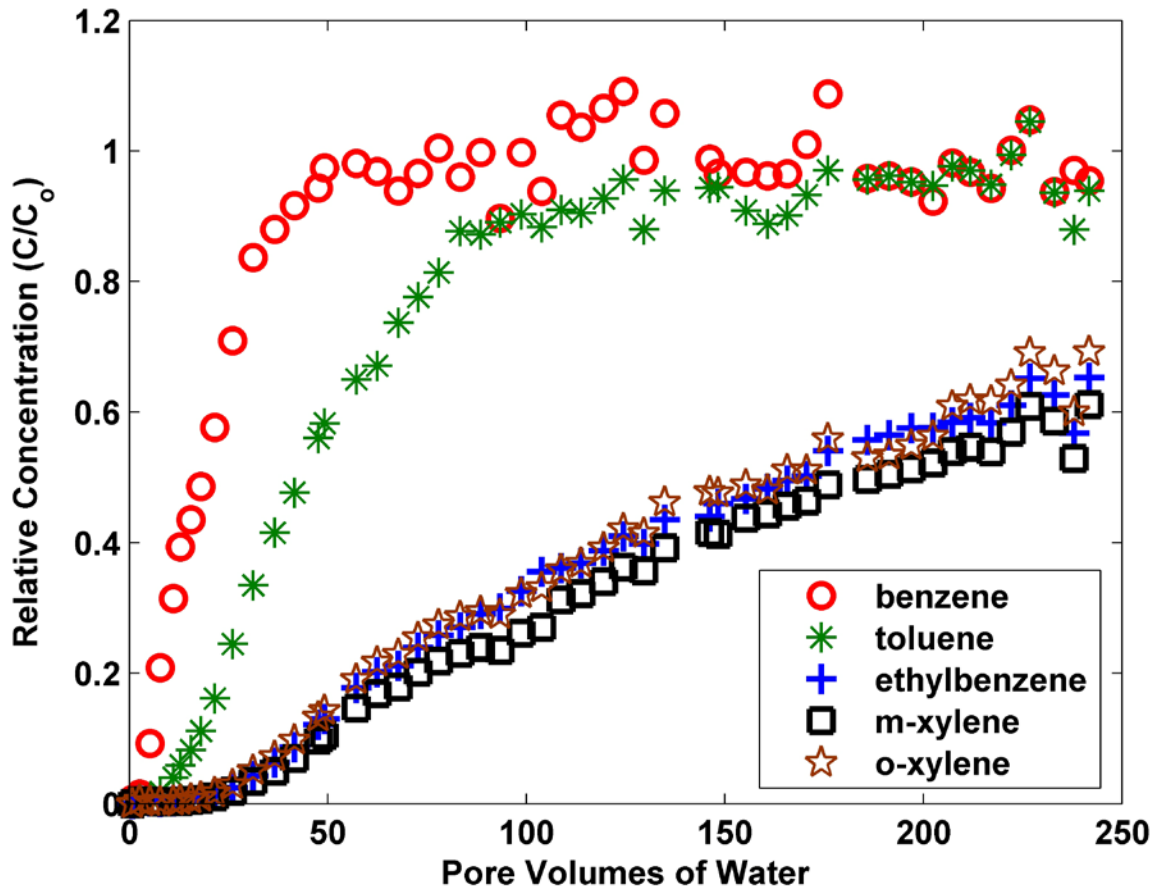


Figure 18. BTEX breakthrough curves for Column 2B.

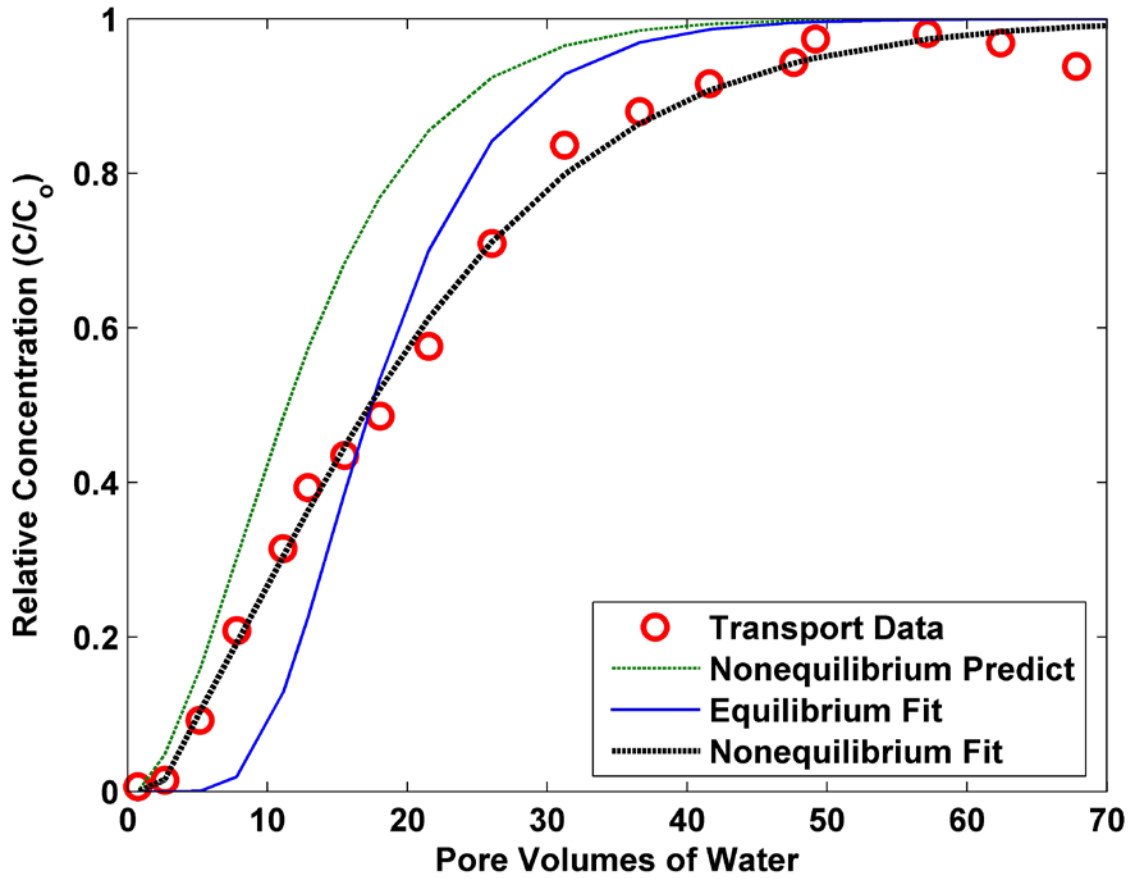


Figure 19. Benzene Column 2B data with nonequilibrium model prediction and equilibrium and nonequilibrium model fits.

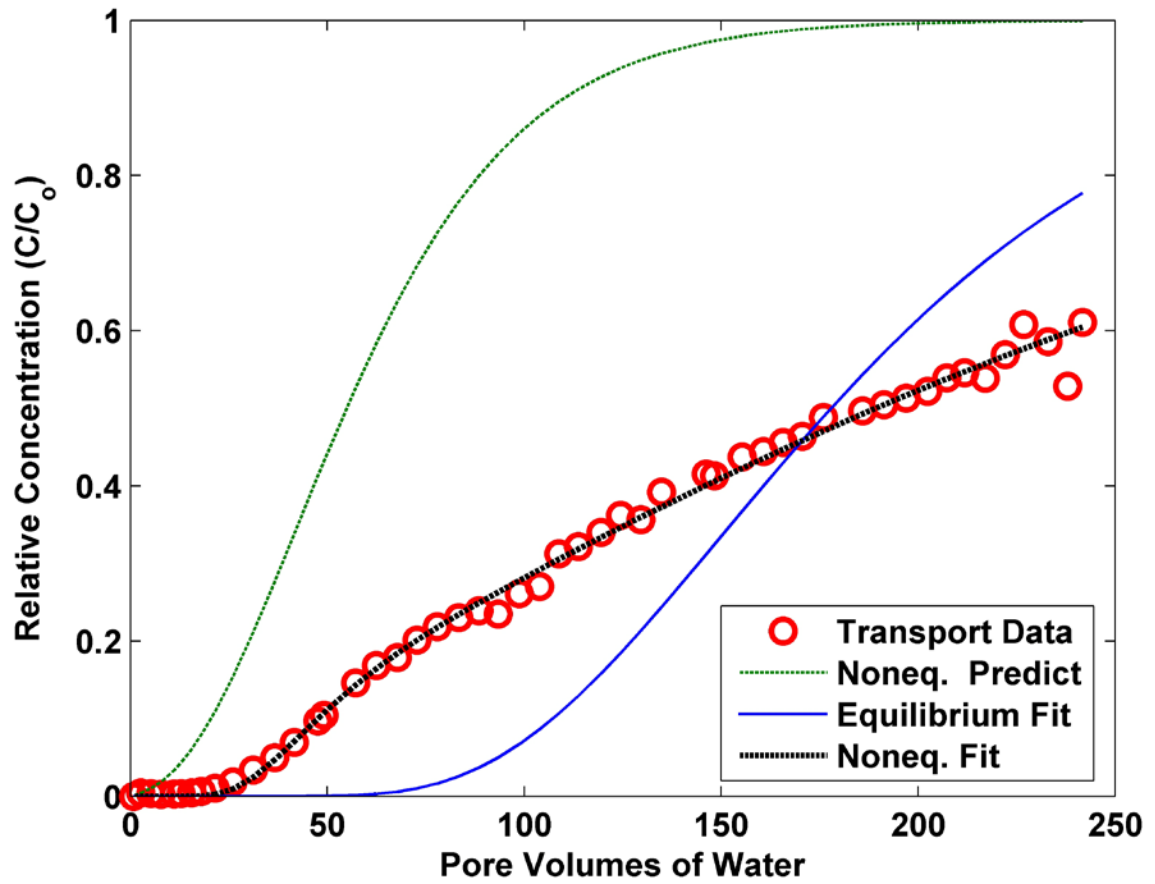


Figure 20. *m*-Xylene Column 2B data with nonequilibrium model prediction and equilibrium and nonequilibrium model fits.

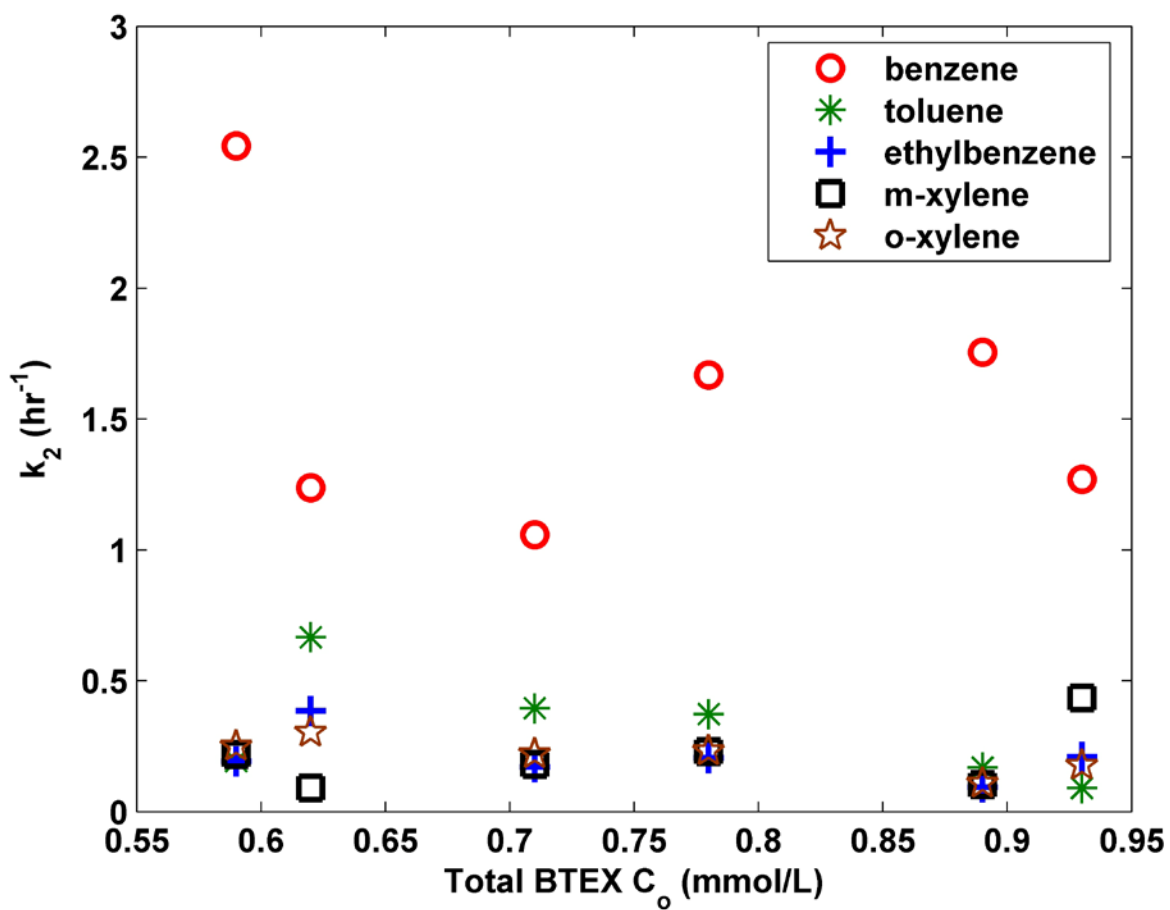


Figure 21. The k_2 calculated from the nonequilibrium model having R , β , and ω inversely fit, termed transport-determined values.

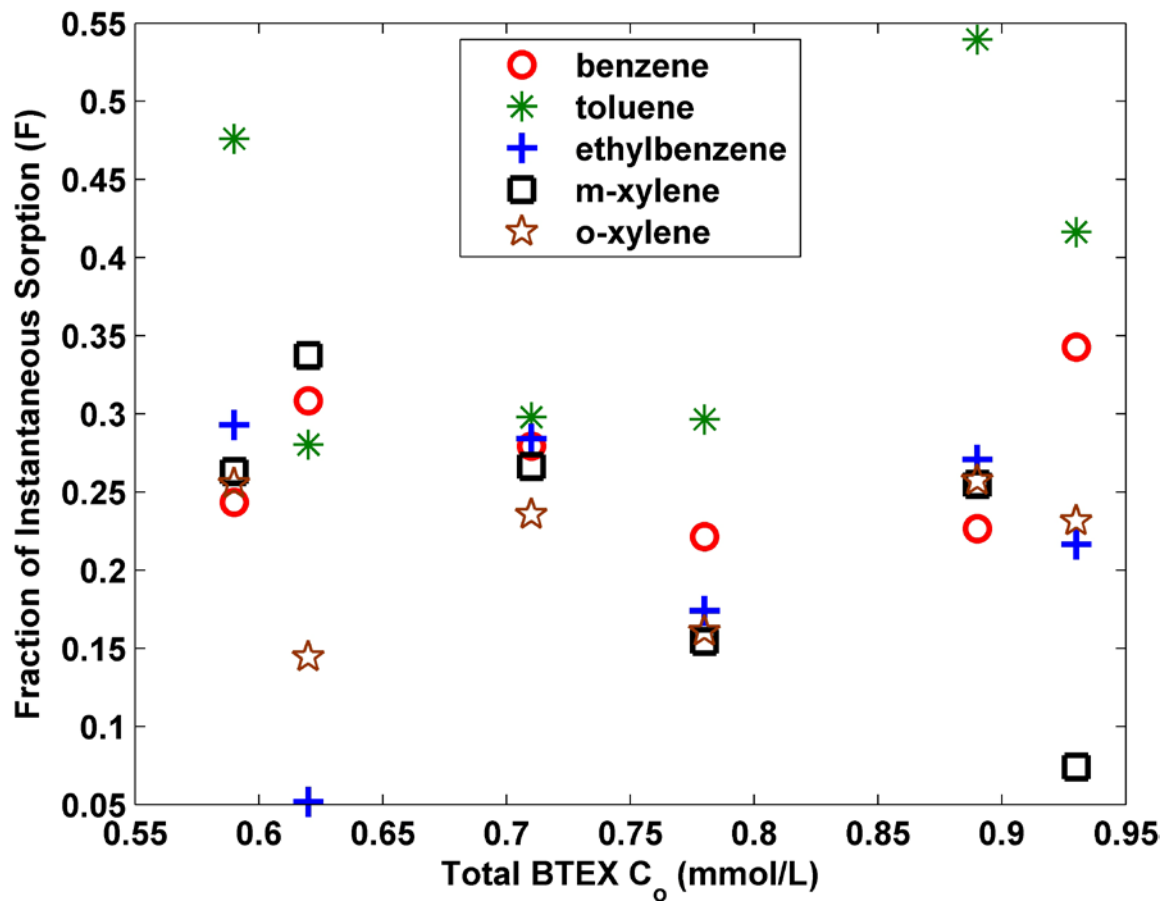


Figure 22. F calculated from the nonequilibrium model having R, β , and ω inversely fit, termed transport-determined values.

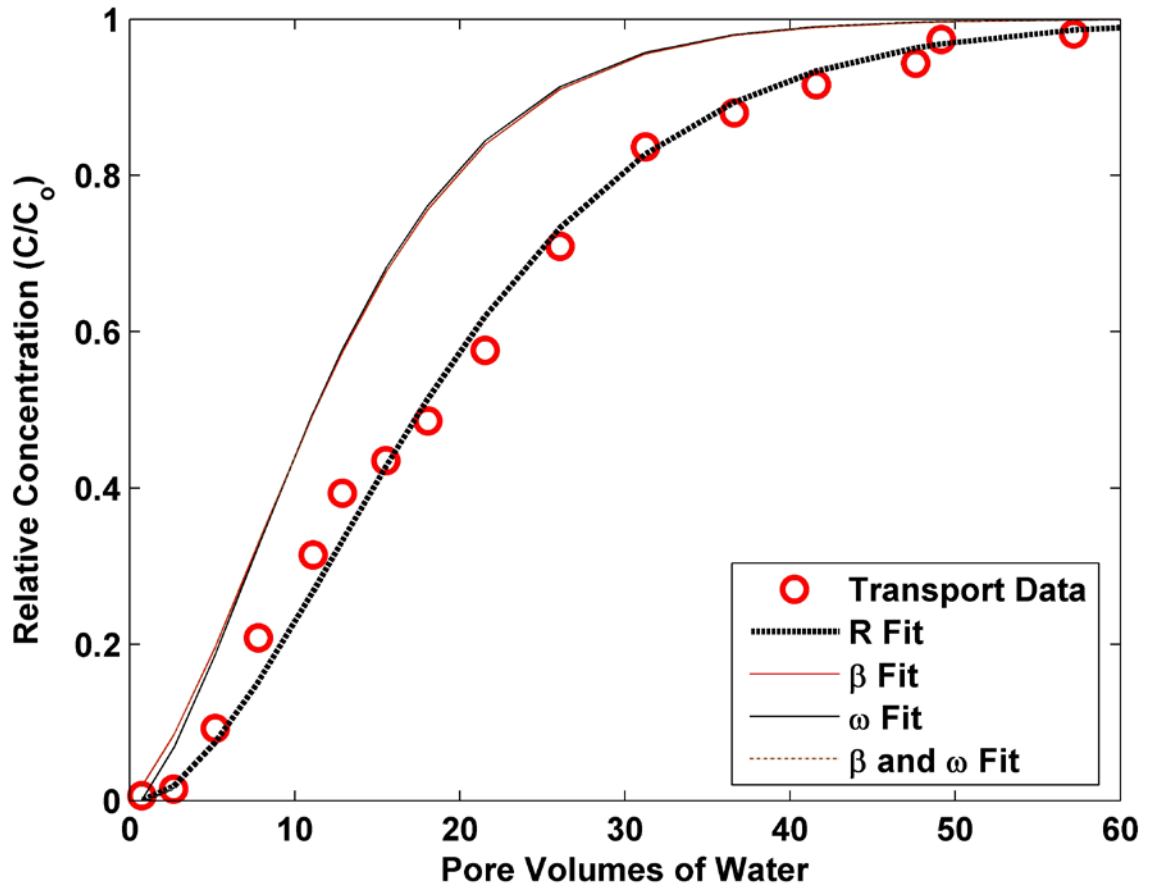


Figure 23. Nonequilibrium prediction model's individual parameter fits to Column 2B benzene data.

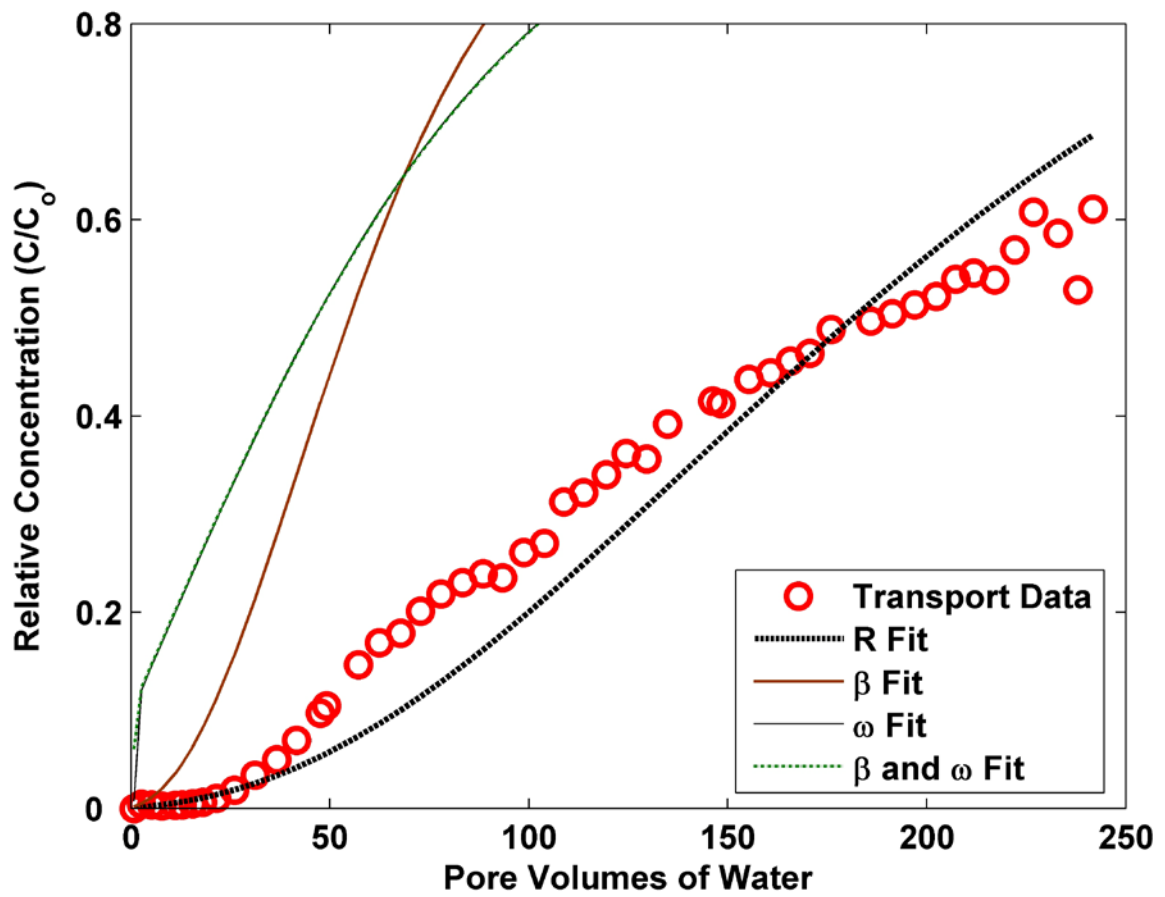


Figure 24. Nonequilibrium prediction model's individual parameter fits to Column 2B *m*-xylene data.

APPENDIX A. SINGLE-SOLUTE AND INITIAL MULTIPLE-SOLUTE BATCH EXPERIMENT RESULTS.

The results from the single-solute batch experiments are contained in this appendix. Six single-solute batch experiments—containing benzene, toluene, ethylbenzene, *m*-xylene, *p*-xylene, and *o*-xylene alone—were conducted. The experimental procedure is discussed in the main text. Tables A-1 through A-6 present the data from the single-solute experiments. Overall results from the single-solute batch experiments can be found in Table A-8.

Table A-1. Data from benzene single-solute batch experiment

Sample	Starting Concentration (mM)	Experiment Time (min)	Final Concentration (mM)	Amount Sorbed (mmol/kg)
0.5-1	0.26	0.5	0.16	0.34
0.5-2	0.27	0.5	0.17	0.30
0.5-3	0.26	0.5	0.17	0.31
1-1	0.26	1	0.15	0.36
1-2	0.27	1	0.15	0.37
1-3	0.27	1	0.17	0.33
2-1	0.26	2.6	0.10	0.53
2-2	0.27	2	0.12	0.49
2-3	0.26	2	0.12	0.47
4-1	0.26	4	0.09	0.56
4-2	0.26	4	0.09	0.55
4-3	0.27	4	0.09	0.56
6-1	0.26	6	0.09	0.57
6-2	0.26	6	0.09	0.57
6-3	0.26	7.2	0.08	0.58
9-1	0.26	9	0.09	0.57
9-2	0.26	9	0.08	0.60
9-3	0.27	10.5	0.08	0.61
12-1	0.26	12	0.08	0.61
12-2	0.26	12	0.08	0.61
12-3	0.27	12	0.08	0.60
15-1	0.27	15	0.07	0.65
15-2	0.26	15	0.07	0.63
15-3	0.24	15	0.07	0.62
20-1	0.26	20	0.08	0.60
20-2	0.25	20	0.08	0.59
20-3	0.27	20.75	0.07	0.62
25-1	0.26	25	0.07	0.63
25-2	0.25	25	0.07	0.61
25-3	0.26	25	0.07	0.62
30-1	0.27	30	0.07	0.62
30-2	0.26	30	0.07	0.65
40-1	0.26	40	0.08	0.61
40-2	0.25	40	0.08	0.60
40-3	0.26	40	0.08	0.61
50-1	0.27	50	0.07	0.63
50-2	0.26	50	0.06	0.66
50-3	0.27	50	0.06	0.67
60-1	0.26	60	0.07	0.62
60-2	0.26	60	0.08	0.61
60-3	0.27	60	0.08	0.62
90-1	0.26	90	0.07	0.62
90-2	0.27	90	0.08	0.62
90-3	0.27	90	0.07	0.63

Table A-2. Data from toluene single-solute batch experiment

Sample	Starting Concentration (mM)	Experiment Time (min)	Final Concentration (mM)	Amount Sorbed (mmol/kg)
0.5-1	0.18	0.5	0.10	0.25
0.5-2	0.18	0.67	0.10	0.29
1-1	0.18	1	0.08	0.33
1-2	0.19	1	0.09	0.32
1-3	0.18	1	0.08	0.33
2-1	0.19	2	0.05	0.44
2-2	0.18	2	0.06	0.39
2-3	0.18	2	0.05	0.42
4-1	0.18	4	0.04	0.45
4-2	0.18	4	0.04	0.47
4-3	0.18	4	0.04	0.46
6-1	0.18	6	0.04	0.47
6-2	0.18	6	0.04	0.47
6-3	0.19	6	0.04	0.48
9-1	0.18	9	0.03	0.50
9-2	0.18	9	0.03	0.50
9-3	0.18	9	0.03	0.49
12-1	0.18	12	0.03	0.49
12-2	0.18	15	0.03	0.49
15-1	0.18	15	0.04	0.48
15-2	0.19	15	0.04	0.49
15-3	0.18	25	0.03	0.50
20-1	0.18	20	0.03	0.49
20-2	0.18	20	0.03	0.50
20-3	0.19	20	0.03	0.50
25-1	0.18	25	0.03	0.51
25-2	0.18	25	0.03	0.51
25-3	0.18	25	0.03	0.51
30-1	0.19	30	0.03	0.50
30-2	0.18	30	0.03	0.51
30-3	0.18	30	0.03	0.51
40-1	0.18	40	0.03	0.51
40-2	0.19	40	0.02	0.52
40-3	0.18	40	0.03	0.52
60-1	0.18	60	0.03	0.51
60-2	0.18	60	0.02	0.52
60-3	0.19	60	0.03	0.52
90-1	0.18	90	0.03	0.51
90-2	0.19	90	0.02	0.52
90-3	0.18	90	0.02	0.52

Table A-3. Data from ethylbenzene single-solute batch experiment

Sample	Starting Concentration (mM)	Experiment Time (min)	Final Concentration (mM)	Amount Sorbed (mmol/kg)
0.5-1	0.21	0.57	0.09	0.38
0.5-2	0.21	0.50	0.09	0.39
0.5-3	0.21	0.60	0.08	0.44
1-1	0.21	1	0.06	0.49
1-2	0.21	1	0.07	0.44
1-3	0.21	1	0.08	0.43
2-1	0.21	2	0.05	0.53
2-2	0.21	2	0.05	0.52
2-3	0.21	2	0.05	0.54
4-1	0.21	4	0.03	0.59
4-2	0.21	4	0.03	0.59
4-3	0.21	4	0.03	0.60
6-1	0.21	6	0.03	0.58
6-2	0.21	6	0.03	0.60
6-3	0.21	6	0.03	0.59
9-1	0.21	9	0.02	0.61
9-2	0.21	9	0.02	0.62
9-3	0.21	9	0.02	0.62
12-1	0.21	12	0.02	0.62
12-2	0.21	12	0.02	0.62
12-3	0.21	12	0.02	0.62
15-1	0.21	16	0.02	0.62
15-2	0.21	15	0.02	0.62
15-3	0.21	15	0.02	0.63
20-1	0.21	20	0.02	0.63
20-2	0.21	20	0.02	0.63
20-3	0.21	20	0.03	0.60
25-1	0.21	25	0.02	0.62
25-2	0.21	25	0.02	0.62
25-3	0.21	25	0.02	0.62
30-1	0.21	30	0.02	0.62
30-2	0.21	30	0.02	0.62
30-3	0.21	30	0.02	0.63
40-1	0.21	40	0.02	0.62
40-2	0.21	40	0.02	0.63
40-3	0.21	40	0.02	0.63
60-1	0.21	60	0.02	0.63
60-2	0.21	60	0.02	0.63
60-3	0.22	60	0.02	0.64
90-1	0.21	90	0.02	0.62
90-2	0.21	90	0.02	0.63
90-3	0.21	90	0.01	0.64

Table A-4. Data from *m*-xylene single-solute batch experiment

Sample	Starting Concentration (mg/L)	Experiment Time (min)	Final Concentration (mg/L)	Amount Sorbed (mg/kg)
0.5-1	0.21	0.5	0.11	0.31
0.5-2	0.21	0.5	0.10	0.34
0.5-3	0.21	0.5	0.11	0.32
1-1	0.20	1	0.08	0.42
1-2	0.21	1	0.08	0.41
1-3	0.21	1	0.08	0.43
2-1	0.21	2	0.05	0.51
2-2	0.21	2	0.05	0.51
2-3	0.21	2	0.05	0.50
4-1	0.21	4	0.03	0.58
4-2	0.21	4	0.03	0.58
4-3	0.21	4	0.03	0.58
6-1	0.21	6	0.03	0.59
6-2	0.20	6	0.03	0.58
6-3	0.21	6	0.03	0.59
9-1	0.20	9	0.02	0.60
9-2	0.21	9	0.02	0.61
9-3	0.21	9	0.02	0.61
12-1	0.21	12.53	0.02	0.60
12-2	0.21	12	0.02	0.61
12-3	0.20	12	0.02	0.60
15-1	0.21	15	0.02	0.61
15-2	0.21	15	0.02	0.61
15-3	0.21	14.18	0.02	0.61
20-1	0.21	20	0.02	0.62
20-2	0.21	20	0.02	0.62
20-3	0.21	20	0.02	0.62
25-1	0.21	25.33	0.02	0.62
25-2	0.21	25.1	0.02	0.62
25-3	0.20	25	0.02	0.62
30-1	0.21	30.7	0.02	0.62
30-2	0.21	30	0.02	0.62
30-3	0.20	30	0.02	0.62
40-1	0.21	40	0.01	0.63
40-2	0.21	40	0.01	0.63
40-3	0.21	40	0.02	0.63
60-1	0.21	60	0.02	0.62
60-2	0.21	60	0.02	0.63
60-3	0.21	60	0.01	0.63
90-1	0.21	90	0.02	0.62
90-2	0.21	90	0.01	0.63
90-3	0.20	90	0.01	0.63

Table A-5. Data from *o*-xylene single-solute batch experiment

Sample	Starting Concentration (mg/L)	Experiment Time (min)	Final Concentration (mg/L)	Amount Sorbed (mg/kg)
0.5-1	0.19	0.5	0.08	0.33
0.5-2	0.19	0.5	0.08	0.34
0.5-3	0.19	0.5	0.08	0.35
1-1	0.19	1	0.07	0.39
1-2	0.19	1	0.07	0.39
1-3	0.19	0.93	0.07	0.40
2-1	0.19	2	0.05	0.45
2-2	0.19	2	0.04	0.48
2-3	0.19	2	0.04	0.47
4-1	0.19	4	0.02	0.53
4-2	0.18	4	0.03	0.52
4-3	0.18	4	0.03	0.51
6-1	0.18	6	0.03	0.52
6-2	0.19	6.38	0.03	0.52
6-3	0.19	6	0.03	0.52
9-1	0.19	9	0.02	0.54
9-2	0.19	9	0.02	0.54
9-3	0.19	9	0.02	0.54
12-1	0.19	12	0.02	0.54
12-2	0.19	12	0.02	0.56
12-3	0.19	12.2	0.02	0.55
15-1	0.18	15	0.02	0.55
15-2	0.19	15	0.02	0.55
15-3	0.19	15	0.02	0.55
20-1	0.18	20.2	0.01	0.56
20-2	0.19	20	0.01	0.57
20-3	0.19	20	0.01	0.56
25-1	0.19	25	0.01	0.56
25-2	0.19	25.27	0.02	0.56
25-3	0.18	25	0.02	0.56
30-1	0.19	30	0.02	0.56
30-2	0.19	30	0.02	0.56
30-3	0.19	30	0.02	0.55
40-1	0.19	40	0.01	0.56
40-2	0.18	40	0.01	0.57
40-3	0.19	40	0.01	0.57
60-1	0.19	60	0.02	0.55
60-2	0.19	60	0.01	0.56
60-3	0.19	60	0.01	0.57
90-1	0.18	90	0.02	0.56
90-2	0.19	90	0.01	0.56
90-3	0.19	90	0.01	0.57

Table A-6. Data from *p*-xylene single-solute batch experiment

Sample	Starting Concentration (mg/L)	Experiment Time (min)	Final Concentration (mg/L)	Amount Sorbed (mg/kg)
0.5-1	0.20	0.5	0.11	0.28
0.5-2	0.19	0.8	0.09	0.33
0.5-3	0.19	0.9	0.09	0.33
1-1	0.20	1	0.09	0.36
1-2	0.20	1	0.08	0.37
1-3	0.19	1	0.07	0.39
2-1	0.19	2	0.05	0.48
2-2	0.19	2	0.05	0.48
2-3	0.20	2	0.05	0.48
4-1	0.19	4	0.03	0.54
4-2	0.20	4	0.03	0.54
4-3	0.20	4	0.03	0.54
6-1	0.20	6	0.03	0.55
6-2	0.20	6	0.03	0.55
6-3	0.19	6	0.03	0.54
9-1	0.20	9	0.02	0.56
9-2	0.20	9	0.02	0.57
9-3	0.20	9	0.02	0.57
12-1	0.19	12	0.02	0.56
12-2	0.20	12	0.02	0.57
12-3	0.20	12	0.02	0.57
15-1	0.19	15	0.02	0.57
15-2	0.20	15	0.02	0.57
15-3	0.20	15	0.02	0.57
20-1	0.19	20	0.01	0.59
20-2	0.19	20	0.01	0.59
20-3	0.20	20	0.02	0.58
25-1	0.19	25	0.02	0.58
25-2	0.19	25	0.02	0.58
25-3	0.19	25	0.02	0.58
30-1	0.20	30	0.02	0.58
30-2	0.19	30	0.02	0.58
30-3	0.19	30	0.02	0.58
40-1	0.20	40	0.01	0.59
40-2	0.20	40	0.01	0.59
40-3	0.20	40	0.01	0.59
60-1	0.19	60	0.02	0.58
60-2	0.20	60	0.01	0.59
60-3	0.19	60	0.01	0.59
90-1	0.20	90	0.01	0.59
90-2	0.19	90	0.01	0.59
90-3	0.20	90	0.02	0.58

Table A-7. Results from the single-solute batch experiments

Constituent	K_d (L/kg)	k₂ (1/hr)	F	Bicontinuum fit (r²)	Starting Conc. (mM)	Water Added (ml)	Zeolite Added (g)	Log K_{ow}¹	Solubility (mg/L)¹
benzene	8.4	7.74	0.15	0.921	0.26	9.87	3	2.13	1850
toluene	18.4	4.64	0.09	0.901	0.18	9.82	3	2.69	470
ethylbenzene	33.8	3.69	0.09	0.916	0.21	9.78	3	3.15	140
m-xylene	38.1	3.13	0.05	0.956	0.21	9.77	3	3.2	173
o-xylene	39.0	3.12	0.08	0.955	0.19	9.76	3	3.15	204
p-xylene	37.5	3.16	0.06	0.939	0.20	9.75	3	3.15	200

¹ Mackay et al., 1992

APPENDIX B. MULTIPLE-SOLUTE BATCH EXPERIMENT DATA.

The data from the multiple-solute batch experiments are presented in this appendix. Four multiple-solute experiments (benzene, toluene, ethylbenzene, m-xylene, and o-xylene) were run with the same initial concentration for each BTEX constituent in order to determine concentration effects on the nonequilibrium sorption parameters. Eight multiple-solute experiments were run in order to determine preferential influences of individual constituents on the nonequilibrium sorption parameters. The experimental procedure is discussed in the main text. The definitions for each experiment are found in Table B-1. Tables B-2 through B-5 represent data from the first four experiments. Tables B-6 through B-13 represent data from the final eight experiments. Tables B-14 through B-25 present the overall results from each experiment.

Table B-1. Multiple-solute kinetic batch experiment definitions. In description field: B = benzene, T = toluene, E = ethylbenzene, M = *m*-xylene, O = *o*-xylene.

Batch Experiment	Description
MSB-0.05	All BTEX constituents' initial aqueous concentrations were 0.05 mM. Total initial aqueous BTEX equaled 0.25 mM.
MSB-0.1	All BTEX constituents' initial aqueous concentrations were 0.1 mM. Total initial aqueous BTEX equaled 0.5 mM.
MSB-0.2	All BTEX constituents' initial aqueous concentrations were 0.2 mM. Total initial aqueous BTEX equaled 1.0 mM.
MSB-0.3	All BTEX constituents' initial aqueous concentrations were 0.3 mM. Total initial aqueous BTEX equaled 1.5 mM.
MSB-0.35T	Initial aqueous concentrations were: B, E, M, and O = 0.2 mM; T = 0.35 mM. Total initial aqueous BTEX concentration equaled 1.15 mM.
MSB-0.35E	Initial aqueous concentrations were: B, T, M, and O = 0.2 mM; E = 0.35 mM. Total initial aqueous BTEX concentration equaled 1.15 mM.
MSB-0.35M	Initial aqueous concentrations were: B, T, E, and O = 0.2 mM; M = 0.35 mM. Total initial aqueous BTEX concentration equaled 1.15 mM.
MSB-0.35O	Initial aqueous concentrations were: B, T, E, and M = 0.2 mM; O = 0.35 mM. Total initial aqueous BTEX concentration equaled 1.15 mM.
MSB-0.5T	Initial aqueous concentrations were: B, E, M, and O = 0.2 mM; T = 0.5 mM. Total initial aqueous BTEX concentration equaled 1.3 mM.
MSB-0.5E	Initial aqueous concentrations were: B, T, M, and O = 0.2 mM; E = 0.5 mM. Total initial aqueous BTEX concentration equaled 1.3 mM.
MSB-0.5M	Initial aqueous concentrations were: B, T, E, and O = 0.2 mM; M = 0.5 mM. Total initial aqueous BTEX concentration equaled 1.3 mM.
MSB-0.5O	Initial aqueous concentrations were: B, T, E, and M = 0.2 mM; O = 0.5 mM. Total initial aqueous BTEX concentration equaled 1.3 mM.

Table B-2. BTEX sorption data from MSB-0.05 batch experiment.

Sample	Experiment Time (min)	Amount Sorbed (mmol/kg)				
		Benzene	Toluene	Ethylbenzene	M-Xylene	O-Xylene
0.5-1	0.5	0.064	0.079	0.090	0.088	0.089
0.5-2	0.5	0.060	0.077	0.091	0.089	0.090
0.5-3	0.5	0.060	0.078	0.093	0.092	0.092
1-2	1	0.078	0.096	0.111	0.102	0.108
1-3	1	0.071	0.088	0.102	0.102	0.099
2-1	2	0.084	0.108	0.124	0.122	0.122
2-2	2	0.089	0.112	0.129	0.128	0.128
2-3	2	0.089	0.114	0.132	0.130	0.131
6-1	6	0.103	0.128	0.144	0.142	0.143
6-2	8	0.102	0.128	0.145	0.144	0.144
6-3	6.2	0.103	0.128	0.144	0.143	0.144
9-1	9	0.101	0.128	0.145	0.144	0.145
9-2	9	0.106	0.131	0.147	0.145	0.146
9-3	9	0.103	0.129	0.147	0.145	0.146
12-1	12	0.111	0.134	0.149	0.148	0.149
12-2	12	0.103	0.130	0.147	0.146	0.147
12-3	12	0.108	0.134	0.149	0.148	0.149
15-1	15	0.108	0.129	0.146	0.144	0.144
15-2	15	0.107	0.133	0.148	0.147	0.148
15-3	15	0.110	0.134	0.149	0.148	0.149
20-1	20	0.108	0.137	0.151	0.149	0.151
20-2	20	0.109	0.134	0.150	0.148	0.149
20-3	20	0.108	0.134	0.149	0.147	0.149
25-1	25.2	0.106	0.133	0.148	0.148	0.149
25-2	25	0.110	0.135	0.149	0.149	0.150
25-3	25	0.105	0.132	0.145	0.144	0.144
30-1	30	0.106	0.133	0.149	0.148	0.149
30-2	30	0.108	0.134	0.150	0.148	0.149
30-3	30	0.115	0.138	0.152	0.150	0.152
40-1	40	0.111	0.137	0.152	0.150	0.151
40-2	40	0.111	0.136	0.152	0.150	0.151
40-3	40	0.111	0.135	0.150	0.148	0.150
60-1	60	0.107	0.135	0.151	0.149	0.151
60-2	60	0.109	0.136	0.152	0.150	0.151
60-3	60	0.109	0.135	0.149	0.148	0.149
90-1	90	0.111	0.138	0.153	0.151	0.152
90-2	90	0.112	0.138	0.153	0.151	0.153

Table B-3. BTEX sorption data from MSB-0.1 batch experiment.

Sample	Experiment Time (min)	Amount Sorbed (mmol/kg)				
		Benzene	Toluene	Ethylbenzene	M-Xylene	O-Xylene
0.5-1	0.5	0.117	0.157	0.155	0.151	0.166
0.5-2	0.5	0.109	0.151	0.154	0.150	0.164
0.5-3	0.5	0.098	0.134	0.129	0.123	0.137
1-1	1	0.137	0.192	0.195	0.164	0.209
1-2	1	0.132	0.196	0.201	0.173	0.218
2-1	2	0.185	0.250	0.245	0.244	0.265
2-2	2	0.178	0.240	0.238	0.237	0.259
2-3	2	0.163	0.230	0.232	0.231	0.251
4-1	2.4	0.175	0.244	0.242	0.241	0.263
4-2	4	0.190	0.265	0.265	0.265	0.290
4-3	4	0.187	0.262	0.262	0.262	0.286
6-2	6	0.221	0.293	0.283	0.284	0.310
6-3	6	0.212	0.288	0.282	0.282	0.308
9-1	9	0.216	0.286	0.279	0.280	0.306
9-2	9	0.230	0.300	0.287	0.288	0.315
9-3	9	0.224	0.293	0.284	0.285	0.312
12-1	12	0.214	0.289	0.282	0.283	0.309
12-2	12	0.218	0.292	0.283	0.284	0.311
12-3	12	0.239	0.302	0.288	0.288	0.316
15-2	15	0.238	0.304	0.290	0.290	0.318
15-3	15	0.224	0.298	0.288	0.289	0.316
20-1	20	0.232	0.303	0.289	0.290	0.317
20-2	20	0.230	0.302	0.290	0.291	0.318
20-3	20	0.232	0.303	0.290	0.291	0.319
25-1	25	0.227	0.302	0.284	0.291	0.318
25-2	25	0.230	0.303	0.285	0.291	0.319
25-3	25	0.224	0.301	0.284	0.291	0.319
30-1	31.5	0.238	0.308	0.292	0.292	0.319
30-2	30	0.234	0.307	0.293	0.294	0.321
30-3	30	0.237	0.308	0.294	0.294	0.322
40-1	40	0.226	0.304	0.290	0.291	0.318
40-2	40	0.232	0.307	0.294	0.295	0.323
40-3	40	0.233	0.308	0.295	0.296	0.324
60-1	60	0.230	0.305	0.292	0.292	0.321
60-2	60	0.232	0.309	0.295	0.296	0.325
60-3	60	0.236	0.312	0.297	0.298	0.327
90-1	90	0.233	0.307	0.292	0.293	0.322
90-2	90	0.231	0.309	0.295	0.296	0.325
90-3	90	0.236	0.312	0.298	0.298	0.328

Table B-4. BTEX sorption data from MSB-0.2 batch experiment.

Sample	Experiment Time (min)	Amount Sorbed (mmol/kg)				
		Benzene	Toluene	Ethylbenzene	M-Xylene	O-Xylene
0.5-1	0.5	0.251	0.254	0.268	0.259	0.286
0.5-2	0.58	0.257	0.267	0.275	0.265	0.295
0.5-3	0.5	0.232	0.225	0.228	0.218	0.236
1-1	1	0.295	0.321	0.340	0.213	0.365
1-3	1	0.283	0.310	0.325	0.186	0.351
2-1	2	0.325	0.415	0.442	0.422	0.481
2-2	2	0.335	0.426	0.460	0.441	0.499
2-3	2	0.317	0.409	0.445	0.427	0.484
4-1	4	0.395	0.457	0.512	0.498	0.555
4-2	4	0.374	0.460	0.504	0.489	0.547
4-3	4	0.385	0.444	0.498	0.483	0.541
6-1	6	0.453	0.509	0.550	0.530	0.595
6-2	6	0.447	0.495	0.543	0.523	0.589
6-3	6	0.451	0.498	0.545	0.525	0.591
9-1	9	0.459	0.507	0.558	0.540	0.605
9-2	9	0.461	0.508	0.558	0.541	0.607
9-3	9	0.457	0.507	0.559	0.543	0.607
12-1	12	0.469	0.519	0.568	0.552	0.618
12-2	12	0.465	0.529	0.572	0.556	0.623
12-3	12	0.461	0.533	0.575	0.558	0.625
15-2	15	0.484	0.528	0.575	0.555	0.625
15-3	15	0.478	0.526	0.574	0.554	0.625
20-1	20	0.484	0.537	0.580	0.562	0.630
20-2	20	0.478	0.536	0.581	0.564	0.632
20-3	20	0.480	0.537	0.581	0.564	0.633
25-1	25	0.485	0.533	0.578	0.562	0.631
25-2	25	0.482	0.533	0.579	0.563	0.631
25-3	25	0.471	0.525	0.574	0.558	0.626
30-1	30.3	0.481	0.529	0.572	0.552	0.621
30-2	30	0.490	0.535	0.579	0.559	0.630
30-3	30	0.501	0.542	0.584	0.565	0.636
40-1	40	0.470	0.531	0.579	0.568	0.630
40-2	40	0.493	0.539	0.583	0.566	0.635
40-3	40	0.481	0.535	0.583	0.566	0.635
60-1	60	0.480	0.529	0.573	0.557	0.626
60-2	60	0.490	0.539	0.583	0.566	0.636
60-3	60	0.485	0.539	0.585	0.568	0.638
90-1	90	0.486	0.535	0.578	0.561	0.631
90-3	90	0.500	0.546	0.589	0.572	0.642

Table B-5. BTEX sorption data from MSB-0.3 batch experiment.

Sample	Experiment Time (min)	Amount Sorbed (mmol/kg)				
		Benzene	Toluene	Ethylbenzene	M-Xylene	O-Xylene
0.5-1	0.5	0.277	0.353	0.417	0.402	0.403
0.5-2	0.5	0.218	0.285	0.361	0.350	0.346
0.5-3	0.5	0.179	0.300	0.435	0.423	0.419
1-1	1	0.444	0.497	0.505	0.466	0.490
1-3	1	0.411	0.488	0.512	0.472	0.500
2-1	2	0.467	0.585	0.588	0.566	0.580
2-2	2	0.453	0.580	0.589	0.568	0.583
2-3	2	0.464	0.589	0.582	0.562	0.577
4-1	4	0.543	0.707	0.740	0.712	0.733
4-2	4	0.542	0.694	0.705	0.678	0.701
4-3	4.1	0.564	0.717	0.741	0.711	0.734
6-1	6	0.607	0.752	0.781	0.752	0.772
6-2	6	0.607	0.749	0.777	0.747	0.768
6-3	6	0.609	0.751	0.781	0.752	0.771
9-1	9	0.628	0.774	0.807	0.775	0.795
9-2	9	0.623	0.777	0.813	0.782	0.802
9-3	9	0.610	0.765	0.805	0.775	0.796
12-2	12	0.636	0.788	0.822	0.790	0.813
12-3	12	0.639	0.790	0.824	0.792	0.813
15-1	15	0.658	0.806	0.834	0.801	0.823
15-2	14.8	0.661	0.821	0.840	0.807	0.829
15-3	15	0.655	0.799	0.829	0.797	0.819
20-1	20	0.667	0.807	0.832	0.799	0.821
20-3	20	0.677	0.821	0.845	0.811	0.836
25-1	20	0.671	0.808	0.838	0.808	0.831
25-2	25	0.676	0.812	0.842	0.812	0.835
25-3	25	0.677	0.810	0.839	0.809	0.833
30-1	30.2	0.687	0.828	0.847	0.813	0.836
30-2	30	0.688	0.832	0.853	0.819	0.843
30-3	30	0.680	0.826	0.849	0.815	0.839
40-1	40	0.689	0.833	0.853	0.819	0.843
40-2	40	0.653	0.816	0.847	0.814	0.838
40-3	40	0.670	0.827	0.853	0.820	0.845
60-1	60	0.657	0.813	0.839	0.807	0.831
60-2	60	0.674	0.828	0.852	0.819	0.845
60-3	60	0.675	0.831	0.855	0.822	0.847
90-2	90	0.663	0.822	0.841	0.809	0.834
90-3	90	0.683	0.835	0.855	0.821	0.847

Table B-6. BTEX sorption data from MSB-0.5T batch experiment.

Sample	Experiment Time (min)	Amount Sorbed (mmol/kg)				
		Benzene	Toluene	Ethylbenzene	M-Xylene	O-Xylene
0.5-1	0.5	0.196	0.575	0.272	0.261	0.259
0.5-2	0.5	0.189	0.524	0.190	0.180	0.183
1-1	1	0.282	0.788	0.308	0.234	0.300
1-2	1	0.281	0.784	0.315	0.239	0.302
1-3	1	0.273	0.807	0.311	0.233	0.301
2-1	2	0.348	0.994	0.390	0.368	0.374
2-2	2	0.332	0.928	0.365	0.345	0.353
2-3	2	0.347	0.998	0.393	0.373	0.383
4-1	4	0.377	1.122	0.482	0.459	0.467
4-2	4	0.384	1.130	0.477	0.454	0.464
4-3	4.2	0.380	1.133	0.488	0.465	0.474
6-1	6	0.423	1.228	0.521	0.495	0.504
6-2	6	0.435	1.243	0.535	0.507	0.516
6-3	6	0.439	1.249	0.533	0.506	0.515
9-1	9	0.448	1.272	0.544	0.516	0.526
9-2	2.8	0.363	1.067	0.447	0.425	0.431
9-3	9	0.443	1.266	0.541	0.514	0.524
12-1	12	0.449	1.283	0.555	0.527	0.537
12-3	12	0.442	1.275	0.549	0.522	0.532
15-1	15	0.454	1.294	0.554	0.526	0.536
15-2	15	0.455	1.294	0.554	0.526	0.536
15-3	15	0.460	1.311	0.559	0.530	0.540
20-1	20	0.457	1.317	0.557	0.528	0.538
20-2	20	0.458	1.307	0.566	0.537	0.548
20-3	20	0.455	1.324	0.574	0.545	0.555
25-1	25	0.462	1.283	0.555	0.524	0.534
25-2	25	0.454	1.312	0.565	0.534	0.544
25-3	25	0.464	1.318	0.565	0.534	0.545
30-1	30	0.468	1.324	0.559	0.531	0.540
30-2	30.2	0.462	1.318	0.562	0.534	0.544
40-1	40	0.462	1.326	0.564	0.534	0.545
40-2	40	0.466	1.329	0.566	0.538	0.549
40-3	40	0.463	1.329	0.567	0.538	0.549
60-1	60	0.462	1.317	0.559	0.532	0.543
60-2	60	0.466	1.330	0.566	0.538	0.549
60-3	60	0.467	1.336	0.569	0.540	0.552
90-1	90	0.456	1.318	0.564	0.536	0.547
90-3	90	0.458	1.327	0.569	0.540	0.552

Table B-7. BTEX sorption data from MSB-0.5E batch experiment.

Sample	Experiment Time (min)	Amount Sorbed (mmol/kg)				
		Benzene	Toluene	Ethylbenzene	M-Xylene	O-Xylene
0.5-1	0.5	0.176	0.223	0.684	0.269	0.266
0.5-2	0.5	0.161	0.220	0.744	0.294	0.292
0.5-3	0.63	0.172	0.240	0.746	0.294	0.296
1-1	1	0.272	0.331	0.935	0.339	0.374
1-2	1	0.278	0.330	0.836	0.294	0.337
1-3	1.1	0.189	0.269	0.804	0.282	0.324
2-1	2	0.321	0.406	1.046	0.415	0.434
2-2	2	0.326	0.419	1.087	0.433	0.452
2-3	2	0.324	0.417	1.103	0.439	0.458
4-1	4	0.335	0.454	1.240	0.493	0.514
4-2	4	0.349	0.462	1.245	0.497	0.520
6-1	6	0.385	0.496	1.336	0.534	0.558
6-2	6	0.393	0.499	1.331	0.533	0.556
6-3	6	0.378	0.496	1.347	0.539	0.563
9-1	9	0.401	0.510	1.364	0.546	0.571
9-2	9	0.411	0.519	1.382	0.554	0.579
9-3	9	0.415	0.523	1.389	0.556	0.583
12-1	12	0.427	0.533	1.411	0.563	0.592
12-2	12	0.416	0.527	1.405	0.563	0.590
12-3	12	0.414	0.524	1.396	0.559	0.585
15-1	15	0.417	0.527	1.407	0.563	0.591
15-2	15	0.413	0.524	1.405	0.563	0.589
15-3	15	0.414	0.525	1.408	0.564	0.590
20-1	20	0.429	0.536	1.414	0.566	0.593
20-2	20	0.419	0.533	1.418	0.568	0.595
20-3	20	0.431	0.540	1.425	0.571	0.599
25-1	25	0.418	0.532	1.411	0.567	0.595
25-2	25	0.422	0.538	1.422	0.572	0.600
30-1	30	0.419	0.533	1.421	0.567	0.593
30-2	29.3	0.422	0.537	1.431	0.573	0.601
30-3	30	0.424	0.536	1.425	0.571	0.599
40-1	40	0.419	0.540	1.437	0.573	0.601
40-2	40	0.416	0.538	1.434	0.574	0.603
40-3	40	0.427	0.544	1.441	0.577	0.606
60-1	60	0.425	0.539	1.420	0.568	0.597
60-2	60	0.427	0.549	1.444	0.578	0.608
60-3	60	0.433	0.554	1.455	0.582	0.613
90-1	90	0.420	0.537	1.413	0.566	0.595
90-2	90	0.423	0.544	1.437	0.575	0.605
90-3	90	0.429	0.549	1.446	0.579	0.609

Table B-8. BTEX sorption data from MSB-0.5M batch experiment.

Sample	Experiment Time (min)	Amount Sorbed (mmol/kg)				
		Benzene	Toluene	Ethylbenzene	M-Xylene	O-Xylene
0.5-1	0.5	0.202	0.223	0.295	0.695	0.274
0.5-2	0.5	0.194	0.203	0.258	0.604	0.235
0.5-3	0.5	0.212	0.224	0.269	0.633	0.252
1-1	1	0.266	0.289	0.344	0.713	0.323
1-2	1	0.237	0.287	0.374	0.793	0.357
2-1	2	0.292	0.358	0.415	0.968	0.394
2-2	2	0.315	0.382	0.436	1.015	0.418
2-3	2	0.307	0.373	0.421	0.983	0.403
4-1	4	0.355	0.448	0.523	1.220	0.501
4-2	4	0.344	0.442	0.526	1.226	0.506
4-3	4	0.328	0.424	0.501	1.167	0.483
6-1	6	0.356	0.455	0.545	1.272	0.525
6-2	6	0.367	0.487	0.570	1.324	0.546
6-3	6	0.381	0.474	0.558	1.297	0.536
9-1	9	0.408	0.497	0.583	1.352	0.557
9-2	9	0.412	0.504	0.590	1.367	0.565
9-3	9	0.420	0.507	0.592	1.371	0.567
12-1	12	0.420	0.502	0.594	1.378	0.570
12-2	12	0.422	0.513	0.599	1.388	0.575
15-1	15	0.431	0.535	0.612	1.415	0.586
15-2	15	0.422	0.534	0.614	1.421	0.589
20-1	20	0.431	0.523	0.606	1.403	0.581
20-3	20	0.435	0.528	0.613	1.418	0.588
25-1	25	0.431	0.526	0.613	1.416	0.586
25-2	25	0.423	0.522	0.611	1.412	0.585
25-3	25	0.428	0.525	0.613	1.416	0.587
30-1	30	0.434	0.534	0.614	1.425	0.587
30-2	30	0.419	0.529	0.614	1.424	0.589
30-3	30	0.428	0.531	0.612	1.418	0.588
40-1	40	0.434	0.532	0.615	1.428	0.589
40-2	40	0.429	0.532	0.618	1.432	0.593
40-3	40	0.434	0.534	0.618	1.431	0.594
60-1	60	0.422	0.520	0.605	1.402	0.582
60-2	60	0.426	0.529	0.615	1.423	0.591
60-3	60	0.432	0.534	0.619	1.434	0.596
90-1	90	0.422	0.528	0.617	1.429	0.593
90-2	90	0.426	0.531	0.620	1.435	0.596
90-3	90	0.432	0.542	0.625	1.446	0.601

Table B-9. BTEX sorption data from MSB-0.5O batch experiment.

Sample	Experiment Time (min)	Amount Sorbed (mmol/kg)				
		Benzene	Toluene	Ethylbenzene	M-Xylene	O-Xylene
0.5-1	0.5	0.186	0.224	0.251	0.254	0.656
0.5-2	0.5	0.207	0.238	0.267	0.270	0.691
1-2	1	0.265	0.360	0.353	0.294	0.931
1-3	1	0.250	0.339	0.351	0.293	0.920
2-1	2	0.308	0.390	0.397	0.403	1.051
2-2	2	0.337	0.417	0.431	0.438	1.139
2-3	2.1	0.322	0.410	0.419	0.426	1.115
4-1	4	0.392	0.494	0.520	0.529	1.378
4-2	4	0.380	0.485	0.510	0.528	1.351
4-3	4	0.369	0.469	0.492	0.502	1.301
6-1	6	0.408	0.511	0.537	0.547	1.416
6-3	6	0.422	0.519	0.542	0.552	1.429
9-1	9	0.447	0.534	0.554	0.563	1.459
9-2	9	0.429	0.520	0.546	0.556	1.441
12-1	12	0.442	0.535	0.559	0.569	1.473
12-2	12.3	0.433	0.536	0.562	0.572	1.485
12-3	12	0.447	0.542	0.565	0.575	1.490
15-1	15	0.458	0.558	0.575	0.585	1.517
15-2	15	0.458	0.555	0.573	0.583	1.510
15-3	15	0.442	0.543	0.568	0.578	1.497
20-1	20	0.456	0.551	0.570	0.580	1.502
20-2	20	0.473	0.560	0.576	0.586	1.519
20-3	20	0.476	0.567	0.579	0.589	1.528
25-1	25	0.458	0.553	0.568	0.583	1.515
25-2	25.3	0.463	0.556	0.571	0.585	1.518
25-3	25	0.463	0.556	0.572	0.587	1.522
30-1	30	0.463	0.557	0.574	0.584	1.520
30-2	30	0.469	0.562	0.580	0.590	1.533
30-3	30	0.447	0.553	0.577	0.587	1.524
40-1	40	0.471	0.563	0.579	0.589	1.534
40-2	40	0.468	0.565	0.582	0.592	1.539
40-3	40	0.468	0.565	0.583	0.593	1.541
60-1	60	0.449	0.551	0.571	0.581	1.511
60-2	60	0.476	0.584	0.590	0.600	1.560
60-3	60	0.459	0.563	0.582	0.593	1.540
90-1	90	0.456	0.558	0.575	0.586	1.523
90-2	90	0.468	0.568	0.585	0.595	1.547
90-3	90	0.464	0.567	0.585	0.595	1.547

Table B-10. BTEX sorption data from MSB-0.35T batch experiment.

Sample	Experiment Time (min)	Amount Sorbed (mmol/kg)				
		Benzene	Toluene	Ethylbenzene	M-Xylene	O-Xylene
0.5-1	0.5	0.173	0.356	0.253	0.262	0.253
0.5-2	0.5	0.150	0.322	0.251	0.258	0.246
0.5-3	4	0.396	0.812	0.511	0.523	0.513
1-1	1	0.250	0.502	0.314	0.271	0.314
1-2	1	0.259	0.507	0.313	0.268	0.312
1-3	1	0.256	0.521	0.326	0.284	0.325
2-1	2	0.345	0.680	0.402	0.412	0.408
2-2	2	0.333	0.674	0.394	0.403	0.401
2-3	2	0.337	0.672	0.398	0.408	0.404
4-1	4	0.382	0.800	0.501	0.513	0.504
4-2	4	0.378	0.786	0.488	0.500	0.491
4-3	4	0.372	0.788	0.494	0.506	0.497
6-1	6	0.433	0.861	0.538	0.550	0.538
6-2	6	0.434	0.838	0.528	0.541	0.530
6-3	5.9	0.438	0.877	0.544	0.556	0.544
9-1	9	0.448	0.891	0.558	0.571	0.559
9-2	2.8	0.370	0.755	0.449	0.459	0.453
9-3	9	0.460	0.905	0.565	0.578	0.565
12-1	12	0.462	0.886	0.558	0.571	0.560
12-2	12	0.477	0.903	0.565	0.578	0.567
15-1	15.1	0.471	0.923	0.573	0.586	0.574
15-2	15	0.490	0.936	0.576	0.589	0.577
15-3	15	0.484	0.936	0.578	0.591	0.580
20-1	20	0.486	0.940	0.579	0.592	0.579
20-2	20	0.491	0.947	0.583	0.596	0.584
20-3	20	0.475	0.934	0.579	0.593	0.581
25-1	25	0.480	0.931	0.577	0.592	0.581
25-2	25	0.480	0.930	0.577	0.591	0.580
25-3	25	0.478	0.934	0.580	0.594	0.583
30-1	30	0.477	0.941	0.579	0.592	0.580
30-2	30	0.475	0.940	0.583	0.596	0.585
40-1	40	0.487	0.953	0.585	0.598	0.586
40-2	40	0.470	0.941	0.585	0.598	0.586
40-3	40	0.483	0.952	0.588	0.601	0.590
60-1	60	0.494	0.965	0.594	0.607	0.596
60-2	60	0.485	0.956	0.590	0.603	0.592
60-3	60	0.483	0.950	0.586	0.599	0.588
90-1	90	0.490	0.956	0.587	0.600	0.589
90-2	90	0.490	0.965	0.595	0.608	0.598
90-3	90	0.489	0.964	0.594	0.608	0.597

Table B-11. BTEX sorption data from MSB-0.35E batch experiment.

Sample	Experiment Time (min)	Amount Sorbed (mmol/kg)				
		Benzene	Toluene	Ethylbenzene	M-Xylene	O-Xylene
0.5-1	0.5	0.162	0.202	0.486	0.261	0.271
0.5-2	0.5	0.195	0.227	0.480	0.256	0.267
0.5-3	0.5	0.158	0.186	0.363	0.189	0.203
1-1	1	0.274	0.320	0.608	0.281	0.352
1-2	1	0.231	0.281	0.550	0.244	0.319
2-1	2	0.328	0.395	0.753	0.409	0.433
2-2	2	0.316	0.398	0.724	0.391	0.420
2-3	2	0.328	0.397	0.708	0.384	0.412
4-1	4	0.381	0.489	0.945	0.515	0.547
4-2	4	0.382	0.485	0.917	0.499	0.534
4-3	4	0.374	0.483	0.925	0.505	0.540
6-1	6	0.413	0.513	0.973	0.539	0.567
6-2	6	0.425	0.516	0.966	0.528	0.563
6-3	6	0.420	0.518	0.976	0.534	0.570
9-1	9	0.438	0.533	1.000	0.546	0.582
9-2	9	0.446	0.541	1.015	0.555	0.591
9-3	9	0.425	0.528	1.002	0.548	0.583
12-1	12	0.454	0.549	1.022	0.558	0.595
12-2	12	0.432	0.547	1.036	0.567	0.603
12-3	12	0.430	0.530	1.011	0.554	0.590
15-1	15	0.452	0.550	1.028	0.562	0.600
15-2	15	0.443	0.545	1.027	0.562	0.600
15-3	15	0.441	0.540	1.024	0.560	0.597
20-1	20	0.464	0.559	1.038	0.567	0.604
20-2	20	0.467	0.567	1.045	0.571	0.610
20-3	20	0.452	0.553	1.035	0.566	0.604
25-1	25	0.461	0.558	1.036	0.568	0.606
25-2	25	0.460	0.560	1.041	0.571	0.610
30-1	30	0.466	0.562	1.044	0.569	0.606
30-2	30	0.464	0.564	1.050	0.574	0.612
30-3	30	0.457	0.559	1.043	0.570	0.609
40-1	40	0.451	0.559	1.047	0.571	0.609
40-2	40	0.471	0.569	1.057	0.577	0.617
40-3	40	0.469	0.569	1.056	0.577	0.617
60-1	60	0.463	0.565	1.050	0.574	0.614
60-2	60	0.472	0.573	1.063	0.581	0.622
60-3	60	0.469	0.571	1.059	0.579	0.620
90-1	90	0.462	0.567	1.055	0.577	0.617
90-2	90	0.468	0.572	1.064	0.582	0.622
90-3	90	0.468	0.572	1.062	0.581	0.622

Table B-12. BTEX sorption data from MSB-0.35M batch experiment.

Sample	Experiment Time (min)	Amount Sorbed (mmol/kg)				
		Benzene	Toluene	Ethylbenzene	M-Xylene	O-Xylene
0.5-1	0.5	0.139	0.185	0.238	0.423	0.231
0.5-2	0.5	0.113	0.159	0.206	0.367	0.199
0.5-3	0.5	0.161	0.214	0.252	0.447	0.245
1-1	1	0.263	0.333	0.359	0.622	0.351
1-2	1	0.216	0.284	0.301	0.513	0.289
1-3	1	0.275	0.346	0.350	0.595	0.335
2-2	2	0.318	0.397	0.410	0.715	0.400
2-3	2	0.305	0.380	0.409	0.716	0.395
4-1	4	0.379	0.463	0.505	0.883	0.488
4-2	4	0.340	0.443	0.497	0.867	0.482
4-3	4	0.360	0.466	0.526	0.917	0.510
6-1	6	0.408	0.506	0.558	0.970	0.538
6-2	6	0.419	0.510	0.559	0.972	0.539
6-3	6	0.418	0.512	0.564	0.981	0.545
9-2	9	0.435	0.525	0.579	1.005	0.559
9-3	9	0.435	0.527	0.582	1.011	0.562
12-1	12	0.443	0.511	0.571	0.995	0.553
12-2	12	0.428	0.520	0.579	1.007	0.560
12-3	12	0.448	0.545	0.590	1.025	0.570
15-1	15	0.448	0.534	0.587	1.020	0.567
15-3	15	0.455	0.538	0.590	1.024	0.570
20-1	20	0.459	0.548	0.595	1.032	0.574
20-2	20	0.467	0.555	0.602	1.044	0.582
25-1	25	0.462	0.543	0.598	1.039	0.578
25-2	25	0.458	0.540	0.596	1.036	0.577
25-3	25	0.461	0.540	0.595	1.035	0.576
30-1	30	0.478	0.560	0.602	1.046	0.580
30-2	30	0.471	0.556	0.603	1.047	0.583
30-3	30	0.457	0.550	0.602	1.045	0.582
40-1	40	0.465	0.556	0.604	1.050	0.583
40-2	40	0.449	0.550	0.603	1.049	0.584
40-3	40	0.454	0.552	0.605	1.050	0.585
60-1	60	0.468	0.555	0.601	1.043	0.582
60-2	60	0.460	0.557	0.607	1.053	0.588
60-3	60	0.459	0.556	0.607	1.054	0.588
90-1	90	0.458	0.553	0.602	1.046	0.583
90-2	90	0.462	0.559	0.609	1.057	0.590
90-3	90	0.464	0.560	0.609	1.058	0.590

Table B-13. BTEX sorption data from MSB-0.35O batch experiment.

Sample	Experiment Time (min)	Amount Sorbed (mmol/kg)				
		Benzene	Toluene	Ethylbenzene	M-Xylene	O-Xylene
0.5-1	0.5	0.168	0.223	0.270	0.268	0.473
0.5-2	0.5	0.154	0.208	0.237	0.235	0.420
0.5-3	0.5	0.118	0.177	0.231	0.230	0.403
1-1	1	0.187	0.259	0.312	0.291	0.547
1-2	1	0.244	0.304	0.311	0.288	0.543
1-3	1	0.260	0.337	0.351	0.329	0.617
2-1	2	0.337	0.434	0.434	0.427	0.767
2-2	2	0.351	0.440	0.431	0.424	0.765
2-3	2	0.308	0.408	0.415	0.409	0.737
4-1	4	0.350	0.477	0.500	0.493	0.888
4-2	4	0.344	0.468	0.493	0.486	0.873
4-3	4	0.358	0.479	0.506	0.499	0.893
6-1	6	0.401	0.519	0.539	0.531	0.951
6-3	6	0.403	0.519	0.537	0.529	0.948
9-1	9	0.412	0.530	0.551	0.543	0.971
9-2	9	0.420	0.538	0.559	0.550	0.986
9-3	9	0.425	0.541	0.560	0.551	0.987
12-2	12	0.422	0.538	0.562	0.554	0.991
12-3	12	0.426	0.553	0.569	0.561	1.004
15-1	15	0.435	0.555	0.573	0.564	1.011
15-2	15	0.443	0.562	0.574	0.565	1.012
15-3	15	0.441	0.555	0.572	0.563	1.009
20-1	20	0.432	0.552	0.570	0.562	1.005
20-2	20	0.442	0.560	0.578	0.569	1.021
20-3	20	0.437	0.557	0.575	0.567	1.017
25-1	25.3	0.434	0.559	0.576	0.569	1.023
25-2	25	0.440	0.560	0.576	0.570	1.023
25-3	25	0.424	0.552	0.572	0.566	1.016
30-1	30	0.449	0.564	0.577	0.568	1.020
30-2	30.2	0.445	0.565	0.581	0.573	1.028
30-3	30	0.441	0.563	0.581	0.572	1.026
40-1	40	0.434	0.562	0.580	0.572	1.029
40-2	40	0.439	0.565	0.583	0.574	1.032
40-3	40	0.443	0.567	0.584	0.575	1.034
60-1	60	0.451	0.568	0.581	0.573	1.029
60-2	60	0.434	0.564	0.583	0.575	1.032
60-3	60	0.434	0.566	0.585	0.577	1.036
90-2	90	0.444	0.572	0.589	0.581	1.043
90-3	90	0.439	0.570	0.589	0.581	1.043

Table B-14. Overall results from MSB-0.05 batch experiment.

Constituent	K_d (L/kg)	k_2 (1/hr)	F	Bicontinuum Fit (r^2)	Starting Conc. (mmol/L)	Water Added (mL)	Zeolite Added (g)	Log K_{ow}	Solubility (mg/L)
Benzene	7.76	9.27	0.20	0.957	0.047	9.81	3.002	2.13	1850
Toluene	18.22	4.73	0.11	0.890	0.049	9.81	3.002	2.69	470
Ethylbenzene	36.25	3.59	0.07	0.931	0.05	9.81	3.002	3.15	140
M-Xylene	38.33	3.55	0.06	0.924	0.049	9.81	3.002	3.20	173
O-Xylene	34.39	3.45	0.07	0.912	0.05	9.81	3.002	3.15	204

Table B-15. Overall results from MSB-0.1 batch experiment.

Constituent	K_d (L/kg)	k_2 (1/hr)	F	Bicontinuum Fit (r^2)	Starting Conc. (mmol/L)	Water Added (mL)	Zeolite Added (g)	Log K_{ow}	Solubility (mg/L)
Benzene	7.27	8.52	0.16	0.96	0.103	9.77	3.002	2.13	1850
Toluene	17.53	4.96	0.09	0.939	0.112	9.77	3.002	2.69	470
Ethylbenzene	34.73	3.40	0.04	0.921	0.098	9.77	3.002	3.15	140
M-Xylene	37.25	2.95	0.03	0.947	0.098	9.77	3.002	3.2	173
O-Xylene	34.41	3.19	0.04	0.923	0.108	9.77	3.002	3.15	204

Table B-16. Overall results from MSB-0.2 batch experiment.

Constituent	K_d (L/kg)	k_2 (1/hr)	F	Bicontinuum Fit (r^2)	Starting Conc. (mmol/L)	Water Added (mL)	Zeolite Added (g)	Log K_{ow}	Solubility (mg/L)
Benzene	7.31	7.61	0.2	0.984	0.214	9.85	2.998	2.13	1850
Toluene	17.68	4.45	0.08	0.945	0.194	9.85	2.998	2.69	470
Ethylbenzene	35.37	2.63	0.03	0.944	0.193	9.85	2.998	3.15	140
M-Xylene	37.51	2.14	0.01	0.9	0.187	9.85	2.998	3.2	173
O-Xylene	34.71	2.54	0.03	0.938	0.211	9.85	2.998	3.15	204

Table B-17. Overall results from MSB-0.3 batch experiment.

Constituent	K_d (L/kg)	k_2 (1/hr)	F	Bicontinuum Fit (r^2)	Starting Conc. (mmol/L)	Water Added (mL)	Zeolite Added (g)	Log K_{ow}	Solubility (mg/L)
Benzene	7.67	6.5	0.11	0.925	0.293	9.84	3	2.13	1850
Toluene	17.96	3.84	0.06	0.923	0.296	9.84	3	2.69	470
Ethylbenzene	35.44	2.41	0.04	0.96	0.282	9.84	3	3.15	140
M-Xylene	37.9	1.94	0.04	0.943	0.27	9.84	3	3.2	173
O-Xylene	34.91	2.35	0.04	0.962	0.28	9.84	3	3.15	204

Table B-18. Overall results from MSB-0.35T batch experiment.

Constituent	K_d (L/kg)	k_2 (1/hr)	F	Bicontinuum Fit (r^2)	Starting Conc. (mmol/L)	Water Added (mL)	Zeolite Added (g)	Log K_{ow}	Solubility (mg/L)
Benzene	7.85	7.07	0.14	0.954	0.2	9.78	3.003	2.13	1850
Toluene	18.6	3.63	0.07	0.908	0.476	9.78	3.003	2.69	470
Ethylbenzene	35.09	2.05	0.03	0.926	0.189	9.78	3.003	3.15	140
M-Xylene	36.58	1.87	0.02	0.922	0.179	9.78	3.003	3.2	173
O-Xylene	33.94	2.03	0.03	0.913	0.184	9.78	3.003	3.15	204

Table B-19. Overall results from MSB-0.35E batch experiment.

Constituent	K_d (L/kg)	k_2 (1/hr)	F	Bicontinuum Fit (r^2)	Starting Conc. (mmol/L)	Water Added (mL)	Zeolite Added (g)	Log K_{ow}	Solubility (mg/L)
Benzene	7.13	7.75	0.12	0.924	0.188	9.89	3.004	2.13	1850
Toluene	17.25	4.35	0.06	0.939	0.195	9.89	3.004	2.69	470
Ethylbenzene	35.42	2.34	0.05	0.95	0.475	9.89	3.004	3.15	140
M-Xylene	36.39	2.07	0.03	0.895	0.19	9.89	3.004	3.2	173
O-Xylene	33.14	2.26	0.04	0.925	0.201	9.89	3.004	3.15	204

Table B-20. Overall results from MSB-0.35M batch experiment.

Constituent	K_d (L/kg)	k_2 (1/hr)	F	Bicontinuum Fit (r^2)	Starting Conc. (mmol/L)	Water Added (mL)	Zeolite Added (g)	Log K_{ow}	Solubility (mg/L)
Benzene	7.55	7.08	0.18	0.975	0.188	9.84	3.008	2.13	1850
Toluene	17.3	3.52	0.07	0.957	0.192	9.84	3.008	2.69	470
Ethylbenzene	34.86	2.16	0.04	0.965	0.205	9.84	3.008	3.15	140
M-Xylene	37.98	1.92	0.03	0.947	0.472	9.84	3.008	3.2	173
O-Xylene	33.9	2.1	0.04	0.931	0.197	9.84	3.008	3.15	204

Table B-21. Overall results from MSB-0.35O batch experiment.

Constituent	K_d (L/kg)	k_2 (1/hr)	F	Bicontinuum Fit (r^2)	Starting Conc. (mmol/L)	Water Added (mL)	Zeolite Added (g)	Log K_{ow}	Solubility (mg/L)
Benzene	7.21	6.94	0.15	0.971	0.205	9.87	2.998	2.13	1850
Toluene	17.68	3.33	0.08	0.902	0.202	9.87	2.998	2.69	470
Ethylbenzene	34.77	2.08	0.04	0.908	0.192	9.87	2.998	3.15	140
M-Xylene	37.4	2.16	0.03	0.941	0.192	9.87	2.998	3.2	173
O-Xylene	35.24	1.93	0.04	0.894	0.509	9.87	2.998	3.15	204

Table B-22. Overall results from MSB-0.5T batch experiment.

Constituent	K_d (L/kg)	k_2 (1/hr)	F	Bicontinuum Fit (r^2)	Starting Conc. (mmol/L)	Water Added (mL)	Zeolite Added (g)	Log K_{ow}	Solubility (mg/L)
Benzene	7.27	7.11	0.11	0.966	0.214	9.80	3.005	2.13	1850
Toluene	17.75	3.54	0.05	0.92	0.344	9.80	3.005	2.69	470
Ethylbenzene	35.01	2.21	0.03	0.961	0.196	9.80	3.005	3.15	140
M-Xylene	37.36	2.05	0.02	0.955	0.199	9.80	3.005	3.2	173
O-Xylene	34.72	2.18	0.03	0.954	0.197	9.80	3.005	3.15	204

Table B-23. Overall results from MSB-0.5E batch experiment.

Constituent	K _d (L/kg)	k ₂ (1/hr)	F	Bicontinuum Fit (r ²)	Starting Conc. (mmol/L)	Water Added (mL)	Zeolite Added (g)	Log K _{ow}	Solubility (mg/L)
Benzene	7.64	6.81	0.11	0.961	0.202	9.84	3.003	2.13	1850
Toluene	17.66	3.87	0.05	0.945	0.204	9.84	3.003	2.69	470
Ethylbenzene	36.09	2.35	0.03	0.93	0.349	9.84	3.003	3.15	140
M-Xylene	37.7	2.22	0.02	0.964	0.19	9.84	3.003	3.2	173
O-Xylene	34.8	2.33	0.03	0.961	0.205	9.84	3.003	3.15	204

Table B-24. Overall results from MSB-0.5M batch experiment.

Constituent	K _d (L/kg)	k ₂ (1/hr)	F	Bicontinuum Fit (r ²)	Starting Conc. (mmol/L)	Water Added (mL)	Zeolite Added (g)	Log K _{ow}	Solubility (mg/L)
Benzene	7.43	7.1	0.08	0.971	0.203	9.81	2.999	2.13	1850
Toluene	17.31	4.11	0.05	0.941	0.201	9.81	2.999	2.69	470
Ethylbenzene	34.52	2.35	0.02	0.946	0.202	9.81	2.999	3.15	140
M-Xylene	37.49	2.23	0.02	0.954	0.348	9.81	2.999	3.2	173
O-Xylene	34.14	2.38	0.02	0.944	0.195	9.81	2.999	3.15	204

Table B-25. Overall results from MSB-0.5O batch experiment.

Constituent	K _d (L/kg)	k ₂ (1/hr)	F	Bicontinuum Fit (r ²)	Starting Conc. (mmol/L)	Water Added (mL)	Zeolite Added (g)	Log K _{ow}	Solubility (mg/L)
Benzene	7.53	7.4	0.08	0.932	0.192	9.84	3.001	2.13	1850
Toluene	17.63	3.91	0.04	0.924	0.204	9.84	3.001	2.69	470
Ethylbenzene	34.91	2.46	0.03	0.96	0.194	9.84	3.001	3.15	140
M-Xylene	37.4	2.23	0.02	0.938	0.19	9.84	3.001	3.2	173
O-Xylene	34.98	2.4	0.03	0.957	0.343	9.84	3.001	3.15	204

APPENDIX C. MONOLAYER SMZ BATCH EXPERIMENT DATA

The monolayer batch experiment data is contained in this appendix. Tables C-1 through C-3 contain the BTEX sorption data from each experiment. The overall results from each experiment are displayed in Tables C-4 through C-6. Three replicate batch experiments with the same initial conditions were run, and are referred to as M1, M2, and M3 batch experiments.

Table C-1. BTEX sorption data from M1 monolayer batch experiment.

Sample	Experiment Time (min)	Amount Sorbed (mmol/kg)				
		Benzene	Toluene	Ethylbenzene	M-Xylene	O-Xylene
0.5-1	0.5	0.176	0.240	0.271	0.326	0.279
0.5-2	0.5	0.154	0.228	0.264	0.318	0.272
0.5-3	0.5	0.140	0.233	0.274	0.331	0.284
1-1	1	0.132	0.195	0.253	0.307	0.264
1-2	1	0.140	0.200	0.255	0.310	0.267
1-3	1	0.152	0.206	0.260	0.316	0.271
2-1	2	0.180	0.248	0.286	0.344	0.298
2-2	2	0.173	0.233	0.271	0.327	0.282
2-3	2	0.158	0.230	0.273	0.330	0.285
4-1	4	0.170	0.236	0.276	0.334	0.289
4-2	4	0.148	0.224	0.271	0.329	0.285
4-3	4	0.170	0.242	0.283	0.342	0.297
6-1	6.67	0.197	0.262	0.295	0.355	0.309
6-2	6	0.198	0.262	0.295	0.355	0.308
6-3	6	0.185	0.247	0.288	0.347	0.301
9-1	9	0.210	0.266	0.296	0.355	0.309
9-2	9	0.188	0.259	0.294	0.355	0.308
9-3	9	0.214	0.279	0.304	0.365	0.317
12-1	12	0.177	0.252	0.292	0.352	0.306
12-2	12	0.178	0.252	0.291	0.351	0.306
12-3	12	0.187	0.258	0.295	0.356	0.310
15-2	15	0.215	0.277	0.305	0.367	0.319
15-3	15	0.229	0.285	0.309	0.371	0.324
20-1	20	0.205	0.272	0.302	0.364	0.317
20-2	20	0.223	0.284	0.310	0.372	0.325
25-1	25	0.219	0.281	0.309	0.371	0.323
25-2	25	0.215	0.281	0.309	0.372	0.324
25-3	25	0.215	0.281	0.310	0.372	0.325
30-1	30	0.242	0.295	0.313	0.375	0.325
30-2	30	0.215	0.280	0.308	0.370	0.322
30-3	30	0.238	0.289	0.312	0.374	0.326
40-1	40	0.211	0.278	0.306	0.368	0.319
40-2	40	0.206	0.276	0.306	0.368	0.321
40-3	40	0.219	0.284	0.310	0.373	0.326
60-1	60	0.228	0.286	0.309	0.372	0.324
60-2	60	0.224	0.286	0.311	0.374	0.327
60-3	60	0.217	0.284	0.311	0.374	0.327
90-1	90	0.208	0.280	0.309	0.372	0.325
90-2	90	0.222	0.288	0.314	0.378	0.330
90-3	90	0.219	0.287	0.315	0.379	0.331

Table C-2. BTEX sorption data from M2 monolayer batch experiment.

Sample	Experiment Time (min)	Amount Sorbed (mmol/kg)				
		Benzene	Toluene	Ethylbenzene	M-Xylene	O-Xylene
0.5-1	0.5	0.187	0.237	0.272	0.281	0.291
0.5-2	0.5	0.176	0.231	0.272	0.281	0.290
0.5-3	0.5	0.165	0.224	0.265	0.274	0.284
1-1	1	0.154	0.230	0.279	0.287	0.301
1-2	1	0.166	0.240	0.287	0.295	0.310
1-3	1	0.157	0.235	0.284	0.293	0.306
2-1	2	0.193	0.258	0.292	0.301	0.314
2-2	2	0.206	0.265	0.296	0.305	0.318
2-3	2	0.220	0.276	0.303	0.312	0.326
4-1	4	0.213	0.280	0.309	0.318	0.332
4-2	4	0.209	0.274	0.305	0.313	0.327
4-3	4	0.216	0.282	0.311	0.320	0.335
6-1	6	0.201	0.265	0.303	0.313	0.328
6-2	6	0.207	0.268	0.303	0.312	0.326
6-3	6	0.211	0.284	0.316	0.325	0.341
9-1	9	0.220	0.297	0.320	0.329	0.345
9-2	9	0.239	0.308	0.326	0.334	0.351
9-3	9	0.228	0.301	0.322	0.330	0.346
12-1	12	0.221	0.288	0.317	0.325	0.341
12-2	12	0.228	0.294	0.320	0.329	0.346
12-3	12	0.225	0.292	0.319	0.328	0.345
15-1	15	0.212	0.283	0.316	0.325	0.341
15-2	15	0.215	0.285	0.316	0.326	0.342
15-3	15	0.237	0.301	0.324	0.333	0.350
20-1	20	0.246	0.307	0.328	0.336	0.354
20-2	20	0.231	0.295	0.320	0.328	0.345
20-3	20	0.256	0.313	0.329	0.337	0.354
25-1	25	0.239	0.303	0.326	0.335	0.352
25-2	25	0.241	0.303	0.325	0.333	0.350
25-3	25	0.235	0.302	0.327	0.335	0.352
30-1	30	0.246	0.307	0.327	0.335	0.351
30-2	30	0.235	0.300	0.324	0.333	0.349
30-3	30	0.250	0.310	0.329	0.338	0.355
40-1	40	0.246	0.306	0.325	0.333	0.349
40-2	40	0.238	0.305	0.328	0.336	0.353
40-3	40	0.233	0.302	0.327	0.336	0.353
60-1	60	0.236	0.297	0.322	0.331	0.349
60-2	60	0.227	0.294	0.323	0.332	0.350
90-1	90	0.233	0.300	0.326	0.335	0.353
90-2	90	0.238	0.305	0.330	0.339	0.357
90-3	90	0.240	0.307	0.331	0.339	0.358

Table C-3. BTEX sorption data from M3 monolayer batch experiment.

Sample	Experiment Time (min)	Amount Sorbed (mmol/kg)				
		Benzene	Toluene	Ethylbenzene	M-Xylene	O-Xylene
0.5-1	0.5	0.149	0.221	0.278	0.277	0.291
0.5-2	0.5	0.156	0.220	0.274	0.273	0.286
0.5-3	0.5	0.123	0.190	0.246	0.247	0.260
1-1	1	0.131	0.212	0.273	0.271	0.288
1-2	1	0.119	0.199	0.263	0.261	0.277
1-3	1	0.127	0.207	0.268	0.267	0.283
2-1	2	0.180	0.247	0.290	0.288	0.305
2-2	2	0.183	0.261	0.302	0.299	0.317
2-3	2	0.191	0.264	0.302	0.300	0.318
4-1	4	0.182	0.250	0.293	0.291	0.307
4-3	4	0.192	0.262	0.304	0.302	0.320
6-1	6	0.188	0.261	0.304	0.302	0.321
6-2	6	0.176	0.251	0.298	0.296	0.314
9-1	9	0.201	0.270	0.309	0.307	0.325
9-2	9	0.209	0.272	0.310	0.306	0.325
9-3	9	0.210	0.272	0.308	0.305	0.324
12-1	12	0.200	0.270	0.310	0.307	0.327
12-2	12	0.187	0.263	0.306	0.304	0.323
12-3	12	0.199	0.268	0.308	0.305	0.324
15-1	15	0.201	0.270	0.311	0.308	0.328
15-2	15	0.195	0.268	0.310	0.307	0.327
15-3	15	0.205	0.272	0.311	0.308	0.328
20-1	20	0.216	0.281	0.316	0.312	0.332
20-2	20	0.228	0.288	0.320	0.316	0.336
20-3	20	0.233	0.294	0.322	0.318	0.338
25-1	24.57	0.219	0.281	0.316	0.311	0.330
25-2	25	0.222	0.285	0.320	0.314	0.335
25-3	25	0.223	0.283	0.318	0.312	0.332
30-1	30	0.222	0.285	0.317	0.313	0.332
30-2	30	0.226	0.286	0.318	0.315	0.335
30-3	30	0.232	0.292	0.322	0.319	0.340
40-1	40	0.222	0.294	0.321	0.316	0.336
40-2	40	0.225	0.288	0.321	0.317	0.337
40-3	40	0.225	0.294	0.323	0.319	0.340
60-1	60	0.221	0.284	0.316	0.313	0.333
60-2	60	0.225	0.288	0.320	0.317	0.337
60-3	60	0.224	0.288	0.320	0.317	0.338
90-1	90	0.213	0.282	0.317	0.314	0.335
90-2	90	0.204	0.279	0.318	0.315	0.335
90-3	90	0.216	0.285	0.321	0.317	0.338

Table C-4. Overall results from M1 monolayer batch experiment.

Constituent	K_d (L/kg)	k₂ (1/hr)	F	Bicontinuum Fit (r²)	Starting Conc. (mmol/L)	Water Added (mL)	Zeolite Added (g)	Log K_{ow}	Solubility (mg/L)
Benzene	5.25	4.97	0.43	0.784	0.108	9.94	2.997	2.13	1850
Toluene	12.86	4.08	0.39	0.811	0.107	9.94	2.997	2.69	470
Ethylbenzene	26.61	3.59	0.36	0.889	0.105	9.94	2.997	3.15	140
M-Xylene	28.26	3.8	0.36	0.895	0.125	9.94	2.997	3.2	173
O-Xylene	25.33	3.48	0.35	0.908	0.111	9.94	2.997	3.15	204

Table C-5. Overall results from M2 monolayer batch experiment.

Constituent	K_d (L/kg)	k₂ (1/hr)	F	Bicontinuum Fit (r²)	Starting Conc. (mmol/L)	Water Added (mL)	Zeolite Added (g)	Log K_{ow}	Solubility (mg/L)
Benzene	6.22	5.91	0.44	0.781	0.11	9.97	2.996	2.13	1850
Toluene	13.53	5.18	0.36	0.864	0.114	9.97	2.996	2.69	470
Ethylbenzene	26.85	4.97	0.33	0.907	0.11	9.97	2.996	3.15	140
M-Xylene	28.52	4.26	0.32	0.897	0.113	9.97	2.996	3.2	173
O-Xylene	25.57	4.57	0.33	0.904	0.12	9.97	2.996	3.15	204

Table C-6. Overall results from M3 monolayer batch experiment.

Constituent	K_d (L/kg)	k₂ (1/hr)	F	Bicontinuum Fit (r²)	Starting Conc. (mmol/L)	Water Added (mL)	Zeolite Added (g)	Log K_{ow}	Solubility (mg/L)
Benzene	5.99	6.35	0.38	0.766	0.105	9.97	3.004	2.13	1850
Toluene	13.83	4.25	0.36	0.772	0.107	9.97	3.004	2.69	470
Ethylbenzene	28.3	4.49	0.35	0.817	0.107	9.97	3.004	3.15	140
M-Xylene	30.09	4.71	0.35	0.816	0.105	9.97	3.004	3.2	173
O-Xylene	27	4.85	0.36	0.831	0.113	9.97	3.004	3.15	204

APPENDIX D. BTEX ISOTHERMS FROM BATCH EXPERIMENT'S EQUILIBRIUM DATA.

Overall, nineteen batch experiments were run for the current research project. Because each vial was essentially an independent batch experiment, hundreds of equilibrium data points (vials allowed to shake for greater than twenty minutes) for each constituent were gathered. Batch equilibrium isotherms for individual constituents were constructed using the equilibrium data from each test. The equilibrium batch experiment data can be seen in Tables D-1 through D-5, and the overall isotherm results can be seen in Table D-6. Figures D-1 through D-5 represent the isotherm results from the equilibrium batch experiment data. Prior to this analysis, complete equilibrium was assumed to occur after twenty minutes. However, inspection of Figures D-1 through D-5 reveals that only a “quasi” equilibrium was reached over the entire batch experiment time period. Minimal changes (3-5.5%) in total sorption are observed; however, a 10-30% change in “equilibrium” aqueous concentration is observed for all five constituents at maximum concentrations (see Table D-7). As expected, a closer inspection of the data revealed a decreasing trend in aqueous concentration over the entire “equilibrium” period. The data from twenty minutes and ninety minutes (batch experiment completion) can be seen in Tables D-8 through D-12, with the overall data trends in Table D-7. Figures D-6 through D-10 display the “equilibrium” conditions for the twenty and ninety minute samples. These results indicate an increase in K_d from the ninety-minute samples, representing a decrease in aqueous concentration.

Table D-1. Benzene equilibrium data from kinetic batch experiments

Aqueous Concentration (mmol/L)	Amount Sorbed (mg/kg)	Aqueous Concentration (mmol/L)	Amount Sorbed (mg/kg)	Aqueous Concentration (mmol/L)	Amount Sorbed (mg/kg)
0.081	0.596	0.015	0.107	0.064	0.490
0.081	0.586	0.014	0.108	0.067	0.485
0.074	0.625	0.013	0.113	0.065	0.486
0.073	0.626	0.013	0.112	0.059	0.500
0.074	0.607	0.013	0.111	0.089	0.667
0.073	0.625	0.014	0.111	0.086	0.677
0.074	0.624	0.014	0.107	0.088	0.671
0.066	0.647	0.014	0.110	0.085	0.676
0.078	0.609	0.014	0.109	0.088	0.677
0.075	0.599	0.013	0.112	0.085	0.687
0.078	0.609	0.013	0.112	0.084	0.688
0.075	0.619	0.032	0.232	0.086	0.680
0.077	0.609	0.032	0.230	0.083	0.689
0.076	0.617	0.032	0.232	0.089	0.653
0.075	0.619	0.035	0.227	0.090	0.670
0.079	0.615	0.032	0.230	0.092	0.657
0.073	0.626	0.034	0.224	0.089	0.674
0.081	0.551	0.030	0.238	0.087	0.675
0.084	0.539	0.031	0.234	0.092	0.652
0.085	0.541	0.030	0.237	0.092	0.663
0.083	0.552	0.033	0.226	0.085	0.683
0.078	0.560	0.031	0.232	0.061	0.457
0.083	0.539	0.031	0.233	0.059	0.458
0.076	0.562	0.033	0.230	0.060	0.455
0.077	0.564	0.032	0.232	0.059	0.462
0.076	0.561	0.030	0.236	0.062	0.454
0.078	0.562	0.032	0.233	0.058	0.464
0.072	0.582	0.031	0.231	0.057	0.468
0.074	0.579	0.032	0.236	0.058	0.462
0.076	0.574	0.067	0.484	0.058	0.462
0.079	0.568	0.068	0.478	0.057	0.466
0.077	0.569	0.067	0.480	0.057	0.463
0.077	0.562	0.066	0.485	0.059	0.462
0.075	0.576	0.067	0.482	0.056	0.466
0.076	0.565	0.071	0.471	0.057	0.467
0.013	0.109	0.067	0.481	0.061	0.456
0.013	0.115	0.065	0.490	0.060	0.458
0.014	0.110	0.063	0.501	0.058	0.429
0.014	0.110	0.071	0.470	0.060	0.419
0.015	0.107	0.064	0.493	0.057	0.431
0.014	0.111	0.066	0.481	0.062	0.418
0.015	0.107	0.068	0.480	0.060	0.422

Aqueous Concentration (mmol/L)	Amount Sorbed (mg/kg)	Aqueous Concentration (mmol/L)	Amount Sorbed (mg/kg)	Aqueous Concentration (mmol/L)	Amount Sorbed (mg/kg)
0.062	0.419	0.066	0.459	0.061	0.461
0.060	0.422	0.067	0.456	0.057	0.478
0.059	0.424	0.063	0.468	0.058	0.471
0.060	0.419	0.063	0.464	0.063	0.457
0.061	0.416	0.066	0.486	0.061	0.465
0.058	0.427	0.064	0.491	0.067	0.449
0.059	0.425	0.068	0.475	0.064	0.454
0.058	0.427	0.066	0.480	0.062	0.468
0.057	0.433	0.066	0.480	0.063	0.460
0.060	0.420	0.068	0.478	0.062	0.459
0.058	0.423	0.068	0.477	0.063	0.458
0.059	0.429	0.069	0.475	0.062	0.462
0.056	0.431	0.066	0.487	0.062	0.464
0.057	0.435	0.070	0.470	0.060	0.432
0.056	0.431	0.066	0.483	0.057	0.442
0.059	0.423	0.064	0.494	0.059	0.437
0.057	0.428	0.067	0.485	0.059	0.434
0.056	0.434	0.067	0.483	0.058	0.440
0.059	0.419	0.064	0.490	0.063	0.424
0.057	0.428	0.066	0.490	0.056	0.449
0.055	0.434	0.065	0.489	0.055	0.445
0.056	0.429	0.061	0.464	0.057	0.441
0.056	0.434	0.058	0.467	0.059	0.434
0.059	0.422	0.063	0.452	0.059	0.439
0.057	0.426	0.063	0.461	0.056	0.443
0.055	0.432	0.062	0.460	0.057	0.451
0.058	0.422	0.060	0.466	0.059	0.434
0.056	0.426	0.060	0.464	0.060	0.434
0.055	0.432	0.062	0.457	0.058	0.444
0.066	0.456	0.062	0.451	0.057	0.439
0.062	0.473	0.060	0.471		
0.063	0.458	0.058	0.469		
0.064	0.463	0.061	0.463		
0.065	0.463	0.060	0.472		
0.064	0.463	0.060	0.469		
0.063	0.469	0.061	0.462		
0.068	0.447	0.060	0.468		
0.062	0.471	0.059	0.468		
0.063	0.468	0.064	0.459		
0.062	0.468	0.062	0.467		
0.068	0.449	0.061	0.462		
0.061	0.476	0.062	0.458		

Table D-2. Toluene equilibrium data from kinetic batch experiments

Aqueous Concentration (mmol/L)	Amount Sorbed (mg/kg)	Aqueous Concentration (mmol/L)	Amount Sorbed (mg/kg)	Aqueous Concentration (mmol/L)	Amount Sorbed (mg/kg)
0.033	0.492	0.008	0.133	0.029	0.539
0.032	0.496	0.008	0.134	0.030	0.539
0.031	0.500	0.007	0.138	0.031	0.535
0.029	0.508	0.007	0.137	0.024	0.558
0.028	0.508	0.007	0.136	0.026	0.546
0.029	0.506	0.007	0.135	0.050	0.807
0.030	0.503	0.008	0.135	0.046	0.821
0.028	0.511	0.007	0.136	0.050	0.808
0.027	0.511	0.007	0.135	0.048	0.812
0.027	0.513	0.007	0.138	0.050	0.810
0.024	0.521	0.007	0.138	0.044	0.828
0.026	0.517	0.019	0.303	0.043	0.832
0.028	0.510	0.018	0.302	0.045	0.826
0.024	0.523	0.018	0.303	0.043	0.833
0.025	0.522	0.019	0.302	0.045	0.816
0.029	0.508	0.018	0.303	0.045	0.827
0.024	0.523	0.019	0.301	0.048	0.813
0.024	0.520	0.017	0.308	0.044	0.828
0.040	0.615	0.017	0.307	0.043	0.831
0.041	0.609	0.017	0.308	0.046	0.822
0.042	0.610	0.018	0.304	0.042	0.835
0.041	0.615	0.017	0.307	0.073	1.317
0.038	0.621	0.017	0.308	0.075	1.307
0.041	0.609	0.018	0.305	0.070	1.324
0.037	0.622	0.017	0.309	0.084	1.283
0.037	0.625	0.016	0.312	0.075	1.312
0.037	0.621	0.017	0.307	0.072	1.318
0.036	0.626	0.016	0.309	0.071	1.324
0.033	0.638	0.016	0.312	0.071	1.318
0.034	0.635	0.030	0.537	0.065	1.335
0.037	0.626	0.031	0.536	0.069	1.326
0.037	0.628	0.030	0.537	0.068	1.329
0.035	0.630	0.031	0.533	0.067	1.329
0.037	0.623	0.032	0.533	0.072	1.317
0.034	0.635	0.034	0.525	0.067	1.330
0.034	0.632	0.032	0.529	0.066	1.336
0.007	0.137	0.031	0.535	0.073	1.318
0.008	0.134	0.029	0.542	0.069	1.327
0.008	0.134	0.032	0.531	0.033	0.536
0.008	0.133	0.030	0.539	0.033	0.533
0.007	0.135	0.030	0.535	0.032	0.540
0.008	0.132	0.033	0.529	0.034	0.532

Aqueous Concentration (mmol/L)	Amount Sorbed (mg/kg)	Aqueous Concentration (mmol/L)	Amount Sorbed (mg/kg)	Aqueous Concentration (mmol/L)	Amount Sorbed (mg/kg)
0.032	0.538	0.030	0.565	0.029	0.572
0.034	0.533	0.035	0.551	0.033	0.548
0.032	0.537	0.025	0.584	0.031	0.555
0.032	0.536	0.031	0.563	0.037	0.536
0.031	0.540	0.033	0.558	0.034	0.543
0.031	0.538	0.030	0.568	0.035	0.540
0.030	0.544	0.029	0.567	0.035	0.540
0.031	0.539	0.056	0.940	0.030	0.560
0.029	0.549	0.054	0.947	0.030	0.556
0.027	0.554	0.057	0.934	0.032	0.550
0.032	0.537	0.058	0.931	0.030	0.556
0.029	0.544	0.058	0.930	0.033	0.550
0.029	0.549	0.058	0.934	0.031	0.552
0.033	0.523	0.055	0.941	0.031	0.555
0.028	0.536	0.056	0.940	0.030	0.557
0.032	0.528	0.048	0.964	0.030	0.556
0.032	0.526	0.053	0.953	0.031	0.553
0.033	0.522	0.055	0.941	0.029	0.559
0.032	0.525	0.051	0.952	0.030	0.560
0.030	0.534	0.049	0.965	0.035	0.552
0.031	0.529	0.052	0.956	0.032	0.560
0.030	0.531	0.053	0.950	0.034	0.557
0.030	0.532	0.051	0.956	0.032	0.559
0.030	0.532	0.050	0.965	0.033	0.560
0.030	0.534	0.049	0.964	0.035	0.552
0.034	0.520	0.034	0.559	0.032	0.564
0.031	0.529	0.030	0.567	0.030	0.565
0.029	0.534	0.035	0.553	0.031	0.563
0.031	0.528	0.035	0.558	0.032	0.562
0.029	0.531	0.033	0.560	0.031	0.565
0.027	0.542	0.036	0.548	0.030	0.567
0.035	0.551	0.032	0.562	0.031	0.568
0.032	0.560	0.032	0.564	0.031	0.564
0.030	0.567	0.033	0.559	0.031	0.566
0.033	0.553	0.032	0.559	0.034	0.558
0.033	0.556	0.031	0.569	0.030	0.572
0.033	0.556	0.030	0.569	0.029	0.570
0.033	0.557	0.031	0.565		
0.032	0.562	0.030	0.573		
0.034	0.553	0.030	0.571		
0.031	0.563	0.031	0.567		
0.031	0.565	0.030	0.572		

Table D-3. Ethylbenzene equilibrium data from kinetic batch experiments

Aqueous Concentration (mmol/L)	Amount Sorbed (mg/kg)	Aqueous Concentration (mmol/L)	Amount Sorbed (mg/kg)	Aqueous Concentration (mmol/L)	Amount Sorbed (mg/kg)
0.017	0.628	0.005	0.145	0.019	0.573
0.018	0.627	0.004	0.148	0.015	0.583
0.027	0.598	0.004	0.149	0.015	0.585
0.020	0.621	0.004	0.151	0.017	0.578
0.020	0.620	0.004	0.151	0.012	0.597
0.019	0.623	0.004	0.151	0.014	0.589
0.020	0.622	0.004	0.149	0.028	0.832
0.019	0.622	0.004	0.150	0.022	0.857
0.018	0.625	0.004	0.151	0.024	0.845
0.021	0.616	0.004	0.148	0.026	0.838
0.018	0.626	0.004	0.152	0.025	0.842
0.018	0.628	0.003	0.152	0.026	0.839
0.016	0.631	0.009	0.289	0.024	0.847
0.016	0.633	0.009	0.290	0.022	0.853
0.016	0.635	0.009	0.290	0.024	0.849
0.019	0.622	0.011	0.284	0.022	0.853
0.017	0.630	0.010	0.285	0.023	0.847
0.015	0.638	0.011	0.284	0.022	0.853
0.021	0.563	0.008	0.292	0.026	0.839
0.021	0.561	0.008	0.293	0.023	0.852
0.021	0.561	0.008	0.294	0.021	0.855
0.021	0.562	0.009	0.290	0.026	0.841
0.019	0.567	0.007	0.294	0.021	0.855
0.021	0.559	0.007	0.295	0.019	0.557
0.019	0.568	0.009	0.292	0.016	0.566
0.018	0.570	0.007	0.295	0.013	0.574
0.018	0.568	0.007	0.297	0.020	0.555
0.018	0.572	0.008	0.292	0.016	0.565
0.016	0.578	0.007	0.295	0.016	0.565
0.017	0.577	0.007	0.298	0.018	0.559
0.021	0.563	0.017	0.580	0.017	0.562
0.019	0.571	0.017	0.581	0.016	0.564
0.017	0.573	0.016	0.581	0.016	0.564
0.019	0.566	0.017	0.578	0.016	0.566
0.017	0.576	0.017	0.579	0.015	0.567
0.016	0.577	0.019	0.574	0.018	0.559
0.004	0.148	0.019	0.572	0.015	0.566
0.004	0.150	0.017	0.579	0.015	0.569
0.004	0.149	0.016	0.584	0.017	0.564
0.005	0.148	0.017	0.579	0.012	0.576
0.004	0.148	0.016	0.583	0.015	0.569
0.004	0.149	0.015	0.583	0.045	1.414

Aqueous Concentration (mmol/L)	Amount Sorbed (mg/kg)	Aqueous Concentration (mmol/L)	Amount Sorbed (mg/kg)	Aqueous Concentration (mmol/L)	Amount Sorbed (mg/kg)
0.043	1.418	0.017	0.577	0.026	1.059
0.042	1.425	0.016	0.579	0.027	1.055
0.047	1.411	0.015	0.582	0.025	1.064
0.043	1.422	0.015	0.583	0.024	1.062
0.043	1.421	0.019	0.571	0.020	0.595
0.040	1.431	0.013	0.590	0.018	0.602
0.041	1.425	0.015	0.582	0.020	0.593
0.038	1.437	0.018	0.575	0.019	0.598
0.038	1.434	0.015	0.585	0.019	0.596
0.036	1.441	0.014	0.585	0.019	0.595
0.042	1.420	0.019	0.579	0.018	0.602
0.036	1.444	0.017	0.583	0.017	0.603
0.033	1.455	0.018	0.579	0.017	0.602
0.045	1.413	0.019	0.577	0.017	0.604
0.037	1.437	0.019	0.577	0.017	0.603
0.036	1.446	0.018	0.580	0.017	0.605
0.020	0.606	0.018	0.579	0.018	0.601
0.017	0.616	0.018	0.583	0.016	0.607
0.019	0.613	0.015	0.589	0.015	0.607
0.019	0.613	0.017	0.585	0.017	0.602
0.019	0.611	0.017	0.585	0.015	0.609
0.018	0.613	0.016	0.588	0.015	0.609
0.018	0.614	0.014	0.594	0.020	0.570
0.018	0.614	0.015	0.590	0.017	0.578
0.018	0.612	0.016	0.586	0.018	0.575
0.018	0.615	0.016	0.587	0.017	0.576
0.017	0.618	0.014	0.595	0.018	0.576
0.017	0.618	0.014	0.594	0.019	0.572
0.020	0.605	0.033	1.038	0.018	0.577
0.017	0.615	0.030	1.045	0.016	0.581
0.016	0.619	0.033	1.035	0.016	0.581
0.017	0.617	0.034	1.036	0.017	0.580
0.016	0.620	0.032	1.041	0.016	0.583
0.014	0.625	0.034	1.032	0.015	0.584
0.019	0.570	0.030	1.044	0.017	0.581
0.017	0.576	0.029	1.050	0.015	0.583
0.016	0.579	0.031	1.043	0.015	0.585
0.019	0.568	0.029	1.047	0.017	0.579
0.019	0.571	0.028	1.057	0.014	0.589
0.019	0.572	0.026	1.056	0.014	0.589
0.018	0.574	0.028	1.050		
0.016	0.580	0.026	1.063		

Table D-4. *m*-Xylene equilibrium data from kinetic batch experiments

Aqueous Concentration (mmol/L)	Amount Sorbed (mg/kg)	Aqueous Concentration (mmol/L)	Amount Sorbed (mg/kg)	Aqueous Concentration (mmol/L)	Amount Sorbed (mg/kg)
0.018	0.620	0.004	0.148	0.017	0.636
0.018	0.620	0.004	0.148	0.017	0.638
0.017	0.620	0.003	0.150	0.019	0.631
0.017	0.623	0.004	0.150	0.013	0.649
0.017	0.623	0.003	0.150	0.015	0.642
0.018	0.619	0.004	0.148	0.026	0.799
0.017	0.620	0.004	0.149	0.020	0.822
0.017	0.620	0.003	0.150	0.022	0.811
0.018	0.619	0.004	0.148	0.023	0.808
0.015	0.630	0.003	0.151	0.022	0.812
0.015	0.629	0.003	0.151	0.023	0.809
0.016	0.628	0.009	0.290	0.022	0.813
0.018	0.619	0.009	0.291	0.020	0.819
0.015	0.627	0.008	0.291	0.021	0.815
0.014	0.632	0.009	0.291	0.020	0.819
0.017	0.624	0.008	0.291	0.020	0.814
0.014	0.633	0.009	0.291	0.020	0.820
0.014	0.630	0.008	0.292	0.024	0.807
0.019	0.553	0.008	0.294	0.020	0.819
0.019	0.553	0.008	0.294	0.019	0.822
0.019	0.554	0.009	0.291	0.023	0.809
0.019	0.555	0.007	0.295	0.019	0.821
0.017	0.559	0.007	0.296	0.017	0.528
0.019	0.552	0.008	0.292	0.014	0.537
0.016	0.560	0.007	0.296	0.012	0.545
0.016	0.562	0.006	0.298	0.019	0.524
0.016	0.560	0.008	0.293	0.015	0.534
0.015	0.564	0.007	0.296	0.015	0.534
0.014	0.569	0.007	0.298	0.016	0.531
0.014	0.568	0.020	0.630	0.015	0.534
0.018	0.556	0.019	0.632	0.015	0.535
0.016	0.563	0.018	0.633	0.015	0.534
0.015	0.565	0.019	0.631	0.014	0.538
0.017	0.558	0.019	0.631	0.013	0.538
0.014	0.567	0.021	0.626	0.016	0.532
0.014	0.568	0.021	0.621	0.014	0.538
0.004	0.149	0.019	0.630	0.013	0.540
0.004	0.148	0.018	0.636	0.015	0.536
0.004	0.147	0.020	0.630	0.011	0.547
0.004	0.148	0.017	0.635	0.013	0.540
0.004	0.149	0.017	0.635	0.018	0.566
0.005	0.144	0.021	0.626	0.017	0.568

Aqueous Concentration (mmol/L)	Amount Sorbed (mg/kg)	Aqueous Concentration (mmol/L)	Amount Sorbed (mg/kg)	Aqueous Concentration (mmol/L)	Amount Sorbed (mg/kg)
0.016	0.571	0.016	0.589	0.014	0.577
0.017	0.567	0.015	0.592	0.013	0.582
0.016	0.572	0.014	0.593	0.013	0.581
0.018	0.567	0.018	0.581	0.032	1.032
0.016	0.573	0.013	0.600	0.029	1.044
0.016	0.571	0.014	0.593	0.033	1.030
0.015	0.573	0.017	0.586	0.030	1.039
0.015	0.574	0.014	0.595	0.030	1.036
0.014	0.577	0.013	0.595	0.031	1.035
0.017	0.568	0.018	0.592	0.028	1.046
0.014	0.578	0.017	0.596	0.027	1.047
0.013	0.582	0.017	0.593	0.028	1.045
0.018	0.566	0.018	0.592	0.026	1.050
0.015	0.575	0.018	0.591	0.027	1.049
0.014	0.579	0.017	0.594	0.026	1.050
0.043	1.403	0.018	0.592	0.029	1.043
0.037	1.426	0.017	0.596	0.026	1.053
0.040	1.418	0.015	0.602	0.025	1.054
0.041	1.416	0.016	0.598	0.027	1.046
0.041	1.412	0.016	0.598	0.024	1.057
0.039	1.416	0.015	0.601	0.024	1.058
0.038	1.425	0.014	0.607	0.018	0.562
0.037	1.424	0.015	0.603	0.016	0.569
0.039	1.418	0.016	0.599	0.017	0.567
0.036	1.428	0.015	0.600	0.016	0.569
0.035	1.432	0.013	0.608	0.016	0.570
0.035	1.431	0.013	0.608	0.017	0.566
0.044	1.402	0.017	0.567	0.016	0.568
0.037	1.423	0.016	0.571	0.015	0.573
0.034	1.434	0.017	0.566	0.015	0.572
0.036	1.429	0.017	0.568	0.015	0.572
0.033	1.435	0.016	0.571	0.014	0.574
0.030	1.446	0.017	0.566	0.014	0.575
0.018	0.580	0.016	0.569	0.015	0.573
0.017	0.586	0.015	0.574	0.014	0.575
0.016	0.589	0.016	0.570	0.014	0.577
0.017	0.583	0.016	0.571	0.016	0.570
0.017	0.585	0.015	0.577	0.013	0.581
0.016	0.587	0.014	0.577	0.013	0.581
0.017	0.584	0.015	0.574		
0.015	0.590	0.013	0.581		
0.016	0.587	0.013	0.579		

Table D-5. o-Xylene equilibrium data from kinetic batch experiments

Aqueous Concentration (mmol/L)	Amount Sorbed (mg/kg)	Aqueous Concentration (mmol/L)	Amount Sorbed (mg/kg)	Aqueous Concentration (mmol/L)	Amount Sorbed (mg/kg)
0.015	0.560	0.005	0.149	0.017	0.636
0.013	0.565	0.005	0.149	0.017	0.638
0.013	0.564	0.004	0.152	0.019	0.631
0.015	0.561	0.004	0.151	0.013	0.649
0.015	0.558	0.004	0.151	0.015	0.642
0.015	0.558	0.004	0.150	0.029	0.821
0.016	0.558	0.004	0.151	0.022	0.846
0.015	0.556	0.004	0.151	0.025	0.836
0.017	0.553	0.004	0.149	0.026	0.831
0.014	0.563	0.004	0.152	0.025	0.835
0.013	0.564	0.004	0.153	0.026	0.833
0.012	0.569	0.011	0.317	0.025	0.836
0.017	0.554	0.010	0.318	0.023	0.843
0.014	0.562	0.010	0.319	0.024	0.839
0.013	0.564	0.011	0.318	0.023	0.843
0.016	0.555	0.010	0.319	0.023	0.838
0.014	0.564	0.010	0.319	0.022	0.845
0.013	0.566	0.010	0.319	0.026	0.831
0.017	0.548	0.009	0.321	0.022	0.845
0.017	0.546	0.009	0.322	0.021	0.847
0.018	0.546	0.010	0.318	0.025	0.834
0.018	0.546	0.009	0.323	0.021	0.847
0.016	0.550	0.008	0.324	0.019	0.538
0.018	0.543	0.010	0.321	0.016	0.548
0.016	0.550	0.008	0.325	0.014	0.555
0.015	0.552	0.008	0.327	0.020	0.534
0.015	0.551	0.009	0.322	0.017	0.544
0.014	0.556	0.008	0.325	0.017	0.545
0.013	0.559	0.008	0.328	0.018	0.540
0.014	0.558	0.020	0.630	0.017	0.544
0.017	0.548	0.019	0.632	0.016	0.545
0.015	0.555	0.018	0.633	0.017	0.545
0.014	0.557	0.019	0.631	0.015	0.549
0.017	0.548	0.019	0.631	0.015	0.549
0.014	0.558	0.021	0.626	0.017	0.543
0.013	0.559	0.021	0.621	0.015	0.549
0.004	0.151	0.019	0.630	0.014	0.552
0.004	0.149	0.018	0.636	0.016	0.547
0.005	0.149	0.020	0.630	0.012	0.558
0.005	0.149	0.017	0.635	0.014	0.552
0.004	0.150	0.017	0.635	0.021	0.593
0.006	0.144	0.021	0.626	0.019	0.595

Aqueous Concentration (mmol/L)	Amount Sorbed (mg/kg)	Aqueous Concentration (mmol/L)	Amount Sorbed (mg/kg)	Aqueous Concentration (mmol/L)	Amount Sorbed (mg/kg)
0.019	0.599	0.042	1.534	0.016	0.617
0.020	0.595	0.040	1.539	0.015	0.622
0.018	0.600	0.039	1.541	0.014	0.622
0.021	0.593	0.049	1.511	0.020	0.574
0.018	0.601	0.035	1.560	0.017	0.582
0.019	0.599	0.040	1.540	0.020	0.574
0.018	0.601	0.047	1.523	0.018	0.578
0.017	0.603	0.039	1.547	0.018	0.577
0.016	0.606	0.037	1.547	0.019	0.576
0.019	0.597	0.019	0.579	0.018	0.580
0.016	0.608	0.018	0.584	0.017	0.583
0.015	0.613	0.018	0.581	0.017	0.582
0.020	0.595	0.018	0.581	0.017	0.583
0.017	0.605	0.019	0.580	0.017	0.584
0.016	0.609	0.018	0.583	0.016	0.585
0.020	0.581	0.019	0.580	0.017	0.582
0.017	0.591	0.018	0.585	0.015	0.588
0.019	0.588	0.016	0.591	0.015	0.588
0.019	0.586	0.018	0.586	0.017	0.583
0.019	0.585	0.017	0.586	0.015	0.590
0.018	0.587	0.016	0.590	0.015	0.590
0.019	0.587	0.014	0.596	0.036	1.005
0.018	0.589	0.016	0.592	0.031	1.021
0.018	0.588	0.017	0.588	0.033	1.017
0.018	0.589	0.016	0.589	0.030	1.023
0.016	0.593	0.014	0.598	0.031	1.023
0.016	0.594	0.014	0.597	0.033	1.016
0.020	0.582	0.020	0.604	0.031	1.020
0.017	0.591	0.018	0.610	0.028	1.028
0.015	0.596	0.020	0.604	0.029	1.026
0.016	0.593	0.020	0.606	0.029	1.029
0.015	0.596	0.019	0.610	0.028	1.032
0.014	0.601	0.020	0.604	0.027	1.034
0.051	1.502	0.019	0.606	0.030	1.029
0.047	1.519	0.018	0.612	0.027	1.032
0.044	1.528	0.019	0.609	0.027	1.036
0.046	1.515	0.018	0.609	0.031	1.024
0.047	1.518	0.017	0.617	0.025	1.043
0.046	1.522	0.016	0.617	0.024	1.043
0.046	1.520	0.017	0.614		
0.043	1.533	0.015	0.622		
0.044	1.524	0.015	0.620		

Table D-6. Overall isotherm results from equilibrium data of batch experiments

Constituent	Number of Samples	Average K_d (L/kg)	Linear Isotherm r^2
Benzene	240	7.50	0.951
Toluene	247	17.77	0.959
Ethylbenzene	250	34.54	0.922
M-Xylene	249	36.87	0.933
O-Xylene	249	34.57	0.935

Table D-7. Overall “quasi” equilibrium results from batch experiment data

Constituent	20-Minute		90-Minute		Aqueous Concentration difference (%)	Amount Sorbed difference (%)
	K_d (L/kg)	r^2	K_d (L/kg)	r^2		
Benzene	7.32	0.944	7.57	0.964	9.9	5.5
Toluene	16.91	0.971	18.77	0.971	21.9	3.9
Ethylbenzene	32.1	0.936	37.54	0.913	29.0	3.1
M-Xylene	34.09	0.958	41.21	0.931	31.3	3.0
O-Xylene	31.88	0.953	37.93	0.928	31.6	3.7

Table D-8. Twenty and ninety-minute data from benzene batch experiments

20 Minute Data		90 Minute Data	
Aqueous Concentration (mmol/L)	Amount Sorbed (mmol/kg)	Aqueous Concentration (mmol/L)	Amount Sorbed (mmol/kg)
0.081	0.596	0.075	0.619
0.081	0.586	0.079	0.615
0.074	0.625	0.073	0.626
0.081	0.551	0.077	0.562
0.084	0.539	0.075	0.576
0.085	0.541	0.076	0.565
0.014	0.109	0.014	0.111
0.015	0.108	0.014	0.112
0.032	0.232	0.032	0.233
0.032	0.230	0.031	0.231
0.032	0.232	0.032	0.236
0.067	0.484	0.065	0.486
0.068	0.478	0.059	0.500
0.067	0.480	0.092	0.652
0.089	0.667	0.092	0.663
0.086	0.677	0.085	0.683
0.061	0.457	0.061	0.456
0.059	0.458	0.060	0.458
0.060	0.455	0.060	0.420
0.058	0.429	0.058	0.423
0.060	0.419	0.059	0.429
0.057	0.431	0.058	0.422
0.056	0.431	0.056	0.426
0.057	0.435	0.055	0.432
0.066	0.456	0.067	0.456
0.062	0.473	0.063	0.468
0.066	0.486	0.063	0.464
0.064	0.491	0.064	0.490
0.068	0.475	0.066	0.490
0.061	0.464	0.065	0.489
0.058	0.467	0.061	0.462
0.063	0.452	0.060	0.468
0.064	0.459	0.059	0.468
0.062	0.467	0.063	0.458
0.060	0.432	0.062	0.462
0.057	0.442	0.062	0.464
0.059	0.437	0.058	0.444
		0.057	0.439

Table D-9. Twenty and ninety-minute data from toluene batch experiments

20 Minute Data		90 Minute Data	
Aqueous Concentration (mmol/L)	Amount Sorbed (mmol/kg)	Aqueous Concentration (mmol/L)	Amount Sorbed (mmol/kg)
0.033	0.492	0.029	0.508
0.032	0.496	0.024	0.523
0.031	0.500	0.024	0.520
0.040	0.615	0.037	0.623
0.041	0.609	0.034	0.635
0.042	0.610	0.034	0.632
0.007	0.137	0.007	0.138
0.008	0.134	0.007	0.138
0.008	0.134	0.017	0.307
0.019	0.303	0.016	0.309
0.018	0.302	0.016	0.312
0.018	0.303	0.031	0.535
0.030	0.537	0.024	0.558
0.031	0.536	0.026	0.546
0.030	0.537	0.046	0.822
0.050	0.807	0.042	0.835
0.046	0.821	0.073	1.318
0.050	0.808	0.069	1.327
0.073	1.317	0.032	0.537
0.075	1.307	0.029	0.544
0.070	1.324	0.029	0.549
0.033	0.536	0.031	0.528
0.033	0.533	0.029	0.531
0.032	0.540	0.027	0.542
0.033	0.523	0.033	0.558
0.028	0.536	0.030	0.568
0.032	0.528	0.029	0.567
0.035	0.551	0.051	0.956
0.032	0.560	0.050	0.965
0.030	0.567	0.049	0.964
0.056	0.940	0.031	0.567
0.054	0.947	0.030	0.572
0.057	0.934	0.029	0.572
0.034	0.559	0.031	0.553
0.030	0.567	0.029	0.559
0.035	0.553	0.030	0.560
0.033	0.548	0.034	0.558
0.031	0.555	0.030	0.572
0.037	0.536	0.029	0.570
0.035	0.552		
0.032	0.560		
0.034	0.557		

Table D-10. Twenty and ninety-minute data from ethylbenzene batch experiments

20 Minute Data		90 Minute Data	
Aqueous Concentration (mmol/L)	Amount Sorbed (mmol/kg)	Aqueous Concentration (mmol/L)	Amount Sorbed (mmol/kg)
0.017	0.628	0.019	0.622
0.018	0.627	0.017	0.630
0.027	0.598	0.015	0.638
0.021	0.563	0.019	0.566
0.021	0.561	0.017	0.576
0.021	0.561	0.016	0.577
0.004	0.148	0.004	0.152
0.004	0.150	0.003	0.152
0.004	0.149	0.008	0.292
0.009	0.289	0.007	0.295
0.009	0.290	0.007	0.298
0.009	0.290	0.017	0.578
0.017	0.580	0.012	0.597
0.017	0.581	0.014	0.589
0.016	0.581	0.026	0.841
0.028	0.832	0.021	0.855
0.022	0.857	0.017	0.564
0.024	0.845	0.012	0.576
0.019	0.557	0.015	0.569
0.016	0.566	0.045	1.413
0.013	0.574	0.037	1.437
0.045	1.414	0.036	1.446
0.043	1.418	0.017	0.617
0.042	1.425	0.016	0.620
0.020	0.606	0.014	0.625
0.017	0.616	0.018	0.575
0.019	0.613	0.015	0.585
0.019	0.570	0.014	0.585
0.017	0.576	0.016	0.587
0.016	0.579	0.014	0.595
0.019	0.579	0.014	0.594
0.017	0.583	0.027	1.055
0.018	0.579	0.025	1.064
0.033	1.038	0.024	1.062
0.030	1.045	0.017	0.602
0.033	1.035	0.015	0.609
0.020	0.595	0.015	0.609
0.018	0.602	0.017	0.579
0.020	0.593	0.014	0.589
0.020	0.570	0.014	0.589
0.017	0.578		
0.018	0.575		

Table D-11. Twenty and ninety-minute data from *m*-xylene batch experiments

20 Minute Data		90 Minute Data	
Aqueous Concentration (mmol/L)	Amount Sorbed (mmol/kg)	Aqueous Concentration (mmol/L)	Amount Sorbed (mmol/kg)
0.018	0.620	0.017	0.624
0.018	0.620	0.014	0.633
0.017	0.620	0.014	0.630
0.019	0.553	0.017	0.558
0.019	0.553	0.014	0.567
0.019	0.554	0.014	0.568
0.004	0.149	0.003	0.151
0.004	0.148	0.003	0.151
0.004	0.147	0.008	0.293
0.009	0.290	0.007	0.296
0.009	0.291	0.007	0.298
0.008	0.291	0.019	0.631
0.020	0.630	0.013	0.649
0.019	0.632	0.015	0.642
0.018	0.633	0.023	0.809
0.026	0.799	0.019	0.821
0.020	0.822	0.015	0.536
0.022	0.811	0.011	0.547
0.017	0.528	0.013	0.540
0.014	0.537	0.018	0.566
0.012	0.545	0.015	0.575
0.018	0.566	0.014	0.579
0.017	0.568	0.036	1.429
0.016	0.571	0.033	1.435
0.043	1.403	0.030	1.446
0.037	1.426	0.017	0.586
0.040	1.418	0.014	0.595
0.018	0.580	0.013	0.595
0.017	0.586	0.015	0.600
0.016	0.589	0.013	0.608
0.018	0.592	0.013	0.608
0.017	0.596	0.014	0.577
0.017	0.593	0.013	0.582
0.017	0.567	0.013	0.581
0.016	0.571	0.027	1.046
0.017	0.566	0.024	1.057
0.032	1.032	0.024	1.058
0.029	1.044	0.016	0.570
0.033	1.030	0.013	0.581
0.018	0.562	0.013	0.581
0.016	0.569		
0.017	0.567		

Table D-12. Twenty and ninety-minute data from *o*-xylene batch experiments

20 Minute Data		90 Minute Data	
Aqueous Concentration (mmol/L)	Amount Sorbed (mmol/kg)	Aqueous Concentration (mmol/L)	Amount Sorbed (mmol/kg)
0.015	0.560	0.016	0.555
0.013	0.565	0.014	0.564
0.013	0.564	0.013	0.566
0.017	0.548	0.017	0.548
0.017	0.546	0.014	0.558
0.018	0.546	0.013	0.559
0.004	0.151	0.004	0.152
0.004	0.149	0.004	0.153
0.005	0.149	0.009	0.322
0.011	0.317	0.008	0.325
0.010	0.318	0.008	0.328
0.010	0.319	0.019	0.631
0.020	0.630	0.013	0.649
0.019	0.632	0.015	0.642
0.018	0.633	0.025	0.834
0.029	0.821	0.021	0.847
0.022	0.846	0.016	0.547
0.025	0.836	0.012	0.558
0.019	0.538	0.014	0.552
0.016	0.548	0.020	0.595
0.014	0.555	0.017	0.605
0.021	0.593	0.016	0.609
0.019	0.595	0.016	0.593
0.019	0.599	0.015	0.596
0.020	0.581	0.014	0.601
0.017	0.591	0.047	1.523
0.019	0.588	0.039	1.547
0.051	1.502	0.037	1.547
0.047	1.519	0.016	0.589
0.044	1.528	0.014	0.598
0.019	0.579	0.014	0.597
0.018	0.584	0.016	0.617
0.018	0.581	0.015	0.622
0.020	0.604	0.014	0.622
0.018	0.610	0.017	0.583
0.020	0.604	0.015	0.590
0.020	0.574	0.015	0.590
0.017	0.582	0.031	1.024
0.020	0.574	0.025	1.043
0.036	1.005	0.024	1.043
0.031	1.021		
0.033	1.017		

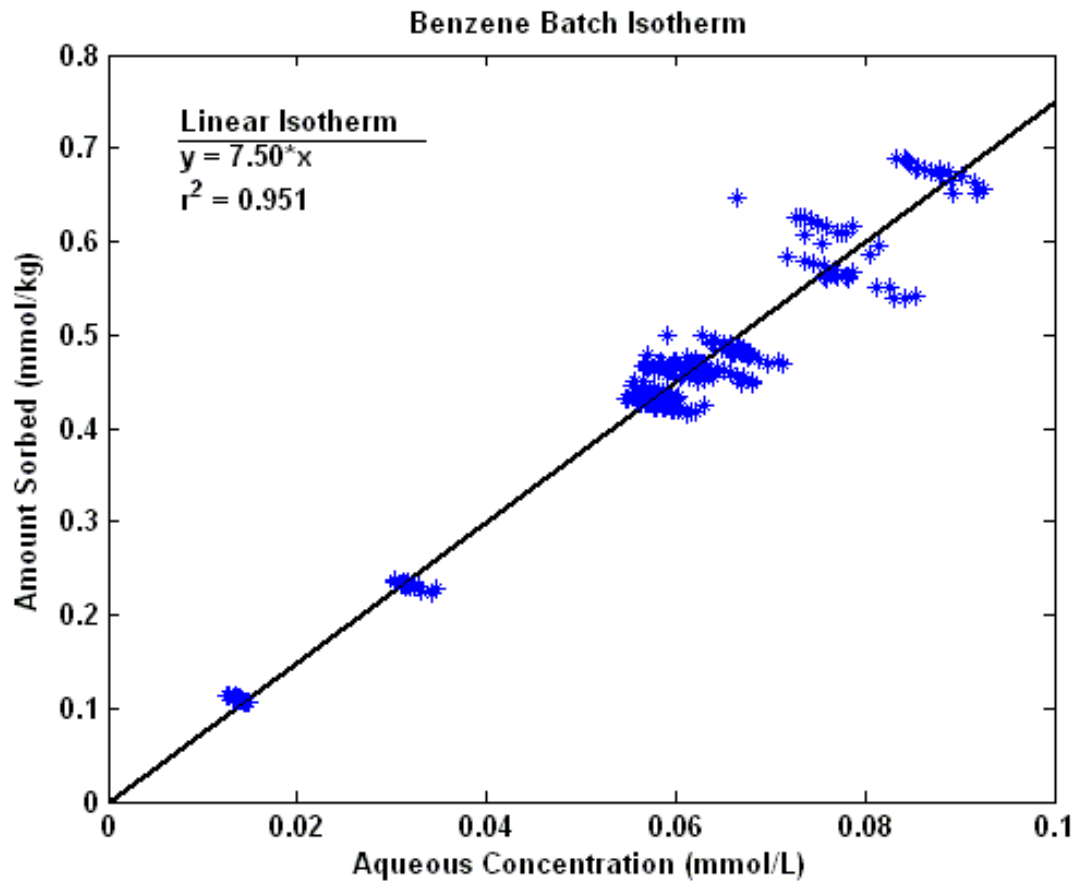


Figure D-1. Isotherm results for benzene equilibrium batch experiment data.

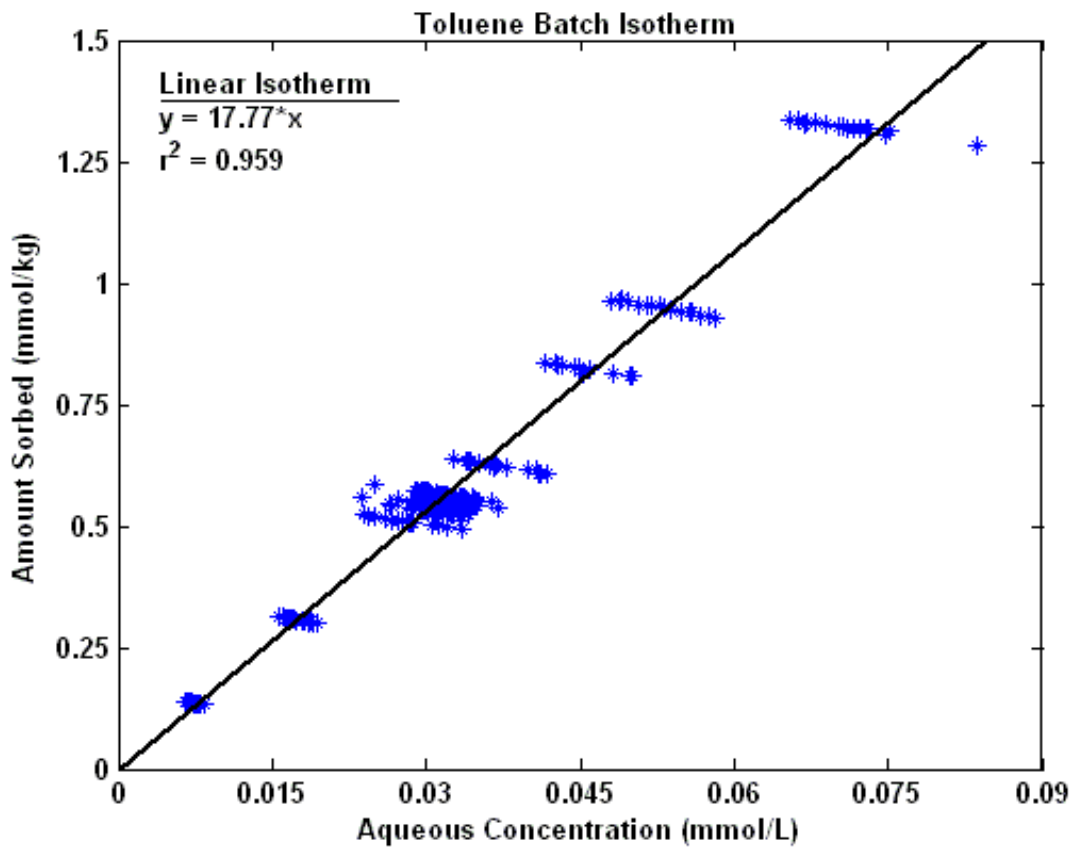


Figure D-2. Isotherm results for toluene equilibrium batch experiment data.

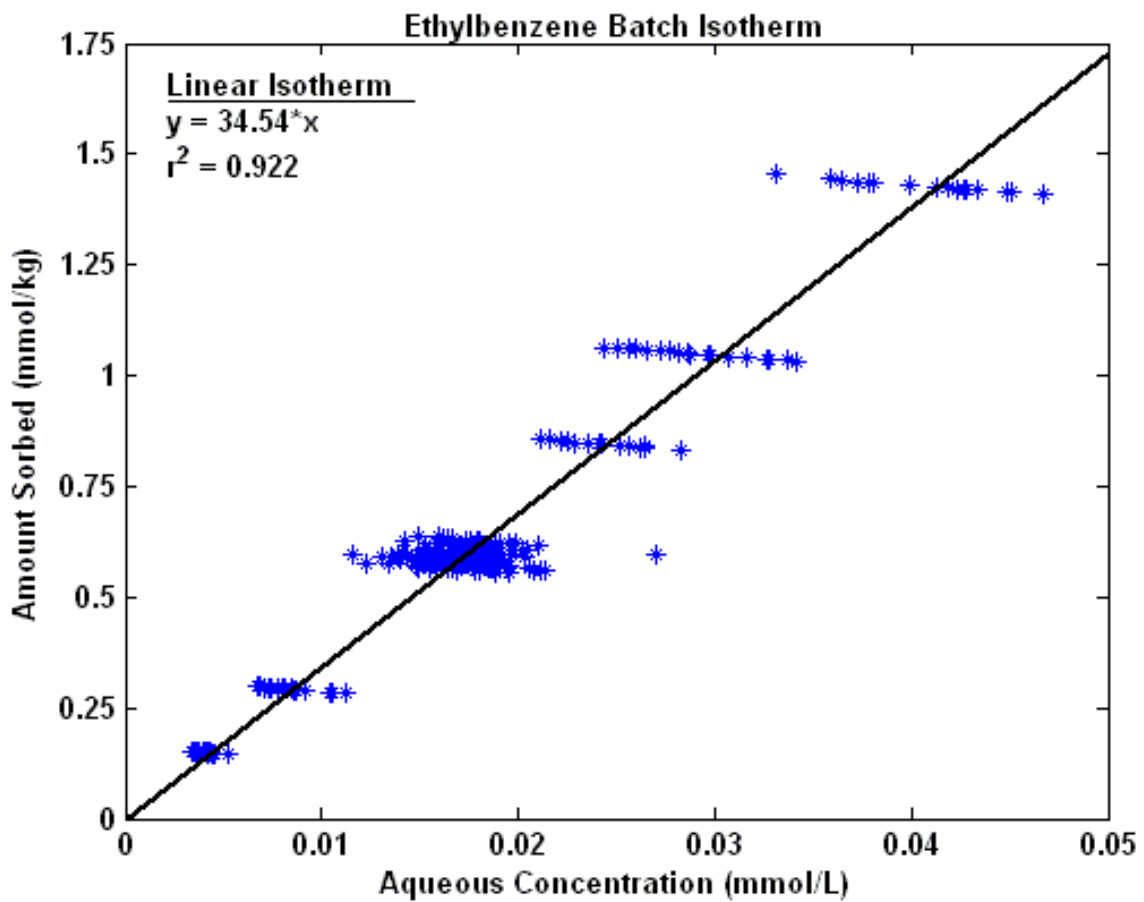


Figure D-3. Isotherm results for ethylbenzene equilibrium batch experiment data.

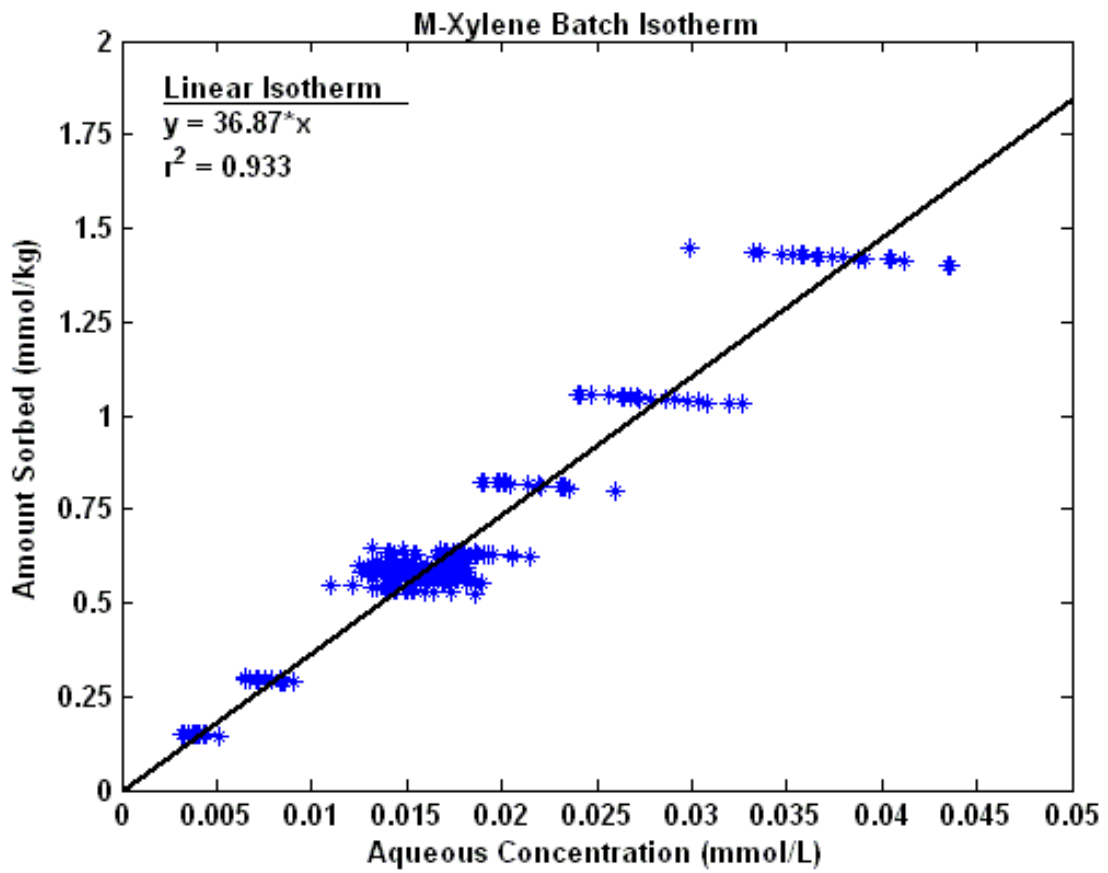


Figure D-4. Isotherm results for *m*-xylene equilibrium batch experiment data.

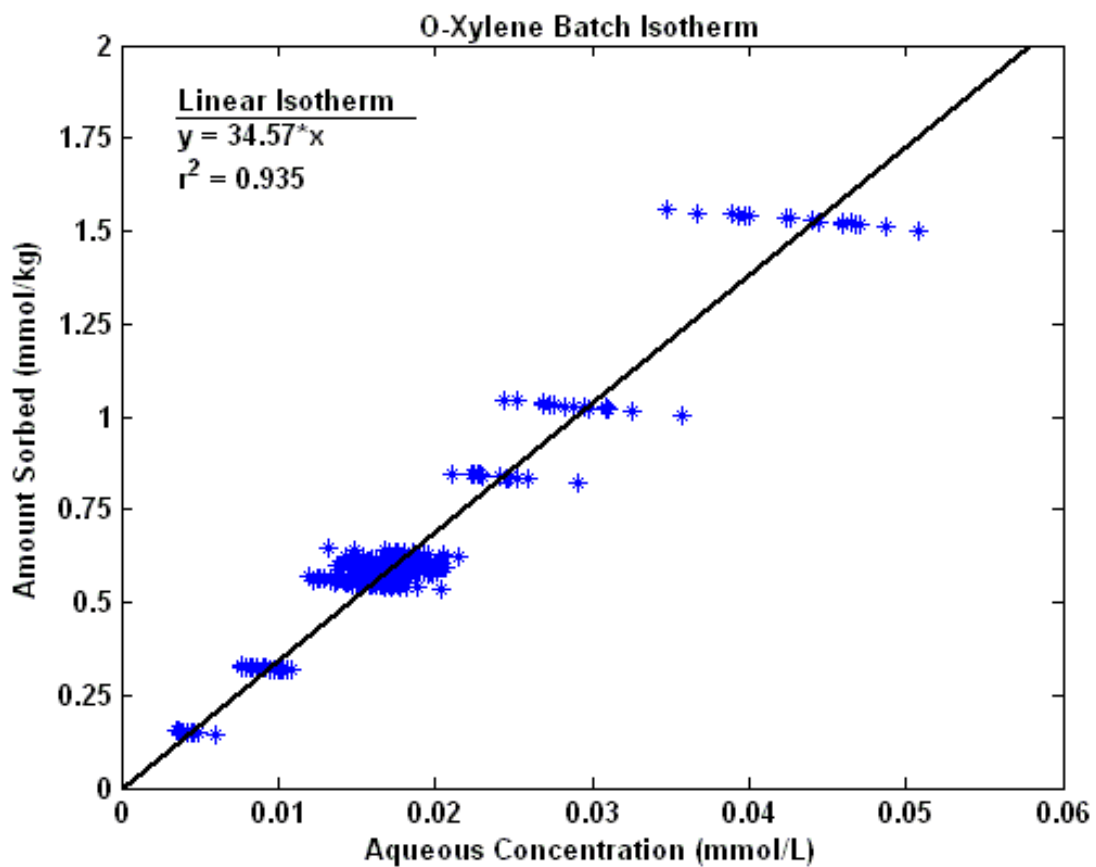


Figure D-5. Isotherm results for *o*-xylene equilibrium batch experiment data.

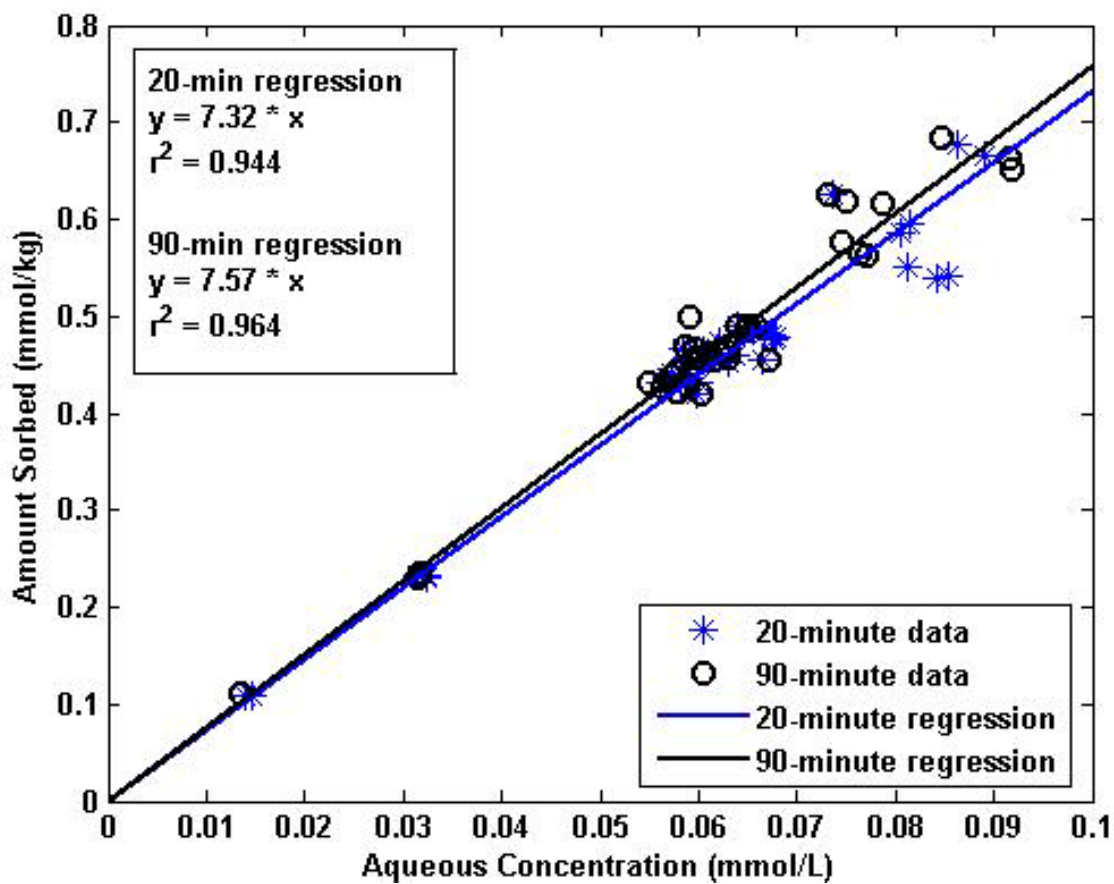


Figure D-6. Twenty and ninety-minute data from the benzene batch experiments fitted with linear isotherms.

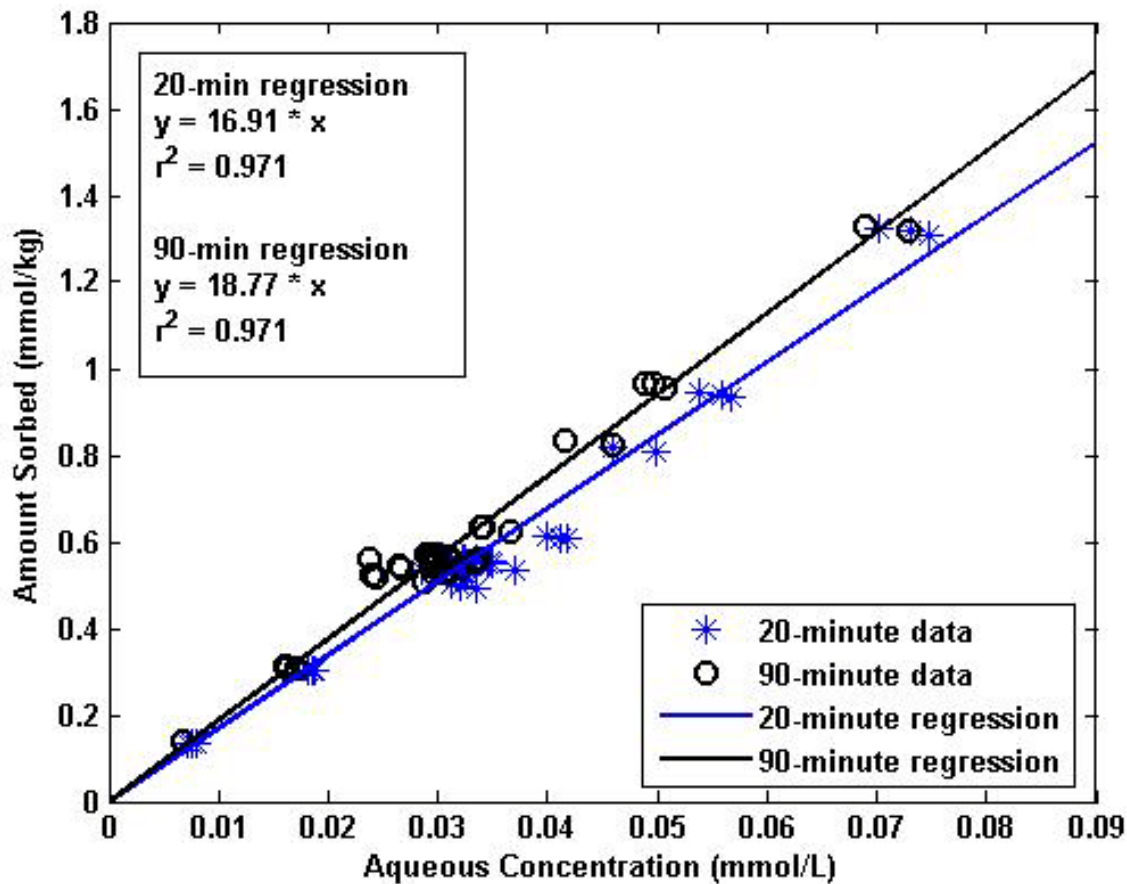


Figure D-7. Twenty and ninety-minute data from the toluene batch experiments fitted with linear isotherms.

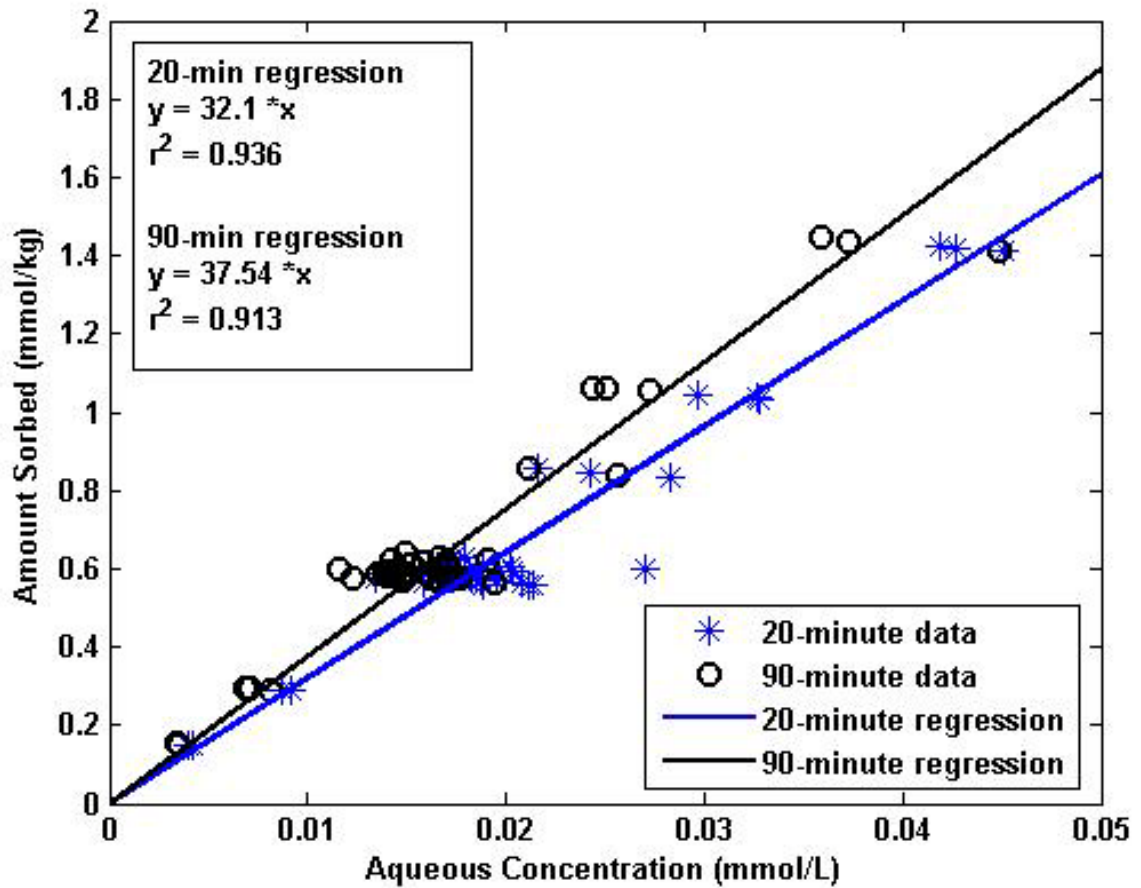


Figure D-8. Twenty and ninety-minute data from the ethylbenzene batch experiments fitted with linear isotherms.

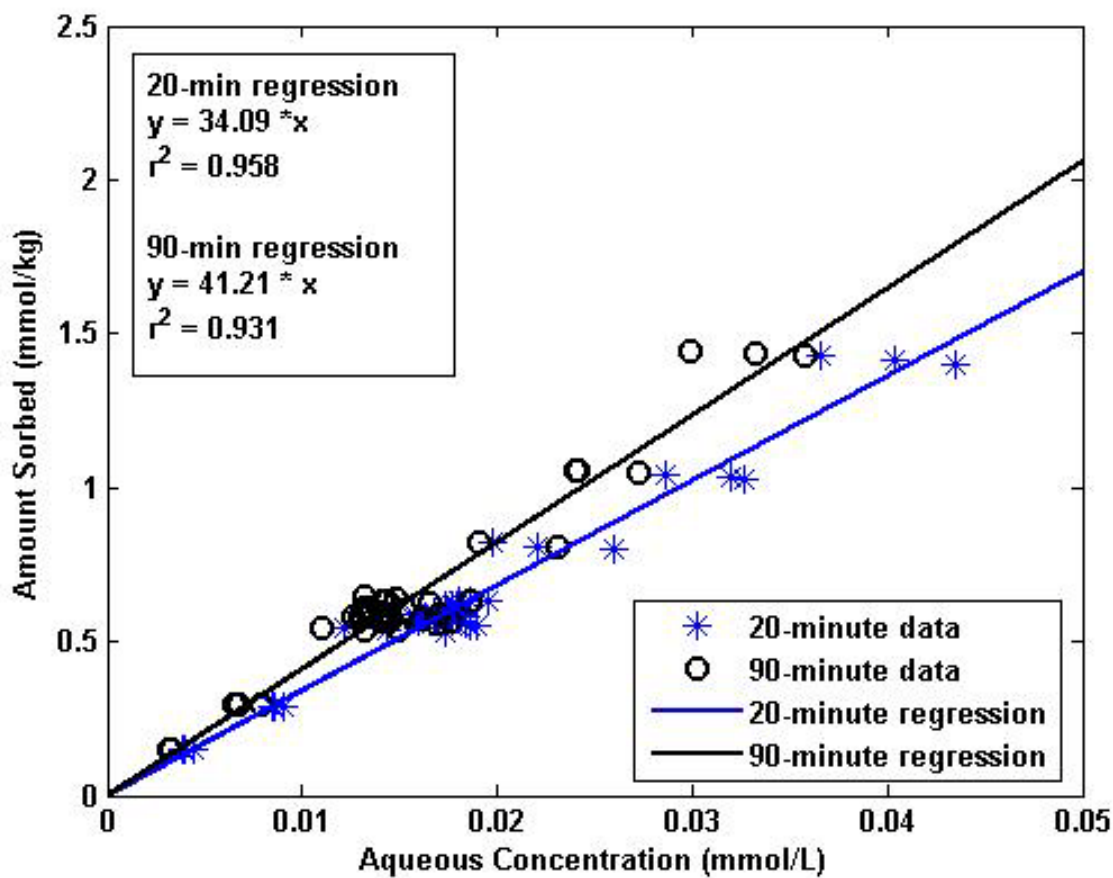


Figure D-9. Twenty and ninety-minute data from the *m*-xylene batch experiments fitted linear isotherms.

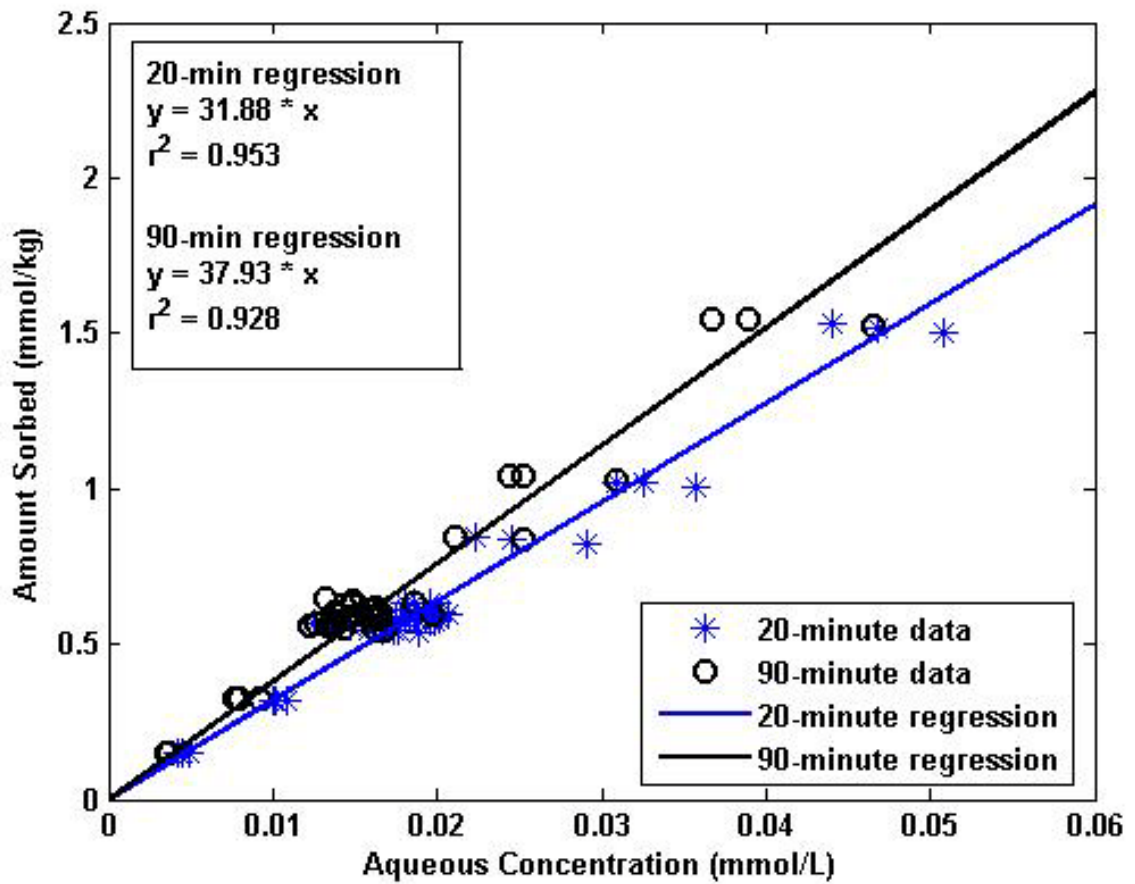


Figure D-10. Twenty and ninety-minute data from the *o*-xylene batch experiments fitted with linear isotherms.

APPENDIX E. TRITIUM BTC DATA.

The data from the tritium transport experiments can be seen in Tables E-1 through E-6. These data are represented in relative concentration as a function of pore volumes. A single tritium experiment was run prior to each BTEX transport experiment in order to obtain column parameters. These results are seen in Table V of the manuscript. Figures E-1 through E-6 show the chemical equilibrium model (CXTFIT version 2.1 (Toride et al., 1999)) inversely fit to the experimental data.

Table E-1. Tritium BTC data from column 1A.

Sample	Pore Volumes	Observed C/C₀	Fit C/C₀	Sample	Pore Volumes	Observed C/C₀	Fit C/C₀
1	0.060	0.000	0.000	28	3.307	0.272	0.319
2	0.180	0.000	0.000	29	3.427	0.211	0.247
3	0.301	0.000	0.000	30	3.548	0.159	0.189
4	0.421	0.003	0.008	31	3.668	0.117	0.143
5	0.541	0.022	0.042	32	3.788	0.090	0.108
6	0.661	0.077	0.112	33	3.908	0.068	0.081
7	0.782	0.168	0.214	34	4.029	0.051	0.060
8	0.902	0.280	0.330	35	4.149	0.041	0.045
9	1.022	0.391	0.447	36	4.269	0.031	0.033
10	1.142	0.532	0.554	37	4.389	0.025	0.025
11	1.263	0.613	0.649	38	4.510	0.019	0.018
12	1.383	0.708	0.727	39	4.630	0.016	0.013
13	1.503	0.781	0.790	40	4.750	0.012	0.010
14	1.623	0.829	0.840	41	4.870	0.010	0.007
15	1.744	0.856	0.879	42	4.991	0.008	0.005
16	1.864	0.905	0.909	43	5.111	0.007	0.004
17	1.984	0.917	0.932	44	5.231	0.006	0.003
18	2.104	0.933	0.950	45	5.351	0.005	0.002
19	2.225	0.952	0.963	46	5.472	0.004	0.002
20	2.345	0.955	0.971	47	5.592	0.003	0.001
21	2.465	0.937	0.963	48	5.712	0.003	0.001
22	2.585	0.890	0.922	49	5.832	0.002	0.001
23	2.706	0.811	0.842	50	5.953	0.002	0.000
24	2.826	0.703	0.736	51	6.073	0.002	0.000
25	2.946	0.585	0.621	52	6.193	0.001	0.000
26	3.067	0.472	0.507	53	6.313	0.001	0.000
27	3.187	0.369	0.406	54	6.434	0.001	0.000

Table E-2. Tritium BTC data from column 1B.

Sample	Pore Volumes	Observed C/C₀	Fit C/C₀	Sample	Pore Volumes	Observed C/C₀	Fit C/C₀
1	0.117	0.000	0.000	28	3.285	0.250	0.313
2	0.235	0.000	0.000	29	3.402	0.202	0.245
3	0.352	0.000	0.003	30	3.519	0.157	0.190
4	0.469	0.000	0.026	31	3.637	0.122	0.146
5	0.587	0.014	0.083	32	3.754	0.098	0.111
6	0.704	0.074	0.174	33	3.871	0.077	0.085
7	0.821	0.197	0.284	34	3.989	0.060	0.064
8	0.939	0.306	0.400	35	4.106	0.047	0.049
9	1.056	0.460	0.509	36	4.223	0.038	0.037
10	1.173	0.569	0.605	37	4.341	0.029	0.028
11	1.290	0.660	0.688	38	4.458	0.023	0.021
12	1.408	0.737	0.757	39	4.575	0.019	0.016
13	1.525	0.786	0.812	40	4.693	0.015	0.012
14	1.642	0.826	0.855	41	4.810	0.012	0.009
15	1.760	0.872	0.889	42	4.927	0.010	0.007
16	1.877	0.896	0.916	43	5.044	0.008	0.005
17	1.994	0.917	0.936	44	5.162	0.006	0.004
18	2.112	0.934	0.952	45	5.279	0.005	0.003
19	2.229	0.949	0.964	46	5.396	0.004	0.002
20	2.346	0.956	0.970	47	5.514	0.003	0.002
21	2.464	0.945	0.956	48	5.631	0.003	0.001
22	2.581	0.881	0.905	49	5.748	0.002	0.001
23	2.698	0.769	0.820	50	5.866	0.002	0.001
24	2.816	0.639	0.713	51	5.983	0.002	0.001
25	2.933	0.507	0.600	52	6.100	0.001	0.000
26	3.050	0.415	0.492	53	6.218	0.001	0.000
27	3.167	0.322	0.396	54	6.335	0.001	0.000

Table E-3. Tritium BTC data from column 2A.

Sample	Pore Volumes	Observed C/C₀	Fit C/C₀	Sample	Pore Volumes	Observed C/C₀	Fit C/C₀
1	0.119	0.000	0.000	28	3.334	0.184	0.245
2	0.238	0.000	0.000	29	3.453	0.142	0.180
3	0.357	0.000	0.002	30	3.573	0.106	0.130
4	0.476	0.002	0.019	31	3.692	0.079	0.093
5	0.595	0.019	0.073	32	3.811	0.060	0.066
6	0.715	0.073	0.169	33	3.930	0.046	0.047
7	0.834	0.187	0.293	34	4.049	0.034	0.033
8	0.953	0.327	0.423	35	4.168	0.027	0.023
9	1.072	0.478	0.546	36	4.287	0.021	0.016
10	1.191	0.610	0.652	37	4.406	0.016	0.011
11	1.310	0.705	0.740	38	4.525	0.013	0.008
12	1.429	0.778	0.808	39	4.644	0.010	0.005
13	1.548	0.834	0.861	40	4.763	0.008	0.004
14	1.667	0.869	0.900	41	4.882	0.006	0.003
15	1.786	0.904	0.929	42	5.002	0.005	0.002
16	1.905	0.930	0.949	43	5.121	0.003	0.001
17	2.024	0.945	0.964	44	5.240	0.002	0.001
18	2.144	0.964	0.975	45	5.359	0.002	0.001
19	2.263	0.973	0.983	46	5.478	0.001	0.000
20	2.382	0.967	0.985	47	5.597	0.001	0.000
21	2.501	0.947	0.965	48	5.716	0.001	0.000
22	2.620	0.862	0.905	49	5.835	0.001	0.000
23	2.739	0.739	0.803	50	5.954	0.001	0.000
24	2.858	0.591	0.678	51	6.073	0.001	0.000
25	2.977	0.447	0.549	52	6.192	0.001	0.000
26	3.096	0.341	0.430	53	6.311	0.000	0.000
27	3.215	0.259	0.328	54	6.431	0.000	0.000

Table E-4. Tritium BTC data from column 2B.

Sample	Pore Volumes	Observed C/C₀	Fit C/C₀	Sample	Pore Volumes	Observed C/C₀	Fit C/C₀
1	0.126	0.000	0.000	28	3.525	0.172	0.181
2	0.252	0.000	0.000	29	3.651	0.128	0.133
3	0.378	0.000	0.003	30	3.777	0.100	0.097
4	0.504	0.007	0.028	31	3.903	0.074	0.070
5	0.629	0.053	0.093	32	4.029	0.057	0.051
6	0.755	0.166	0.197	33	4.154	0.043	0.037
7	0.881	0.320	0.323	34	4.280	0.032	0.026
8	1.007	0.446	0.450	35	4.406	0.024	0.019
9	1.133	0.556	0.567	36	4.532	0.019	0.013
10	1.259	0.660	0.667	37	4.658	0.015	0.010
11	1.385	0.743	0.748	38	4.784	0.011	0.007
12	1.511	0.801	0.812	39	4.910	0.009	0.005
13	1.637	0.855	0.862	40	5.036	0.007	0.003
14	1.763	0.885	0.899	41	5.162	0.006	0.002
15	1.888	0.902	0.927	42	5.288	0.004	0.002
16	2.014	0.933	0.947	43	5.413	0.003	0.001
17	2.140	0.948	0.962	44	5.539	0.003	0.001
18	2.266	0.967	0.973	45	5.665	0.002	0.001
19	2.392	0.971	0.976	46	5.791	0.002	0.000
20	2.518	0.961	0.953	47	5.917	0.002	0.000
21	2.644	0.898	0.886	48	6.043	0.001	0.000
22	2.770	0.772	0.781	49	6.169	0.001	0.000
23	2.896	0.640	0.657	50	6.295	0.001	0.000
24	3.021	0.502	0.533	51	6.421	0.001	0.000
25	3.147	0.386	0.419	52	6.546	0.001	0.000
26	3.273	0.300	0.322	53	6.672	0.001	0.000
27	3.399	0.230	0.243	54	6.798	0.001	0.000

Table E-5. Tritium BTC data from column 3A.

Sample	Pore Volumes	Observed C/C₀	Fit C/C₀	Sample	Pore Volumes	Observed C/C₀	Fit C/C₀
1	0.124	0.000	0.000	28	3.475	0.206	0.289
2	0.248	0.000	0.001	29	3.599	0.164	0.237
3	0.372	0.001	0.018	30	3.724	0.152	0.194
4	0.496	0.023	0.069	31	3.848	0.127	0.159
5	0.621	0.088	0.151	32	3.972	0.103	0.130
6	0.745	0.185	0.250	33	4.096	0.082	0.105
7	0.869	0.296	0.355	34	4.220	0.063	0.086
8	0.993	0.387	0.453	35	4.344	0.052	0.070
9	1.117	0.475	0.542	36	4.468	0.041	0.057
10	1.241	0.563	0.620	37	4.592	0.032	0.046
11	1.365	0.636	0.686	38	4.717	0.027	0.038
12	1.489	0.702	0.743	39	4.841	0.022	0.031
13	1.614	0.770	0.789	40	4.965	0.018	0.025
14	1.738	0.811	0.827	41	5.089	0.015	0.020
15	1.862	0.846	0.859	42	5.213	0.012	0.017
16	1.986	0.874	0.885	43	5.337	0.010	0.014
17	2.110	0.895	0.907	44	5.461	0.009	0.011
18	2.234	0.922	0.924	45	5.585	0.008	0.009
19	2.358	0.936	0.935	46	5.710	0.006	0.007
20	2.482	0.910	0.923	47	5.834	0.006	0.006
21	2.607	0.812	0.873	48	5.958	0.005	0.005
22	2.731	0.733	0.792	49	6.082	0.004	0.004
23	2.855	0.660	0.696	50	6.206	0.004	0.003
24	2.979	0.553	0.599	51	6.330	0.003	0.003
25	3.103	0.464	0.506	52	6.454	0.003	0.002
26	3.227	0.391	0.423	53	6.578	0.002	0.002
27	3.351	0.246	0.351	54	6.702	0.002	0.002

Table E-6. Tritium BTC data from column 3B.

Sample	Pore Volumes	Observed C/C₀	Fit C/C₀	Sample	Pore Volumes	Observed C/C₀	Fit C/C₀
1	0.121	0.000	0.000	28	3.392	0.246	0.289
2	0.242	0.000	0.000	29	3.513	0.202	0.233
3	0.363	0.000	0.008	30	3.635	0.163	0.186
4	0.485	0.001	0.041	31	3.756	0.133	0.149
5	0.606	0.022	0.109	32	3.877	0.109	0.119
6	0.727	0.105	0.203	33	3.998	0.087	0.094
7	0.848	0.244	0.308	34	4.119	0.067	0.075
8	0.969	0.366	0.413	35	4.240	0.054	0.059
9	1.090	0.478	0.511	36	4.362	0.042	0.047
10	1.212	0.578	0.598	37	4.483	0.033	0.037
11	1.333	0.650	0.673	38	4.604	0.026	0.029
12	1.454	0.719	0.736	39	4.725	0.020	0.023
13	1.575	0.760	0.787	40	4.846	0.016	0.018
14	1.696	0.806	0.830	41	4.967	0.013	0.015
15	1.817	0.841	0.864	42	5.088	0.010	0.012
16	1.938	0.870	0.892	43	5.210	0.008	0.009
17	2.060	0.890	0.914	44	5.331	0.006	0.007
18	2.181	0.914	0.932	45	5.452	0.005	0.006
19	2.302	0.927	0.944	46	5.573	0.004	0.005
20	2.423	0.941	0.937	47	5.694	0.003	0.004
21	2.544	0.896	0.896	48	5.815	0.003	0.003
22	2.665	0.791	0.821	49	5.937	0.002	0.002
23	2.787	0.671	0.725	50	6.058	0.002	0.002
24	2.908	0.553	0.623	51	6.179	0.002	0.001
25	3.029	0.447	0.524	52	6.300	0.001	0.001
26	3.150	0.362	0.434	53	6.421	0.001	0.001
27	3.271	0.298	0.356	54	6.542	0.001	0.001

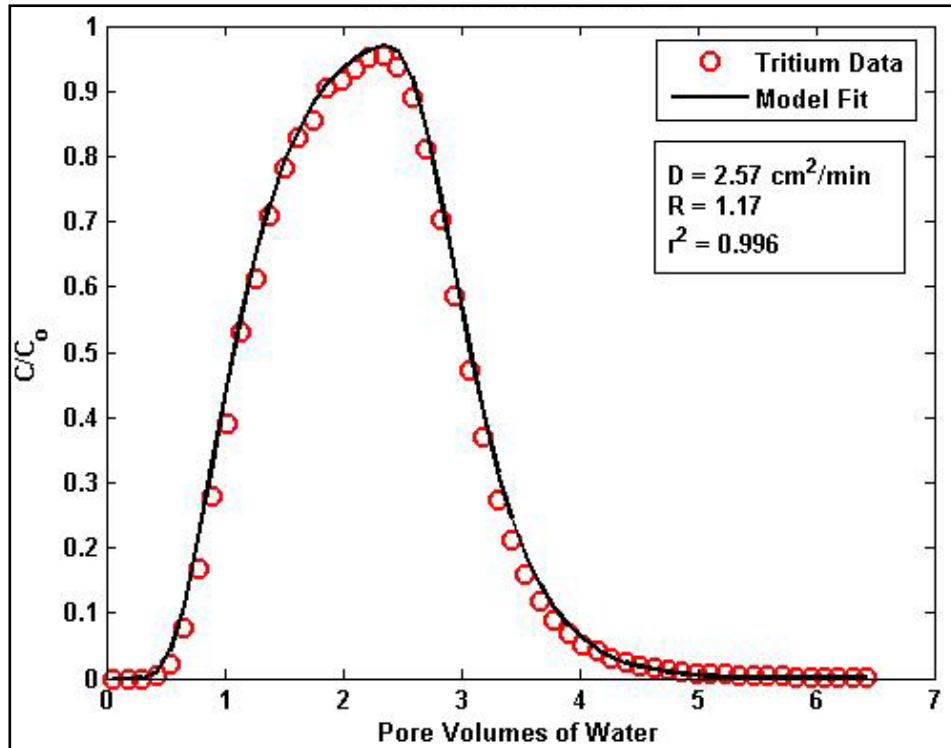


Figure E-1. Tritium BTC data from column 1A. The solid line represents the physical equilibrium model inversely fit to the data.

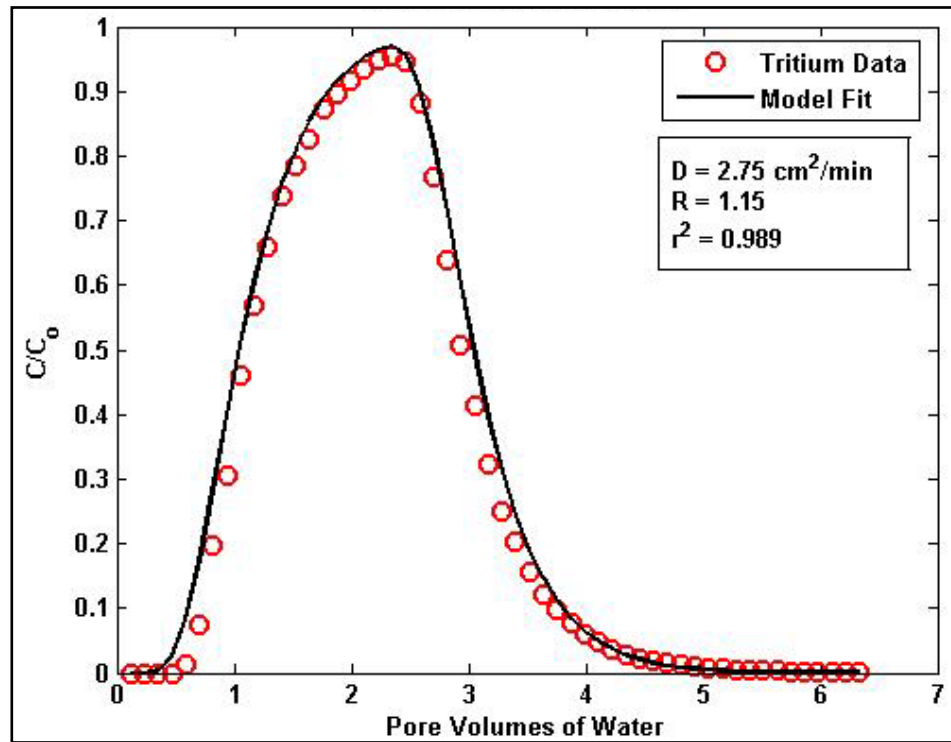


Figure E-2. Tritium BTC data from column 1B. The solid line represents the physical equilibrium model inversely fit to the data.

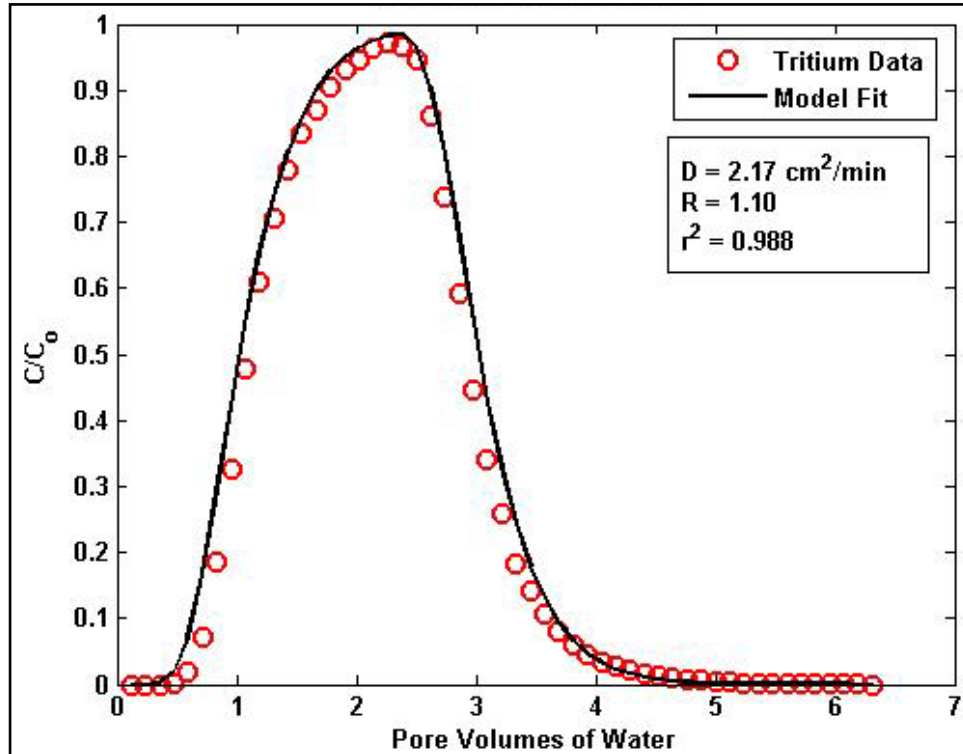


Figure E-3. Tritium BTC data from column 2A. The solid line represents the physical equilibrium model inversely fit to the data.

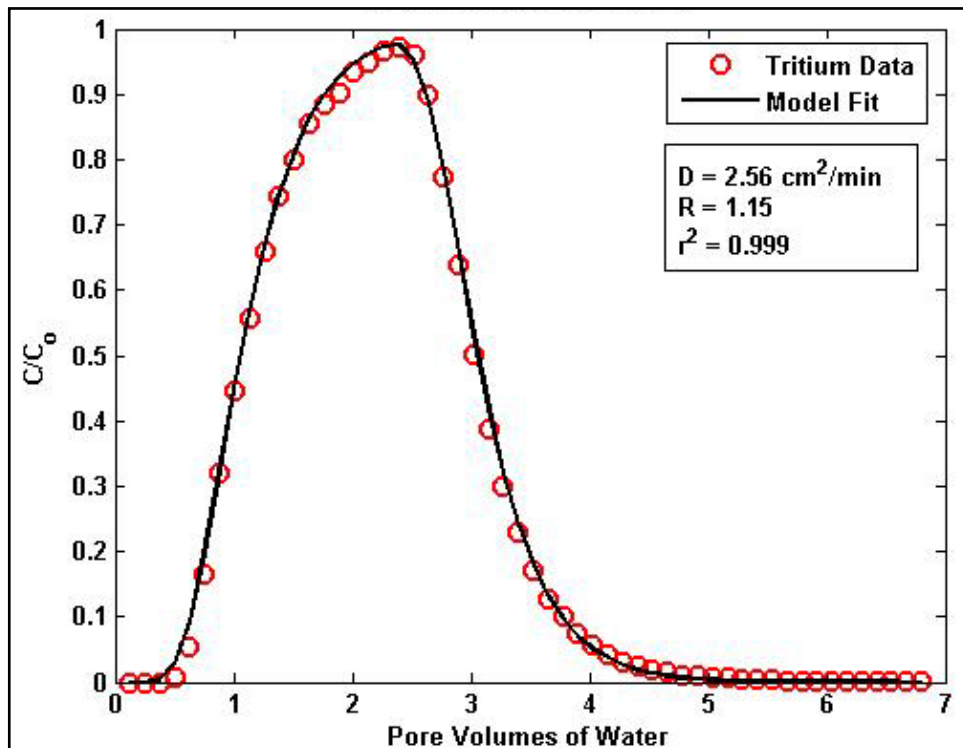


Figure E-4. Tritium BTC data from column 2B. The solid line represents the physical equilibrium model inversely fit to the data.

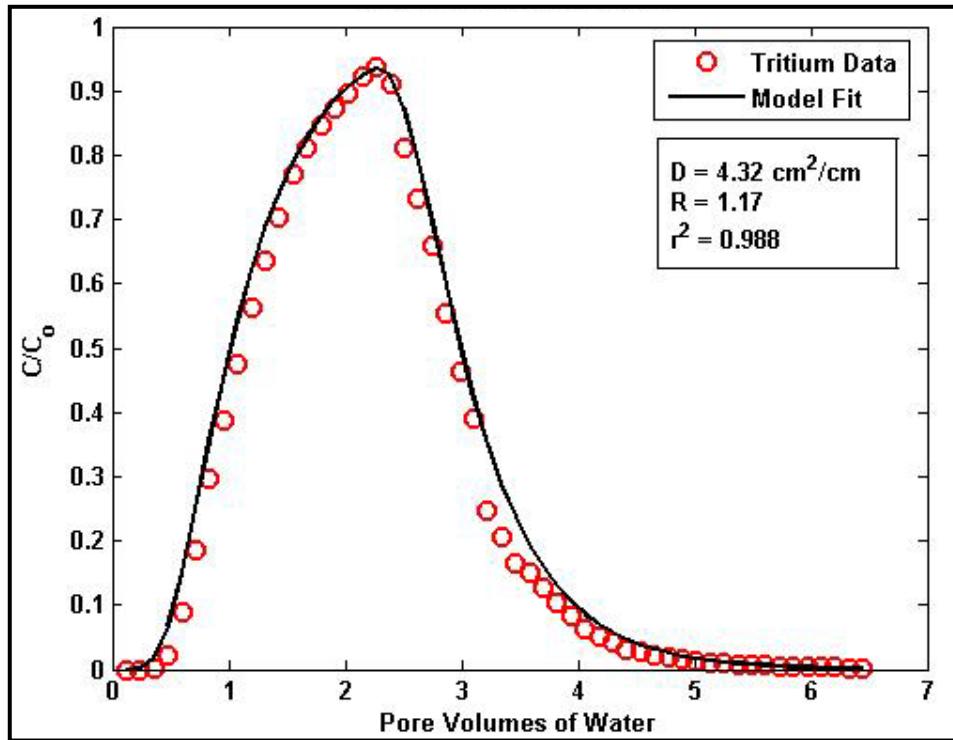


Figure E-5. Tritium BTC data from column 3A. The solid line represents the physical equilibrium model inversely fit to the data.

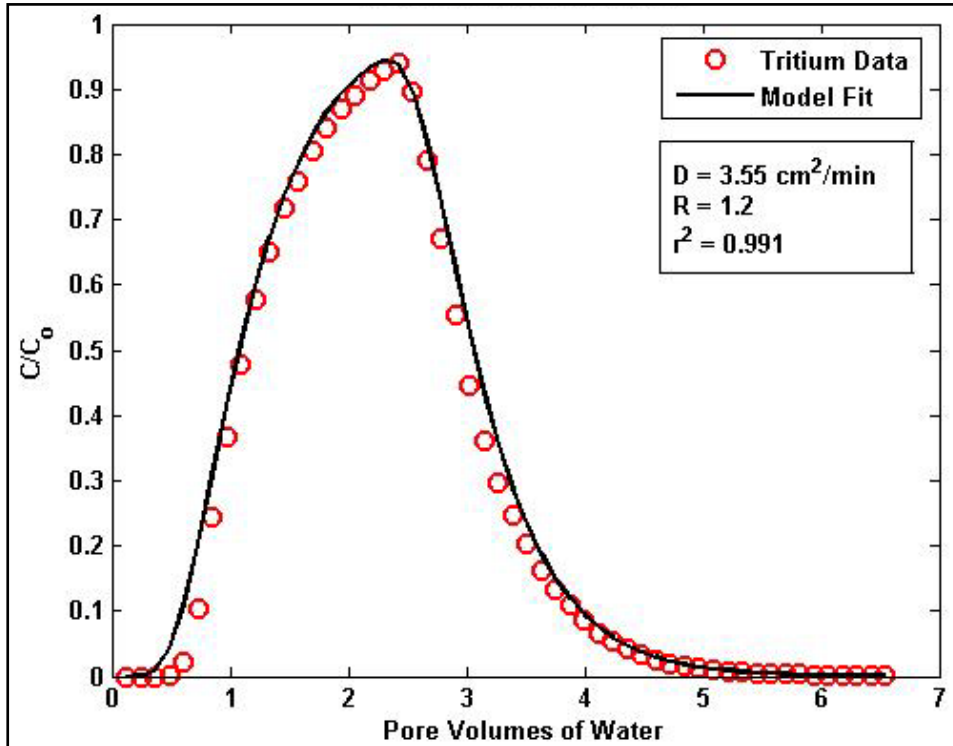


Figure E-6. Tritium BTC data from column 3B. The solid line represents the physical equilibrium model inversely fit to the data.

APPENDIX F. LABORATORY COLUMN BTEX BTC AND MODEL PREDICTION DATA.

This appendix contains the BTEX BTC data and modeling results from each laboratory transport experiment. Tables F-1 through F-6 contain the BTEX BTC data. The nonequilibrium prediction results are seen in Tables F-7 through F-12. Tables F-13 through F-18 present the equilibrium model data inversely fit to the BTEX BTC data, while the inverse nonequilibrium fit is presented in Tables F-19 through F-24. The data is presented as relative effluent concentrations as a function of effluent pore volumes. The parameters obtained from the equilibrium model fits are presented in Table F-25, while the parameters obtained from the nonequilibrium model fits are presented in Table F-26.

Table F-1. BTEX BTC data from column 1A transport experiment.

Sample	Pore Volumes	C/C _o				
		Benzene	Toluene	Ethylbenzene	M-xylene	O-xylene
1	1.2	0.004	0.002	0.003	0.002	0.003
2	2.8	0.040	0.006	0.002	0.002	0.002
3	5.2	0.147	0.025	0.004	0.004	0.005
4	7.5	0.267	0.053	0.008	0.007	0.010
5	9.8	0.368	0.081	0.013	0.011	0.016
6	12.3	0.446	0.112	0.019	0.016	0.022
7	14.9	0.501	0.144	0.025	0.021	0.029
8	17.2	0.610	0.213	0.038	0.032	0.043
9	19.6	0.623	0.219	0.041	0.035	0.047
10	24.5	0.724	0.302	0.061	0.051	0.068
11	29.6	0.784	0.378	0.083	0.071	0.094
12	34.3	0.842	0.486	0.109	0.092	0.117
13	39.6	0.924	0.469	0.117	0.099	0.127
14	44.2	0.917	0.579	0.147	0.124	0.157
15	49.5	1.010	0.681	0.186	0.156	0.195
16	53.1	0.964	0.677	0.193	0.164	0.204
17	57.7	0.987	0.716	0.214	0.181	0.225
18	62.9	1.032	0.780	0.220	0.211	0.258
19	68.3	1.056	0.814	0.244	0.255	0.282
20	73.3	1.060	0.836	0.257	0.282	0.287
21	78.1	0.959	0.850	0.247	0.281	0.295
22	83.1	0.988	0.888	0.267	0.316	0.324
23	88.1	0.971	0.887	0.274	0.340	0.340
24	92.6	0.975	0.899	0.281	0.363	0.359
25	97.4	0.949	0.877	0.270	0.360	0.353
26	102.3	1.133	0.964	0.329	0.440	0.419
27	107.2	1.070	0.920	0.325	0.437	0.416
28	112.0	1.067	0.927	0.339	0.457	0.433
29	117.3	1.064	0.934	0.354	0.481	0.452
30	122.0	0.937	0.956	0.325	0.445	0.421
31	127.0	0.847	0.949	0.358	0.499	0.472
32	133.7	0.891	0.919	0.393	0.522	0.501
33	136.3	0.989	1.006	0.442	0.554	0.543
34	141.3	0.911	0.956	0.442	0.532	0.535
35	146.0	1.023	0.921	0.455	0.538	0.547
36	151.1	0.948	1.007	0.444	0.548	0.575
37	156.0	0.927	1.004	0.466	0.559	0.587
38	161.8	0.977	0.888	0.509	0.573	0.610
39	165.7	1.031	0.936	0.551	0.588	0.640
40	170.5	0.888	0.828	0.511	0.557	0.606
41	175.6	0.996	0.922	0.571	0.597	0.663
42	180.3	1.092	1.099	0.583	0.614	0.683
43	185.2	0.977	0.921	0.605	0.554	0.694

Table F-1 (continued).

Sample	Pore Volumes	C/C_o				
		Benzene	Toluene	Ethylbenzene	M-xylene	O-xylene
44	190.4	1.127	1.080	0.622	0.657	0.720
45	195.0	1.171	1.113	0.662	0.686	0.763
46	200.0	1.133	1.082	0.650	0.679	0.754
47	205.2	1.047	1.002	0.705	0.640	0.709
48	215.0	1.078	1.095	0.734	0.669	0.751
49	219.6	1.061	0.971	0.734	0.673	0.753
50	224.9	1.028	0.956	0.740	0.683	0.767
51	231.1	1.082	0.986	0.751	0.691	0.797

Table F-2. BTEX BTC data from column 1B transport experiment.

Sample	Pore Volumes	C/C _o				
		Benzene	Toluene	Ethylbenzene	M-xylene	O-xylene
1	0.5	0.011	0.015	0.008	0.009	0.009
2	2.7	0.029	0.005	0.003	0.004	0.004
3	5.0	0.126	0.010	0.002	0.003	0.002
4	7.4	0.266	0.028	0.003	0.003	0.003
5	10.0	0.400	0.058	0.004	0.003	0.005
6	12.4	0.420	0.076	0.006	0.005	0.007
7	14.7	0.557	0.116	0.009	0.007	0.011
8	17.1	0.628	0.153	0.012	0.010	0.015
9	19.4	0.704	0.193	0.017	0.013	0.020
10	24.5	0.825	0.279	0.029	0.022	0.034
11	29.2	0.900	0.355	0.046	0.037	0.055
12	34.3	0.930	0.381	0.054	0.042	0.062
13	38.8	0.976	0.498	0.077	0.060	0.087
14	43.5	0.984	0.537	0.094	0.073	0.105
15	48.4	1.033	0.610	0.118	0.092	0.129
16	53.4	1.007	0.639	0.137	0.108	0.152
17	58.1	1.047	0.764	0.174	0.138	0.189
18	62.9	1.026	0.714	0.181	0.146	0.198
19	67.3	1.032	0.818	0.216	0.173	0.229
20	72.1	1.025	0.838	0.239	0.192	0.253
21	76.9	0.987	0.759	0.236	0.193	0.252
22	82.2	1.070	0.843	0.277	0.229	0.294
23	86.2	1.036	0.831	0.287	0.238	0.306
24	91.2	0.955	0.788	0.291	0.242	0.308
25	95.8	0.937	0.783	0.309	0.258	0.325
26	100.6	1.017	0.902	0.337	0.289	0.363
27	105.6	0.993	0.892	0.364	0.310	0.387
28	110.1	1.104	0.982	0.410	0.348	0.428
29	114.9	0.990	0.908	0.401	0.345	0.421
30	119.5	1.024	0.945	0.432	0.373	0.454
31	124.8	0.991	0.922	0.437	0.380	0.457
32	143.5	0.954	0.949	0.491	0.435	0.513
33	148.1	0.856	0.903	0.476	0.424	0.501
34	152.9	1.001	0.829	0.545	0.484	0.569
35	158.0	0.981	0.952	0.555	0.496	0.576
36	162.6	0.935	0.938	0.552	0.498	0.578
37	167.5	0.950	0.906	0.565	0.512	0.594
38	172.4	0.987	0.925	0.596	0.544	0.620
39	177.6	1.041	0.975	0.628	0.573	0.656
40	182.1	0.915	0.862	0.574	0.528	0.603
41	186.5	1.063	0.994	0.658	0.605	0.695
42	191.6	0.984	0.933	0.640	0.591	0.674
43	196.3	1.014	1.015	0.699	0.644	0.727

Table F-2 (continued).

Sample	Pore Volumes	C/C_o				
		Benzene	Toluene	Ethylbenzene	M-xylene	O-xylene
44	201.1	1.066	1.057	0.732	0.672	0.755
45	205.9	0.968	0.972	0.690	0.635	0.725
46	210.4	1.016	1.008	0.730	0.671	0.767
47	215.5	0.957	0.957	0.712	0.660	0.746
48	219.7	1.014	1.006	0.755	0.698	0.792
49	224.9	0.990	0.905	0.648	0.605	0.703
50	225.1	1.028	0.953	0.696	0.652	0.746
51	225.3	1.112	1.032	0.753	0.707	0.795

Table F-3. BTEX BTC data from column 2A transport experiment.

Sample	Pore Volumes	C/C ₀				
		Benzene	Toluene	Ethylbenzene	M-xylene	O-xylene
1	0.6	0.008	0.006	0.006	0.006	0.006
2	2.5	0.011	0.002	0.002	0.003	0.002
3	5.0	0.079	0.005	0.002	0.002	0.002
4	7.5	0.214	0.014	0.002	0.002	0.002
5	9.7	0.325	0.027	0.002	0.002	0.002
6	12.4	0.460	0.050	0.003	0.003	0.004
7	14.7	0.443	0.062	0.004	0.003	0.004
8	17.3	0.578	0.100	0.006	0.004	0.007
9	21.8	0.665	0.157	0.010	0.007	0.012
10	24.4	0.741	0.236	0.015	0.011	0.018
11	29.4	0.836	0.284	0.025	0.020	0.031
12	34.7	0.936	0.380	0.033	0.025	0.038
13	39.9	0.944	0.435	0.043	0.032	0.049
14	44.2	0.962	0.489	0.054	0.040	0.062
15	49.1	1.024	0.562	0.070	0.052	0.079
16	54.1	0.967	0.573	0.080	0.060	0.090
17	58.8	0.955	0.597	0.090	0.068	0.102
18	64.9	0.965	0.644	0.113	0.085	0.123
19	68.6	0.955	0.656	0.134	0.106	0.148
20	73.2	1.065	0.748	0.147	0.113	0.161
21	78.3	0.977	0.716	0.155	0.120	0.169
22	83.0	0.953	0.716	0.165	0.129	0.181
23	88.2	0.976	0.750	0.184	0.145	0.201
24	92.6	0.895	0.761	0.185	0.146	0.204
25	97.2	0.905	0.779	0.201	0.162	0.221
26	102.3	0.985	0.784	0.246	0.197	0.261
27	107.0	1.023	0.793	0.266	0.214	0.282
28	111.8	1.069	0.828	0.298	0.239	0.312
29	116.8	0.926	0.781	0.266	0.217	0.285
30	121.9	1.071	0.900	0.310	0.253	0.325
31	126.7	0.988	0.846	0.312	0.258	0.333
32	131.5	0.940	0.812	0.311	0.258	0.332
33	136.4	0.918	0.801	0.318	0.266	0.338
34	141.1	0.965	0.847	0.345	0.290	0.367
35	145.9	1.026	0.896	0.372	0.312	0.391
36	150.9	0.966	0.855	0.371	0.315	0.393
37	155.8	0.843	0.757	0.342	0.291	0.364
38	160.5	0.953	0.858	0.396	0.338	0.419
39	165.6	0.953	0.860	0.407	0.351	0.429
40	165.8	0.977	0.879	0.424	0.366	0.438
41	176.0	0.912	0.835	0.419	0.367	0.435
42	179.9	0.921	0.844	0.438	0.397	0.468
43	184.6	1.050	0.901	0.499	0.458	0.492

Table F-3 (continued).

Sample	Pore Volumes	C/C₀				
		Benzene	Toluene	Ethylbenzene	M-xylene	O-xylene
44	189.7	0.970	0.841	0.486	0.450	0.478
45	194.4	1.084	0.942	0.550	0.507	0.529
46	199.2	1.111	0.961	0.563	0.521	0.551
47	204.3	1.074	0.937	0.561	0.521	0.561
48	209.7	1.065	0.927	0.566	0.526	0.581
49	213.9	1.015	0.885	0.557	0.517	0.586
50	219.1	0.933	0.902	0.568	0.532	0.555
51	223.5	0.979	0.944	0.582	0.559	0.589
52	228.7	1.000	0.968	0.577	0.566	0.608

Table F-4. BTEX BTC data from column 2B transport experiment.

Sample	Pore Volumes	C/C ₀				
		Benzene	Toluene	Ethylbenzene	M-xylene	O-xylene
1	0.7	0.006	0.000	0.000	0.000	0.000
2	2.7	0.015	0.005	0.005	0.004	0.005
3	5.2	0.092	0.007	0.003	0.003	0.003
4	7.8	0.208	0.018	0.003	0.003	0.003
5	11.1	0.314	0.040	0.004	0.003	0.004
6	12.9	0.394	0.059	0.004	0.003	0.005
7	15.5	0.435	0.082	0.006	0.005	0.007
8	18.1	0.486	0.111	0.008	0.006	0.010
9	21.5	0.576	0.161	0.013	0.010	0.016
10	26.1	0.709	0.245	0.024	0.019	0.029
11	31.2	0.837	0.335	0.043	0.034	0.051
12	36.6	0.880	0.415	0.063	0.050	0.072
13	41.6	0.916	0.477	0.087	0.069	0.097
14	47.6	0.944	0.560	0.121	0.097	0.133
15	49.2	0.974	0.583	0.130	0.105	0.143
16	57.2	0.981	0.650	0.177	0.146	0.190
17	62.4	0.969	0.671	0.202	0.169	0.217
18	67.8	0.939	0.737	0.211	0.179	0.229
19	72.8	0.966	0.776	0.239	0.201	0.255
20	77.9	1.005	0.814	0.258	0.219	0.274
21	83.3	0.960	0.877	0.270	0.230	0.286
22	88.5	0.998	0.872	0.291	0.239	0.294
23	93.4	0.897	0.891	0.299	0.235	0.290
24	98.7	0.998	0.903	0.325	0.261	0.322
25	103.9	0.938	0.883	0.355	0.270	0.331
26	108.8	1.055	0.910	0.361	0.312	0.358
27	113.8	1.036	0.905	0.369	0.322	0.368
28	119.5	1.066	0.927	0.387	0.340	0.392
29	124.4	1.091	0.956	0.410	0.362	0.421
30	129.6	0.986	0.880	0.398	0.356	0.414
31	134.9	1.058	0.939	0.435	0.392	0.462
32	146.2	0.988	0.944	0.440	0.415	0.478
33	148.3	0.966	0.944	0.460	0.413	0.476
34	155.3	0.967	0.909	0.467	0.437	0.488
35	160.8	0.962	0.888	0.482	0.444	0.481
36	165.7	0.965	0.901	0.495	0.456	0.511
37	170.6	1.010	0.932	0.502	0.464	0.511
38	175.9	1.088	0.970	0.541	0.488	0.559
39	185.9	0.958	0.956	0.557	0.497	0.530
40	191.3	0.962	0.962	0.565	0.505	0.534
41	197.0	0.953	0.953	0.576	0.513	0.549
42	202.4	0.923	0.947	0.576	0.522	0.563
43	207.3	0.981	0.977	0.584	0.539	0.609

Table F-4 (continued).

Sample	Pore Volumes	C/C₀				
		Benzene	Toluene	Ethylbenzene	M-xylene	O-xylene
44	211.8	0.968	0.970	0.591	0.546	0.618
45	217.0	0.943	0.948	0.583	0.539	0.617
46	222.1	1.001	0.994	0.610	0.569	0.641
47	226.8	1.047	1.045	0.652	0.608	0.691
48	233.0	0.938	0.936	0.626	0.586	0.663
49	237.9	0.970	0.879	0.567	0.529	0.600
50	241.7	0.954	0.939	0.653	0.611	0.692

Table F-5. BTEX BTC data from column 3A transport experiment.

Sample	Pore Volumes	C/Co				
		Benzene	Toluene	Ethylbenzene	M-xylene	O-xylene
1	0.6	0.007	0.005	0.009	0.006	0.009
2	3.4	0.109	0.019	0.007	0.005	0.007
3	5.1	0.169	0.033	0.008	0.006	0.008
4	7.7	0.302	0.070	0.013	0.011	0.015
5	10.1	0.351	0.091	0.017	0.014	0.020
6	13.4	0.388	0.114	0.022	0.019	0.026
7	15.6	0.554	0.185	0.035	0.029	0.039
8	18.5	0.574	0.191	0.039	0.033	0.043
9	20.9	0.720	0.251	0.052	0.043	0.056
10	26.5	0.806	0.318	0.068	0.057	0.075
11	31.3	0.781	0.346	0.081	0.070	0.090
12	36.5	0.874	0.424	0.100	0.085	0.110
13	41.4	0.995	0.519	0.126	0.107	0.135
14	46.7	0.872	0.499	0.128	0.110	0.139
15	51.9	0.930	0.562	0.148	0.126	0.159
16	58.4	1.007	0.651	0.182	0.154	0.192
17	60.9	0.924	0.616	0.174	0.149	0.186
18	69.7	0.905	0.644	0.184	0.156	0.198
19	72.3	0.901	0.655	0.195	0.165	0.208
20	77.4	0.959	0.717	0.218	0.184	0.232
21	82.6	0.991	0.702	0.227	0.192	0.242
22	87.9	1.017	0.736	0.236	0.204	0.248
23	93.7	1.094	0.764	0.279	0.242	0.294
24	98.2	0.990	0.787	0.279	0.243	0.297
25	103.9	0.972	0.808	0.326	0.288	0.349
26	109.9	1.037	0.877	0.372	0.320	0.382
27	112.7	1.053	0.902	0.384	0.334	0.395
28	118.4	1.021	0.901	0.407	0.360	0.417
29	126.6	0.992	0.889	0.415	0.370	0.425
30	129.0	0.931	0.881	0.385	0.348	0.402
31	133.0	0.921	0.881	0.392	0.359	0.413
32	139.1	0.946	0.911	0.421	0.385	0.437
33	143.8	0.940	0.907	0.439	0.398	0.455
34	153.8	0.911	1.077	0.464	0.423	0.483
35	159.7	1.037	0.956	0.523	0.472	0.539
36	164.7	1.081	0.982	0.546	0.492	0.556
37	169.2	0.914	0.887	0.500	0.455	0.522
38	179.7	0.916	0.901	0.533	0.488	0.558
39	184.2	1.027	1.004	0.596	0.548	0.621
40	190.0	0.924	0.911	0.549	0.507	0.576
41	196.2	0.989	0.857	0.555	0.514	0.579
42	200.5	1.107	1.060	0.591	0.550	0.604
43	205.3	1.019	0.979	0.552	0.517	0.569

Table F-5 (continued).

Sample	Pore Volumes	C/Co				
		Benzene	Toluene	Ethylbenzene	M-xylene	O-xylene
44	211.4	1.062	1.021	0.588	0.555	0.613
45	215.3	1.064	1.027	0.613	0.580	0.636
46	221.0	0.938	0.899	0.560	0.532	0.593
47	226.0	1.048	0.998	0.634	0.597	0.665
48	230.8	1.010	0.958	0.610	0.583	0.650
49	235.7	0.945	0.895	0.577	0.553	0.620
50	238.3	1.038	0.975	0.637	0.609	0.669

Table F-6. BTEX BTC data from column 3B transport experiment.

Sample	Pore Volumes	C/Co				
		Benzene	Toluene	Ethylbenzene	M-xylene	O-xylene
1	0.3	0.009	0.011	0.011	0.009	0.011
2	2.7	0.052	0.006	0.005	0.004	0.004
3	5.2	0.215	0.026	0.005	0.004	0.005
4	7.6	0.321	0.053	0.006	0.005	0.007
5	9.8	0.370	0.074	0.008	0.007	0.010
6	12.8	0.505	0.124	0.014	0.011	0.017
7	15.4	0.558	0.155	0.019	0.015	0.022
8	18.7	0.662	0.224	0.030	0.024	0.034
9	20.3	0.703	0.237	0.033	0.027	0.038
10	24.8	0.751	0.278	0.044	0.036	0.051
11	30.4	0.809	0.324	0.062	0.051	0.071
12	35.9	0.874	0.421	0.085	0.069	0.095
13	39.8	0.943	0.483	0.102	0.083	0.114
14	45.1	0.908	0.505	0.117	0.096	0.129
15	49.8	0.918	0.541	0.134	0.111	0.146
16	54.6	0.947	0.588	0.155	0.128	0.168
17	59.9	0.960	0.626	0.175	0.146	0.188
18	64.8	0.910	0.661	0.184	0.154	0.198
19	73.1	1.019	0.732	0.235	0.197	0.249
20	74.8	1.000	0.732	0.241	0.206	0.259
21	79.5	1.010	0.757	0.258	0.220	0.275
22	84.5	1.074	0.823	0.292	0.249	0.308
23	89.8	0.966	0.791	0.307	0.259	0.311
24	95.2	1.011	0.808	0.312	0.269	0.331
25	99.5	1.004	0.855	0.340	0.296	0.357
26	104.5	1.009	0.865	0.359	0.323	0.373
27	109.5	1.069	0.899	0.388	0.339	0.404
28	113.3	1.074	0.910	0.404	0.353	0.421
29	119.0	1.040	0.892	0.410	0.361	0.425
30	125.7	1.020	0.885	0.423	0.374	0.441
31	131.7	1.077	0.944	0.470	0.417	0.486
32	134.3	0.965	0.895	0.459	0.415	0.480
33	139.4	1.047	0.963	0.497	0.445	0.507
34	144.2	0.975	0.914	0.490	0.442	0.509
35	148.6	0.994	0.944	0.519	0.470	0.535
36	154.4	0.911	0.915	0.549	0.499	0.564
37	164.0	0.996	0.912	0.533	0.482	0.549
38	168.7	1.035	0.946	0.563	0.511	0.580
39	175.1	0.984	0.914	0.565	0.516	0.587
40	179.3	1.109	1.025	0.633	0.577	0.646
41	184.1	0.969	0.903	0.597	0.544	0.622
42	188.6	1.027	0.966	0.636	0.585	0.658
43	193.1	1.014	0.956	0.634	0.586	0.651

Table F-6 (continued).

Sample	Pore Volumes	C/Co				
		Benzene	Toluene	Ethylbenzene	M-xylene	O-xylene
44	197.2	0.922	0.879	0.601	0.557	0.621
45	202.8	1.000	0.943	0.640	0.595	0.665
46	207.1	0.931	0.891	0.648	0.573	0.638
47	212.3	1.013	0.978	0.659	0.624	0.692
48	217.2	1.043	0.993	0.666	0.631	0.699
49	222.3	1.041	0.999	0.682	0.651	0.722
50	227.5	0.988	0.946	0.696	0.652	0.735
51	232.6	0.961	0.920	0.680	0.641	0.720

Table F-7. Nonequilibrium prediction model results for column 1A experiment.

Sample	Pore Volumes	C/Co				
		Benzene	Toluene	Ethylbenzene	M-xylene	O-xylene
1	1.2	0.012	0.001	0.001	0.001	0.001
2	2.8	0.080	0.014	0.004	0.004	0.005
3	5.2	0.215	0.042	0.010	0.010	0.012
4	7.5	0.358	0.082	0.019	0.019	0.023
5	9.8	0.493	0.131	0.032	0.030	0.037
6	12.3	0.617	0.192	0.048	0.045	0.055
7	14.9	0.723	0.263	0.070	0.065	0.079
8	17.2	0.795	0.328	0.093	0.085	0.103
9	19.6	0.852	0.396	0.119	0.109	0.130
10	24.5	0.927	0.530	0.182	0.166	0.196
11	29.6	0.965	0.648	0.253	0.231	0.269
12	34.3	0.983	0.739	0.325	0.297	0.341
13	39.6	0.992	0.817	0.405	0.372	0.422
14	44.2	0.996	0.867	0.473	0.436	0.489
15	49.5	0.998	0.910	0.547	0.508	0.562
16	53.1	0.999	0.932	0.594	0.554	0.608
17	57.7	1.000	0.952	0.649	0.609	0.663
18	62.9	1.000	0.969	0.706	0.666	0.718
19	68.3	1.000	0.980	0.756	0.719	0.767
20	73.3	1.000	0.986	0.796	0.761	0.805
21	78.1	1.000	0.991	0.830	0.797	0.838
22	83.1	1.000	0.994	0.859	0.829	0.866
23	88.1	1.000	0.996	0.885	0.858	0.891
24	92.6	1.000	0.997	0.904	0.879	0.909
25	97.4	1.000	0.998	0.921	0.899	0.925
26	102.3	1.000	0.999	0.935	0.916	0.939
27	107.2	1.000	0.999	0.947	0.931	0.950
28	112.0	1.000	1.000	0.957	0.942	0.959
29	117.3	1.000	1.000	0.966	0.953	0.968
30	122.0	1.000	1.000	0.972	0.961	0.974
31	127.0	1.000	1.000	0.978	0.968	0.979
32	133.7	1.000	1.000	0.983	0.976	0.984
33	136.3	1.000	1.000	0.985	0.978	0.986
34	141.3	1.000	1.000	0.988	0.982	0.989
35	146.0	1.000	1.000	0.990	0.985	0.991
36	151.1	1.000	1.000	0.992	0.988	0.993
37	156.0	1.000	1.000	0.994	0.990	0.994
38	161.8	1.000	1.000	0.995	0.993	0.996
39	165.7	1.000	1.000	0.996	0.994	0.996
40	170.5	1.000	1.000	0.997	0.995	0.997
41	175.6	1.000	1.000	0.998	0.996	0.998
42	180.3	1.000	1.000	0.998	0.997	0.998
43	185.2	1.000	1.000	0.998	0.997	0.999

Table F-7 (continued).

Sample	Pore Volumes	C/Co				
		Benzene	Toluene	Ethylbenzene	M-xylene	O-xylene
44	190.4	1.000	1.000	0.999	0.998	0.999
45	195.0	1.000	1.000	0.999	0.998	0.999
46	200.0	1.000	1.000	0.999	0.999	0.999
47	205.2	1.000	1.000	0.999	0.999	0.999
48	215.0	1.000	1.000	1.000	0.999	1.000
49	219.6	1.000	1.000	1.000	0.999	1.000
50	224.9	1.000	1.000	1.000	1.000	1.000
51	231.1	1.000	1.000	1.000	1.000	1.000

Table F-8. Nonequilibrium prediction model results for column 1B experiment.

Sample	Pore Volumes	C/Co				
		Benzene	Toluene	Ethylbenzene	M-xylene	O-xylene
1	0.5	0.000	0.000	0.000	0.000	0.000
2	2.7	0.050	0.011	0.003	0.003	0.003
3	5.0	0.160	0.033	0.007	0.008	0.009
4	7.4	0.303	0.069	0.015	0.015	0.018
5	10.0	0.458	0.119	0.027	0.026	0.031
6	12.4	0.587	0.175	0.042	0.039	0.048
7	14.7	0.688	0.233	0.058	0.054	0.066
8	17.1	0.776	0.299	0.080	0.073	0.088
9	19.4	0.839	0.363	0.103	0.094	0.113
10	24.5	0.926	0.498	0.162	0.147	0.174
11	29.2	0.965	0.610	0.224	0.203	0.239
12	34.3	0.985	0.710	0.297	0.270	0.312
13	38.8	0.993	0.782	0.362	0.331	0.379
14	43.5	0.997	0.840	0.431	0.396	0.447
15	48.4	0.999	0.886	0.500	0.461	0.515
16	53.4	0.999	0.920	0.565	0.525	0.580
17	58.1	1.000	0.943	0.622	0.582	0.636
18	62.9	1.000	0.960	0.675	0.634	0.687
19	67.3	1.000	0.972	0.718	0.679	0.730
20	72.1	1.000	0.980	0.760	0.722	0.770
21	76.9	1.000	0.986	0.797	0.761	0.806
22	82.2	1.000	0.991	0.832	0.799	0.840
23	86.2	1.000	0.994	0.855	0.824	0.862
24	91.2	1.000	0.996	0.879	0.852	0.886
25	95.8	1.000	0.997	0.899	0.874	0.904
26	100.6	1.000	0.998	0.916	0.893	0.920
27	105.6	1.000	0.999	0.931	0.911	0.935
28	110.1	1.000	0.999	0.942	0.924	0.945
29	114.9	1.000	0.999	0.952	0.937	0.955
30	119.5	1.000	1.000	0.960	0.946	0.963
31	124.8	1.000	1.000	0.968	0.956	0.970
32	143.5	1.000	1.000	0.985	0.979	0.986
33	148.1	1.000	1.000	0.988	0.982	0.989
34	152.9	1.000	1.000	0.990	0.985	0.991
35	158.0	1.000	1.000	0.992	0.988	0.993
36	162.6	1.000	1.000	0.993	0.990	0.994
37	167.5	1.000	1.000	0.995	0.992	0.995
38	172.4	1.000	1.000	0.996	0.993	0.996
39	177.6	1.000	1.000	0.997	0.994	0.997
40	182.1	1.000	1.000	0.997	0.995	0.997
41	186.5	1.000	1.000	0.998	0.996	0.998
42	191.6	1.000	1.000	0.998	0.997	0.998
43	196.3	1.000	1.000	0.998	0.997	0.999

Table F-8 (continued).

Sample	Pore Volumes	C/Co				
		Benzene	Toluene	Ethylbenzene	M-xylene	O-xylene
44	201.1	1.000	1.000	0.999	0.998	0.999
45	205.9	1.000	1.000	0.999	0.998	0.999
46	210.4	1.000	1.000	0.999	0.999	0.999
47	215.5	1.000	1.000	0.999	0.999	0.999
48	219.7	1.000	1.000	0.999	0.999	1.000
49	224.9	1.000	1.000	1.000	0.999	1.000
50	225.1	1.000	1.000	1.000	0.999	1.000
51	225.3	1.000	1.000	1.000	0.999	1.000

Table F-9. Nonequilibrium prediction model results for column 2A experiment.

Sample	Pore Volumes	C/Co				
		Benzene	Toluene	Ethylbenzene	M-xylene	O-xylene
1	0.6	0.000	0.000	0.000	0.000	0.000
2	2.5	0.042	0.010	0.003	0.004	0.004
3	5.0	0.153	0.033	0.009	0.009	0.010
4	7.5	0.298	0.070	0.017	0.017	0.020
5	9.7	0.428	0.110	0.027	0.027	0.031
6	12.4	0.571	0.168	0.042	0.041	0.048
7	14.7	0.680	0.226	0.059	0.057	0.067
8	17.3	0.774	0.294	0.081	0.076	0.090
9	21.8	0.882	0.414	0.126	0.117	0.137
10	24.4	0.922	0.481	0.156	0.144	0.168
11	29.4	0.965	0.598	0.218	0.200	0.232
12	34.7	0.986	0.705	0.291	0.267	0.307
13	39.9	0.994	0.787	0.365	0.335	0.381
14	44.2	0.997	0.840	0.426	0.392	0.442
15	49.1	0.999	0.886	0.492	0.455	0.508
16	54.1	1.000	0.920	0.556	0.517	0.571
17	58.8	1.000	0.944	0.613	0.573	0.628
18	64.9	1.000	0.965	0.680	0.639	0.692
19	68.6	1.000	0.974	0.715	0.675	0.727
20	73.2	1.000	0.982	0.756	0.717	0.767
21	78.3	1.000	0.988	0.796	0.759	0.805
22	83.0	1.000	0.992	0.827	0.792	0.835
23	88.2	1.000	0.995	0.857	0.825	0.864
24	92.6	1.000	0.996	0.879	0.849	0.885
25	97.2	1.000	0.998	0.899	0.872	0.904
26	102.3	1.000	0.998	0.917	0.893	0.922
27	107.0	1.000	0.999	0.931	0.910	0.935
28	111.8	1.000	0.999	0.943	0.924	0.947
29	116.8	1.000	1.000	0.954	0.937	0.957
30	121.9	1.000	1.000	0.963	0.948	0.965
31	126.7	1.000	1.000	0.970	0.957	0.971
32	131.5	1.000	1.000	0.975	0.964	0.977
33	136.4	1.000	1.000	0.980	0.971	0.981
34	141.1	1.000	1.000	0.984	0.976	0.985
35	145.9	1.000	1.000	0.987	0.980	0.988
36	150.9	1.000	1.000	0.989	0.984	0.990
37	155.8	1.000	1.000	0.991	0.987	0.992
38	160.5	1.000	1.000	0.993	0.989	0.994
39	165.6	1.000	1.000	0.994	0.991	0.995
40	165.8	1.000	1.000	0.995	0.991	0.995
41	176.0	1.000	1.000	0.997	0.994	0.997
42	179.9	1.000	1.000	0.997	0.995	0.997
43	184.6	1.000	1.000	0.998	0.996	0.998

Table F-9 (continued).

Sample	Pore Volumes	C/Co				
		Benzene	Toluene	Ethylbenzene	M-xylene	O-xylene
44	189.7	1.000	1.000	0.998	0.997	0.998
45	194.4	1.000	1.000	0.999	0.997	0.999
46	199.2	1.000	1.000	0.999	0.998	0.999
47	204.3	1.000	1.000	0.999	0.998	0.999
48	209.7	1.000	1.000	0.999	0.999	0.999
49	213.9	1.000	1.000	0.999	0.999	0.999
50	219.1	1.000	1.000	1.000	0.999	1.000
51	223.5	1.000	1.000	1.000	0.999	1.000
52	228.7	1.000	1.000	1.000	0.999	1.000

Table F-10. Nonequilibrium prediction model results for column 2B experiment.

Sample	Pore Volumes	C/Co				
		Benzene	Toluene	Ethylbenzene	M-xylene	O-xylene
1	0.7	0.000	0.000	0.000	0.001	0.000
2	2.7	0.048	0.012	0.004	0.004	0.005
3	5.2	0.159	0.036	0.009	0.010	0.011
4	7.8	0.302	0.073	0.018	0.019	0.022
5	11.1	0.484	0.135	0.034	0.034	0.039
6	12.9	0.572	0.173	0.045	0.043	0.051
7	15.5	0.684	0.235	0.064	0.061	0.071
8	18.1	0.770	0.298	0.085	0.080	0.094
9	21.5	0.855	0.386	0.118	0.109	0.129
10	26.1	0.924	0.496	0.167	0.154	0.180
11	31.2	0.965	0.610	0.231	0.212	0.245
12	36.6	0.985	0.709	0.301	0.276	0.317
13	41.6	0.993	0.782	0.367	0.338	0.384
14	47.6	0.998	0.850	0.447	0.413	0.463
15	49.2	0.998	0.864	0.467	0.432	0.483
16	57.2	1.000	0.920	0.565	0.526	0.580
17	62.4	1.000	0.944	0.623	0.583	0.637
18	67.8	1.000	0.962	0.678	0.638	0.690
19	72.8	1.000	0.973	0.723	0.684	0.734
20	77.9	1.000	0.982	0.764	0.726	0.774
21	83.3	1.000	0.988	0.802	0.766	0.811
22	88.5	1.000	0.992	0.833	0.800	0.841
23	93.4	1.000	0.994	0.859	0.828	0.866
24	98.7	1.000	0.996	0.883	0.855	0.889
25	103.9	1.000	0.997	0.902	0.877	0.907
26	108.8	1.000	0.998	0.918	0.895	0.923
27	113.8	1.000	0.999	0.932	0.911	0.936
28	119.5	1.000	0.999	0.945	0.927	0.948
29	124.4	1.000	1.000	0.954	0.938	0.957
30	129.6	1.000	1.000	0.963	0.949	0.965
31	134.9	1.000	1.000	0.969	0.957	0.971
32	146.2	1.000	1.000	0.980	0.972	0.982
33	148.3	1.000	1.000	0.982	0.974	0.983
34	155.3	1.000	1.000	0.986	0.980	0.987
35	160.8	1.000	1.000	0.989	0.983	0.990
36	165.7	1.000	1.000	0.991	0.986	0.992
37	170.6	1.000	1.000	0.993	0.988	0.993
38	175.9	1.000	1.000	0.994	0.991	0.995
39	185.9	1.000	1.000	0.996	0.994	0.996
40	191.3	1.000	1.000	0.997	0.995	0.997
41	197.0	1.000	1.000	0.998	0.996	0.998
42	202.4	1.000	1.000	0.998	0.997	0.998
43	207.3	1.000	1.000	0.998	0.997	0.999

Table F-10 (continued).

Sample	Pore Volumes	C/Co				
		Benzene	Toluene	Ethylbenzene	M-xylene	O-xylene
44	211.8	1.000	1.000	0.999	0.998	0.999
45	217.0	1.000	1.000	0.999	0.998	0.999
46	222.1	1.000	1.000	0.999	0.998	0.999
47	226.8	1.000	1.000	0.999	0.999	0.999
48	233.0	1.000	1.000	0.999	0.999	1.000
49	237.9	1.000	1.000	1.000	0.999	1.000
50	241.7	1.000	1.000	1.000	0.999	1.000

Table F-11. Nonequilibrium prediction model results for column 3A experiment.

Sample	Pore Volumes	C/Co				
		Benzene	Toluene	Ethylbenzene	M-xylene	O-xylene
1	0.6	0.001	0.001	0.001	0.002	0.001
2	3.4	0.119	0.034	0.011	0.012	0.014
3	5.1	0.213	0.061	0.019	0.020	0.022
4	7.7	0.365	0.113	0.035	0.034	0.040
5	10.1	0.493	0.167	0.053	0.051	0.058
6	13.4	0.643	0.249	0.082	0.078	0.090
7	15.6	0.724	0.308	0.105	0.099	0.114
8	18.5	0.803	0.381	0.138	0.128	0.148
9	20.9	0.852	0.440	0.166	0.154	0.177
10	26.5	0.928	0.568	0.240	0.222	0.252
11	31.3	0.961	0.659	0.305	0.282	0.318
12	36.5	0.980	0.742	0.377	0.350	0.391
13	41.4	0.990	0.802	0.442	0.411	0.455
14	46.7	0.995	0.853	0.508	0.475	0.521
15	51.9	0.997	0.891	0.568	0.534	0.581
16	58.4	0.999	0.925	0.636	0.601	0.647
17	60.9	0.999	0.935	0.660	0.625	0.671
18	69.7	1.000	0.961	0.734	0.700	0.743
19	72.3	1.000	0.967	0.753	0.720	0.762
20	77.4	1.000	0.976	0.787	0.756	0.795
21	82.6	1.000	0.982	0.817	0.788	0.825
22	87.9	1.000	0.987	0.843	0.816	0.850
23	93.7	1.000	0.991	0.869	0.844	0.875
24	98.2	1.000	0.993	0.886	0.863	0.891
25	103.9	1.000	0.995	0.904	0.883	0.908
26	109.9	1.000	0.996	0.920	0.902	0.924
27	112.7	1.000	0.997	0.927	0.909	0.930
28	118.4	1.000	0.998	0.939	0.923	0.942
29	126.6	1.000	0.999	0.952	0.939	0.955
30	129.0	1.000	0.999	0.956	0.943	0.958
31	133.0	1.000	0.999	0.961	0.950	0.963
32	139.1	1.000	0.999	0.968	0.958	0.970
33	143.8	1.000	1.000	0.972	0.963	0.974
34	153.8	1.000	1.000	0.980	0.973	0.981
35	159.7	1.000	1.000	0.983	0.977	0.984
36	164.7	1.000	1.000	0.986	0.980	0.987
37	169.2	1.000	1.000	0.987	0.983	0.988
38	179.7	1.000	1.000	0.991	0.987	0.992
39	184.2	1.000	1.000	0.992	0.989	0.993
40	190.0	1.000	1.000	0.993	0.990	0.994
41	196.2	1.000	1.000	0.995	0.992	0.995
42	200.5	1.000	1.000	0.995	0.993	0.996
43	205.3	1.000	1.000	0.996	0.994	0.996

Table F-11 (continued).

Sample	Pore Volumes	C/Co				
		Benzene	Toluene	Ethylbenzene	M-xylene	O-xylene
44	211.4	1.000	1.000	0.997	0.995	0.997
45	215.3	1.000	1.000	0.997	0.995	0.997
46	221.0	1.000	1.000	0.998	0.996	0.998
47	226.0	1.000	1.000	0.998	0.997	0.998
48	230.8	1.000	1.000	0.998	0.997	0.998
49	235.7	1.000	1.000	0.998	0.998	0.999
50	238.3	1.000	1.000	0.999	0.998	0.999

Table F-12. Nonequilibrium prediction model results for column 3B experiment.

Sample	Pore Volumes	C/Co				
		Benzene	Toluene	Ethylbenzene	M-xylene	O-xylene
1	0.3	0.000	0.000	0.000	0.000	0.000
2	2.7	0.076	0.021	0.007	0.007	0.008
3	5.2	0.207	0.055	0.016	0.016	0.019
4	7.6	0.353	0.101	0.029	0.029	0.033
5	9.8	0.474	0.149	0.043	0.042	0.049
6	12.8	0.624	0.225	0.068	0.064	0.076
7	15.4	0.724	0.293	0.093	0.087	0.102
8	18.7	0.818	0.380	0.129	0.120	0.140
9	20.3	0.854	0.423	0.149	0.138	0.160
10	24.8	0.921	0.532	0.206	0.190	0.219
11	30.4	0.964	0.651	0.284	0.262	0.298
12	35.9	0.984	0.743	0.362	0.334	0.376
13	39.8	0.991	0.795	0.415	0.384	0.430
14	45.1	0.996	0.851	0.486	0.452	0.500
15	49.8	0.998	0.889	0.545	0.509	0.558
16	54.6	0.999	0.918	0.601	0.564	0.614
17	59.9	1.000	0.942	0.657	0.620	0.669
18	64.8	1.000	0.958	0.703	0.667	0.714
19	73.1	1.000	0.976	0.769	0.736	0.779
20	74.8	1.000	0.978	0.782	0.749	0.791
21	79.5	1.000	0.984	0.812	0.781	0.820
22	84.5	1.000	0.989	0.840	0.811	0.847
23	89.8	1.000	0.992	0.866	0.839	0.872
24	95.2	1.000	0.994	0.888	0.864	0.893
25	99.5	1.000	0.996	0.903	0.881	0.908
26	104.5	1.000	0.997	0.918	0.898	0.922
27	109.5	1.000	0.998	0.931	0.913	0.935
28	113.3	1.000	0.998	0.940	0.923	0.943
29	119.0	1.000	0.999	0.951	0.936	0.953
30	125.7	1.000	0.999	0.961	0.949	0.963
31	131.7	1.000	1.000	0.968	0.958	0.970
32	134.3	1.000	1.000	0.971	0.961	0.973
33	139.4	1.000	1.000	0.976	0.967	0.977
34	144.2	1.000	1.000	0.980	0.972	0.981
35	148.6	1.000	1.000	0.983	0.976	0.984
36	154.4	1.000	1.000	0.986	0.980	0.987
37	164.0	1.000	1.000	0.990	0.985	0.991
38	168.7	1.000	1.000	0.992	0.988	0.992
39	175.1	1.000	1.000	0.993	0.990	0.994
40	179.3	1.000	1.000	0.994	0.991	0.995
41	184.1	1.000	1.000	0.995	0.993	0.996
42	188.6	1.000	1.000	0.996	0.994	0.996
43	193.1	1.000	1.000	0.996	0.995	0.997

Table F-12 (continued).

Sample	Pore Volumes	C/Co				
		Benzene	Toluene	Ethylbenzene	M-xylene	O-xylene
44	197.2	1.000	1.000	0.997	0.995	0.997
45	202.8	1.000	1.000	0.998	0.996	0.998
46	207.1	1.000	1.000	0.998	0.997	0.998
47	212.3	1.000	1.000	0.998	0.997	0.998
48	217.2	1.000	1.000	0.999	0.998	0.999
49	222.3	1.000	1.000	0.999	0.998	0.999
50	227.5	1.000	1.000	0.999	0.998	0.999
51	232.6	1.000	1.000	0.999	0.999	0.999

Table F-13. Equilibrium model inversely fit to column 1A data results.

Sample	Pore Volumes	C/Co				
		Benzene	Toluene	Ethylbenzene	M-xylene	O-xylene
1	1.2	0.000	0.000	0.000	0.000	0.000
2	2.8	0.000	0.000	0.000	0.000	0.000
3	5.2	0.004	0.000	0.000	0.000	0.000
4	7.5	0.048	0.000	0.000	0.000	0.000
5	9.8	0.163	0.000	0.000	0.000	0.000
6	12.3	0.332	0.001	0.000	0.000	0.000
7	14.9	0.515	0.006	0.000	0.000	0.000
8	17.2	0.650	0.017	0.000	0.000	0.000
9	19.6	0.758	0.037	0.000	0.000	0.000
10	24.5	0.895	0.115	0.000	0.000	0.000
11	29.6	0.957	0.231	0.000	0.000	0.000
12	34.3	0.982	0.357	0.000	0.000	0.000
13	39.6	0.993	0.493	0.000	0.001	0.001
14	44.2	0.997	0.598	0.001	0.002	0.002
15	49.5	0.999	0.700	0.002	0.004	0.006
16	53.1	1.000	0.756	0.003	0.007	0.010
17	57.7	1.000	0.816	0.007	0.013	0.018
18	62.9	1.000	0.867	0.013	0.024	0.032
19	68.3	1.000	0.906	0.022	0.039	0.050
20	73.3	1.000	0.932	0.033	0.057	0.072
21	78.1	1.000	0.951	0.048	0.078	0.097
22	83.1	1.000	0.965	0.066	0.104	0.127
23	88.1	1.000	0.975	0.088	0.134	0.160
24	92.6	1.000	0.982	0.110	0.163	0.193
25	97.4	1.000	0.987	0.136	0.195	0.229
26	102.3	1.000	0.991	0.165	0.231	0.267
27	107.2	1.000	0.993	0.195	0.268	0.306
28	112.0	1.000	0.995	0.226	0.304	0.345
29	117.3	1.000	0.997	0.263	0.345	0.388
30	122.0	1.000	0.998	0.295	0.381	0.425
31	127.0	1.000	0.998	0.329	0.419	0.463
32	133.7	1.000	0.999	0.377	0.469	0.513
33	136.3	1.000	0.999	0.394	0.487	0.531
34	141.3	1.000	0.999	0.429	0.522	0.566
35	146.0	1.000	1.000	0.461	0.554	0.598
36	151.1	1.000	1.000	0.494	0.587	0.630
37	156.0	1.000	1.000	0.525	0.617	0.658
38	161.8	1.000	1.000	0.560	0.650	0.690
39	165.7	1.000	1.000	0.583	0.671	0.710
40	170.5	1.000	1.000	0.610	0.696	0.734
41	175.6	1.000	1.000	0.637	0.721	0.757
42	180.3	1.000	1.000	0.660	0.742	0.777
43	185.2	1.000	1.000	0.684	0.762	0.796

Table F-13 (continued).

Sample	Pore Volumes	C/Co				
		Benzene	Toluene	Ethylbenzene	M-xylene	O-xylene
44	190.4	1.000	1.000	0.708	0.783	0.814
45	195.0	1.000	1.000	0.727	0.800	0.830
46	200.0	1.000	1.000	0.747	0.816	0.845
47	205.2	1.000	1.000	0.767	0.833	0.859
48	215.0	1.000	1.000	0.800	0.860	0.884
49	219.6	1.000	1.000	0.815	0.871	0.894
50	224.9	1.000	1.000	0.830	0.883	0.904
51	231.1	1.000	1.000	0.846	0.896	0.915

Table F-14. Equilibrium model inversely fit to column 1B data results.

Sample	Pore Volumes	C/Co				
		benzene	toluene	ethylbenzene	m-xylene	o-xylene
1	0.5	0.000	0.000	0.000	0.000	0.000
2	2.7	0.000	0.000	0.000	0.000	0.000
3	5.0	0.007	0.000	0.000	0.000	0.000
4	7.4	0.073	0.000	0.000	0.000	0.000
5	10.0	0.234	0.000	0.000	0.000	0.000
6	12.4	0.417	0.001	0.000	0.000	0.000
7	14.7	0.573	0.004	0.000	0.000	0.000
8	17.1	0.709	0.012	0.000	0.000	0.000
9	19.4	0.803	0.028	0.000	0.000	0.000
10	24.5	0.920	0.092	0.000	0.000	0.000
11	29.2	0.967	0.184	0.000	0.000	0.000
12	34.3	0.987	0.304	0.000	0.000	0.000
13	38.8	0.995	0.413	0.000	0.000	0.001
14	43.5	0.998	0.521	0.001	0.000	0.002
15	48.4	0.999	0.619	0.003	0.001	0.004
16	53.4	1.000	0.704	0.006	0.003	0.009
17	58.1	1.000	0.769	0.012	0.006	0.016
18	62.9	1.000	0.822	0.020	0.011	0.027
19	67.3	1.000	0.861	0.030	0.017	0.040
20	72.1	1.000	0.894	0.044	0.026	0.057
21	76.9	1.000	0.920	0.061	0.038	0.078
22	82.2	1.000	0.941	0.084	0.054	0.105
23	86.2	1.000	0.954	0.105	0.069	0.128
24	91.2	1.000	0.966	0.132	0.090	0.159
25	95.8	1.000	0.974	0.160	0.111	0.191
26	100.6	1.000	0.981	0.190	0.136	0.224
27	105.6	1.000	0.986	0.223	0.163	0.260
28	110.1	1.000	0.989	0.255	0.190	0.294
29	114.9	1.000	0.992	0.289	0.219	0.330
30	119.5	1.000	0.994	0.321	0.248	0.364
31	124.8	1.000	0.996	0.359	0.282	0.404
32	143.5	1.000	0.999	0.488	0.403	0.535
33	148.1	1.000	0.999	0.518	0.433	0.564
34	152.9	1.000	0.999	0.548	0.462	0.594
35	158.0	1.000	0.999	0.578	0.493	0.623
36	162.6	1.000	1.000	0.605	0.520	0.649
37	167.5	1.000	1.000	0.631	0.548	0.675
38	172.4	1.000	1.000	0.657	0.575	0.699
39	177.6	1.000	1.000	0.682	0.602	0.723
40	182.1	1.000	1.000	0.703	0.625	0.742
41	186.5	1.000	1.000	0.722	0.646	0.760
42	191.6	1.000	1.000	0.743	0.669	0.779
43	196.3	1.000	1.000	0.761	0.690	0.796

Table F-14 (continued).

Sample	Pore Volumes	C/Co				
		Benzene	Toluene	Ethylbenzene	M-xylene	O-xylene
44	201.1	1.000	1.000	0.779	0.710	0.812
45	205.9	1.000	1.000	0.795	0.729	0.827
46	210.4	1.000	1.000	0.809	0.745	0.840
47	215.5	1.000	1.000	0.824	0.763	0.853
48	219.7	1.000	1.000	0.836	0.777	0.864
49	224.9	1.000	1.000	0.849	0.793	0.875
50	225.1	1.000	1.000	0.850	0.794	0.876
51	225.3	1.000	1.000	0.850	0.794	0.876

Table F-15. Equilibrium model inversely fit to column 2A data results.

Sample	Pore Volumes	C/Co				
		Benzene	Toluene	Ethylbenzene	M-xylene	O-xylene
1	0.6	0.000	0.000	0.000	0.000	0.000
2	2.5	0.000	0.000	0.000	0.000	0.000
3	5.0	0.001	0.000	0.000	0.000	0.000
4	7.5	0.029	0.000	0.000	0.000	0.000
5	9.7	0.116	0.000	0.000	0.000	0.000
6	12.4	0.290	0.000	0.000	0.000	0.000
7	14.7	0.465	0.000	0.000	0.000	0.000
8	17.3	0.633	0.001	0.000	0.000	0.000
9	21.8	0.827	0.009	0.000	0.000	0.000
10	24.4	0.893	0.020	0.000	0.000	0.000
11	29.4	0.959	0.062	0.000	0.000	0.000
12	34.7	0.986	0.139	0.000	0.000	0.000
13	39.9	0.995	0.239	0.000	0.000	0.000
14	44.2	0.998	0.332	0.000	0.000	0.000
15	49.1	0.999	0.436	0.000	0.000	0.000
16	54.1	1.000	0.537	0.000	0.000	0.001
17	58.8	1.000	0.623	0.001	0.001	0.001
18	64.9	1.000	0.717	0.003	0.001	0.003
19	68.6	1.000	0.763	0.004	0.002	0.005
20	73.2	1.000	0.813	0.007	0.004	0.008
21	78.3	1.000	0.857	0.012	0.008	0.014
22	83.0	1.000	0.889	0.018	0.012	0.021
23	88.2	1.000	0.917	0.028	0.018	0.031
24	92.6	1.000	0.935	0.038	0.025	0.042
25	97.2	1.000	0.950	0.051	0.035	0.056
26	102.3	1.000	0.963	0.067	0.047	0.073
27	107.0	1.000	0.972	0.085	0.061	0.092
28	111.8	1.000	0.979	0.105	0.077	0.113
29	116.8	1.000	0.984	0.128	0.096	0.138
30	121.9	1.000	0.988	0.153	0.117	0.165
31	126.7	1.000	0.991	0.179	0.139	0.192
32	131.5	1.000	0.994	0.207	0.162	0.220
33	136.4	1.000	0.995	0.235	0.187	0.250
34	141.1	1.000	0.996	0.264	0.213	0.279
35	145.9	1.000	0.997	0.294	0.240	0.310
36	150.9	1.000	0.998	0.326	0.269	0.342
37	155.8	1.000	0.999	0.356	0.297	0.373
38	160.5	1.000	0.999	0.386	0.325	0.403
39	165.6	1.000	0.999	0.418	0.355	0.435
40	165.8	1.000	0.999	0.419	0.356	0.437
41	176.0	1.000	1.000	0.481	0.417	0.499
42	179.9	1.000	1.000	0.504	0.439	0.522
43	184.6	1.000	1.000	0.531	0.466	0.549

Table F-15 (continued).

Sample	Pore Volumes	C/Co				
		Benzene	Toluene	Ethylbenzene	M-xylene	O-xylene
44	189.7	1.000	1.000	0.559	0.494	0.577
45	194.4	1.000	1.000	0.585	0.520	0.602
46	199.2	1.000	1.000	0.609	0.546	0.627
47	204.3	1.000	1.000	0.635	0.572	0.651
48	209.7	1.000	1.000	0.660	0.599	0.677
49	213.9	1.000	1.000	0.679	0.618	0.695
50	219.1	1.000	1.000	0.701	0.642	0.716
51	223.5	1.000	1.000	0.719	0.662	0.734
52	228.7	1.000	1.000	0.739	0.683	0.754

Table F-16. Equilibrium model inversely fit to column 2B data results.

Sample	Pore Volumes	C/Co				
		Benzene	Toluene	Ethylbenzene	M-xylene	O-xylene
1	0.7	0.000	0.000	0.000	0.000	0.000
2	2.7	0.000	0.000	0.000	0.000	0.000
3	5.2	0.001	0.000	0.000	0.000	0.000
4	7.8	0.019	0.000	0.000	0.000	0.000
5	11.1	0.128	0.000	0.000	0.000	0.000
6	12.9	0.224	0.000	0.000	0.000	0.000
7	15.5	0.386	0.002	0.000	0.000	0.000
8	18.1	0.535	0.008	0.000	0.000	0.000
9	21.5	0.700	0.027	0.000	0.000	0.000
10	26.1	0.842	0.077	0.000	0.000	0.000
11	31.2	0.928	0.170	0.000	0.000	0.000
12	36.6	0.969	0.290	0.000	0.000	0.000
13	41.6	0.986	0.408	0.000	0.000	0.000
14	47.6	0.995	0.542	0.000	0.000	0.001
15	49.2	0.996	0.573	0.001	0.000	0.001
16	57.2	0.999	0.712	0.003	0.001	0.003
17	62.4	1.000	0.782	0.006	0.003	0.007
18	67.8	1.000	0.838	0.011	0.006	0.012
19	72.8	1.000	0.878	0.018	0.010	0.020
20	77.9	1.000	0.909	0.027	0.016	0.031
21	83.3	1.000	0.934	0.041	0.026	0.046
22	88.5	1.000	0.952	0.057	0.037	0.063
23	93.4	1.000	0.964	0.075	0.050	0.082
24	98.7	1.000	0.974	0.098	0.067	0.107
25	103.9	1.000	0.981	0.123	0.086	0.133
26	108.8	1.000	0.986	0.148	0.107	0.160
27	113.8	1.000	0.990	0.177	0.130	0.189
28	119.5	1.000	0.993	0.211	0.158	0.225
29	124.4	1.000	0.995	0.242	0.184	0.257
30	129.6	1.000	0.996	0.275	0.213	0.291
31	134.9	1.000	0.997	0.310	0.244	0.326
32	146.2	1.000	0.999	0.384	0.312	0.402
33	148.3	1.000	0.999	0.398	0.325	0.416
34	155.3	1.000	0.999	0.443	0.367	0.461
35	160.8	1.000	1.000	0.477	0.400	0.496
36	165.7	1.000	1.000	0.507	0.430	0.526
37	170.6	1.000	1.000	0.536	0.459	0.555
38	175.9	1.000	1.000	0.566	0.489	0.584
39	185.9	1.000	1.000	0.620	0.544	0.637
40	191.3	1.000	1.000	0.646	0.572	0.663
41	197.0	1.000	1.000	0.673	0.600	0.690
42	202.4	1.000	1.000	0.697	0.626	0.713
43	207.3	1.000	1.000	0.717	0.648	0.733

Table F-16 (continued).

Sample	Pore Volumes	C/Co				
		Benzene	Toluene	Ethylbenzene	M-xylene	O-xylene
44	211.8	1.000	1.000	0.735	0.668	0.750
45	217.0	1.000	1.000	0.755	0.690	0.769
46	222.1	1.000	1.000	0.773	0.710	0.786
47	226.8	1.000	1.000	0.788	0.727	0.801
48	233.0	1.000	1.000	0.807	0.749	0.820
49	237.9	1.000	1.000	0.821	0.766	0.833
50	241.7	1.000	1.000	0.831	0.777	0.843

Table F-17. Equilibrium model inversely fit to column 3A data results.

Sample	Pore Volumes	C/Co				
		Benzene	Toluene	Ethylbenzene	M-xylene	O-xylene
1	0.6	0.000	0.000	0.000	0.000	0.000
2	3.4	0.001	0.000	0.000	0.000	0.000
3	5.1	0.015	0.000	0.000	0.000	0.000
4	7.7	0.098	0.000	0.000	0.000	0.000
5	10.1	0.224	0.000	0.000	0.000	0.000
6	13.4	0.416	0.003	0.000	0.000	0.000
7	15.6	0.533	0.009	0.000	0.000	0.000
8	18.5	0.655	0.024	0.000	0.000	0.000
9	20.9	0.734	0.042	0.000	0.000	0.000
10	26.5	0.861	0.110	0.000	0.000	0.000
11	31.3	0.920	0.186	0.000	0.000	0.000
12	36.5	0.957	0.279	0.001	0.000	0.001
13	41.4	0.976	0.366	0.002	0.001	0.003
14	46.7	0.987	0.455	0.005	0.003	0.007
15	51.9	0.993	0.534	0.011	0.007	0.013
16	58.4	0.997	0.621	0.021	0.014	0.025
17	60.9	0.997	0.651	0.026	0.017	0.031
18	69.7	0.999	0.740	0.048	0.034	0.057
19	72.3	0.999	0.762	0.057	0.041	0.066
20	77.4	1.000	0.800	0.075	0.055	0.087
21	82.6	1.000	0.833	0.096	0.072	0.110
22	87.9	1.000	0.861	0.119	0.091	0.135
23	93.7	1.000	0.887	0.147	0.115	0.165
24	98.2	1.000	0.904	0.169	0.135	0.189
25	103.9	1.000	0.921	0.199	0.160	0.221
26	109.9	1.000	0.936	0.231	0.189	0.255
27	112.7	1.000	0.942	0.246	0.203	0.271
28	118.4	1.000	0.953	0.278	0.232	0.303
29	126.6	1.000	0.964	0.323	0.273	0.350
30	129.0	1.000	0.967	0.336	0.285	0.363
31	133.0	1.000	0.972	0.357	0.306	0.385
32	139.1	1.000	0.977	0.390	0.337	0.419
33	143.8	1.000	0.981	0.415	0.361	0.444
34	153.8	1.000	0.986	0.465	0.410	0.494
35	159.7	1.000	0.989	0.494	0.438	0.523
36	164.7	1.000	0.991	0.517	0.461	0.546
37	169.2	1.000	0.992	0.537	0.481	0.566
38	179.7	1.000	0.994	0.582	0.527	0.611
39	184.2	1.000	0.995	0.600	0.545	0.628
40	190.0	1.000	0.996	0.623	0.569	0.650
41	196.2	1.000	0.997	0.646	0.593	0.673
42	200.5	1.000	0.997	0.661	0.608	0.687
43	205.3	1.000	0.998	0.677	0.626	0.703

Table F-17 (continued).

Sample	Pore Volumes	C/Co				
		Benzene	Toluene	Ethylbenzene	M-xylene	O-xylene
44	211.4	1.000	0.998	0.697	0.646	0.722
45	215.3	1.000	0.998	0.709	0.659	0.733
46	221.0	1.000	0.999	0.725	0.677	0.749
47	226.0	1.000	0.999	0.739	0.692	0.763
48	230.8	1.000	0.999	0.752	0.706	0.775
49	235.7	1.000	0.999	0.765	0.720	0.787
50	238.3	1.000	0.999	0.771	0.727	0.793

Table F-18. Equilibrium model inversely fit to column 3B data results.

Sample	Pore Volumes	C/Co				
		Benzene	Toluene	Ethylbenzene	M-xylene	O-xylene
1	0.3	0.000	0.000	0.000	0.000	0.000
2	2.7	0.000	0.000	0.000	0.000	0.000
3	5.2	0.016	0.000	0.000	0.000	0.000
4	7.6	0.106	0.000	0.000	0.000	0.000
5	9.8	0.237	0.000	0.000	0.000	0.000
6	12.8	0.443	0.001	0.000	0.000	0.000
7	15.4	0.594	0.006	0.000	0.000	0.000
8	18.7	0.739	0.020	0.000	0.000	0.000
9	20.3	0.793	0.032	0.000	0.000	0.000
10	24.8	0.891	0.081	0.000	0.000	0.000
11	30.4	0.953	0.171	0.000	0.000	0.000
12	35.9	0.979	0.276	0.001	0.000	0.001
13	39.8	0.988	0.352	0.002	0.001	0.002
14	45.1	0.995	0.453	0.004	0.002	0.006
15	49.8	0.997	0.535	0.009	0.005	0.011
16	54.6	0.999	0.610	0.016	0.009	0.019
17	59.9	0.999	0.681	0.027	0.016	0.032
18	64.8	1.000	0.737	0.040	0.026	0.047
19	73.1	1.000	0.812	0.069	0.047	0.080
20	74.8	1.000	0.825	0.077	0.053	0.088
21	79.5	1.000	0.856	0.098	0.069	0.112
22	84.5	1.000	0.883	0.123	0.089	0.140
23	89.8	1.000	0.906	0.152	0.113	0.171
24	95.2	1.000	0.926	0.184	0.139	0.204
25	99.5	1.000	0.938	0.211	0.162	0.233
26	104.5	1.000	0.950	0.242	0.189	0.265
27	109.5	1.000	0.960	0.274	0.217	0.299
28	113.3	1.000	0.966	0.299	0.240	0.325
29	119.0	1.000	0.973	0.336	0.273	0.363
30	125.7	1.000	0.980	0.378	0.313	0.406
31	131.7	1.000	0.985	0.416	0.349	0.444
32	134.3	1.000	0.986	0.432	0.364	0.460
33	139.4	1.000	0.989	0.462	0.393	0.491
34	144.2	1.000	0.991	0.491	0.421	0.519
35	148.6	1.000	0.993	0.515	0.445	0.544
36	154.4	1.000	0.994	0.547	0.477	0.575
37	164.0	1.000	0.996	0.596	0.527	0.624
38	168.7	1.000	0.997	0.619	0.551	0.646
39	175.1	1.000	0.998	0.648	0.581	0.674
40	179.3	1.000	0.998	0.666	0.600	0.691
41	184.1	1.000	0.998	0.685	0.621	0.710
42	188.6	1.000	0.999	0.703	0.640	0.727
43	193.1	1.000	0.999	0.720	0.658	0.743

Table F-18 (continued).

Sample	Pore Volumes	C/Co				
		Benzene	Toluene	Ethylbenzene	M-xylene	O-xylene
44	197.2	1.000	0.999	0.734	0.674	0.757
45	202.8	1.000	0.999	0.753	0.694	0.775
46	207.1	1.000	0.999	0.767	0.710	0.788
47	212.3	1.000	1.000	0.782	0.727	0.803
48	217.2	1.000	1.000	0.796	0.742	0.816
49	222.3	1.000	1.000	0.809	0.758	0.828
50	227.5	1.000	1.000	0.822	0.773	0.840
51	232.6	1.000	1.000	0.834	0.786	0.852

Table F-19. Nonequilibrium model inversely fit to column 1A data results.

Sample	Pore Volumes	C/Co				
		Benzene	Toluene	Ethylbenzene	M-xylene	O-xylene
1	1.2	0.000	0.000	0.000	0.000	0.000
2	2.8	0.030	0.000	0.000	0.000	0.000
3	5.2	0.161	0.006	0.009	0.000	0.000
4	7.5	0.266	0.034	0.021	0.000	0.001
5	9.8	0.353	0.076	0.028	0.000	0.007
6	12.3	0.436	0.121	0.034	0.000	0.018
7	14.9	0.516	0.165	0.040	0.000	0.033
8	17.2	0.579	0.202	0.046	0.001	0.045
9	19.6	0.638	0.239	0.052	0.002	0.057
10	24.5	0.738	0.315	0.064	0.009	0.079
11	29.6	0.814	0.388	0.078	0.026	0.098
12	34.3	0.867	0.454	0.091	0.051	0.117
13	39.6	0.909	0.523	0.107	0.085	0.138
14	44.2	0.935	0.577	0.121	0.117	0.156
15	49.5	0.956	0.635	0.138	0.155	0.178
16	53.1	0.967	0.670	0.150	0.179	0.193
17	57.7	0.977	0.711	0.165	0.209	0.212
18	62.9	0.984	0.753	0.183	0.239	0.234
19	68.3	0.990	0.790	0.202	0.268	0.257
20	73.3	0.993	0.820	0.219	0.292	0.278
21	78.1	0.995	0.846	0.236	0.313	0.298
22	83.1	0.997	0.869	0.254	0.333	0.319
23	88.1	0.998	0.889	0.273	0.353	0.341
24	92.6	0.999	0.904	0.289	0.369	0.359
25	97.4	0.999	0.919	0.306	0.386	0.379
26	102.3	0.999	0.931	0.324	0.403	0.399
27	107.2	1.000	0.942	0.342	0.418	0.419
28	112.0	1.000	0.951	0.359	0.433	0.438
29	117.3	1.000	0.959	0.378	0.450	0.458
30	122.0	1.000	0.965	0.395	0.463	0.476
31	127.0	1.000	0.971	0.413	0.478	0.495
32	133.7	1.000	0.977	0.436	0.497	0.520
33	136.3	1.000	0.979	0.445	0.504	0.529
34	141.3	1.000	0.983	0.462	0.517	0.546
35	146.0	1.000	0.986	0.478	0.530	0.563
36	151.1	1.000	0.988	0.495	0.543	0.580
37	156.0	1.000	0.990	0.511	0.555	0.596
38	161.8	1.000	0.992	0.529	0.570	0.614
39	165.7	1.000	0.993	0.541	0.579	0.626
40	170.5	1.000	0.994	0.556	0.590	0.640
41	175.6	1.000	0.995	0.572	0.602	0.655
42	180.3	1.000	0.996	0.585	0.613	0.668
43	185.2	1.000	0.997	0.600	0.623	0.682

Table F-19 (continued).

Sample	Pore Volumes	C/Co				
		Benzene	Toluene	Ethylbenzene	M-xylene	O-xylene
44	190.4	1.000	0.997	0.614	0.634	0.696
45	195.0	1.000	0.998	0.627	0.644	0.707
46	200.0	1.000	0.998	0.640	0.654	0.720
47	205.2	1.000	0.998	0.654	0.665	0.732
48	215.0	1.000	0.999	0.678	0.683	0.755
49	219.6	1.000	0.999	0.689	0.692	0.764
50	224.9	1.000	0.999	0.702	0.701	0.775
51	231.1	1.000	0.999	0.716	0.712	0.788

Table F-20. Nonequilibrium model inversely fit to column 1B data results.

Sample	Pore Volumes	C/Co				
		Benzene	Toluene	Ethylbenzene	M-xylene	O-xylene
1	0.5	0.000	0.000	0.000	0.000	0.000
2	2.7	0.035	0.000	0.000	0.000	0.000
3	5.0	0.134	0.000	0.000	0.000	0.000
4	7.4	0.244	0.001	0.000	0.000	0.000
5	10.0	0.362	0.012	0.000	0.000	0.000
6	12.4	0.467	0.040	0.000	0.000	0.001
7	14.7	0.555	0.080	0.001	0.001	0.003
8	17.1	0.641	0.135	0.003	0.002	0.008
9	19.4	0.710	0.190	0.006	0.005	0.014
10	24.5	0.823	0.302	0.020	0.016	0.033
11	29.2	0.892	0.387	0.038	0.031	0.053
12	34.3	0.938	0.460	0.061	0.048	0.075
13	38.8	0.963	0.513	0.082	0.064	0.094
14	43.5	0.978	0.561	0.103	0.081	0.114
15	48.4	0.988	0.605	0.125	0.098	0.135
16	53.4	0.993	0.644	0.146	0.115	0.156
17	58.1	0.996	0.678	0.167	0.132	0.176
18	62.9	0.998	0.709	0.187	0.149	0.197
19	67.3	0.999	0.735	0.205	0.165	0.216
20	72.1	0.999	0.760	0.225	0.183	0.237
21	76.9	1.000	0.784	0.245	0.200	0.258
22	82.2	1.000	0.807	0.267	0.220	0.281
23	86.2	1.000	0.823	0.284	0.235	0.299
24	91.2	1.000	0.842	0.304	0.254	0.320
25	95.8	1.000	0.857	0.323	0.271	0.340
26	100.6	1.000	0.871	0.342	0.289	0.361
27	105.6	1.000	0.885	0.362	0.308	0.382
28	110.1	1.000	0.896	0.379	0.325	0.401
29	114.9	1.000	0.907	0.398	0.343	0.420
30	119.5	1.000	0.916	0.416	0.359	0.439
31	124.8	1.000	0.925	0.435	0.379	0.460
32	143.5	1.000	0.951	0.503	0.445	0.531
33	148.1	1.000	0.956	0.519	0.461	0.548
34	152.9	1.000	0.961	0.535	0.477	0.565
35	158.0	1.000	0.965	0.551	0.494	0.582
36	162.6	1.000	0.969	0.566	0.509	0.597
37	167.5	1.000	0.972	0.582	0.525	0.613
38	172.4	1.000	0.975	0.596	0.540	0.629
39	177.6	1.000	0.978	0.612	0.556	0.644
40	182.1	1.000	0.980	0.625	0.570	0.658
41	186.5	1.000	0.982	0.637	0.583	0.670
42	191.6	1.000	0.984	0.651	0.597	0.684
43	196.3	1.000	0.986	0.664	0.611	0.697

Table F-20 (continued).

Sample	Pore Volumes	C/Co				
		Benzene	Toluene	Ethylbenzene	M-xylene	O-xylene
44	201.1	1.000	0.987	0.676	0.624	0.710
45	205.9	1.000	0.989	0.688	0.637	0.722
46	210.4	1.000	0.990	0.699	0.648	0.733
47	215.5	1.000	0.991	0.711	0.661	0.745
48	219.7	1.000	0.992	0.721	0.672	0.754
49	224.9	1.000	0.993	0.732	0.684	0.766
50	225.1	1.000	0.993	0.733	0.685	0.766
51	225.3	1.000	0.993	0.733	0.685	0.766

Table F-21. Nonequilibrium model inversely fit to column 2A data results.

Sample	Pore Volumes	C/Co				
		Benzene	Toluene	Ethylbenzene	M-xylene	O-xylene
1	0.6	0.000	0.000	0.000	0.000	0.000
2	2.5	0.002	0.000	0.000	0.000	0.000
3	5.0	0.088	0.000	0.000	0.000	0.000
4	7.5	0.214	0.000	0.000	0.001	0.000
5	9.7	0.308	0.001	0.000	0.003	0.000
6	12.4	0.411	0.006	0.000	0.006	0.000
7	14.7	0.496	0.020	0.000	0.008	0.000
8	17.3	0.578	0.050	0.001	0.010	0.001
9	21.8	0.696	0.135	0.005	0.014	0.005
10	24.4	0.752	0.195	0.010	0.017	0.009
11	29.4	0.833	0.306	0.021	0.022	0.020
12	34.7	0.893	0.407	0.034	0.029	0.037
13	39.9	0.932	0.481	0.048	0.037	0.054
14	44.2	0.954	0.527	0.060	0.043	0.068
15	49.1	0.971	0.566	0.073	0.052	0.083
16	54.1	0.982	0.597	0.086	0.061	0.098
17	58.8	0.988	0.622	0.099	0.070	0.112
18	64.9	0.994	0.648	0.116	0.083	0.131
19	68.6	0.995	0.662	0.126	0.091	0.142
20	73.2	0.997	0.679	0.139	0.102	0.156
21	78.3	0.998	0.696	0.154	0.114	0.171
22	83.0	0.999	0.711	0.168	0.126	0.185
23	88.2	0.999	0.726	0.184	0.139	0.201
24	92.6	1.000	0.739	0.197	0.151	0.215
25	97.2	1.000	0.751	0.211	0.164	0.229
26	102.3	1.000	0.764	0.227	0.178	0.245
27	107.0	1.000	0.776	0.242	0.192	0.260
28	111.8	1.000	0.787	0.257	0.206	0.275
29	116.8	1.000	0.798	0.273	0.221	0.290
30	121.9	1.000	0.808	0.289	0.237	0.306
31	126.7	1.000	0.818	0.304	0.252	0.321
32	131.5	1.000	0.827	0.319	0.267	0.336
33	136.4	1.000	0.836	0.334	0.282	0.351
34	141.1	1.000	0.844	0.349	0.297	0.365
35	145.9	1.000	0.851	0.364	0.313	0.379
36	150.9	1.000	0.859	0.380	0.329	0.395
37	155.8	1.000	0.866	0.395	0.344	0.409
38	160.5	1.000	0.873	0.409	0.359	0.423
39	165.6	1.000	0.880	0.424	0.376	0.438
40	165.8	1.000	0.880	0.425	0.377	0.438
41	176.0	1.000	0.893	0.455	0.409	0.467
42	179.9	1.000	0.897	0.467	0.421	0.478
43	184.6	1.000	0.902	0.480	0.436	0.491

Table F-21 (continued).

Sample	Pore Volumes	C/Co				
		Benzene	Toluene	Ethylbenzene	M-xylene	O-xylene
44	189.7	1.000	0.907	0.495	0.452	0.505
45	194.4	1.000	0.912	0.508	0.466	0.518
46	199.2	1.000	0.916	0.521	0.481	0.530
47	204.3	1.000	0.921	0.535	0.496	0.543
48	209.7	1.000	0.925	0.550	0.512	0.557
49	213.9	1.000	0.929	0.560	0.524	0.568
50	219.1	1.000	0.933	0.574	0.539	0.580
51	223.5	1.000	0.936	0.585	0.552	0.591
52	228.7	1.000	0.939	0.598	0.566	0.603

Table F-22. Nonequilibrium model inversely fit to column 2B data results.

Sample	Pore Volumes	C/Co				
		Benzene	Toluene	Ethylbenzene	M-xylene	O-xylene
1	0.7	0.000	0.000	0.000	0.000	0.000
2	2.7	0.015	0.000	0.000	0.000	0.000
3	5.2	0.104	0.000	0.000	0.000	0.000
4	7.8	0.192	0.000	0.000	0.000	0.000
5	11.1	0.304	0.006	0.000	0.000	0.000
6	12.9	0.363	0.016	0.000	0.000	0.000
7	15.5	0.447	0.045	0.000	0.000	0.000
8	18.1	0.521	0.087	0.001	0.001	0.002
9	21.5	0.612	0.158	0.003	0.003	0.006
10	26.1	0.712	0.256	0.012	0.009	0.019
11	31.2	0.799	0.356	0.030	0.024	0.044
12	36.6	0.865	0.441	0.058	0.047	0.075
13	41.6	0.908	0.506	0.087	0.071	0.105
14	47.6	0.943	0.572	0.124	0.100	0.140
15	49.2	0.949	0.587	0.133	0.108	0.148
16	57.2	0.974	0.655	0.176	0.143	0.187
17	62.4	0.983	0.693	0.201	0.164	0.209
18	67.8	0.990	0.728	0.224	0.184	0.230
19	72.8	0.993	0.757	0.244	0.201	0.248
20	77.9	0.996	0.783	0.262	0.218	0.265
21	83.3	0.997	0.808	0.280	0.234	0.283
22	88.5	0.998	0.830	0.296	0.249	0.299
23	93.4	0.999	0.848	0.311	0.263	0.314
24	98.7	0.999	0.866	0.327	0.278	0.330
25	103.9	1.000	0.881	0.341	0.292	0.345
26	108.8	1.000	0.894	0.355	0.305	0.359
27	113.8	1.000	0.906	0.368	0.319	0.373
28	119.5	1.000	0.918	0.383	0.334	0.389
29	124.4	1.000	0.927	0.396	0.346	0.403
30	129.6	1.000	0.935	0.409	0.360	0.417
31	134.9	1.000	0.943	0.423	0.373	0.431
32	146.2	1.000	0.957	0.450	0.401	0.460
33	148.3	1.000	0.959	0.455	0.406	0.465
34	155.3	1.000	0.965	0.472	0.423	0.483
35	160.8	1.000	0.970	0.484	0.436	0.496
36	165.7	1.000	0.973	0.496	0.447	0.508
37	170.6	1.000	0.976	0.507	0.459	0.520
38	175.9	1.000	0.979	0.518	0.471	0.532
39	185.9	1.000	0.984	0.540	0.493	0.555
40	191.3	1.000	0.986	0.551	0.505	0.567
41	197.0	1.000	0.988	0.562	0.517	0.579
42	202.4	1.000	0.989	0.573	0.528	0.590
43	207.3	1.000	0.991	0.583	0.538	0.600

Table F-22 (continued).

Sample	Pore Volumes	C/Co				
		Benzene	Toluene	Ethylbenzene	M-xylene	O-xylene
44	211.8	1.000	0.992	0.592	0.547	0.609
45	217.0	1.000	0.993	0.602	0.558	0.620
46	222.1	1.000	0.994	0.611	0.568	0.629
47	226.8	1.000	0.994	0.620	0.577	0.638
48	233.0	1.000	0.995	0.631	0.588	0.650
49	237.9	1.000	0.996	0.639	0.598	0.659
50	241.7	1.000	0.996	0.646	0.605	0.665

Table F-23. Nonequilibrium model inversely fit to column 3A data results.

Sample	Pore Volumes	C/Co				
		Benzene	Toluene	Ethylbenzene	M-xylene	O-xylene
1	0.6	0.000	0.000	0.000	0.000	0.000
2	3.4	0.103	0.000	0.000	0.000	0.000
3	5.1	0.180	0.005	0.000	0.000	0.000
4	7.7	0.277	0.036	0.001	0.001	0.001
5	10.1	0.358	0.080	0.003	0.004	0.007
6	13.4	0.463	0.143	0.013	0.013	0.020
7	15.6	0.527	0.180	0.023	0.021	0.031
8	18.5	0.600	0.222	0.037	0.032	0.046
9	20.9	0.653	0.252	0.048	0.041	0.057
10	26.5	0.758	0.317	0.073	0.061	0.080
11	31.3	0.823	0.367	0.091	0.075	0.097
12	36.5	0.876	0.418	0.109	0.089	0.115
13	41.4	0.912	0.462	0.125	0.103	0.131
14	46.7	0.939	0.508	0.141	0.117	0.148
15	51.9	0.958	0.549	0.157	0.131	0.164
16	58.4	0.974	0.597	0.177	0.149	0.185
17	60.9	0.978	0.614	0.185	0.156	0.193
18	69.7	0.988	0.670	0.212	0.181	0.222
19	72.3	0.990	0.685	0.220	0.188	0.230
20	77.4	0.993	0.713	0.236	0.203	0.247
21	82.6	0.995	0.739	0.252	0.218	0.264
22	87.9	0.997	0.763	0.268	0.233	0.281
23	93.7	0.998	0.788	0.286	0.250	0.300
24	98.2	0.999	0.805	0.299	0.263	0.314
25	103.9	0.999	0.825	0.316	0.279	0.332
26	109.9	0.999	0.844	0.334	0.296	0.351
27	112.7	1.000	0.852	0.343	0.304	0.359
28	118.4	1.000	0.868	0.359	0.321	0.377
29	126.6	1.000	0.888	0.383	0.344	0.402
30	129.0	1.000	0.893	0.390	0.350	0.409
31	133.0	1.000	0.901	0.401	0.362	0.421
32	139.1	1.000	0.912	0.418	0.378	0.439
33	143.8	1.000	0.920	0.432	0.391	0.453
34	153.8	1.000	0.935	0.459	0.418	0.481
35	159.7	1.000	0.942	0.474	0.434	0.497
36	164.7	1.000	0.948	0.487	0.447	0.510
37	169.2	1.000	0.952	0.499	0.458	0.522
38	179.7	1.000	0.961	0.525	0.485	0.549
39	184.2	1.000	0.965	0.536	0.496	0.560
40	190.0	1.000	0.969	0.550	0.510	0.574
41	196.2	1.000	0.972	0.564	0.525	0.589
42	200.5	1.000	0.975	0.574	0.535	0.599
43	205.3	1.000	0.977	0.585	0.546	0.610

Table F-23 (continued).

Sample	Pore Volumes	C/Co				
		Benzene	Toluene	Ethylbenzene	M-xylene	O-xylene
44	211.4	1.000	0.980	0.598	0.560	0.624
45	215.3	1.000	0.981	0.607	0.568	0.632
46	221.0	1.000	0.984	0.619	0.581	0.644
47	226.0	1.000	0.985	0.629	0.591	0.655
48	230.8	1.000	0.987	0.639	0.602	0.665
49	235.7	1.000	0.988	0.648	0.612	0.674
50	238.3	1.000	0.989	0.653	0.617	0.679

Table F-24. Nonequilibrium model inversely fit to column 3B data results.

Sample	Pore Volumes	C/Co				
		Benzene	Toluene	Ethylbenzene	M-xylene	O-xylene
1	0.3	0.000	0.000	0.000	0.000	0.000
2	2.7	0.048	0.000	0.000	0.000	0.000
3	5.2	0.212	0.004	0.000	0.000	0.000
4	7.6	0.326	0.028	0.000	0.000	0.000
5	9.8	0.401	0.065	0.000	0.000	0.001
6	12.8	0.494	0.125	0.001	0.001	0.004
7	15.4	0.563	0.171	0.003	0.002	0.010
8	18.7	0.639	0.221	0.010	0.007	0.023
9	20.3	0.673	0.244	0.014	0.011	0.030
10	24.8	0.751	0.299	0.032	0.025	0.051
11	30.4	0.826	0.363	0.058	0.047	0.078
12	35.9	0.878	0.420	0.085	0.069	0.103
13	39.8	0.905	0.458	0.104	0.084	0.119
14	45.1	0.934	0.508	0.128	0.105	0.140
15	49.8	0.952	0.548	0.148	0.122	0.159
16	54.6	0.965	0.587	0.168	0.139	0.178
17	59.9	0.976	0.627	0.190	0.158	0.198
18	64.8	0.983	0.661	0.209	0.175	0.218
19	73.1	0.991	0.712	0.240	0.204	0.250
20	74.8	0.992	0.722	0.247	0.210	0.257
21	79.5	0.994	0.747	0.265	0.226	0.275
22	84.5	0.996	0.772	0.283	0.243	0.294
23	89.8	0.997	0.795	0.303	0.261	0.314
24	95.2	0.998	0.817	0.323	0.280	0.335
25	99.5	0.999	0.833	0.338	0.294	0.351
26	104.5	0.999	0.850	0.356	0.311	0.370
27	109.5	0.999	0.865	0.373	0.328	0.388
28	113.3	1.000	0.876	0.387	0.341	0.402
29	119.0	1.000	0.891	0.407	0.359	0.423
30	125.7	1.000	0.906	0.429	0.381	0.446
31	131.7	1.000	0.917	0.449	0.400	0.467
32	134.3	1.000	0.922	0.457	0.409	0.476
33	139.4	1.000	0.930	0.473	0.424	0.492
34	144.2	1.000	0.938	0.488	0.439	0.508
35	148.6	1.000	0.943	0.502	0.452	0.522
36	154.4	1.000	0.950	0.519	0.470	0.540
37	164.0	1.000	0.960	0.547	0.498	0.569
38	168.7	1.000	0.964	0.561	0.511	0.583
39	175.1	1.000	0.969	0.578	0.529	0.601
40	179.3	1.000	0.972	0.589	0.540	0.612
41	184.1	1.000	0.975	0.602	0.553	0.625
42	188.6	1.000	0.977	0.614	0.565	0.637
43	193.1	1.000	0.980	0.625	0.576	0.649

Table F-24 (continued).

Sample	Pore Volumes	C/Co				
		Benzene	Toluene	Ethylbenzene	M-xylene	O-xylene
44	197.2	1.000	0.982	0.635	0.587	0.659
45	202.8	1.000	0.984	0.648	0.601	0.672
46	207.1	1.000	0.985	0.658	0.611	0.683
47	212.3	1.000	0.987	0.670	0.623	0.694
48	217.2	1.000	0.989	0.681	0.634	0.705
49	222.3	1.000	0.990	0.692	0.646	0.716
50	227.5	1.000	0.991	0.703	0.657	0.727
51	232.6	1.000	0.992	0.713	0.668	0.737

Table F-25. Parameters obtained from equilibrium fit model.

Column	Constituent	P	R	r²
1A	Benzene	11.32	15.96	0.889
	Toluene	11.32	43.36	0.931
	Ethylbenzene	11.32	165.3	0.768
	M-xylene	11.32	150.1	0.684
	O-xylene	11.32	143.4	0.788
1B	Benzene	10.69	14.81	0.944
	Toluene	10.69	46.51	0.928
	Ethylbenzene	10.69	158.8	0.832
	M-xylene	10.69	173.9	0.842
	O-xylene	10.69	151.1	0.852
2A	Benzene	13.29	16.37	0.916
	Toluene	13.29	56.07	0.815
	Ethylbenzene	13.29	192.6	0.761
	M-xylene	13.29	204.9	0.817
	O-xylene	13.29	189.3	0.729
2B	Benzene	11.90	18.88	0.938
	Toluene	11.90	49.45	0.949
	Ethylbenzene	11.90	178.2	0.603
	M-xylene	11.90	192.7	0.622
	O-xylene	11.90	174.9	0.624
3A	Benzene	6.69	17.18	0.922
	Toluene	6.69	56.9	0.91
	Ethylbenzene	6.69	184.7	0.782
	M-xylene	6.69	198.8	0.799
	O-xylene	6.69	177.7	0.803
3B	Benzene	8.11	15.38	0.92
	Toluene	8.11	53.51	0.919
	Ethylbenzene	8.11	163.5	0.828
	M-xylene	8.11	178	0.828
	O-xylene	8.11	158	0.839

Table F-26. Parameters obtained from nonequilibrium fit model.

Column	Constituent	P	R	B	w	r²
1A	Benzene	11.32	18.39	0.346	2.12	0.946
	Toluene	11.32	45.86	0.296	2.74	0.979
	Ethylbenzene	11.32	179.10	0.057	5.04	0.983
	M-xylene	11.32	184.60	0.341	1.54	0.989
	O-xylene	11.32	153.90	0.150	3.72	0.995
1B	Benzene	10.69	15.58	0.292	3.54	0.973
	Toluene	10.69	52.99	0.486	1.05	0.98
	Ethylbenzene	10.69	171.60	0.297	2.98	0.993
	M-xylene	10.69	188.70	0.267	3.62	0.994
	O-xylene	10.69	160.40	0.260	3.51	0.995
2A	Benzene	13.29	18.10	0.379	2.19	0.961
	Toluene	13.29	76.60	0.424	0.68	0.987
	Ethylbenzene	13.29	223.00	0.220	3.95	0.993
	M-xylene	13.29	230.70	0.078	7.46	0.992
	O-xylene	13.29	222.30	0.235	3.38	0.995
2B	Benzene	11.90	20.66	0.264	3.17	0.979
	Toluene	11.90	55.20	0.548	1.00	0.988
	Ethylbenzene	11.90	223.80	0.274	1.83	0.996
	M-xylene	11.90	242.30	0.258	2.18	0.995
	O-xylene	11.90	211.90	0.261	2.01	0.994
3A	Benzene	6.69	18.78	0.263	2.74	0.957
	Toluene	6.69	61.13	0.308	2.06	0.982
	Ethylbenzene	6.69	212.70	0.178	3.57	0.986
	M-xylene	6.69	229.00	0.158	4.21	0.989
	O-xylene	6.69	200.80	0.165	3.76	0.99
3B	Benzene	8.11	17.79	0.320	1.72	0.976
	Toluene	8.11	57.82	0.310	2.07	0.989
	Ethylbenzene	8.11	183.80	0.288	2.80	0.996
	M-xylene	8.11	201.70	0.270	3.20	0.996
	O-xylene	8.11	173.90	0.240	3.30	0.997

APPENDIX G. BICONTINUUM MODEL MODIFICATIONS AND CODE.

During the course of this research, it was noted that the bicontinuum model derived by Selim et al, 1976 was most sensitive to early time data (one to four minute data). Because of the lower sensitivity to late time data, the model was under predicting the amount of time required to reach sorption equilibrium. Consequently, the kinetic rate coefficient was skewed higher than the true data suggested (Figures G-1 and G-2). In order to provide a more accurate estimation of the kinetic rate coefficient, a weighted version of the bicontinuum model was developed. The weighted model included the following two-step process:

- 1) Inversely fit the non-weighted bicontinuum model to the batch experiment data. K_d was calculated from equilibrium data of the batch experiments and allowed to vary by 0.01 L/kg; F and k_2 were inversely fit to the data based on a least sum of squared errors method. Obtain the fraction of instantaneous sorption from this fit.
- 2) Run the weighted bicontinuum model with values for K_d and F determined in part 1. Inversely fit k_2 to the “approaching equilibrium” batch experiment data (six through twenty-minute data) based on a least sum of squared errors method.

Once these two models were sequentially run, the three desired nonequilibrium parameters were obtained. The final MATLAB code used to fit the model can be seen after figure G-1.

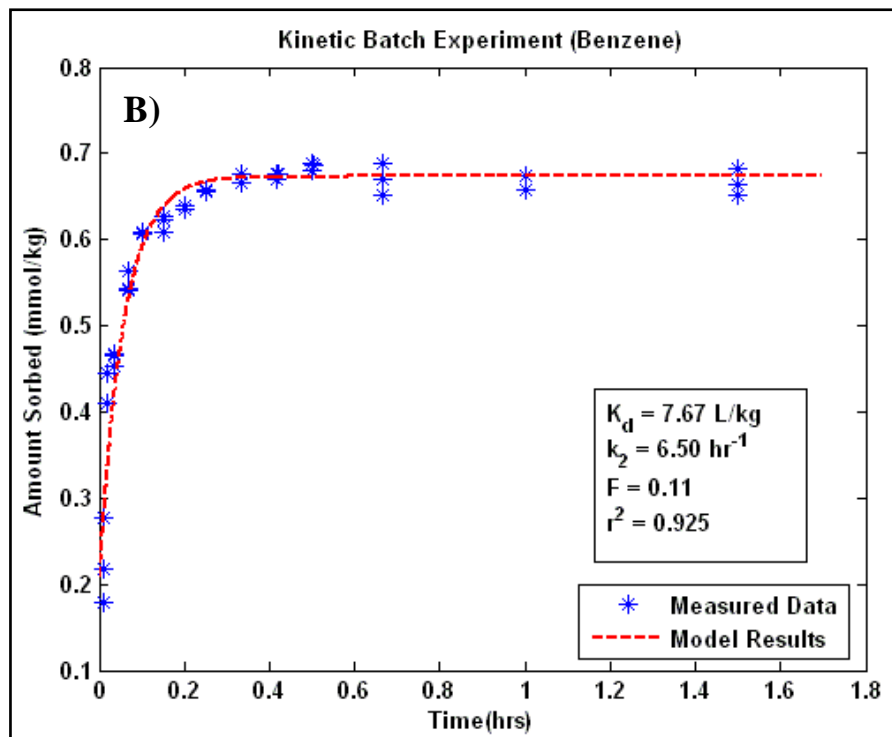
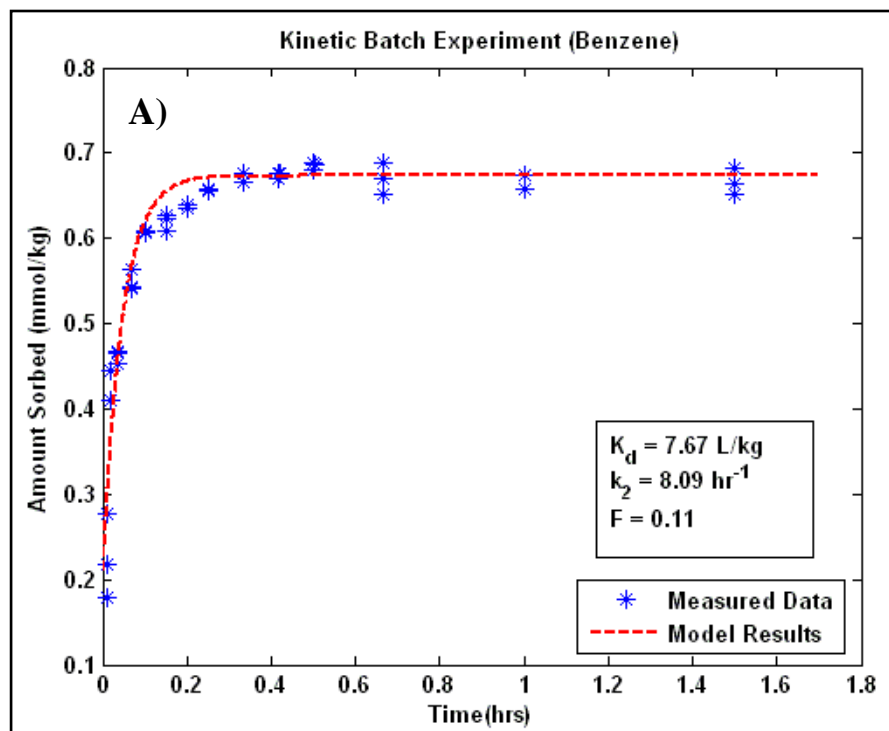


Figure G-1. A) Unmodified model fit to benzene batch data. B) Modified model fit to same benzene dataset.

```

% Josh Simpson

clear;

load SorbedB.txt;

sorb = SorbedB(:, 1);           % sorption data from a batch experiment
timed = SorbedB(:, 2);         % time into experiment that sorption data was taken
ConcAq = SorbedB(:, 3);
meanvalue = mean(sorb);

plot(timed,sorb,'b*')
hold on

Cstart = input('Enter the starting aqueous concentration (mmol/L). ');
WatVol = input('Enter the amount of water added (mL). ');
SoilMass = input('Enter the amount of soil added (g). ');
Kdval = input('Enter the constituents Kd (L/kg). ');

Ctot = Cstart;

[numsamples, columntime] = size(sorb);

S = 0;                         % total amount sorbed
S2new = 0;                     % amount sorbed by rate-limited sites
S1 = 0;                       % amount sorbed by instantaneous sites
deltaS2 = 0;
timestep = 0.001;             % timestep in hrs
Sorbed = ones(1,1700);        % variable to store the model's sorption over time to find Kd and F
Sorbed2 = ones(1,1700);       % variable to store the model's sorption over time to find k2
bestfitline = ones(1,1700);   % will only write to this when the sum of square errors is minimized
bestfitline2 = ones(1,1700);  % will only write to this when the sum of square errors is minimized
bestfit = 100000;             % arbitrary, original sum of square errors value
bestfit2 = 100000;           % arbitrary, original sum of square errors value
big = 0;                      % counting variable for the sorption variable
finaltime = 1.7;

Fkeep = 0;                   % F value for the best-fit line

```

```

Kdkeep = 0;           % Kd value for the best-fit line
k2keep = 0;          % k2 value for the best-fit line
k2keep2 = 0;         % k2 value for the best-fit line

% this loop determines the correct F and Kd

for F = 0.00:0.01:0.35

    for Kd = Kdval-0.01:0.01:Kdval+0.01

        for k2 = 1:0.01:13.5

            big = 0;
            Ctot = Cstart;
            S = 0;
            S2new = 0;

            for time = 0.001:timestep:finaltime

                big = big+1;

                S1 = ((Kd*F*(Ctot-S2new*(SoilMass/WatVol)))/(1+(F*Kd*(SoilMass/WatVol))));
                deltaS2 = (k2*((1-F)*Kd*(Ctot-((S1+S2new)*(SoilMass/WatVol)))-S2new))*(timestep);
% k2 units are 1/hr
                S2old = S2new;
                S2new = deltaS2 + S2old;

                S = S1 + S2new;
                Sorbed(big)=S;
                Caq(big) = Cstart - S*(SoilMass/WatVol);

            end

            sumsquare = 0;

            for i=1:numsamples

                square = (Sorbed(round(timed(i)*1000))-sorb(i))^2;

```

```

        sumsquare = sumsquare + square;
    end

    if sumsquare < bestfit
        bestfitline = Sorbed;
        bestfit = sumsquare;
        Fkeep = F;
        Kdkeep = Kd;
        k2keep = k2;
    end
end
end
end

% time to determine the best-fit k2
for k2 = 1:0.01:16
    F = Fkeep;
    Kd = Kdkeep;

    big = 0;
    Ctot = Cstart;
    S = 0;
    S2new = 0;

    for time = 0.001:timestep:finaltime
        big = big+1;

        S1 = ((Kd*F*(Ctot-2new*(SoilMass/WatVol)))/(1+(F*Kd*(SoilMass/WatVol))));
    end
end
end
end

```

```

        deltaS2 = (k2*((1-F)*Kd*(Ctot-((S1+S2new)*(SoilMass/WatVol)))-S2new))*(timestep);
% k2 units are 1/hr
        S2old = S2new;
        S2new = deltaS2 + S2old;

        S = S1 + S2new;
        Sorbed2(big)=S;
        Caq(big) = Cstart - S*(SoilMass/WatVol);
end

% need conditional statement to find best fit along "approaching equilibrium" curve

sumsquare2 = 0;
sumsquare3 = 0;

for i=1:numsamples

    timevalue = timed(i);

    if (timevalue >=0.0999) & (timevalue <=0.34)
        square2 = (Sorbed2(round(timed(i)*1000))-sorb(i))^2;
        sumsquare2 = sumsquare2 + square2;    % finding best fit of specified points only
    end

end

if sumsquare2 < bestfit2

    for i=1:numsample    % determining total sum of squared error for new line

        square3 = (Sorbed2(round(timed(i)*1000))-sorb(i))^2;
        sumsquare3 = sumsquare3 + square3;

    end

    bestfitline2 = Sorbed2;
    bestfit2 = sumsquare2;

```



```

        bestfit3 = sumsquare3;
            Fkeep = F;
            Kdkeep = Kd;
            k2keep2 = k2;

        end

end

title('Kinetic Batch Experiment (Benzene)');
xlabel('Time(hrs)');
ylabel('Amount Sorbed (mmol/kg)');

t = 0.001:timestep:1.7;

plot(t, bestfitline2, '--r')

legend('Measured Data', 'Model Fit',4)

% Coefficient of determination

ssyy = 0;

for k = 1:numsamples
    syy = (sorb(k) - meanvalue)^2;
    ssyy = ssyy + syy;
end

r2 = 1 - (bestfit3/ssyy);

```

APPENDIX H. PARTICLE SIZE ANALYSIS OF SURFACTANT MODIFIED ZEOLITE FROM THE 2005 FARMINGTON, NM PILOT TEST.

This appendix describes particle size analyses that were conducted on spent SMZ from a field test in 2005. The supporting data are also presented in this appendix.

INTRODUCTION

A pilot test designed to remove organic hydrocarbons from produced water was conducted during the summer of 2005. New Mexico Tech (NMT) and the University of Texas at Austin (UT Austin) carried out the pilot test near Farmington, NM. Two surfactant-modified zeolite (SMZ) columns, A and B, were constructed in order to remove the volatile hydrocarbons—benzene, toluene, ethyl benzene, and xylenes (BTEX)—from the produced water. After the pilot test was completed, SMZ samples were taken from both columns. Duplicate samples were acquired from the top portion and bottom portion of column A; the same procedure was conducted on column B.

Because SMZ breakdown during produced water treatment was previously reported (Ranck et al., 2005), the spent SMZ was analyzed to determine how the produced water had affected the zeolite's particle size distribution. Samples were compared to the particle size distribution results of one virgin SMZ sample. Hydrometer tests were conducted to analyze the particle distribution of fine particles (anything passing the 200 sieve), while sieve analyses measured the distribution of particles retained on and above the 200 sieve. The combination of the two tests produced the particle size distribution data of the spent and virgin SMZ samples.

METHODS AND MATERIALS

Each sample was initially run through a number 10 sieve in order to separate the coarse grained particles from the remaining sample. Both the retained mass and the passing mass were recorded. Since the virgin SMZ did not contain a significant amount of particles larger than the number 10 sieve (<1%), it was unnecessary to perform a particle distribution analysis of the coarse particles. Once the sample was separated, 100 grams of the particles passing the number 10 sieve were measured for the remaining analyses.

The hydrometer test followed ASTM standards (ASTM International, 2002). A dispersing solution (125 mL) containing sodium hexametaphosphate (40 g/L) was mixed with the 100-gram sample in a mixing bowl and allowed to sit for 16 hours in order to minimize sediment flocculation during the hydrometer test. The mixture was then stirred with an electric mixer and poured into a 1,000 mL graduated cylinder. Distilled water was added to the cylinder until the solution reached 1,000 mL. The graduated cylinder was covered and shook by hand for approximately 40 seconds. Once the shaking was completed, hydrometer (152H hydrometer) and temperature readings were recorded according to ASTM standards (after 1, 2, 4, 8, 15, 30, 60, 120, 240, 960, and 1440 minutes). Once the hydrometer readings were complete, the sample was shook on a number 200 sieve. Because particles finer than the 200 sieve were analyzed by the hydrometer test, particles passing the 200 sieve were disregarded. The particles retained on the number 200 sieve were placed on a tin plate and baked in an oven for three days.

The sieve analysis was performed with ASTM number 16, 30, 40, 50, 70, 100, and 200 sieves. Samples were shaken with an electric sieve shaker for approximately 25

minutes. Once the samples had been shaken, the mass retained on each sieve was weighed and recorded. The percentage of mass retained on the sieve was calculated after the sieves were weighed. The results from the sieve test and the hydrometer test provided a particle size distribution for each sample.

The effective grain size is a common parameter used to compare soil samples. 10% of a sample's particles are finer than the effective grain size (d_{10}). The effective grain size is important because flow through a sample is controlled by the fine particles in a sample. Therefore, the smallest 10% of the soil's particles will greatly influence the permeability of a sample. The effective grain size also is important because the finer particles can control the mechanical behavior of a soil (Budhu, 2000). Coarser particles tend to "float" on the smaller particles, so the small particles dictate the movement of the soil. The second influence is not as important in this study because the particles are bound in columns. However, the flow regime is a great concern of the research group. Long-term stability would enhance the effectiveness of the SMZ sorption system.

The d_{60} (60% finer than this particle size) and d_{30} (30% finer than this particle size) values were also recorded. The percentage of gravel, sand, silt, and clay were also calculated from the particle size distribution data. Gravel was defined as anything retained on the ASTM number 4 sieve and larger (4.75 mm and larger). Sand was defined as particles retained between the number 10 sieve and the number 200 sieve (2 mm – 0.075 mm). Silt and clay were combined into a "fines" category, which represented any particle smaller than the 200 sieve. Particle sizes ranging between 0.075 mm and 0.005 mm were defined as silts, while particles smaller than 0.005 mm were defined as a clay particle.

Another parameter used to classify and compare soil samples is the uniformity coefficient. The uniformity coefficient (C_u) is typically calculated for medium to coarse-grained samples and represents the d_{60} value divided by the d_{10} value. For a sample of uniformly sized particles, the uniformity coefficient will equal one (Hillel, 1998). As the sample becomes more poorly sorted, the uniformity coefficient will increase. The C_u is typically less than four for well-sorted soils (Budhu, 2000); but in poorly sorted sands, the uniformity coefficient can reach 1,000 (Hillel, 1998). Therefore, as the grains become more non-uniform, the uniformity coefficient increases.

The coefficient of gradation (C_c) is another parameter that is commonly used to classify soil samples. The C_c is often used to determine if a soil sample is gap graded. For typical well-sorted and poorly-sorted samples, the C_c usually equals between one and three (Budhu, 2000). A gap-graded soil will produce a C_c outside of this range. The sudden change of slope produces the deviations from the normal values. Equation H-1 is used to calculate the coefficient of gradation.

$$C_c = \frac{(d_{30})^2}{d_{10} * d_{60}} \quad (\text{H-1})$$

The primary concern of particle breakdown is the influence on the column's permeability; therefore, the permeability of each sample was calculated. Initially, the Hazen method was used to approximate the hydraulic conductivity of each sample. This method is applicable for sands with a d_{10} value between 0.1 mm and 3.0 mm (Fetter, 2001). The SMZ samples have d_{10} values approximately equaling 0.1 mm; so this method is a valid approximation for the hydraulic conductivity of the SMZ samples. The

Hazen method uses Equation H-2 to approximate the hydraulic conductivity of sandy sediments.

$$K = C(d_{10})^2 \quad (\text{H-2})$$

Where K is the hydraulic conductivity (cm/sec), C is a coefficient based on the properties of the sample, and d_{10} is in cm. Because the majority of the samples were medium to fine grained sands, the constant, C, was set as 80 (Fetter, 2001). Once the hydraulic conductivity was approximated, each sample's permeability was calculated with Equation H-3.

$$K = \frac{k * \rho_w * g}{\mu} \quad (\text{H-3})$$

Where k is permeability (cm^2), g is gravity (m/s^2), ρ_w is the density of water (kg/m^3), and μ is dynamic viscosity ($\text{kg}/(\text{m} * \text{sec})$). These parameters were calculated and compared in order to determine the extent of the particle breakdown that occurred during the pilot test. The permeability and d_{10} values are of particular importance because the flow characteristics through the columns are directly related to these two parameters. When both the permeability and the d_{10} decrease, produced water treatment efficiency decreases. Clogging issues, immobile sections, and backpressure buildups could also be of concern when these parameters decrease.

RESULTS AND DISCUSSION

Tables H-1 through H-9 present the hydrometer and sieve test data. The overall results from the hydrometer and sieve tests are presented in Tables H-10 and H-11.

Samples were defined as top or bottom (T or B), column A or B (A or B), and sample 1

or 2 (-1 or -2). For example, sample BA-2 represents the second sample for the bottom of column B. The percentage of finer particles was calculated for each sieve and for the hydrometer test data. From this data, particle size distribution histograms and graphs were created. Figures H-1 through H-9 show the histograms of each sample's particle size distribution compared to the virgin SMZ. The particle size distribution graphs of each sample are seen in Figures H-10 through H-16. The spent SMZ histograms show similar particle distribution results. The percentages of particles ranging from 0.6 mm – 0.3 mm decreased in the spent SMZ compared to the virgin SMZ. The most consistent and significant loss in percentage occurred on the ASTM number 40 sieve (0.425 mm). This particle size recorded a drop from 27% retained to only approximately 20% retained. Since the medium grained particles all saw a decrease in percentage retained, the fine particles saw the increase in percentage retained. The results show that particles ranging from 0.212 mm – 0.0361 mm consistently had higher percentages retained in the spent SMZ than the virgin SMZ. The increase in percentage retained on these sieves was not significant, but the results show that a definite increase occurred for the majority of the samples. Even though the fines from 0.212 mm – 0.0361 mm showed an increase in percentage retained, the fines below 0.031 mm did not show consistent increases in percentages retained. Both of the samples from the top of column B show an increase in particles between 0.0180 mm – 0.0094 mm; however, no other samples have similar results. Therefore, the medium grained particles were broken down into semi-fine grained particles during the pilot test. However, a consistent increase in extremely fine grained particles was not observed in the results.

The particle size distribution graphs indicate that the percentage of coarse grained particles (2 mm – 0.5 mm) was not significantly affected during the pilot test. A slight increase in the particles retained on the number 10 sieve is seen in some of the samples; however, these results are explained by particles bonding together during the test. Therefore, the increase in percentage is not due to single large particles but to the cementing of multiple particles together. These particle groups were not crushed prior to the hydrometer and sieve analysis because the individual particles could be affected / crushed when attempting to split the group. This process could lead to an increase in fine particles and skew the results. Even though no significant change in the coarse particles was seen from the graphs, the graphs do indicate that the pilot test did alter the percentage of fine grained particles in the majority of the samples. The percentage of particles 0.5 mm and smaller increased for all of the spent SMZ samples compared to the virgin SMZ. Therefore, as expected, an increase in fines occurred during the pilot test due to particle break down. The extent of particle breakdown was examined using the parameters discussed in the methods section. The effective grain size (d_{10}), d_{30} , and d_{60} values were obtained from the particle size distribution graphs. As stated previously, these parameters were used to calculate the uniformity coefficient and the coefficient of gradation. Also, the effective grain size was used to approximate the hydraulic conductivity of each sample using the Hazen Method. The results from these calculations can be seen in Table H-10. Top A 1 and Top A 2 represent the two samples taken from the top of column A. Bot A 1 and Bot A 2 are samples taken from the bottom of column A. The same naming procedure applies to column B. Raw SMZ 1 represents the virgin SMZ sample that underwent both the hydrometer and sieve analyses.

As stated previously, the data in Table H-10 indicates that no change in the d_{60} value is seen between the virgin SMZ and the spent SMZ. The d_{60} value for the virgin SMZ is 0.68 mm, and the average value of the spent SMZ is 0.70 mm. The slight increase in the d_{60} value is caused by the grouping of particles discussed previously. Table H-10 shows that some of the samples had large increases in the d_{60} value (Top B 2), while other samples had significant breakdown of the coarse grained particles and the d_{60} value was substantially smaller (Top A 1). The d_{30} value for the virgin SMZ is 0.44 mm, while the average value from the spent SMZ is 0.41 mm. So, on average the d_{30} particle size decreased during the pilot test by only 7%. Again, the d_{30} value increased for the Top B 2 sample, while it was significantly smaller for the Top A 1 and Bot A 1 samples. These two samples show a decrease of 20% from the original d_{30} value. The data shows that, on average, only a slight decrease of the d_{30} occurred. A significant decrease in the effective grain size for the majority of the samples compared to the virgin SMZ is seen in Table H-10. On average, the d_{10} value for the spent SMZ was 0.12 mm and it was 0.29 mm for the virgin SMZ sample. These values indicate that the effective grain size decreased by 58% during the pilot test.

The uniformity coefficient is used to determine the sorting of a sample. As stated previously, it can range from one (uniform grain size) to around 1000 (poorly sorted). Since the virgin SMZ's C_u equals 2.3, it lies within the typical range of a well-sorted sample. However, the average C_u of 6.1 from the spent SMZ is not in the typical range of a well-sorted soil. Therefore, the pilot test started with well-sorted SMZ and particle break down caused the spent SMZ to be classified as a poorly sorted sample. The maximum change in the uniformity coefficient occurred in the samples from the bottom

of column A. The C_u for these samples ranged from 3 to 4 times the virgin SMZ's uniformity coefficient. Both samples from the top of column B show the least amount of change in the uniformity coefficient as they doubled the original value. If the coefficient of gradation (C_c) is larger than 3, a soil is defined as gap graded. As expected, the results show that none of the SMZ samples are gap graded. All of the samples lie in the range for typical poorly and well sorted soils. The C_c increased for all of the samples because the d_{30} and d_{60} remained constant while the d_{10} decreased. Since you divide the squared d_{30} value by the d_{60} and d_{10} values, a decrease in the d_{10} value will naturally produce a larger coefficient of gradation.

Because the Hazen method is only an approximation of hydraulic conductivity, the results from the virgin SMZ were compared to lab measurements on virgin SMZ. Column measurements in the lab resulted in a hydraulic conductivity range of 31.5 – 35.8 m/day for virgin SMZ (Altare, 2006). The results from the Hazen method indicate that the virgin SMZ has a hydraulic conductivity of 58 m/day. So, the Hazen method slightly overestimates the hydraulic conductivity value; but it provides a good approximation for the virgin and spent SMZ. The average hydraulic conductivity of the spent SMZ is approximately 12 m/day. Therefore, the hydraulic conductivity of the spent SMZ is 1/5 of the virgin SMZ's hydraulic conductivity. Two of the spent SMZ samples are even one order of magnitude less than the virgin SMZ. In order to calculate the permeability, a density of 998.2 kg/m³, and a viscosity of $1.002 * 10^{-3}$ kg/(m*sec) were used. Therefore, only a conversion factor of $1.023 * 10^{-7}$ (m*sec) was needed to convert the hydraulic conductivity to permeability (m²) (Schwartz and Zhang, 2003). These values assume 20°C and water as the fluid. Since the same conversion factor was used to calculate the

permeabilities, the results for the permeability data matched the results from the hydraulic conductivity data. Both the hydraulic conductivity and permeability lie within the typical range for a medium grained, clean sand (Freeze and Cherry, 1979 and Schwartz and Zhang, 2003). Both the particle size analysis in Table H-11 and the particle size distribution graphs (Figures H-9 through H-16) indicate that the majority of the SMZ samples are medium grained sand particles.

The particle classification results are seen in Table H-11. The same sample-naming scheme is used in Table H-11 as was used in Table H-10. The results from this analysis also indicate that the percentage of fines (silt and clay combined) increased during the pilot test because of particles breaking down. Prior to the pilot test, the virgin SMZ contained 98% sand and 2% fines. The average values for the spent SMZ are: 93% sand and 7% fines. Therefore, the spent SMZ has approximately 3.7 times the amount of fines in the virgin SMZ. The same trends within the columns are seen with the particle size analysis. On average, the top sample has a lower amount of fines than the bottom sample in each column. Also, column A was usually the first column in series during the pilot test. The data shows that a greater amount of particle breakdown occurred in this column than column B.

The results from the two virgin SMZ samples that only underwent the sieve analysis show an even greater amount of particle breakdown. The percentage of fines in these two samples was four times smaller than the virgin SMZ that underwent both the hydrometer and sieve analyses. Similar results are seen for the effective grain size, the d_{30} , and the hydraulic conductivity of these two samples. The uniformity constant for these two samples also indicate that the virgin SMZ is a well sorted sample.

CONCLUSIONS

Particles in a media naturally break down when water flows through it, so some particle breakdown was expected. The results from the particle size distribution test confirm that particle break down did occur during the pilot test. Both of the columns show a higher percentage of fines in the lower sample than the upper sample. Since flow occurred from the top of the columns to the bottom of the columns, some fine particles were probably carried downward in the column during the pilot test. The samples were also taken approximately 6 months after the pilot test was completed, so particle settling could have occurred during that period of time. The effective grain size and amount of fines were important parameters because the small grain sizes control the ability for produced water to flow through the columns. The results from these parameters indicate that the fines did increase significantly in some of the samples; for example, in the bottom of column A. Even though the percentage of fines did increase, the histograms show that an increase in the extremely fine grained particles did not occur. Since these particles would greatly influence the flow regime, no consistent increase in these particles is promising. One major effect of particle breakdown is the back pressure will build up when produced water is forced through the columns. No back pressure build up was observed during the field test, which also indicates that the overall particle breakdown did not greatly influence the flow regime. Although particle breakdown is seen in the results, the results do not provide any significant reason for doubting the long term stability of the SMZ particles.

Table H-1. Combined sieve and hydrometer data for sample TA-1.

Grain size (mm)	U.S. Standard Sieve No.	Percent Finer by weight	Percent Retained
75.00	3 in.	100.00	0.00
50.00	2 in.	100.00	0.00
37.50	1-1/2 in.	100.00	0.00
25.00	1 in.	100.00	0.00
19.00	3/4 in.	100.00	0.00
9.50	3/8 in.	100.00	0.00
4.75	4	100.00	0.00
2.00	10	99.70	0.30
1.18	16	98.40	1.30
0.60	30	57.03	41.37
0.43	40	37.54	19.49
0.30	50	24.67	12.87
0.21	70	19.41	5.26
0.15	100	14.56	4.85
0.08	200	8.93	5.63
0.0498	Hydrometer	8.33	0.60
0.0357		5.72	2.61
0.0255		3.63	2.09
0.0180		3.63	0.00
0.0133		3.11	0.52
0.0094		2.59	0.52
0.0066		2.59	0.00
0.0047		2.59	0.00
0.0033		2.59	0.00
0.0017		2.59	0.00
0.0014		2.59	0.00

Table H-2. Combined sieve and hydrometer data for sample TA-2.

Grain size (mm)	U.S. Standard Sieve No.	Percent Finer by weight	Percentage Retained
75.00	3 in.	100.00	0.00
50.00	2 in.	100.00	0.00
37.50	1-1/2 in.	100.00	0.00
25.00	1 in.	100.00	0.00
19.00	3/4 in.	100.00	0.00
9.50	3/8 in.	100.00	0.00
4.75	4	100.00	0.00
2.00	10	99.69	0.31
1.18	16	97.49	2.20
0.60	30	50.85	46.64
0.43	40	30.07	20.78
0.30	50	17.41	12.66
0.21	70	13.31	4.10
0.15	100	10.69	2.62
0.08	200	5.63	5.06
0.0507	Hydrometer	4.68	0.96
0.0361		4.15	0.52
0.0257		3.11	1.04
0.0182		3.11	0.00
0.0133		2.59	0.52
0.0094		2.59	0.00
0.0066		2.59	0.00
0.0047		2.59	0.00
0.0033		2.59	0.00
0.0017		2.59	0.00
0.0014		2.59	0.00

Table H-3. Combined sieve and hydrometer data for sample BA-1.

Grain size (mm)	U.S. Standard Sieve No.	Percent Finer by weight	Percentage Retained
75.00	3 in.	100.00	0.00
50.00	2 in.	100.00	0.00
37.50	1-1/2 in.	100.00	0.00
25.00	1 in.	100.00	0.00
19.00	3/4 in.	100.00	0.00
9.50	3/8 in.	100.00	0.00
4.75	4	100.00	0.00
2.00	10	96.02	3.98
1.18	16	93.79	2.23
0.60	30	52.84	40.95
0.43	40	35.95	16.89
0.30	50	24.41	11.54
0.21	70	20.32	4.10
0.15	100	17.24	3.08
0.08	200	10.03	7.21
0.0501	Hydrometer	7.31	2.72
0.0361		3.78	3.53
0.0257		2.98	0.80
0.0182		2.98	0.00
0.0133		2.48	0.50
0.0094		2.48	0.00
0.0066		2.48	0.00
0.0047		2.48	0.00
0.0033		1.98	0.50
0.0017		2.48	-0.50
0.0014		2.48	0.00

Table H-4. Combined sieve and hydrometer data for sample BA-2.

Grain size (mm)	U.S. Standard Sieve No.	Percent Finer by weight	Percentage Retained
75.00	3 in.	100.00	0.00
50.00	2 in.	100.00	0.00
37.50	1-1/2 in.	100.00	0.00
25.00	1 in.	100.00	0.00
19.00	3/4 in.	100.00	0.00
9.50	3/8 in.	100.00	0.00
4.75	4	100.00	0.00
2.00	10	98.92	1.08
1.18	16	97.04	1.88
0.60	30	48.28	48.76
0.43	40	29.70	18.58
0.30	50	18.71	10.99
0.21	70	15.38	3.33
0.15	100	12.39	2.98
0.08	200	7.18	5.21
0.0505	Hydrometer	5.90	1.28
0.0361		3.58	2.32
0.0257		3.07	0.51
0.0182		3.07	0.00
0.0133		3.07	0.00
0.0094		3.07	0.00
0.0066		2.56	0.51
0.0047		2.56	0.00
0.0033		2.56	0.00
0.0017		2.56	0.00
0.0014		2.56	0.00

Table H-5. Combined sieve and hydrometer data for sample TB-1.

Grain size (mm)	U.S. Standard Sieve No.	Percent Finer by weight	Percentage Retained
75.00	3 in.	100.00	0.00
50.00	2 in.	100.00	0.00
37.50	1-1/2 in.	100.00	0.00
25.00	1 in.	100.00	0.00
19.00	3/4 in.	100.00	0.00
9.50	3/8 in.	100.00	0.00
4.75	4	100.00	0.00
2.00	10	98.65	1.35
1.18	16	97.02	1.63
0.60	30	46.41	50.61
0.43	40	25.92	20.49
0.30	50	14.43	11.49
0.21	70	11.39	3.04
0.15	100	8.72	2.68
0.08	200	8.40	0.29
0.0501	Hydrometer	7.26	1.03
0.0357		5.83	1.44
0.0252		5.62	0.21
0.0179		4.60	1.03
0.0132		4.09	0.51
0.0093		3.57	0.51
0.0066		3.06	0.51
0.0047		3.06	0.00
0.0033		2.55	0.51
0.0017		2.55	0.00
0.0014		2.55	0.00

Table H-6. Combined sieve and hydrometer data for sample TB-2.

Grain size (mm)	U.S. Standard Sieve No.	Percent Finer by weight	Percentage Retained
75.00	3 in.	100.00	0.00
50.00	2 in.	100.00	0.00
37.50	1-1/2 in.	100.00	0.00
25.00	1 in.	100.00	0.00
19.00	3/4 in.	100.00	0.00
9.50	3/8 in.	100.00	0.00
4.75	4	100.00	0.00
2.00	10	92.79	7.21
1.18	16	89.95	2.85
0.60	30	41.12	48.83
0.43	40	23.50	17.62
0.30	50	12.98	10.52
0.21	70	10.24	2.75
0.15	100	8.97	1.26
0.08	200	5.00	3.97
0.0505	Hydrometer	5.53	-0.53
0.0358		4.33	1.21
0.0253		4.33	0.00
0.0180		3.84	0.48
0.0132		3.36	0.48
0.0094		2.88	0.48
0.0066		2.40	0.48
0.0047		2.40	0.00
0.0033		2.40	0.00
0.0017		2.40	0.00
0.0014		2.40	0.00

Table H-7. Combined sieve and hydrometer data for sample BB-1.

Grain size (mm)	U.S. Standard Sieve No.	Percent Finer by weight	Percentage Retained
75.00	3 in.	100.00	0.00
50.00	2 in.	100.00	0.00
37.50	1-1/2 in.	100.00	0.00
25.00	1 in.	100.00	0.00
19.00	3/4 in.	100.00	0.00
9.50	3/8 in.	100.00	0.00
4.75	4	100.00	0.00
2.00	10	99.85	0.15
1.18	16	97.03	2.82
0.60	30	50.13	46.90
0.43	40	29.70	20.43
0.30	50	17.13	12.57
0.21	70	13.54	3.59
0.15	100	10.78	2.76
0.08	200	6.09	4.68
0.0507	Hydrometer	5.48	0.61
0.0363		2.79	2.70
0.0257		2.58	0.21
0.0182		2.06	0.52
0.0133		2.06	0.00
0.0094		1.54	0.52
0.0067		1.54	0.00
0.0047		1.54	0.00
0.0033		1.54	0.00
0.0017		2.06	-0.52
0.0014		2.06	0.00

Table H-8. Combined sieve and hydrometer data for sample BB-2.

Grain size (mm)	U.S. Standard Sieve No.	Percent Finer by weight	Percentage Retained
75.00	3 in.	100.00	0.00
50.00	2 in.	100.00	0.00
37.50	1-1/2 in.	100.00	0.00
25.00	1 in.	100.00	0.00
19.00	3/4 in.	100.00	0.00
9.50	3/8 in.	100.00	0.00
4.75	4	100.00	0.00
2.00	10	99.86	0.14
1.18	16	98.18	1.68
0.60	30	55.32	42.86
0.43	40	33.85	21.47
0.30	50	20.20	13.65
0.21	70	16.01	4.19
0.15	100	12.26	3.74
0.08	200	6.47	5.79
0.0505	Hydrometer	5.69	0.78
0.0361		4.39	1.30
0.0255		3.61	0.78
0.0180		3.61	0.00
0.0133		3.09	0.52
0.0094		3.09	0.00
0.0066		3.09	0.00
0.0047		3.09	0.00
0.0033		3.09	0.00
0.0017		3.09	0.00
0.0014		2.58	0.52

Table H-9. Combined sieve and hydrometer data for sample Virgin SMZ.

Grain size (mm)	U.S. Standard Sieve No.	Percent Finer by weight	Percentage Retained
75.00	3 in.	100.00	0.00
50.00	2 in.	100.00	0.00
37.50	1-1/2 in.	100.00	0.00
25.00	1 in.	100.00	0.00
19.00	3/4 in.	100.00	0.00
9.50	3/8 in.	100.00	0.00
4.75	4	100.00	0.00
2.00	10	99.91	0.09
1.18	16	98.63	1.28
0.60	30	52.80	45.83
0.43	40	26.00	26.80
0.30	50	10.45	15.56
0.21	70	7.71	2.74
0.15	100	5.47	2.24
0.08	200	1.83	3.64
0.0513	Hydrometer	2.63	-0.80
0.0364		2.10	0.53
0.0258		1.57	0.53
0.0182		1.57	0.00
0.0133		1.57	0.00
0.0094		1.57	0.00
0.0067		1.04	0.53
0.0047		1.04	0.00
0.0033		1.04	0.00
0.0017		0.51	0.53
0.0014		0.51	0.00

Table H-10. Overall parameter results from the particle size distribution data.

Sample	d₁₀ (mm)	d₃₀ (mm)	d₆₀ (mm)	C_u	C_c	Hydraulic Conductivity (m/sec)	Permeability (cm²)
Top A 1	0.08	0.34	0.62	7.5	2.25	5.51E-05	5.64E-08
Top A 2	0.13	0.42	0.70	5.4	1.94	1.35E-04	1.38E-07
Bot A 1	0.08	0.36	0.69	9.2	2.50	4.50E-05	4.60E-08
Bot A 2	0.10	0.43	0.71	7.1	2.60	8.00E-05	8.18E-08
Top B 1	0.17	0.46	0.71	4.2	1.75	2.31E-04	2.37E-07
Top B 2	0.20	0.49	0.79	4.0	1.52	3.20E-04	3.27E-07
Bot B 1	0.13	0.43	0.70	5.4	2.03	1.35E-04	1.38E-07
Bot B 2	0.11	0.38	0.66	6.0	1.99	9.68E-05	9.90E-08
Raw Zeolite	0.29	0.44	0.68	2.3	0.98	6.73E-04	6.88E-07
VIR SMZ 1	0.40	0.61	0.82	2.1	1.13	1.28E-03	1.31E-06
VIR SMZ 2	0.43	0.61	0.82	1.9	1.06	1.48E-03	1.51E-06

Table H-11. Particle size breakdown results from particle size distribution data.

Sample	% Gravel	% Sand	% Fines	% Silt	% Clay
Top A 1	0	91.07	8.93	6.34	2.59
Top A 2	0	94.37	5.63	3.04	2.59
Bot A 1	0	89.97	10.03	7.55	2.48
Bot A 2	0	92.82	7.18	4.63	2.56
Top B 1	0	95.60	4.40	1.34	3.06
Top B 2	0	95.00	5.00	2.60	2.40
Bot B 1	0	93.91	6.09	4.55	1.54
Bot B 2	0	93.53	6.47	3.38	3.09
Raw Zeolite	0	98.17	1.83	0.79	1.04
VIR SMZ 1	0	99.32	0.68	0.68	0.00
VIR SMZ 2	0	99.77	0.23	0.22	0.01

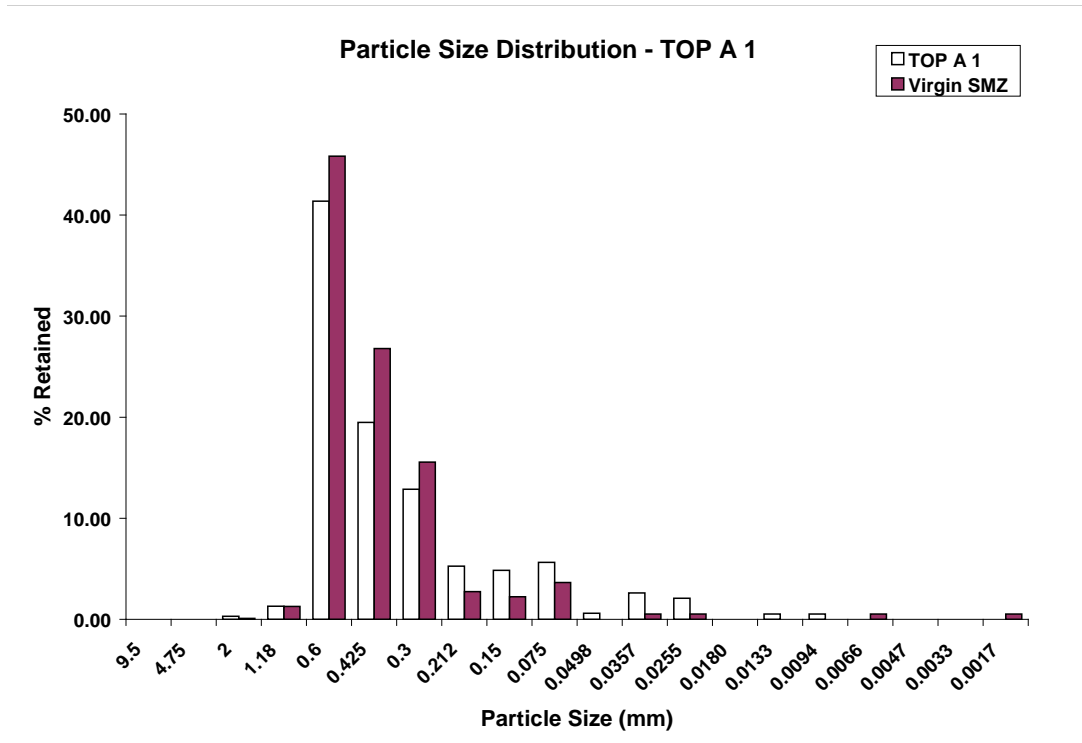


Figure H-1. Bar graph representation of particle size distribution of sample TA-1. Virgin SMZ represents unspent particle size distribution.

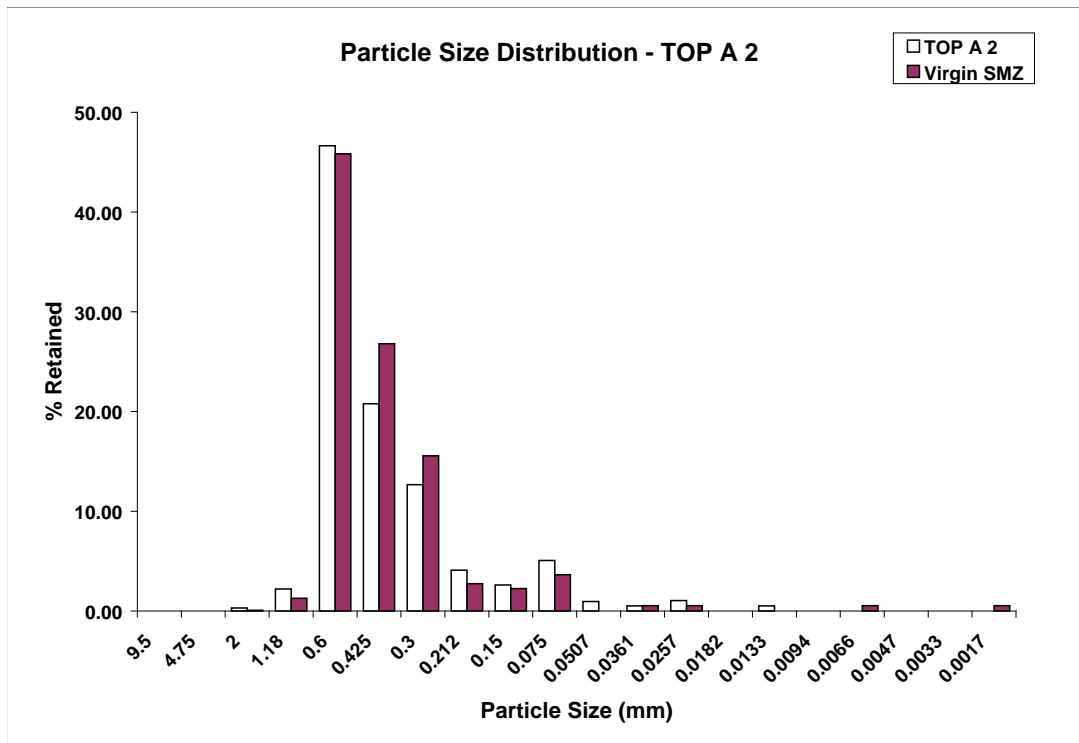


Figure H-2. Bar graph representation of particle size distribution of sample TA-2. Virgin SMZ represents unspent particle size distribution.

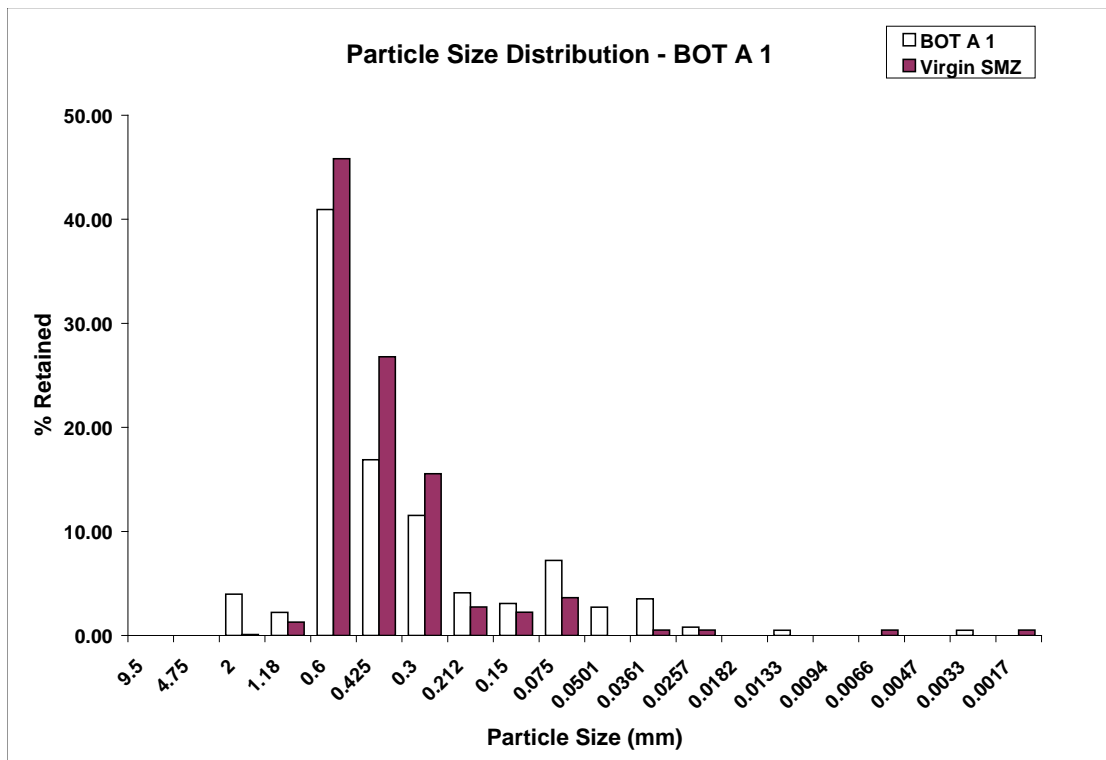


Figure H-3. Bar graph representation of particle size distribution of sample BA-1. Virgin SMZ represents unspent particle size distribution.

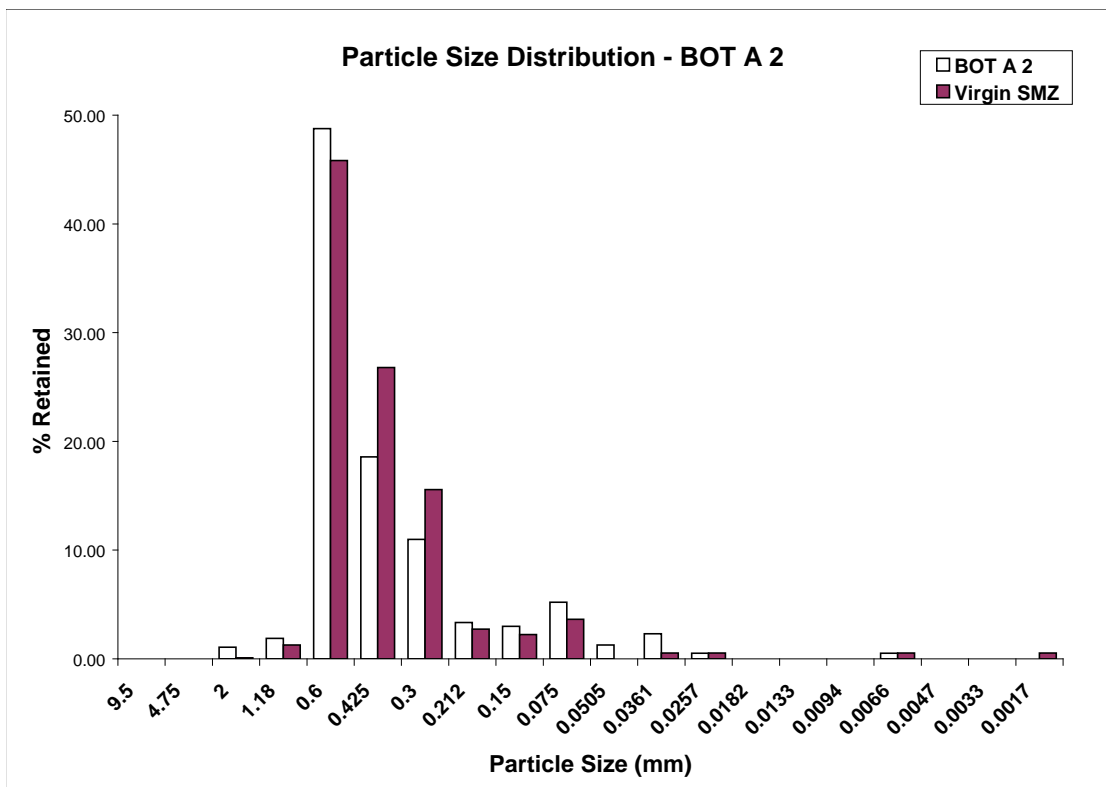


Figure H-4. Bar graph representation of particle size distribution of sample BA-2. Virgin SMZ represents unspent particle size distribution.

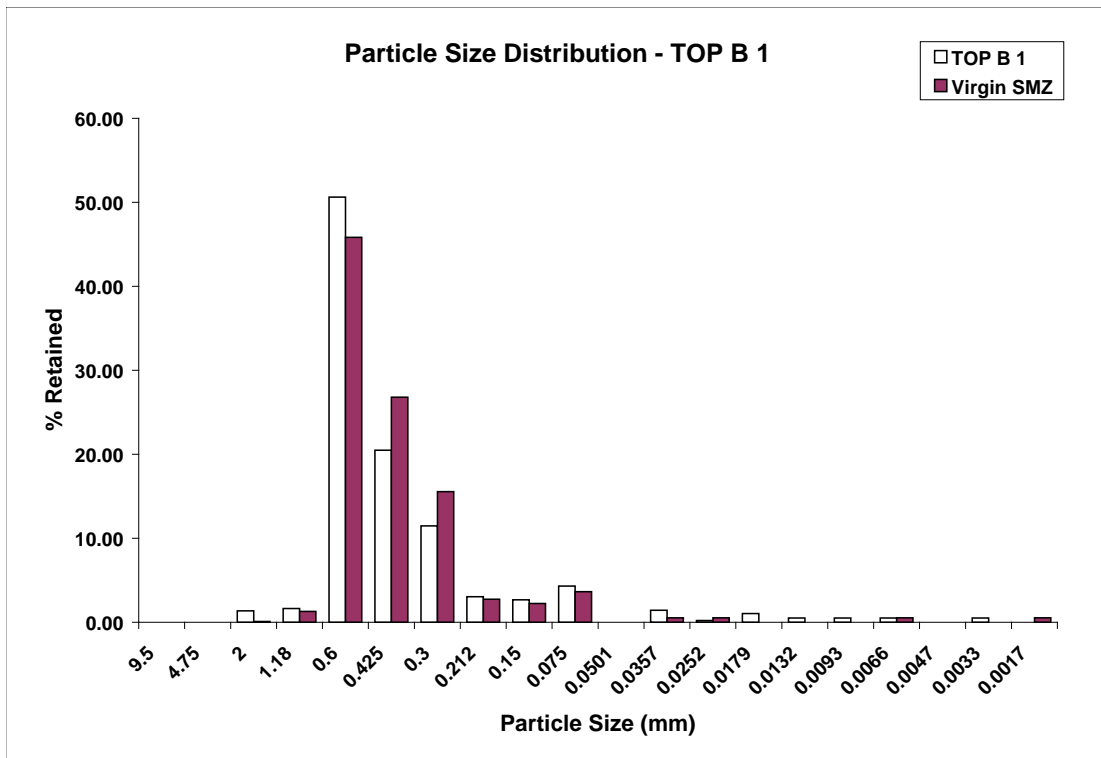


Figure H-5. Bar graph representation of particle size distribution of sample TB-1. Virgin SMZ represents unspent particle size distribution.

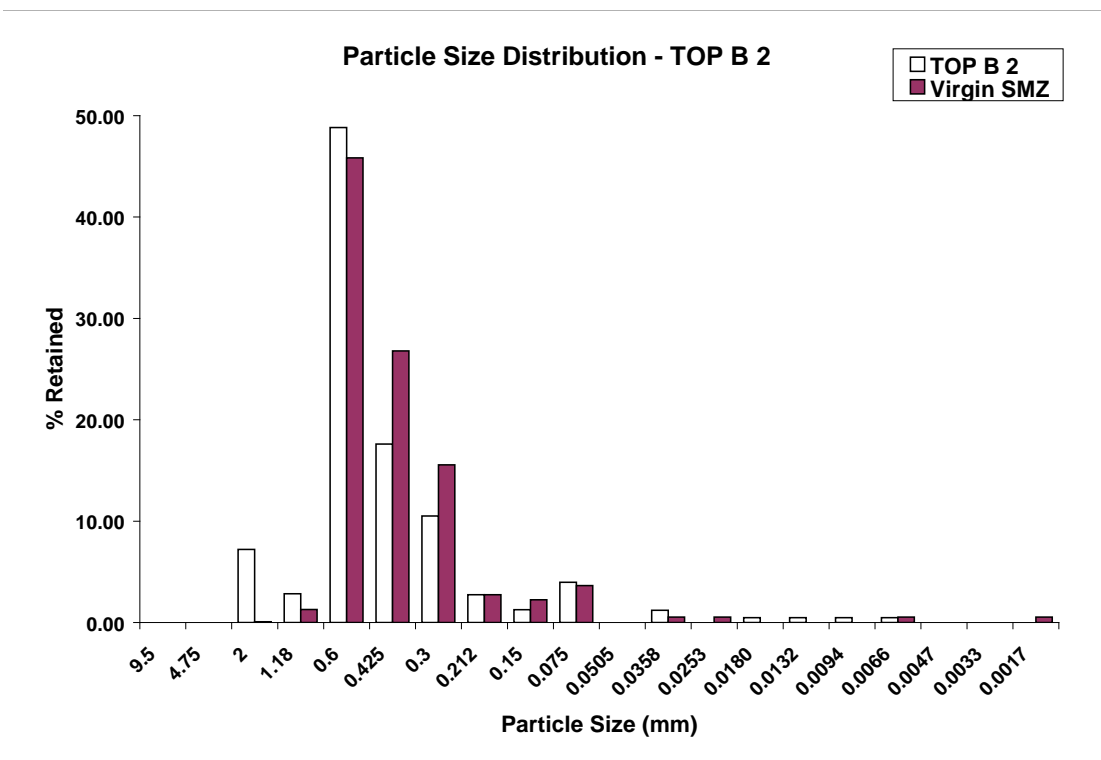


Figure H-6. Bar graph representation of particle size distribution of sample TB-2. Virgin SMZ represents unspent particle size distribution.

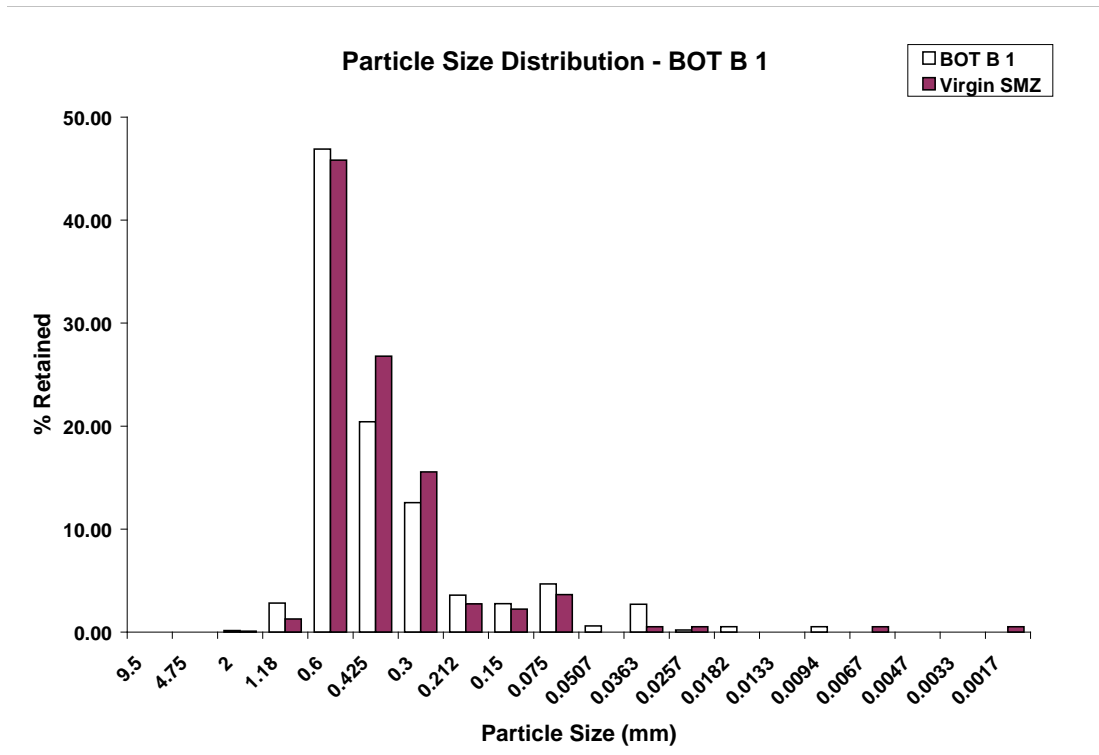


Figure H-7. Bar graph representation of particle size distribution of sample BB-1. Virgin SMZ represents unspent particle size distribution.

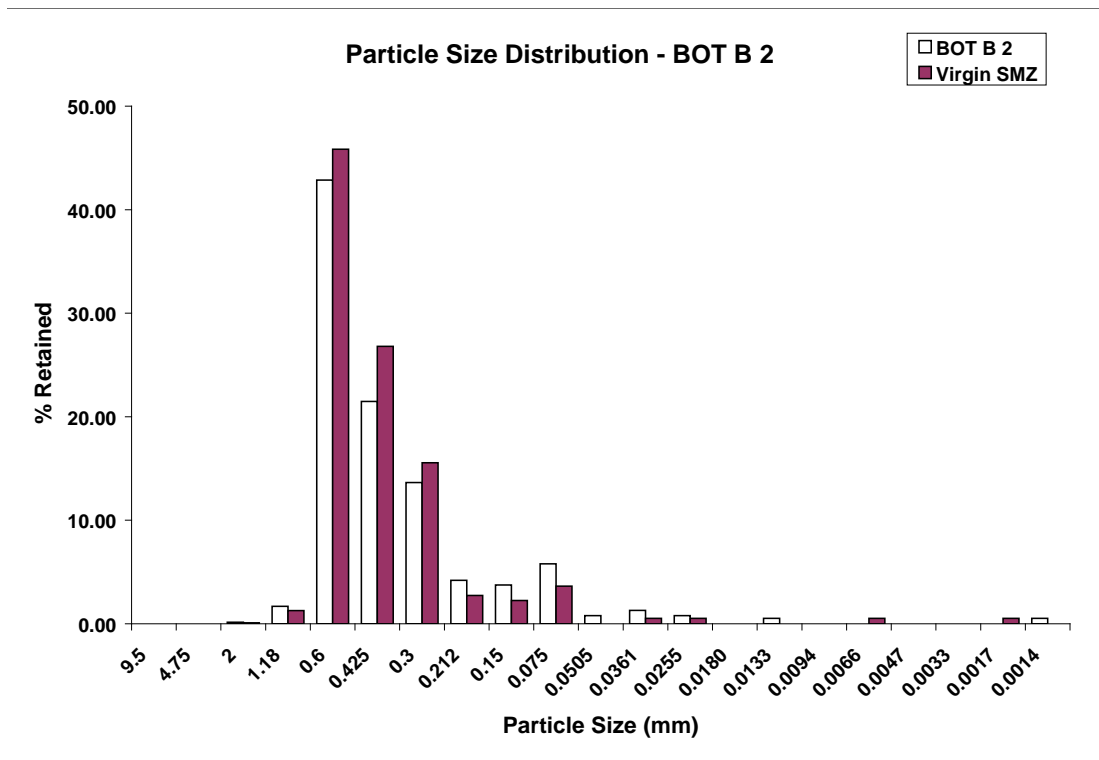


Figure H-8. Bar graph representation of particle size distribution of sample BB-2. Virgin SMZ represents unspent particle size distribution.

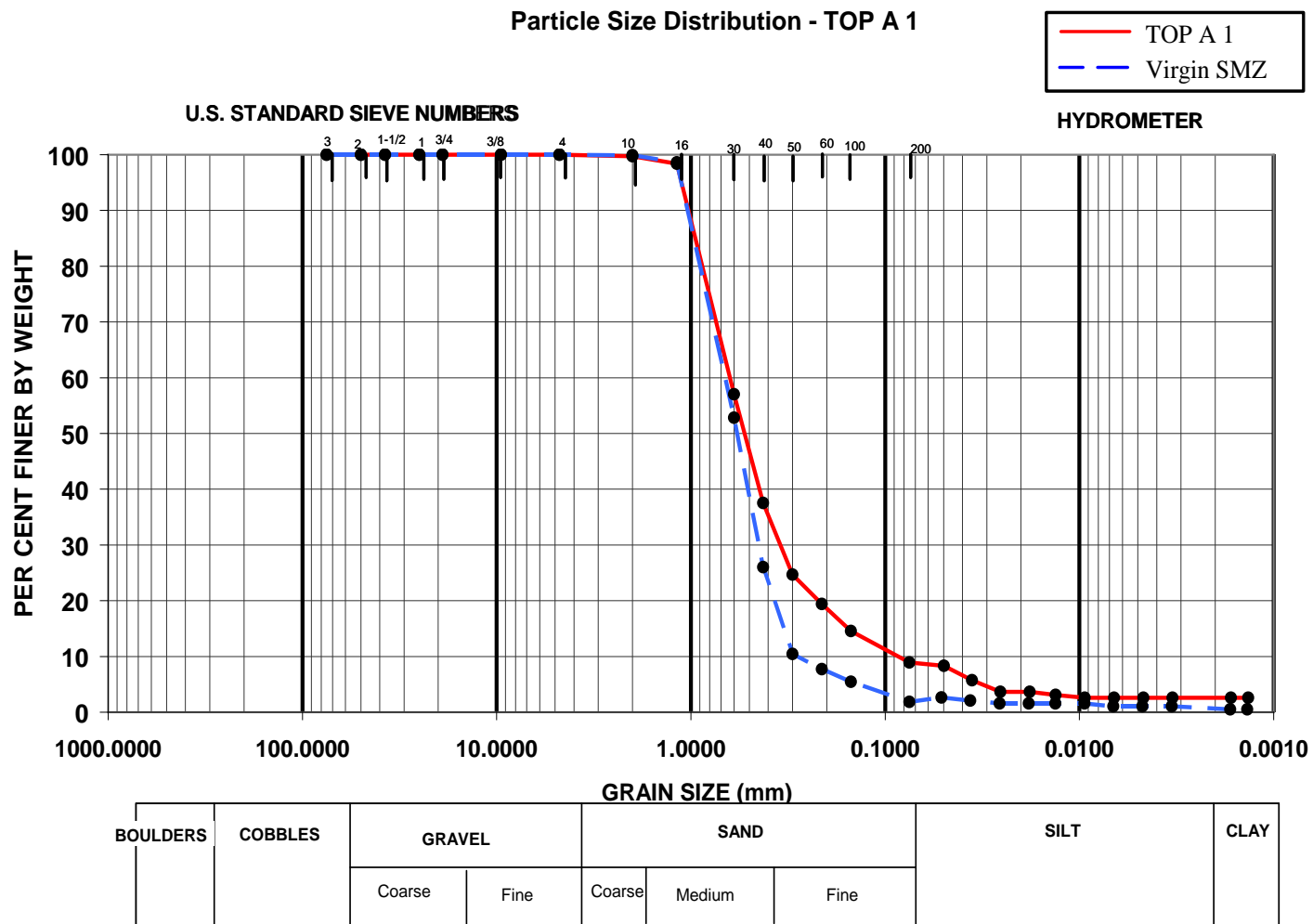


Figure H-9. Particle size distribution results for sample TA-1.

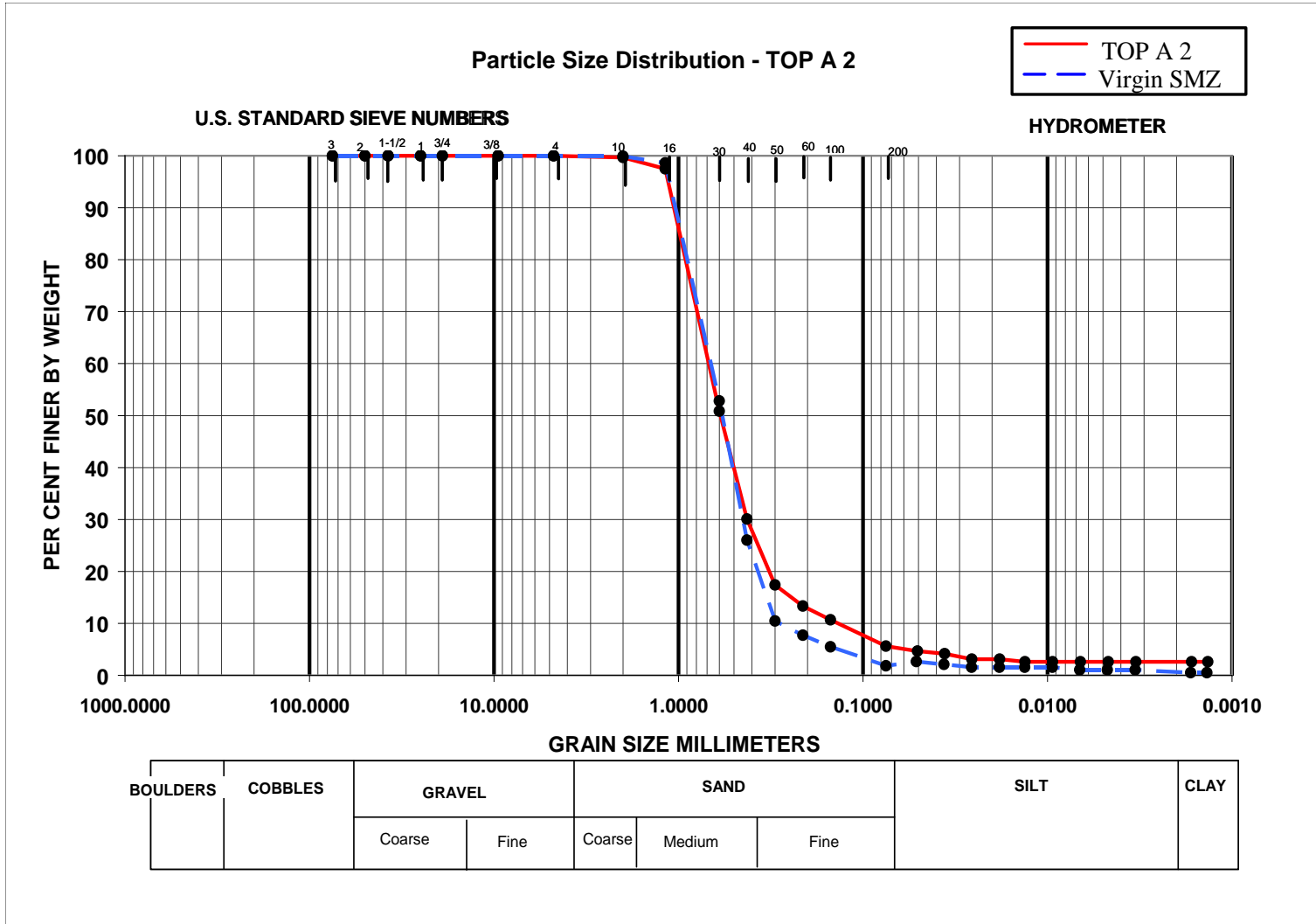


Figure H-10. Particle size distribution results for sample TA-2.

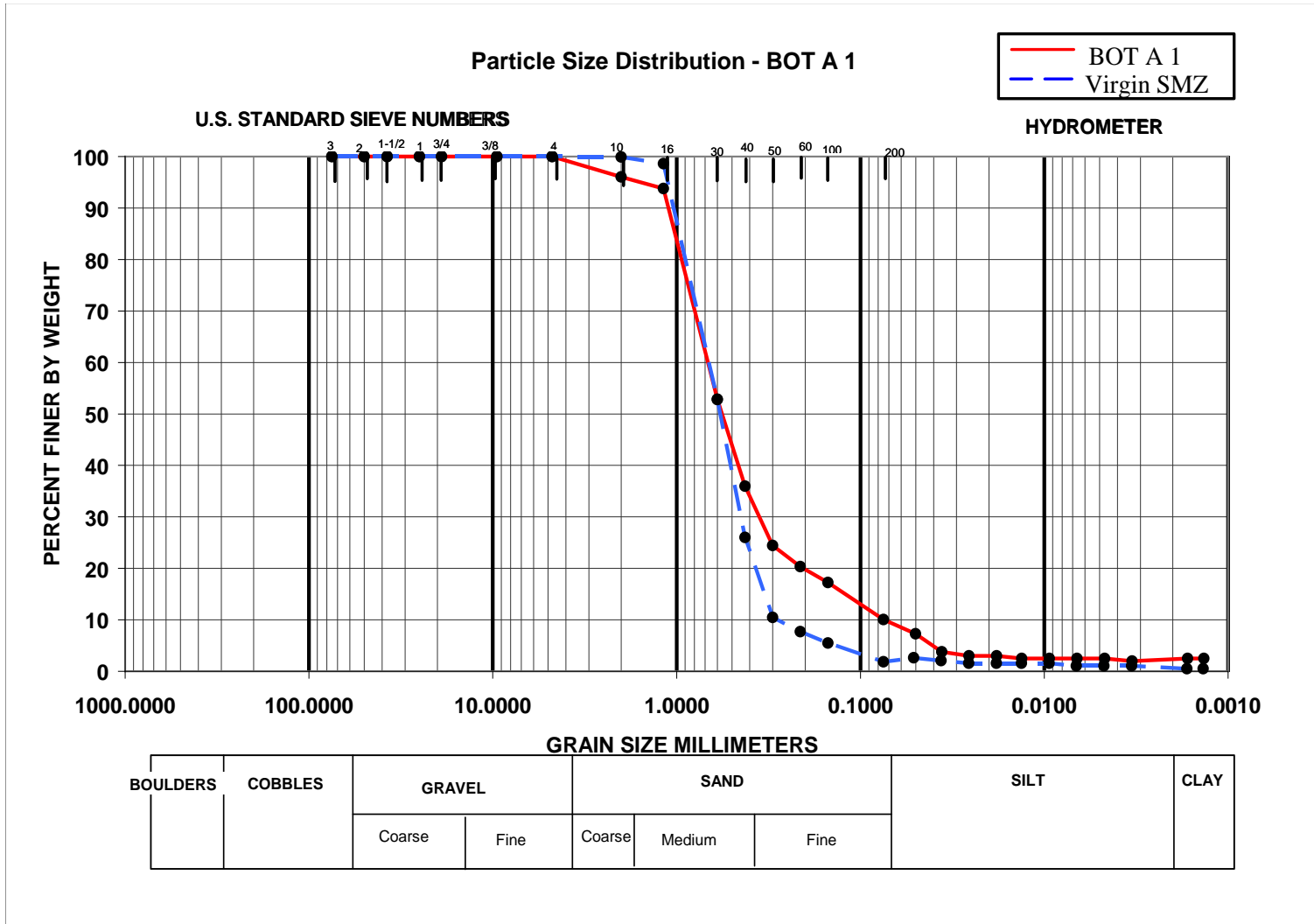


Figure H-11. Particle size distribution results for sample BA-1.

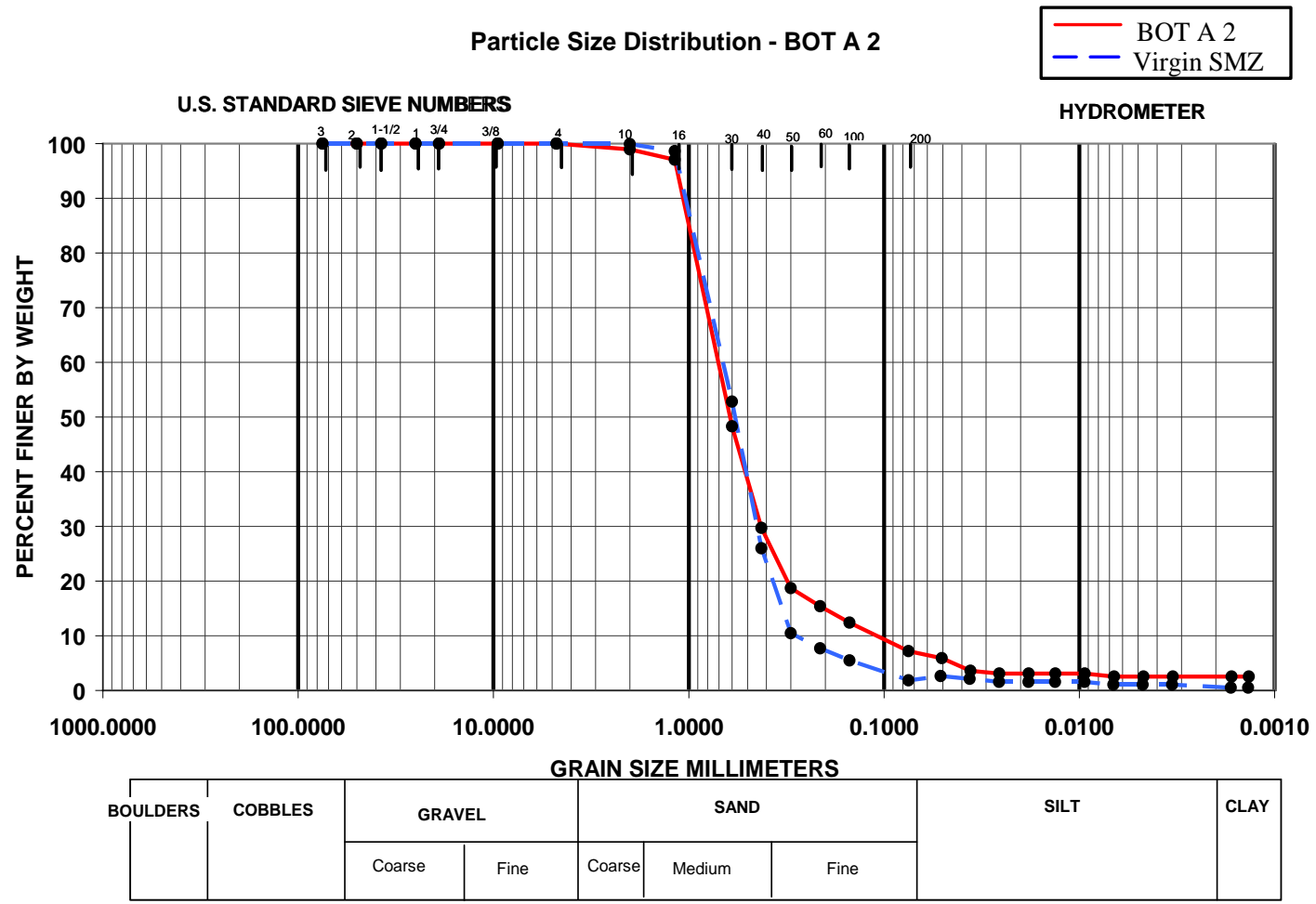


Figure H-12. Particle size distribution results for sample BA-2.

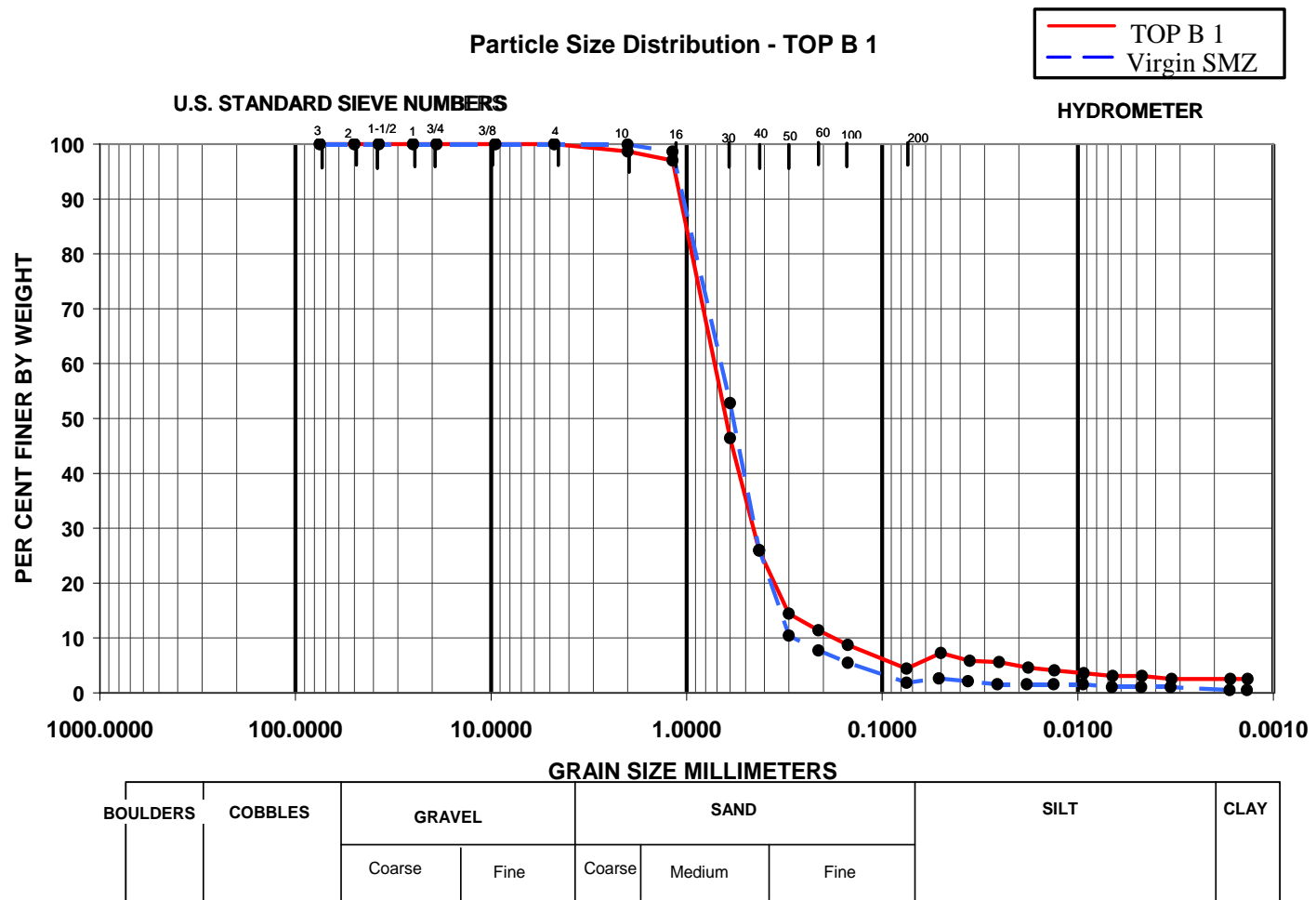


Figure H-13. Particle size distribution results for sample TB-1.

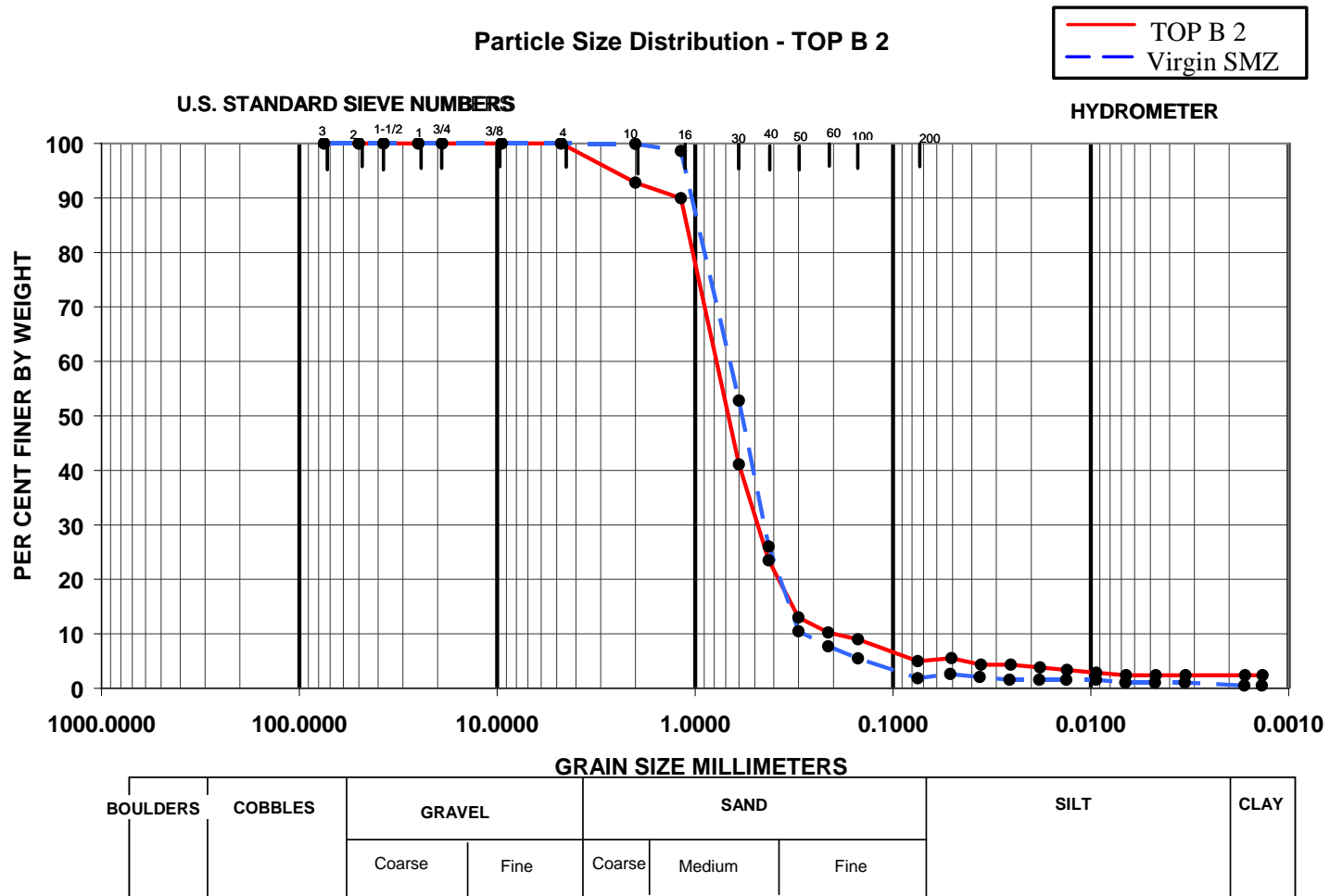


Figure H-14. Particle size distribution results for sample TB-2.

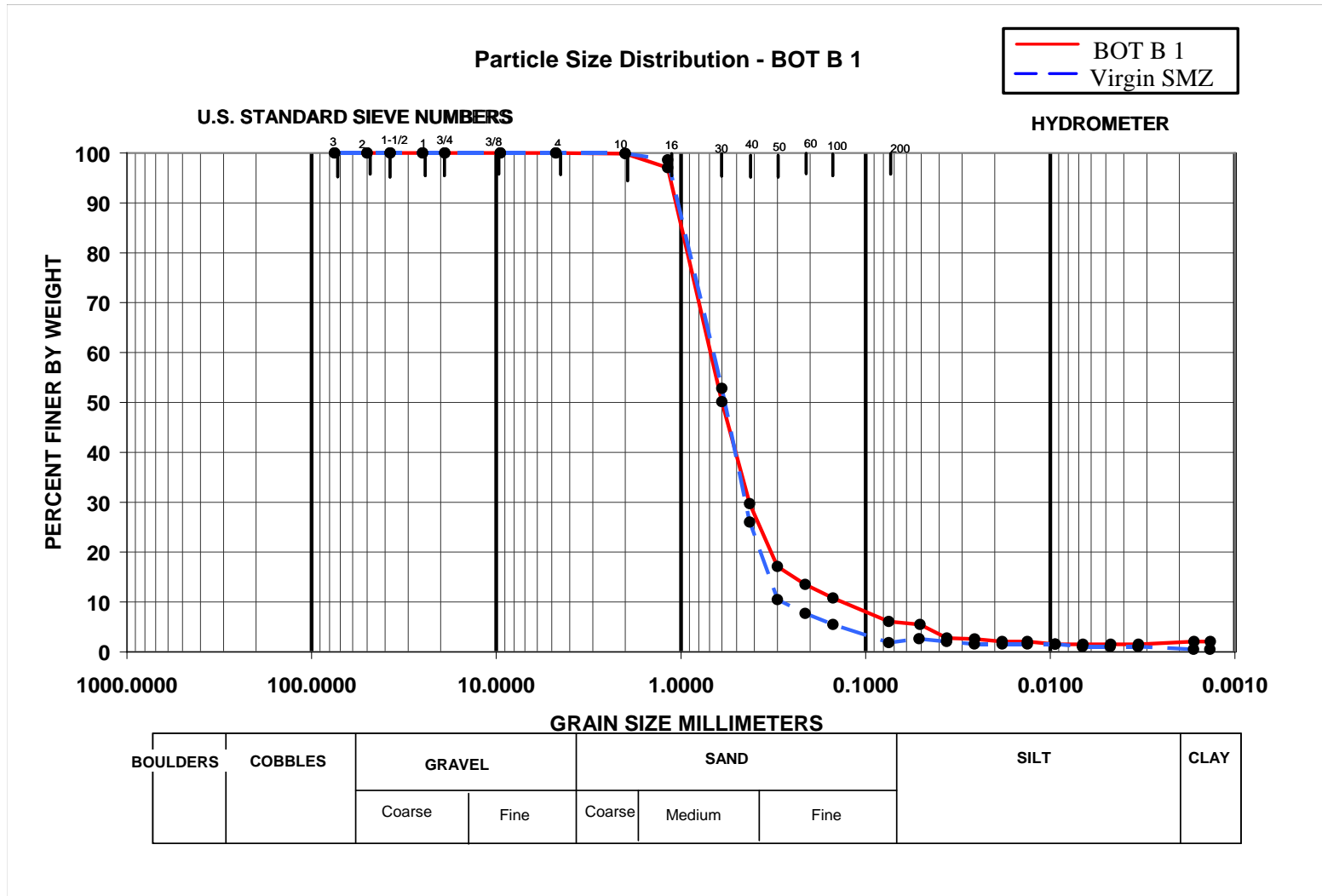


Figure H-15. Particle size distribution results for sample BB-1.

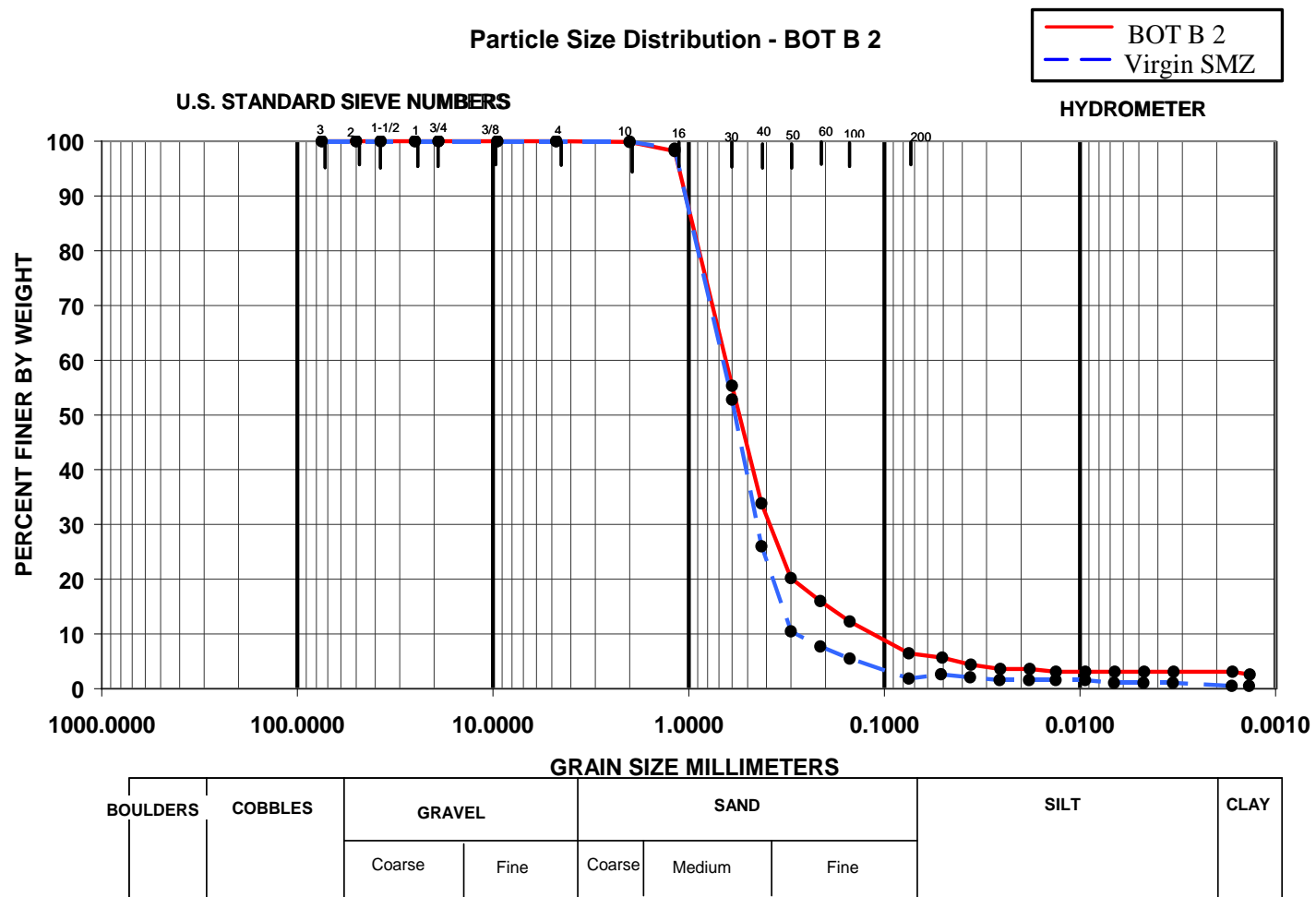


Figure H-16. Particle size distribution results for sample BB-2.

APPENDIX I. APPENDICES REFERENCES.

Altare, Craig. Personal Communication; 2006

ASTM International. *Standard Test Method for Particle-Size Analysis of Soils*, Designation: D 422-63 (Reapproved 2002); pgs. 1-8

Budhu, Muni. *Soil Mechanics and Foundations*, John Wiley and Sons, Inc., New York, 2000; pgs 25-26

Fetter, C.W. *Applied Hydrology*, 4th edition, Prentice-Hall, Inc., Upper Saddle River, New Jersey, 2001, pg 86

Freeze, R. Allan and Cherry, John A. *Groundwater*, Prentice-Hall, Inc., Englewood Cliffs, New Jersey, 1979, pg 29

Hillel, Daniel; *Environmental Soil Physics*; Academic Press, San Diego, 1998, pgs 65-66

Mackay, D., Shiu, W.Y., and Ma, K.C. *Illustrated Handbook of Physical-Chemical Properties and Environmental Fate of Organic Chemicals*, Lewis Publishers, Chelsea, MI, 1992

Schwartz, Franklin W. and Zhang, Hubao. *Fundamentals of Groundwater*, John Wiley and Sons, 2003, pgs 51-52

Selim, H.M, Davidson, J.M. and Mansell, R.S. *Evaluation of a Two-Site Adsorption-Desorption Model for Describing Solute Transport in Soils*, Proc. Summer Computer Simulation Conference, Washington D.C., 1976, pgs 444-448

Toride, N., Lej, F.J., and Van Genuchten, M.T. *The CXTFIT Code for Estimating Transport Parameters from Laboratory or Field Tracer Experiments, Version 2.1*, U.S. Salinity Laboratory, Riverside, California, 1999